Direct Effects of Selective Serotonin Reuptake Inhibitors, Fluoxetine, Sertraline and Paroxetine, and Atypical Antipsychotics, Aripiprazole and Clozapine, on Islet Beta Cell Mass and Function

Toczyska, Klaudia

Awarding institution:
King's College London

Direct Effects of Selective Serotonin Reuptake Inhibitors, Fluoxetine, Sertraline and Paroxetine, and Atypical Antipsychotics, Aripiprazole and Clozapine, on Islet Beta Cell Mass and Function

A thesis submitted by

Klaudia Wiktoria Toczyska

For the award of Doctor in Philosophy from

King's College London

Diabetes Research Group

Department of Diabetes

Faculty of Life Sciences & Medicine

King's College London

to my mum

Acknowledgements

I would like to thank my supervisors Professor Shanta Persaud and Doctor Bo Liu for their continuous support, guidance and encouragement throughout my PhD. Shanta was very patient with me; she was always there for me when I needed help and professional feedback. She introduced me to Diabetes research when I was an undergraduate student, and I cannot imagine doing my PhD with anyone else. I really appreciate her help and I am going to miss working with her. Many thanks to Bo for teaching me all the necessary techniques, her support when I first started islet isolations, and her help with my experiments. I wouldn't be a researcher I am now without her.

I thank Medical Research Council for providing funding for my studies.

My gratitude extends to the members of the Diabetes Research Group. Special thank you to Hannah Rosa who helped me with radioimmunoassays when I struggled with my RSI. Thank you to my favourite lab partner Naila for making me brave to introduce new techniques into my project and for her encouragement. I am going to miss doing experiments with her. Thank you to my students, Le'Vena Tan, Sameeyah Bint-Mahmood, Alokya Balagamage, Georgina Day and Nunzio Guccio, I couldn't imagine better company. Thank you to Tanyel Ashik, Maya Wilson, Dan Egbase, Sian Simpson and Matilda Kennard for their help with setting up the KCL Physiology Society and organising Physiology Fridays with me during my PhD. Thank you to Inmaculada Ruz-Maldonado, Oladapo Olaniru, Patricio Atanes, Lydia Daniels Gatward, Lorna Smith, Anastasia Tsakamki, Sophie Sayers, Eliane Caseiro Soares De Menezes, Aakruti Kaikini and Ella-Louise Hubber for their professional help when I was learning new techniques and with my experiments. I would also like to thank PIs in the group for their support

throughout my PhD and new PhD students who made my last year of PhD very enjoyable.

I would like to thank lecturers in the Departments of Physiology and Biochemistry for giving me the opportunity to help with their teaching and marking. Working as a GTA was one of my favourite activities during my PhD.

Finally, I would like to express my gratitude to my parents, my sisters, Natalia and Julia, and my boyfriend. Without their tremendous understanding and encouragement in the past few years, and especially during writing this thesis, it would be impossible for me to complete my study. Thank you for motivating me, comforting me, and always being there for me, kocham Was.

Abstract

The prevalence of type 2 diabetes (T2D) is 2-3-fold higher among people with severe mental health disorders compared to the general population. Several lines of evidence suggest a bidirectional link between diabetes and mental illness, so prevention of T2D in patients with mental illness and management of psychiatric symptoms in diabetic patients are both clinically important. There are concerns that antidepressant and antipsychotic therapies increase the risk of developing T2D. However, different medications used to control psychiatric conditions vary in side effects related to glucose dysregulation, and the direct actions of individual medications at beta cells are not fully understood. Therefore, the experiments in this thesis focused on the effects on beta cell function of the widely prescribed selective serotonin reuptake inhibitor (SSRI) antidepressants, fluoxetine, sertraline and paroxetine, and atypical antipsychotic drugs (AAPs), aripiprazole and clozapine.

SSRIs block serotonin reuptake by inhibiting the serotonin reuptake transporter (SERT). SERT mRNA was detected by standard polymerase chain reaction (PCR) amplification in MIN6 beta cells, mouse islets and human islets. In addition, SERT expression was confirmed by detection of a 71kDa immunoreactive protein by Western blotting. On the other hand, AAPs act on a range of receptors, including dopamine 2 (D2) receptors, and D2 receptor expression in beta cells was confirmed by quantitative PCR and fluorescent immunohistochemistry. Trypan blue exclusion tests were used to assess viability of MIN6 beta cells and mouse islets, and they showed no impairment in viability following a 48h incubation with 0.1-1μM fluoxetine, 0.1-1μM sertraline, 0.01-0.1μM paroxetine, 0.1-1μM aripiprazole or 0.2-2μM clozapine. Trypan blue uptake was only evident in MIN6 cells or islets treated with fluoxetine, sertraline or aripiprazole at 10μM, paroxetine at 1μM and clozapine at 20μM. Acute exposure of mouse and human

islets to therapeutically relevant concentrations of SSRIs increased glucose-stimulated insulin secretion (GSIS) in perifusions. In addition, exposure of MIN6 cells, mouse islets and human islets to SSRIs or AAPs for 1h or 48h in static incubation experiments significantly potentiated glucose-induced insulin secretion.

The effects of SSRIs and AAPs in regulating beta cell proliferation were investigated by quantifying bromodeoxyuridine (BrdU) incorporation into beta cell DNA. Fluoxetine, sertraline, paroxetine, and aripiprazole, but not clozapine, significantly increased MIN6 beta cell proliferation following a 48h incubation, and aripiprazole and clozapine increased proliferation of islet-derived pseudoislets. In addition, male *ob/ob* mice that were injected with fluoxetine (10mg/kg) 4 times over 14 days showed significant increases in islet size and the number of BrdU-positive beta cells. Moreover, quantitative Western blot analysis revealed that fluoxetine increased phosphorylation of mitogen-activated protein kinase (MAPK), cAMP response element-binding protein (CREB), and protein kinase B, also known as Akt, which are known to be involved in beta cell mass expansion.

Levels of apoptosis of beta cells are low, therefore apoptosis of MIN6 beta cells, mouse islets and human islets was induced by a saturated free fatty acid, palmitate, or a cocktail of proinflammatory cytokines (interleukin-1β, tumour necrosis factor α, and interferon γ). SSRIs and AAPs had no effect on basal apoptosis rates, but they had a protective effect against palmitate- and cytokine-induced apoptosis.

In summary, the data presented in this thesis have demonstrated that therapeutically relevant concentrations of fluoxetine, sertraline, paroxetine, as well as aripiprazole and clozapine, potentiate acute dynamic glucose-stimulated

insulin secretion, with no impairment of viability, and they also promote beta cell proliferation and have a protective effect against palmitate- and cytokine-induced apoptosis. Therefore, these data indicating that these SSRIs and AAPs exert beneficial effects on beta cell mass and function suggest that glucose dysregulation observed with their use is not secondary to adverse effects at beta cells.

Abbreviations

°C	Degree Celsius
µ	micro
5-HT	5-hydroxytryptamine/serotonin
AA	arachidonic acid
AADC	aromatic acid decarboxylase
AAP	atypical antipsychotic
AB	antibody
AC	adenylyl cyclase
Ach	acetylcholine
ACTB	beta actin
ADP	adenosine diphosphate
AG	antigen
AGI	alpha glucosidase inhibitors
AMPK	adenosine monophosphate-activated protein kinase
ANOVA	analysis of variance
AP	action potential
Apaf1	apoptotic protease activating factor 1
ATP	adenosine triphosphate
AUC	area under the curve
Bcl-2	B-cell lymphoma 2
BMI	Body mass index
bp	base pair
BrdU	5-bromo-2'-deoxyuridine
BSA	bovine serum albumin

Ca^{2+}	calcium ion
CaMK	calcium-calmodulin-dependent protein kinases
cAMP	cyclic adenosine 3,5-monophosphate
CBD	common bile duct
CBT	cognitive behavioural therapy
Cch	carbachol
CD80	cluster of differentiation 80
cDNA	complementary DNA
cmp	counts per minute
CNS	central nervous system
CO_2	carbon dioxide
CREB	cAMP response element-binding protein
CRP	C-reactive protein
Cu^{+}	cuprous ion
D	dopamine
DAG	diacylglycerol
DMEM	Dulbecco's modified eagle's medium
DMSO	dimethyl sulfoxide
DNA	deoxyribonucleic acid
dNTPs	deoxyribonucleotide triphosphate
DPP-4	dipeptidyl peptidase-4
EDU	5-ethynyl-2'-deoxyuridine
EGF	epidermal growth factor
ELISA	enzyme-linked immunosorbent assay
ER	endoplasmic reticulum
FBS	foetal bovine serum

FFA	free fatty acid
FGA	first-generation antipsychotic
FGA	first-generation antipsychotics
FSK	forskolin
g	gram
GABA	gamma-aminobutyric acid
GAD	generalised anxiety disorder
GD	gestational diabetes
GEF	guanine-nucleotide exchange factor
GH	growth factor
GIP	glucose-dependent insulinotropic polypeptide
GKA	glucokinase activator
GLP-1	glucagon-like peptide-1
GLUT	glucose transporter
GPCR	G-protein coupled receptor
GSIS	glucose-stimulated insulin secretion
H	hour
H_2O	water
$HbA1_C$	glycated haemoglobin $A1_C$
HNF	hepatocyte nuclear factor
HPA	hypothalamic-pituitary-adrenocortical axis
i	inhibitor
IAPP	islet amyloid polypeptide
IDF	International Diabetes Federation
IGF	insulin-like growth factor
IHC	immunohistochemistry

IL-1β	interleukin-1 beta
IL-2	interleukin-2
INF-γ	interferon gamma
INS1	rat insulinoma beta cell line
IP3	inositol 1,4,5-triphosphate
IPGTT	intraperitoneal glucose tolerance test
ipGTTs	intraperitoneal glucose tolerance test
IRS	insulin receptor substrate
k	kilo
K^+	potassium ion
K_{ATP}	ATP-sensitive potassium channel
kDa	kilodalton
Kir6.2	inward rectifier potassium channel
KO	knockout
l	litre
LDL	low-density lipoprotein
LPS	lipopolysaccharide
m	mili
M	molar
MAO	monoamine oxidase
MAPK	mitogen-activated protein kinase (Erk)
MCP-1	monocyte chemoattractant protein-1
MDD	major depressive disorder
MEM	minimum essential medium
min	minute
MIN6	mouse insulinoma beta cell line

MODY	maturity onset of the young
mRNA	messenger RNA
n	nano
NF-κB	nuclear factor kappa-light-chain-enhancer of activated B cells
nM	nanomolar
NS	nervous system
NSB	non-specific binding
O_2	oxygen
ob/ob	$Lep^{ob/ob}$ / obese
OCD	obsessive-compulsive disorder
P	passage
PAGE	polyacrylamide gel electrophoresis
PBS	phosphate-buffered saline
PCR	polymerase chain reaction
PDGF	platelet-derived growth factor
PDVF	polyvinylidene fluoride
PDX-1	pancreatic and duodenal homeobox 1
PEG	polyethylene glycol
PI	phosphatidylinositol and propidium iodide
PI3K	phosphatidylinositol (3)-kinase
PIP2	phosphatidylinositol (4,5)-biphosphate
PIP3	phosphatidylinositol (3,4,5)-biphosphate
PKA	protein kinase A
PKB	protein kinase B (Akt)
PKC	protein kinase C
PL	placental lactogen

PLC	phospholipase C
PP	pancreatic polypeptide
PPAR	peroxisome proliferator-activated receptor
PSC	pancreatic stellate cell
PTSD	post-traumatic stress disorder
q	quantitative
R	receptor
Raw 264.7	monocyte/macrophage-like cell line
RCT	randomised controlled trial
RIA	radioimmunoassay
RIPA	radioimmunoprecipitation assay
RNA	ribonucleic acid
ROS	reactive oxygen species
RPMI	Roswell Park Memorial Institute
RT	reverse transcriptase
RT-PCR	real-time PCR
SCZ	schizophrenia
SDS	sodium dodecyl sulphate
SEM	standard error of the mean
SERT	serotonin transporter
SGA	second-generation antipsychotic
SGLT-2	sodium-glucose transport protein 2
SNRI	serotonin-noradrenaline reuptake inhibitor
SNS	sympathetic nervous system
SSRI	selective serotonin reuptake inhibitor
SU	sulphonylurea

SUR1	ATP-sensitive sulphonylurea receptor
SV40LT	simian virus 40 large T antigen
T	totals
T1D	type 1 diabetes
T2D	type 2 diabetes
TAP	typical antipsychotic
TCA	tricyclic antidepressants
TNF-α	tumour necrosis factor alpha
TPH	tryptophan hydroxylase
TPH-1	human monocytic cell line
Tris	tris(hydroxymethyl)aminomethane
TRS	treatment-resistant schizophrenia
TRP	tryptophan
TZD	thiazolidinedione
v/v	volume in volume
VDCC	voltage-dependent calcium channel
VLDL	very-low-density lipoprotein
w/v	weight in volume
WHO	World Health Organisation
α	alpha
β	beta
γ	gamma
ζ	zeta

Table of contents

Table of figures

Table of tables

Chapter 1. Introduction

1.1. Diabetes Mellitus

Diabetes mellitus, simply called diabetes, is a group of complex and heterogeneous metabolic disorders that develop when pancreatic beta cells are destroyed or when they do not produce enough insulin, an important hormone that decreases blood glucose levels. Therefore, diabetes is characterised by chronic and sustained hyperglycaemia (high blood glucose levels). Symptoms of hyperglycaemia include frequent urination, abnormal thirst and dry mouth, blurred vision, and tiredness (Umpierrez et al., 2012). The formation of the sugar-haemoglobin linkage indicates sustained hyperglycaemia, and the glycated haemoglobin $A1_C$ ($HbA1_C$) is routinely measured in people with diabetes, as it is easy to detect and gives an indication of glycaemic management. For non-diabetic individuals, the normal range for $HbA1_C$ is 4-6% (20-42mmol/mol). $HbA1_C$ levels between 6-6.5% (42-48mmol/mol) may indicate a pre-diabetic state, whereas levels of 6.5% (48mmol/mol) and higher indicate diabetes (Sherwani et al., 2016).

The history of diabetes starts in antiquity, but it was linked to the pancreas only in the late 19th century. Even though diabetes has been known for thousands of years, it has become a major epidemic very recently. This is highlighted by the fact that in over a decade, the incidence of diabetes increased by 50% (Danaei et al., 2011). It is estimated that 537 million people have diabetes worldwide, and by 2045 this number will reach 700 million (IDF Diabetes Atlas – 10th Edition). This places a vast economic burden on healthcare systems globally and highlights the need for new treatment strategies.

The advances in diabetes research allowed for the identification of the different types of this disorder. However, many patients do not simply fit into a single class due to the complexity of diabetes (Cakan et al., 2012). The American Diabetes Association proposed the classification of diabetes as type 1, type 2, other types, and gestational diabetes (GD).

1.1.1. Type 1 diabetes

1.1.1.1. Epidemiology

Type 1 diabetes (T1D) constitutes 5%-10% of all diabetes cases (Maahs et al., 2010) and 80%-90% of diabetes in children and adolescents (Craig et al., 2009; Dabelea et al., 2014). This type of diabetes mainly affects children and young adults, but it can develop at any age, and it usually presents at 10 to 14 years of age. Due to different genetic and environmental triggers, including exposure to environmental microbes and dietary factors, there are huge variations in the incidence of T1D between different countries. Finland and the UK have high incidence rates, whereas Venezuela and Thailand have low incidence rates (IDF Diabetes Atlas – 10th Edition).

1.1.1.2. Pathogenesis

This type of diabetes develops mainly due to an autoimmune destruction of the beta cells through T cell mediated responses (Devendra et al., 2004) that result in beta cell death and subsequent hyperglycaemia. Islet autoantigens are generated due to contribution of genetic and environmental factors (Figure 1.1). Intra islet macrophages recognise the autoantigen and present it to CD4+ T cells that in turn activate CD8+ T cells to directly damage beta cells and potentiate islet infiltration by macrophages, leading to progression of T1D (Burrack et al., 2017;

Jo and Fan, 2021). T1D can be further divided into autoimmune, idiopathic, and fulminant T1D. Both idiopathic and fulminant are nonimmune-mediated and are often associated with a viral infection (Imagawa et al., 2000). Interestingly, clinical studies report metabolic disturbances in COVID-19 accompanied by new-onset T1D in the absence of autoantibodies (Chee et al., 2020; Hollstein et al., 2020; Marchand et al., 2020). What is more, an 80% increase in new-onset T1D in children during the pandemic has been reported (Unsworth et al., 2020).

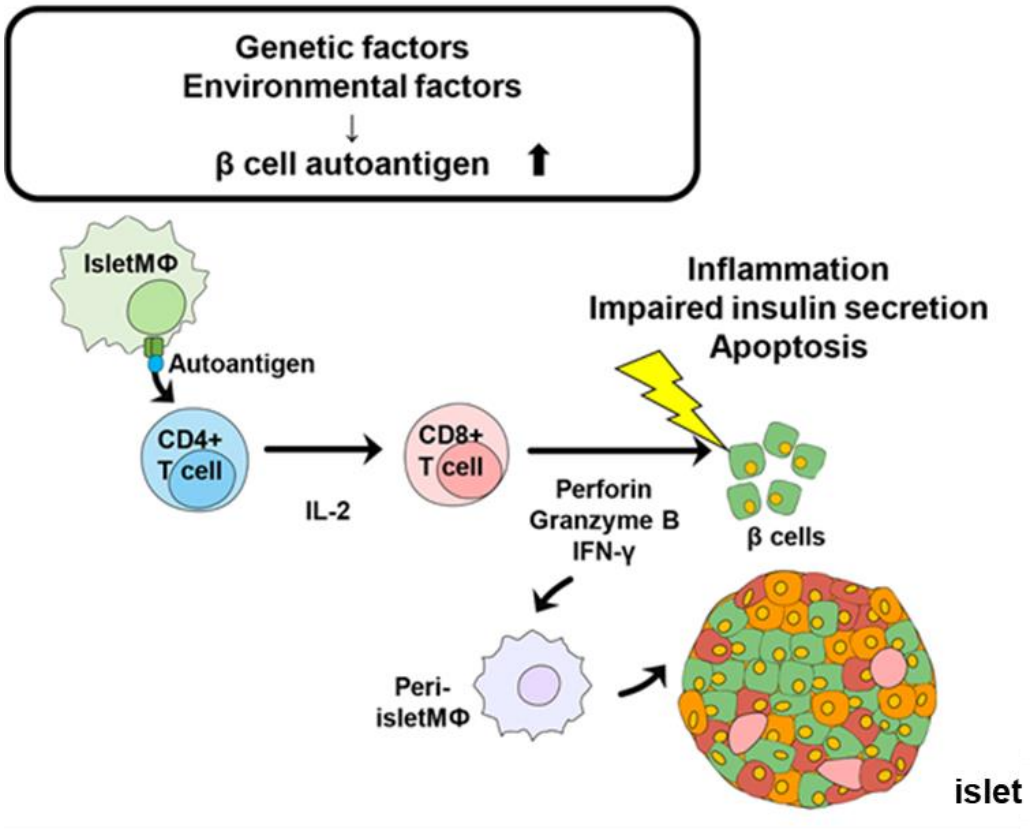

Figure 1.1. Schematic of immune modulation leading to destruction of beta cells in T1D. Genetic and environmental factors lead to generation of the autoantigen, which can be recognised by macrophages. The autoantigen is presented to CD4+ T cells, which in turn secrete interleukin-2 (IL-2) to activate CD8+ T cells to directly destroy beta cells and potentiate islet inflammation. CD8+ T cells destroy beta cell directly via perforin, a glycoprotein that forms pores in cell membranes of target cells, and granzyme B, a cytotoxic serum protease protein, and a cytokine interferon-γ (IFN-γ) (Burrack et al., 2017). Adapted from Jo and Fan, 2021.

1.1.1.3. Treatment

The aim of management of T1D is to promote healthy lifestyle and control glycaemia to prevent severe hypoglycaemia, hyperglycaemia, and ketoacidosis. The main treatment strategy is insulin replacement (administration of exogenous insulin or insulin analogues) to replicate normal physiology as closely as possible, and these are delivered by subcutaneous injections or insulin pumps. Insulin replacement, as well as blood glucose monitoring, are initiated in all newly diagnosed T1D patients. Recombinant insulin analogues can be long-acting (glargine, degludec, detmir) or short-acting (aspart, lispro). Long-acting insulin analogues, having durations of action of 20–42h, are used to provide basal insulin throughout the day. Short-acting analogues have an onset of action of approximately 15min and a duration of action of up to 4h, and they are used for rapid reductions in blood glucose levels after a meal or to treat high glucose levels acutely (Melo et al., 2019; Vardi et al., 2008). Management of T1D extends to adjunctive therapies that help to complement insulin replacement, and these include the use of metformin to improve insulin sensitivity and hence provide better control glycaemic management (Holt et al., 2021; Liu et al., 2020). The development of the artificial pancreas, immunotherapy and human islet transplantation or stem cell strategies are the goals to improve the lives of T1D patients in the future.

1.1.2. Type 2 diabetes

1.1.2.1. Epidemiology

Approximately 90%-95% of diabetes patients are diagnosed with T2D, and most of these patients are adults. Nevertheless, it is increasingly seen in children and adolescents due to rising levels of obesity, and the age of diagnosis of T2D has been decreasing. Although genetic predisposition in part determines susceptibility to T2D, an unhealthy diet and physical inactivity are important drivers of the epidemic as T2D continues to increase in prevalence and incidence globally. Certain regions of the world, for example China and India, show a disproportionately high burden (IDF Diabetes Atlas – 10th Edition).

1.1.2.2. Pathogenesis

T2D is associated with insulin resistance, during which insulin is less effective in transducing its glucose-lowering actions. Insulin resistance is initially countered by an increase in insulin production by beta cells to maintain normoglycaemia (Cerf, 2013). However, over time, beta cells fail to release sufficient levels of insulin, resulting in hyperglycaemia and T2D (Figure 1.2). The onset of T2D is slow and difficult to determine due to the lack of acute metabolic disturbances as seen in T1D. Nevertheless, a decline in beta cell function can be detected 10 years before the onset of diabetes (King et al., 1999). Insulin resistance usually begins long before the onset of T2D due to the interaction of several genetic and environmental factors (Stumvoll et al., 2005). The major contributors to the development of T2D are being overweight and obese (Belkina and Denis, 2010; Kahn et al., 2006; Wu et al., 2014), but they could also include high blood pressure, polycystic ovary syndrome and a family history of diabetes, as well as heavy alcohol consumption and smoking (Figure 1.2). In addition, individuals with

T2D are usually present with islet alpha cell dysfunction that results in glucagon secretion under conditions of hyperglycaemia and reduced secretion of prandial glucagon-like peptide 1 (GLP-1) (Nauck et al., 2011). With obesity and T2D reaching epidemic proportions, the development of new treatments is gaining prominence (Dyson, 2010; Leitner et al., 2017; Wilcox, 2005).

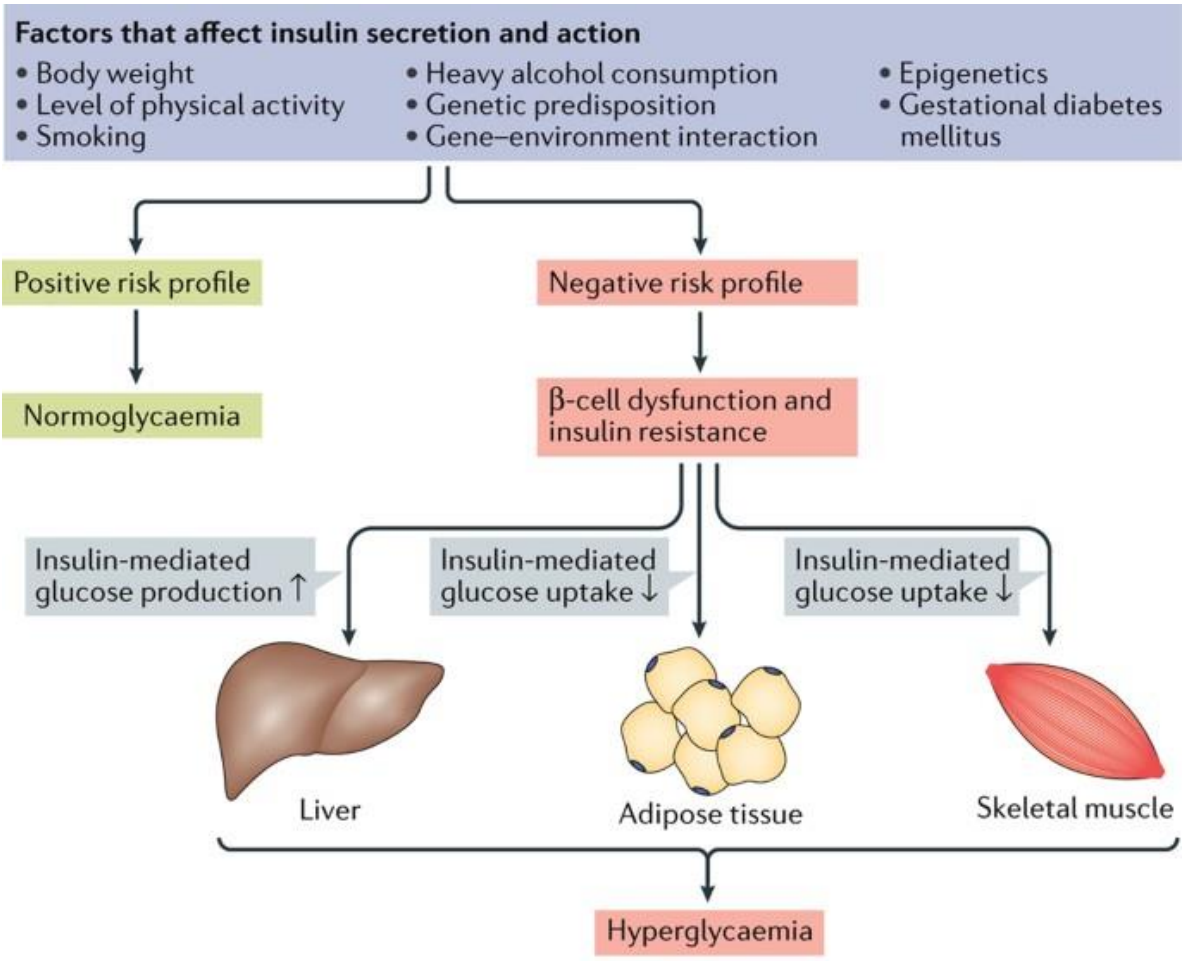

Figure 1.2. Pathophysiology of hyperglycaemia in type 2 diabetes. Insulin secreted from beta cells acts on its target tissues to reduce glucose output by the liver and to increase glucose uptake by skeletal muscle and adipose tissue. Hyperglycaemia develops when beta cell failure and insulin resistance in the peripheral tissues occurs. Some of the factors that affect insulin secretion and insulin action include obesity and genetic predisposition (Zheng et al., 2017).

1.1.2.3. Treatment

Type 2 diabetes is initially managed with diet and exercise. Moreover, weight loss is an effective strategy for reducing the incidence of T2D of those at risk (Feldman et al., 2017). The major treatments include pharmacological interventions for individuals with uncontrolled T2D after lifestyle modifications (Marin-Penalver et al., 2016). Lifestyle changes are often difficult to maintain, but with relevant weight management programmes, remission of T2D can be achieved within a year (Xin et al., 2020). For advanced T2D, differently acting drugs are required at different stages of the disease due to the progressive pathophysiological changes associated with T2D (Kahn et al., 2006) (Figure 1.3). The year of the submission of this thesis marks the 100th anniversary of the discovery of insulin, which has been the first treatment strategy for diabetes. Nowadays, there are several classes of non-insulin antidiabetic drugs available, and the choice of treatment is individualised and based on the risk to benefit ratio (Tahrani et al., 2011).

The prevalence of diabetes imposes extensive research in this area. Approximately 7,000 drug trials are currently registered around the world (Perreault et al., 2021). Among established and widely used pharmacological compounds for the treatment of T2D are GLP-1 analogues, dipeptidyl peptidase 4 (DPP-4) inhibitors and sulphonylureas that target beta cell dysfunction, alpha-glucosidase inhibitors that lower glucose absorption in the intestine, thiazolidinediones and biguanides (mainly metformin) that enhance insulin action, and sodium–glucose cotransporter 2 (SGLT2) inhibitors that increase glucose excretion by the kidneys (Fellner, 2016; Tahrani et al., 2011; Perreaut et a., 2021). In addition to their favourable effects to decrease plasma glucose levels, GLP-1 receptor agonists and SGLT2 inhibitors exert desirable off-target effects, such as weight loss and lowering of blood pressure, and they are not

associated with a risk of hypoglycaemia. In addition, SGLT2 inhibitors reduce the risk of renal and cardiovascular complications, and their use is associated with decreased risk of heart attack and stroke (Zinman et al., 2015), slower progression of kidney disease (Wanner et al., 2016) and decreased risk of kidney failure in people with T2D and nephropathy (Perkovic et al., 2019). These beneficial effects lead to less hospitalisations and decreased mortality due to heart and kidney failure (Gerstein et al., 2019; Hernandez et al., 2018; Marso et al., 2016; Neal et al., 2017; Wiviott et al., 2019; Zinman et al., 2015). Nevertheless, many T2D therapies have a number of side effects, including weight gain (thiazolidinediones) and hypoglycaemia (insulin, sulphonylureas), and therefore potential new treatment targets and novel compounds are being studied. The current goals are to reduce hyperglycaemia, weight gain, as well as cardiovascular and renal complications, and to preserve beta cell mass. Combinations of different agents are often used to target different aspects of T2D, manage blood glucose levels more efficiently and prevent diabetes-related complications. Additionally, to be competitive against the current therapies in use, new agents should exhibit additional features, such as contributing to weight loss, having no increased risk for hypoglycaemia, or being long-acting and decreasing the frequency of use.

New compounds that are currently under investigation include glucokinase activators (GKAs) and agonists of free fatty acid receptor-1 (FFAR1), glucose-dependent insulinotropic polypeptide (GIP) receptor agonists, triple GLP1–GIP–glucagon receptor agonists and agonists of G-protein coupled receptor 119 (GPCR119). These new agents act to increase beta cell function. Other new agents act on the liver to decrease glucose production or increase glucose uptake, and these include glucagon receptor antagonists, antisense oligonucleotide inhibitors and liver-selective GKAs. Lastly, some of the newest

agents that increase insulin sensitivity include fibroblast growth factor 21 (FGF21) analogues, new selective peroxisome proliferator-activated receptor (PPAR) agonists, stimulators of GLUT-4 transporter, NF-κB inhibitors, ghrelin analogues, and more. The mechanisms of action of some novel agents, including imeglimin, are still under investigation (Doupis et al., 2021; Hallakou-Bozec et al., 2021).

Metformin is the first-line medication for the treatment of T2D. However, it was initially used to treat influenza, and only in 1957 was it redirected to lower blood glucose levels. On the other hand, SGLT2 inhibitors, recently introduced to block glucose reuptake into the blood from the renal filtrate in patients with T2D, were initially used to treat infectious diseases, such as malaria. Redirecting known agents to be used in the treatment of different conditions is desired because their safety and side-effects have been already recognised. In addition, there is growing interest in the use of natural anti-diabetic plants in the treatment of T2D, including A. *latifolia* and M. *indica* that inhibit DPP-4 to improve glucose homeostasis (Ansari et al., 2021) or H. *rosa-sinensis* that promotes insulin secretion and blocks digestion of carbohydrates in rodents (Ansari et al., 2020). In this context, fluoxetine, a selective serotonin reuptake inhibitor (SSRI), which is a safe drug commonly used in the treatment of depression and anxiety, has been reported to improve glycaemic management in depressed patients with T2D. Fluoxetine, and other SSRIs: sertraline and paroxetine, were investigated in this thesis and further background information is provided in Section 1.7.

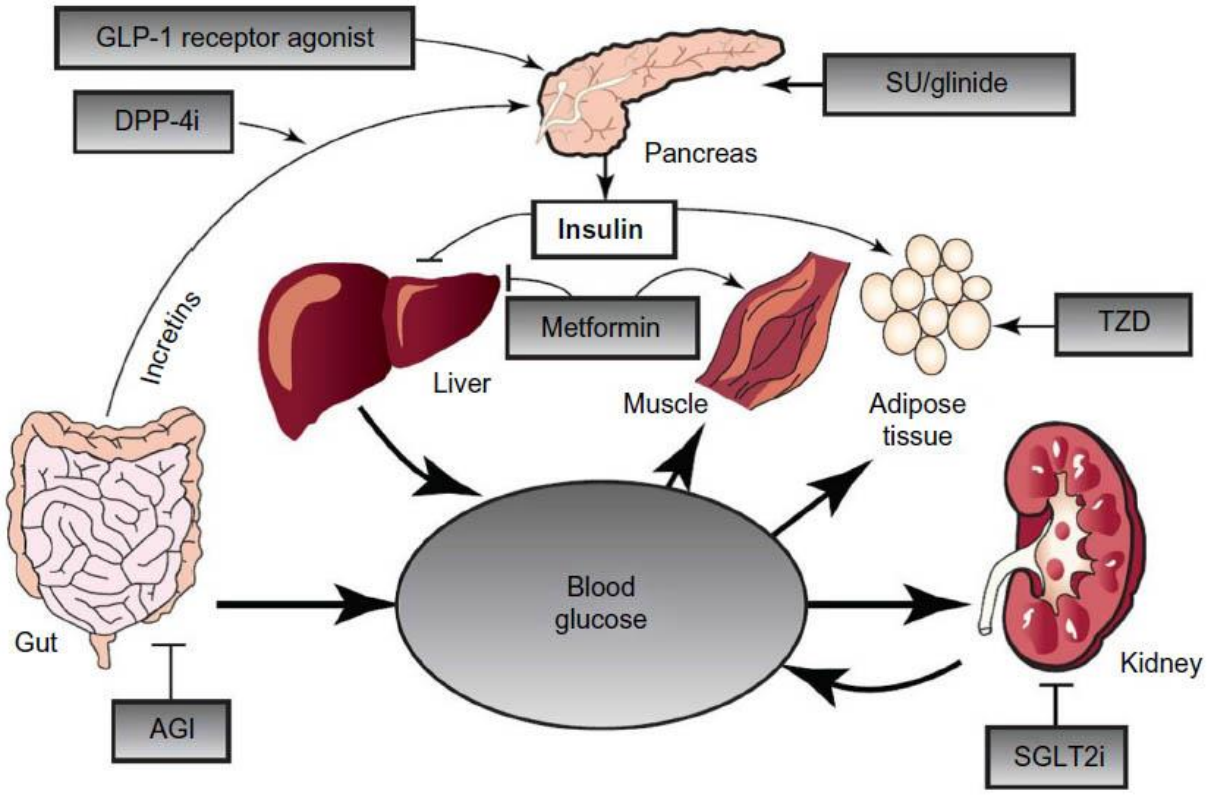

Figure 1.3. Available therapies for T2D. Incretin mimetics (GLP-1 receptor agonists), DPP-4 inhibitors, glinides and sulphonylureas (SU) target impaired insulin secretion, thiazolidinediones (TZD) act by activating PPAR-γ to inhibit insulin resistance, α-glucosidase inhibitors (AGI) act as competitive inhibitors of enzymes required for carbohydrate digestion, metformin reduces hepatic gluconeogenesis by activating AMP-activated protein kinase, and SGLT2 inhibitors block glucose re-uptake into the blood from the renal filtrate in the kidneys (Kuecker and Vivian, 2015).

1.1.3. Gestational diabetes Mellitus

Hyperglycaemia during pregnancy, usually first detected during the second or third trimesters, is classified as gestational diabetes. There are 700,000 pregnancies each year in England and Wales: 5% of these are complicated by hyperglycaemia, of which 87.5% develop gestational diabetes (National Institute for Clinical Excellence, 2015). In the short-term, gestational diabetes has several risks, including pregnancy-induced hypertension, pre-eclampsia, caesarean section and macrosomia (King, 2017; Shakya and Zhang, 2015). What is more, the offspring of women who have had gestational diabetes are at risk of developing T2D in the future (Garcia-Vargas et al., 2012).

1.1.4. Monogenic diabetes

A single genetic mutation in an autosomal dominant gene may lead to monogenic diabetes. It accounts for less than 5% of all diabetes cases (Yang and Chan, 2016). This type of diabetes can be further divided into neonatal diabetes and maturity-onset diabetes of the young (MODY).

Neonatal diabetes is very rare, affecting 1 in 500,000 births (Habeb et al., 2012). It is usually diagnosed in children under 6 months, and it can be confirmed by genetic testing. Neonatal diabetes may result in a number of complications, including developmental delay, such as muscle weakness or learning disability, and epilepsy, depending on the gene mutation. The most common treatment options for this type of diabetes are SU or insulin (Aguilar-Bryan and Bryan, 2008; Nansseu et al., 2016).

MODY is a rare type of diabetes accounting for only 1%–3% of all diabetes cases (Shields et al., 2010), and around 90% of people with MODY are at first mistakenly

diagnosed with other types of diabetes. The most commonly mutated genes in MODY are HNF1-α, HNF4-α, HNF1-β, all carrying a risk of diabetic complications, as well as glucokinase, which does not require treatment because blood glucose is only slightly increased in this type (5.5-8mM) (Urakami, 2019), mainly due to the compensatory action of glucokinase isozymes. Treatment of MODY depends on the mutated gene, but usually SU are used (Urakami, 2019).

1.1.5. Secondary diabetes

Secondary diabetes develops as a result of complications from other pancreas diseases (pancreatitis), endocrine diseases (Cushing's disease), following drug treatment (corticosteroids) or viral infections (Nomiyama and Yanase, 2015). Some forms of secondary diabetes result in a partial loss of pancreatic function that is managed with medications or insulin injections. In some cases, diabetes is permanent and must be managed with insulin injections, as for T1D.

1.1.6. Diabetic complications

When diabetes remains unrecognised or uncontrolled for a prolonged time, the complications of chronic hyperglycaemia may start to develop. Sustained hyperglycaemia and associated metabolic abnormalities can lead to life-threatening health complications (Greenstein and Wood, 2011; King et al., 1999). Complications are very common among people with diabetes, and they are responsible for significant morbidity and mortality. Prevalence of cardiovascular disease and stroke are 10.6% and 1.1%, respectively, while those of diabetic retinopathy, neuropathy, nephropathy and diabetic foot are 26.1%, 62.6%, 50.8%, 2.6%, respectively (Arambewela et al., 2018). In the UK, diabetes is responsible for 530 heart failures and 175 amputations every week (Whicher et al., 2019). The chronic complications of diabetes can be microvascular due to damage to small blood vessels (neuropathy, nephropathy, and retinopathy) or macrovascular due to damage to the arteries (cardiovascular disease and stroke), often resulting from high blood glucose levels (Papatheodoru et al., 2018). On the other hand, diabetic foot syndrome results from a combination of neuropathy, artery peripheral disease and infection, and it is a major cause of lower limb amputation (Tuttolomondo et al., 2015). Other complications of diabetes that do not fall into these categories are dental problems, decreased resistance to infections, as well as birth complications in women suffering from GD (Deshpande et al., 2008), dementia (Cukierman et al., 2005), neuropathy (Thorve et al., 2011) and depression (Nouwen et al., 2011).

As of August 2021, there have been over 211 million confirmed cases of COVID-19, caused by SARS-CoV-2, of which 2.09% have resulted in death (WHO Coronavirus (COVID-19) Dashboard, 2021). In the light of the COVID-19 pandemic, infection has been identified as an important complication of diabetes since people with diabetes have decreased immunity and are more susceptible to infections, including COVID-19 (Holt et al., 2021). People who suffer from both diabetes and COVID-19 have a worse prognosis than individuals who do not have diabetes. Initially, COVID-19 was only considered a lung disease (Zhu et al., 2020), but accumulating evidence suggests that SARS-CoV-2 also affects other organs, including heart, brain and the endocrine organs (Gupta et al., 2020; Puelles et al., 2020; Song et al., 2021; Wichmann et al., 2020), and recent evidence shows that SARS-CoV-2 affects pancreatic function, leading to pancreatitis in 33% of severely ill patients (Geravandi et al., 2021; Muller at el., 2021). What is more, severe COVID-19 has been linked to elevated blood glucose levels and metabolic dysregulation, and COVID-19 patients with T2D present with elevated hyperglycaemia and ketoacidosis (Chen et al., 2020; Ebekozien et al., 2020). Importantly, there is evidence that SARS-CoV-2 can perturb islet beta cell integrity (Muller at el., 2021), but the direct effects of the virus at beta cells are yet to be determined.

1.2. Pancreas

The pancreas is a glandular organ located in the abdominal cavity behind the stomach, with the body near the duodenum and its tail by the spleen. The main pancreatic duct and a smaller accessory pancreatic duct join with the common bile duct near the ampulla of Vater, also known as the hepatopancreatic duct. The intricacy of the pancreas relies on its complex architecture as it is divided into exocrine and endocrine tissues (Jones and Persaud, 2017) (Figure 1.4).

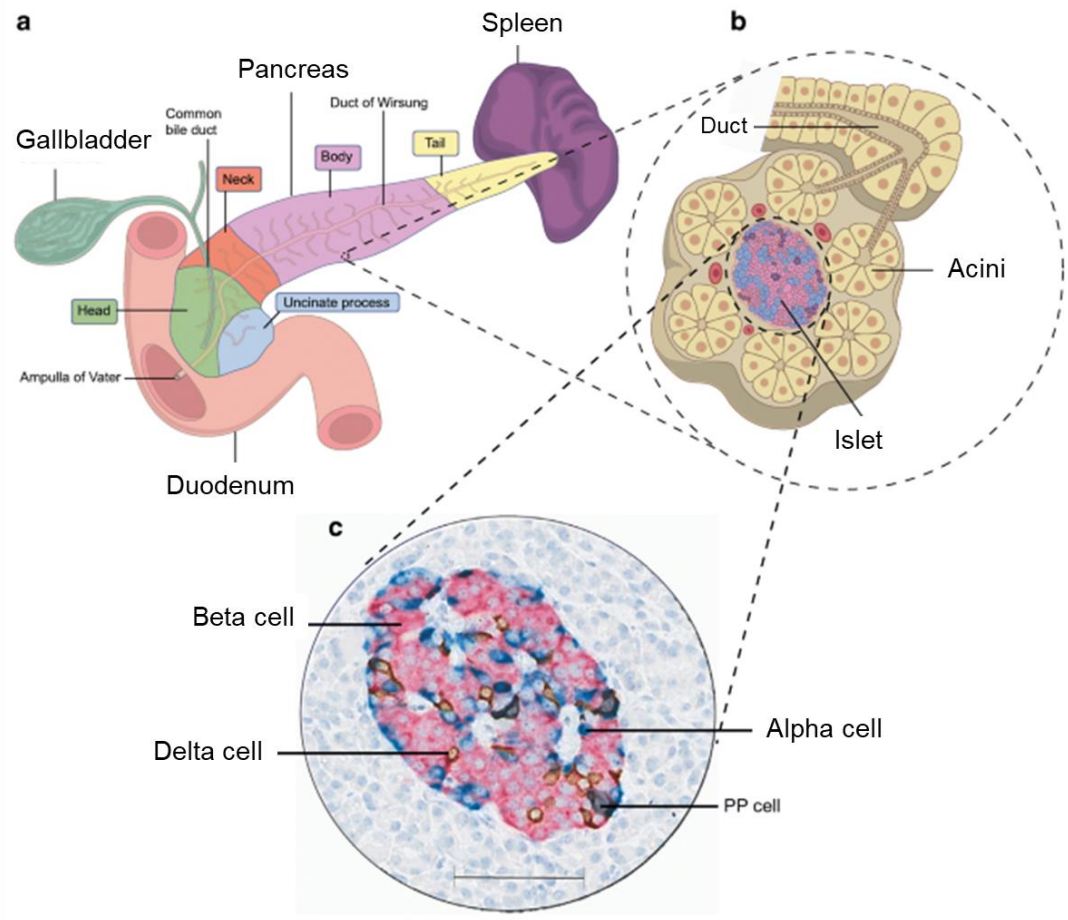

Figure 1.4. Anatomical organisation of the pancreas (a). The exocrine pancreas is composed of a complex of ducts and acinar cells that secrete digestive enzymes (b). The endocrine pancreas is made up of the hormone-releasing cells within the islets of Langerhans: alpha cells (blue), beta cells (pink) and delta cells (red) (Atkinson et al., 2020).

1.2.1. Exocrine pancreas

The majority of the pancreas is composed of the exocrine tissue. The cells with a digestive role form clusters called acini around the small intercalated ducts. The acinar cells secrete proenzymes into the ducts, which drain into larger interlobular ducts and the main pancreatic duct. The inactive enzymes are secreted into the duodenum to protect the pancreas from self-digestion, where they are activated by enterokinase (Pandiri, 2014). The active enzymes produced by acinar cells break down proteins (trypsin), fats (lipase) and carbohydrates (amylase) in the duodenum (Keller and Layer, 2005).

1.2.2. Endocrine pancreas

The cells with an endocrine role form clusters that are distributed throughout the pancreas. The clusters of endocrine cells, so-called pancreatic islets or islets of Langerhans, account for less than 3% of the total organ mass (Jones and Persaud, 2017). The islets are formed when cells of an endocrine fate cluster close to the capillaries during embryonic development to ensure that the produced hormones reach the bloodstream. Each islet cell secretes a different hormone. Endocrine cells within the islets that produce insulin, glucagon and somatostatin are named beta, alpha and delta cells, respectively. Two more cell types that can be found within islets are ghrelin- and pancreatic polypeptide-producing cells (Cabrera et al., 2006).

1.2.3. Species differences in islet architecture

Although the sizes of the islets are comparable (500-700µm), it has been recognised that the cytoarchitecture of islets differs between species (Brissova et al., 2005). Both microscopic and macroscopic anatomies of the pancreas differ between mice and humans. In mice, the pancreas is not as well-defined as in humans, but it is diffusely distributed within the mesentery of the proximal small intestine (Cabrera et al., 2006). The human pancreas is also more richly innervated and vascularised when compared to a mouse pancreas. In mice, beta cells are perfused centre-to-periphery and constitute 60%-80% of the islet cell population. On the other hand, beta cells are equally scattered throughout the human islet and make up 50%-70% of the human islet cell population (Dolensek et al., 2015) (Figure 1.5). The number of islets also differs between species. Mouse pancreas contains 1,000-5,000 islets and only approximately 200-250 islets can be recovered following the isolation procedure, whereas the number of islets in the human pancreas is much higher and can range between 1,000,000 to 15,000,000 islets, each having its own complex anatomy, blood supply, and innervation (Dolensek et al., 2015) (Table 1.1).

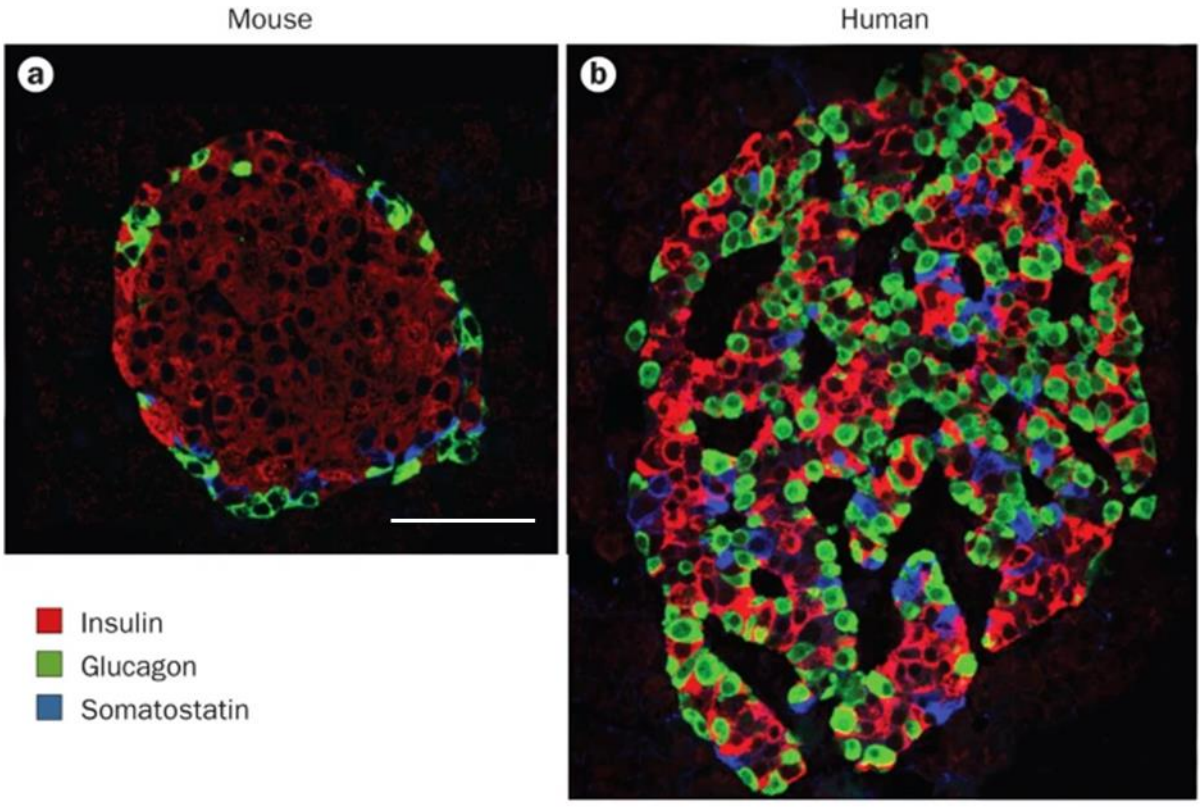

Figure 1.5. Cytoarchitecture of islets from mouse (a) and human (b) adult pancreas. Sections of adult mouse and human pancreases were stained for insulin (red), glucagon (red) and somatostatin (blue). Scale bar = 50µm. Mouse beta cells are located in the core of an islet surrounded by a thin mantle of alpha cells. The section through a human pancreas shows the less organised structure of the human islet where beta cells are intermingled with alpha cells (Cabrera et al., 2006; Wang et al., 2015).

Table 1.1. Differences between the mouse and human pancreas. Adapted from Dolensek et al., 2015.

Scale	Property	Mouse	Human
Organ	Anatomical type	Diffuse/dendritic, lobular, soft	Solitary, compact, firm
Tissue	Diameter of islets	500-700µm	500-700µm
	Number of islets	1,000-5,000	1,000,000-15,000,000
	Location of islets	More random, interlobular	Uniform, intralobular
Cells	% of beta cells	60-80%	50-70%
	% of alpha cells	10-20%	20-40%
	Microarchitecture of islets	Mantle islets predominate	Trilaminar islets predominate
	Sympathetic nerve fibres	Scarce innervation of exocrine tissue, contact with alpha cells and vascular smooth muscle cells	Rich innervation of exocrine tissue, contact with vascular smooth muscle cells
	Parasympathetic nerve fibres	Scarce innervation of exocrine tissue, contact all types of endocrine cells	Rich innervation of exocrine tissue, contact beta and delta cells, possibly alpha cells

1.2.4. Paracrine and autocrine signalling in islets

Hormone secretion is regulated by paracrine and autocrine signalling, as well as the nervous system and presence of glucose and other nutrients, including amino acids and fatty acids (Fu et al., 2013; Rorsman and Braun, 2013). The paracrine and autocrine signalling within islets allows for tight coordination of hormone secretion. Paracrine signalling within the islets involves the effects of somatostatin to decrease (Kailey et al., 2012) and glucagon to increase insulin secretion (Song et al., 2017), whereas autocrine signalling loops include ATP (Bauer et al., 2018) or serotonin that also stimulate insulin release from beta cells (Almaça et al., 2016). Therefore, islets are considered micro-organs with complex signalling networks.

1.2.4.1. Insulin

Islet beta cells are the only site of insulin production in the body, a hormone that is crucial to ensure that blood glucose levels remain within the narrow physiological range of 4-6mM. Insulin is a storage hormone that exerts its metabolic effects on peripheral tissues; muscle (both cardiac and skeletal), fat and liver. Plasma concentrations of insulin increase and decrease during the absorptive and postabsorptive states, respectively (Raju and Cryer, 2005; Wilcox, 2005). The plasma half-life of insulin is short: 4-6 min, as expected from a necessity to respond rapidly to changes in blood glucose levels (Hulse et al., 2009).

Insulin secretion is mainly stimulated by glucose that enters beta cells through the glucose transporter GLUT-2 in rodents or GLUT-1, -2 and -3 in humans (McCulloch et al., 2011), where it is converted to glucose-6-phosphate by glucokinase and further metabolised in the cytoplasm and mitochondria.

Oxidative metabolism of glucose in the mitochondria leads to an increase in the ATP:ADP ratio in the cytoplasm, which in turn results in closure of ATP-sensitive potassium channels (K_{ATP}) and reduction of potassium ion efflux. Plasma membrane depolarisation induces voltage-dependent calcium channels (VDCC) to open and allow calcium ions influx. This increase in intracellular calcium ion concentration promotes fusion of insulin-containing vesicles with the plasma membrane, the process dependent on SNARE proteins in the presence of calcium ions (Xiong et al., 2017).

Glucose-stimulated insulin secretion occurs in a biphasic fashion, meaning that an immediate insulin release is followed by a continuous release of both previously stored and newly synthesised insulin. Insulin storage supports high specialisation of beta cells to release insulin rapidly in response to an appropriate signal (Greenstein and Wood, 2011). Moreover, as mentioned in Section 1.2.4, insulin release can be affected by the paracrine and autocrine signalling within the islets, as well as the autonomic nervous system, adrenaline from adrenal glands, and various gastrointestinal hormones (Fu et al., 2013; Henquin, 2021).

1.2.4.2. Glucagon

Another important islet hormone is glucagon that is produced and secreted by alpha cells, which are electrically excitable like beta cells. At low glucose concentrations, alpha cells depolarise. Voltage-gated Na^+ channels and Ca^{2+} channels contribute to the upstroke of action potentials (Aps). The discharge of high-voltage Aps opens VDCC to allow the influx of extracellular calcium ions into the cytosol. This provides calcium signals that trigger glucagon granule exocytosis. When the blood glucose levels increase, glucagon secretion is

suppressed, which is likely to be through the reduction of P/ Q-type Ca^{2+} channel activity in alpha cells (Briant et al., 2016; Gaisano et al., 2012).

Glucagon is secreted from alpha cells when plasma glucose concentration falls below 5mM, and it exerts opposite effects to insulin (Lund et al., 2016; Miyachi et al., 2017). The main function of glucagon is to increase blood glucose concentration to prevent hypoglycaemia, primarily through inactivation of glycolysis and activation of glycogenolysis and gluconeogenesis in the liver (Unger and Cherrington, 2012). In addition, glucagon decreases fatty acid synthesis in adipose tissue and regulates the rate of glucose production by promoting lipolysis (Habegger et al., 2010). Under certain physiological conditions, glucagon stimulates the production of ketone bodies in the liver, which substitute partially for glucose in meeting the brain's energy requirements during fasting. Glucagon and insulin form a feedback system and act simultaneously to maintain glucose levels within the desired range (Bich et al., 2020) (Figure 1.6).

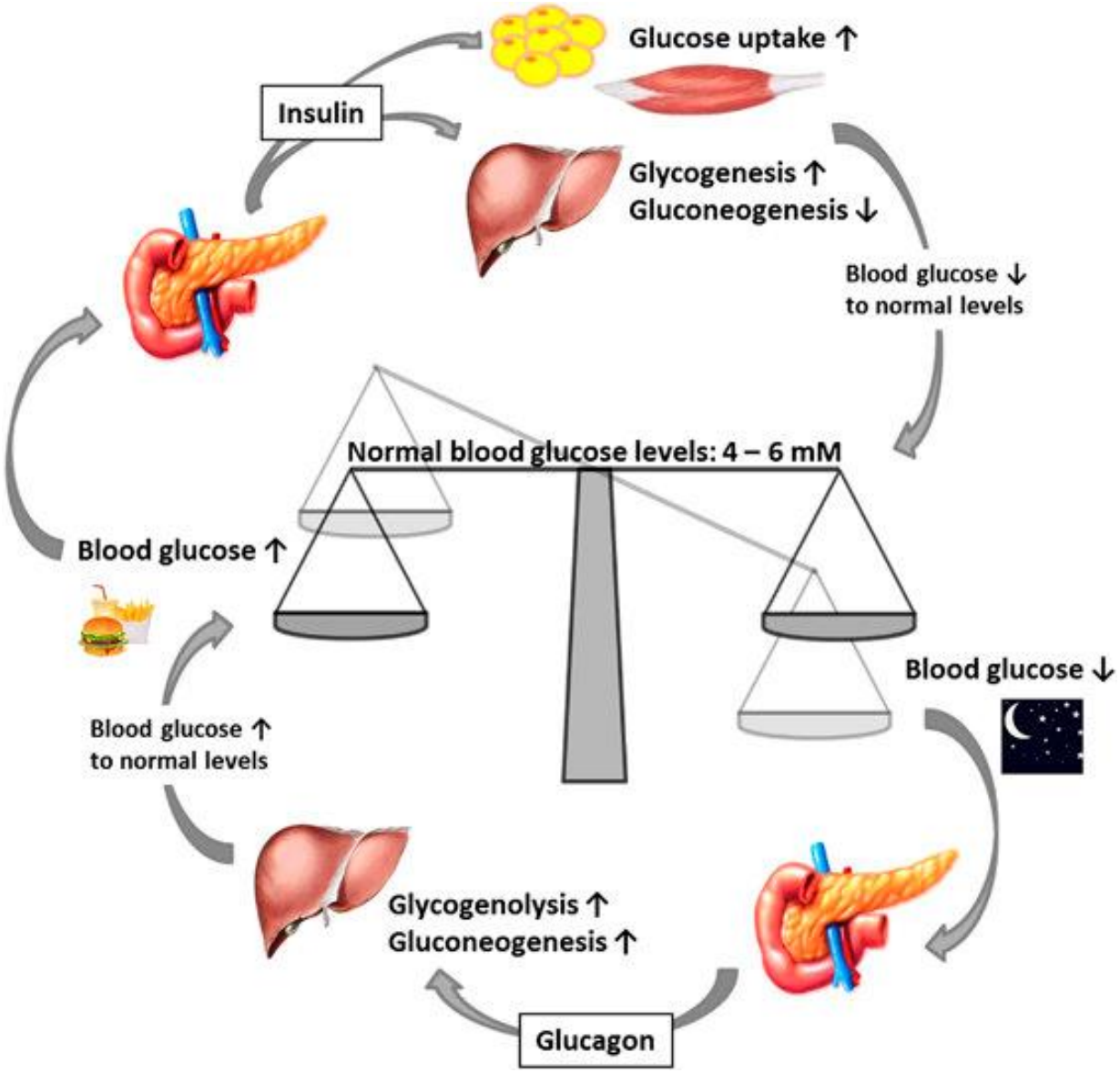

Figure 1.6. Maintenance of blood glucose levels by glucagon and insulin. When blood glucose levels decrease, the islet alpha cells secrete glucagon, which increases endogenous blood glucose levels, for instance, through glycogenolysis. Following food intake, when blood glucose levels increase, insulin is secreted from beta cells to trigger glucose uptake into insulin-dependent muscle and adipose tissues as well as to promote glycogenesis in the liver (Roder et al., 2016).

1.2.4.3. Serotonin

Among a plethora of paracrine and autocrine signals in islets, serotonin presents several unique features. Serotonin (5-hydroxytryptamine, 5-HT) is a bioamine derived from tryptophan through hydroxylation by the enzyme tryptophan hydroxylase (TPH) and decarboxylation by aromatic acid decarboxylase (AADC). Although whether serotonin crosses the blood-brain barrier is still under investigation (Berger et al., 2009; El-Merahbi et al., 2015; Riggio et al., 2021; Robinson, 2009; Young et al., 2016), total body serotonin can be divided into two major pools: brain serotonin and peripheral serotonin. TPH1 is mainly expressed in the periphery, whereas TPH2 is predominant in the brain (El-Merahbi et al., 2015). Interestingly, beta cells express both TPH1 and TPH2, and secrete serotonin in paracrine and autocrine manners. What is more, beta cells share common developmental features with serotonergic neurons. The similarities in the biology of these cell types have important implications for the pathology and treatment of mental and metabolic diseases (Ohta et al., 2011).

There are fourteen subtypes of receptors through which serotonin impacts its target cells leading to different cellular responses, and several serotonin receptors are expressed by beta cells (Darmon et al., 2015) (Figure 1.7). All receptors for serotonin are either stimulatory or inhibitory G-protein coupled receptors (GPCRs; Section 1.3.2), except for the 5-HT3 subtype (Ohara-Imaizumi et al., 2013). The 5-HT1 receptors (1A, C, D, E, and F) are coupled to the $G\alpha i$ protein that inhibits adenylate cyclase, thus inhibiting cAMP formation. The 5-HT2 receptors (2A, B, and C) are $G\alpha q$ protein-coupled and activate phospholipase C (PLC), which results in inositol (1,4,5)-trisphosphate (IP_3) and DAG formation and Ca^{2+} release from the intracellular stores, whereas the 5-HT3 receptors (3A, B, C, D, and F) are ligand-gated ion channels. The 5-HT4, 6, and 7 receptor families

couple to the Gαs protein that is linked to cAMP formation. The downstream signalling to 5-HT5 receptors remains unclear. In addition, intracellular serotonin can bind to small GTPases, in a process known as serotonylation, and through serotonylation of small GTPases involved in insulin granule exocytosis, it promotes insulin release in a receptor-independent manner (El-Merahbi et al., 2015; Paulmann et al., 2009). Serotonin is taken up into the cells by the serotonin transporter or packed into secretory vesicles by the vesicular monoamine transporter 2, reused or catabolised by the enzyme monoamine oxidase (MAO) (Cataldo Bascunan et al., 2017). There is evidence that serotonin receptors are expressed in rodent and human islets, and the level of their expression changes under different physiological conditions such as pregnancy (Kim et al., 2010).

Serotonin is released together with insulin in a glucose-dependent manner in non-diabetic and non-pregnant individuals, and there is evidence that serotonin shapes the secretory profile of the beta and alpha cells, and hence helps to orchestrate islet hormone secretion (Almaca et al., 2016; Cataldo Bascunan et al., 2017). Interestingly, during physiological challenges, such as pregnancy, when the energy requirements of the foetus impose changes in maternal metabolism, serotonin increases responsiveness to glucose and drives beta cell mass expansion downstream of the lactogenic hormones (Kim et al., 2010). There is evidence that human beta cells produce and secrete serotonin under normal physiological conditions, which in turn acts in an autocrine or paracrine manner to drive beta cell proliferation and insulin secretion by activating 5-HT2 and 5-HT3 receptors, or by binding to GTPases in response to high glucose (Almaca et al., 2016; Paulmann et al., 2009; Robinson, 2009).

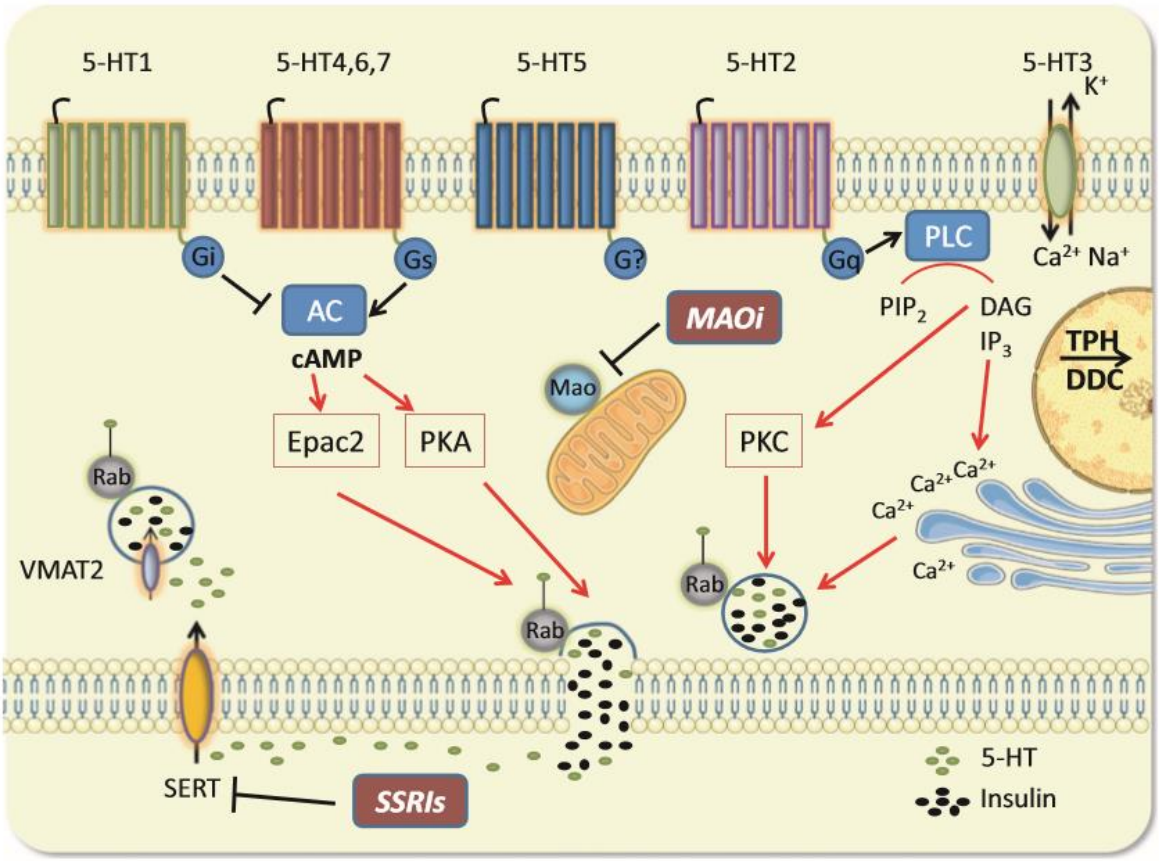

Figure 1.7. Serotonin signalling in beta cells. The 5-HT1 receptors couple negatively via Gαi, 5-HT2 receptors are Gαq protein-coupled, whereas 5-HT3 receptors are ligand-gated ion channels. The 5-HT 4, 6 and 7 receptor families are coupled to Gαs, but the signalling downstream of the 5-HT5 receptors is unclear. Intracellular serotonin binds to small GTPases to stimulate insulin granule exocytosis and extracellular serotonin enters the cell via SERT or is loaded into secretory vesicles by VMAT2 to be reused or catabolised by MAO (Cataldo Bascunan et al., 2017).

1.2.4.4. Dopamine

In the brain, the dopaminergic pathways control motor coordination, motivation, reward, and working memory (Luo and Huang, 2016; Schultz, 1998). Dysfunction of the dopaminergic neurons can cause Parkinson's disease and schizophrenia (SCZ) (Iversen and Iversen, 2007). In addition to these functions in the brain, and as serotonin, dopamine acts outside the nervous system where it is synthesised by, and released from peripheral tissues, including the endocrine pancreas. Peripheral dopamine does not cross the blood-brain barrier, but it exerts autocrine and/or paracrine role in the islets. Although the precise role of dopamine in beta cells has been controversial, there is now strong evidence that dopamine is synthesised in the islets, and it plays a role in modulating hormone secretion. Dopamine may induce changes in insulin secretion through stimulation of Gαi-coupled D2 receptors.

Dopamine receptors are GPCRs (Section 1.3.2), and they include 5 subtypes: D1, D2, D3, D4, and D5. The D1 and D5 receptors usually display a stimulatory function on adenylate cyclase activity, and they are classified as D1-like receptors. On the other hand, the D2, D3, and D4 receptors interact with Gαi proteins and show inhibitory function on adenylate cyclase activity. They are classified as D2-like receptors and are found in beta cells (Rubi et al., 2005; Ustione et al., 2013), and it has been shown that exogenous dopamine inhibits glucose-stimulated insulin secretion from beta cells via D2 receptors (Rubi et al., 2005; Zhang et al., 2015). Although islets are richly innervated and there are peripheral sources of dopamine in the body (Goldstein et al., 2003; Eisenhofer et al., 2005), there is evidence that dopamine is stored in beta and alpha cells and it is co-secreted with insulin and glucagon, and it acts in an autocrine and paracrine manner on these cells to inhibit hormone secretion (Aslanoglou et al., 2021) (Figure 1.8).

Interestingly, expression of the dopamine transporter has been confirmed for both mouse and human beta cells (Simpson et al., 2012; Ustione et al., 2013).

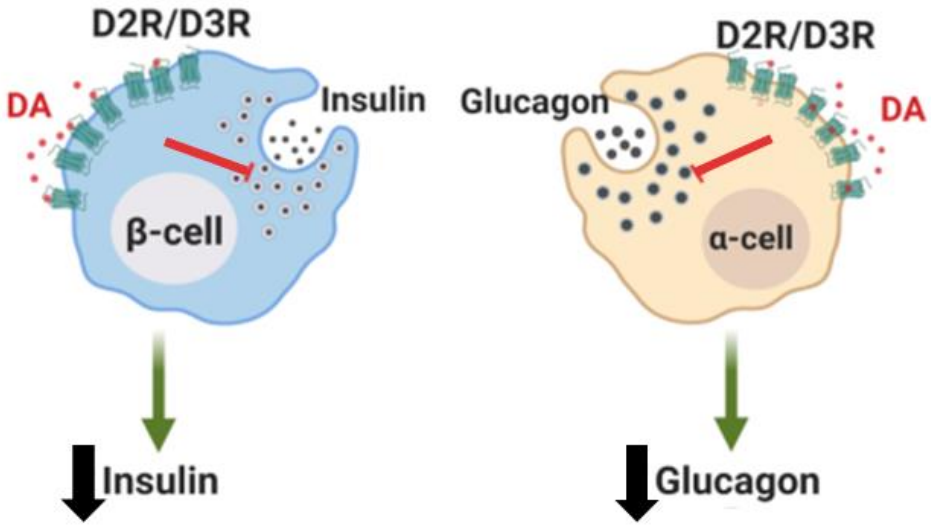

Figure 1.8. Negative feedback of dopamine regulating insulin and glucagon secretion from beta cells and alpha cells, respectively. Beta and alpha cells express the molecular machinery for dopamine synthesis, release, and storage. The dopamine D2-like receptors mediate the inhibition of insulin and glucagon secretion. Adapted from Aslanoglou et al., 2021.

1.3. Regulation of insulin secretion

Insulin secretion is controlled by nutrients (glucose, amino acids, fatty acids) and non-nutrients (e.g., islet hormones, neurotransmitters) to ensure that circulating levels of insulin are appropriate for the current metabolic state (Fu et al., 2013; Jones and Persaud, 2010).

1.3.1. Regulation of insulin secretion by nutrients

Islet beta cells respond to minor changes in extracellular glucose levels. The model for insulin secretion has its origin in the pioneering work of Dean and Matthews (Dean and Matthews, 1968) who, based on the electrophysiological nature of islet beta cells, recorded electrical activity in beta cells for the first time. Nutrient-stimulated insulin secretion involves three distinct components: an initial peak (first phase) triggered by Ca^{2+}, increase in the Ca^{2+}-triggered response (second phase), and a memory that continues with a decrease in circulating nutrients (time-dependent potentiation) (Henquin et al., 2002). The first phase is initiated by ATP derived from glucose metabolism, which leads to membrane depolarisation following closure of K_{ATP} channels and the consequent influx of extracellular calcium ions (Figure 1.9). The elevations of intracellular Ca^{2+} trigger the release of a small pool of secretory granules, resulting in the initial peak of the insulin response (Straub and Sharp, 2002). This is followed by a sustained second phase of insulin release that lasts as long as the nutrients are present in the circulation. The second phase is facilitated through an augmentation of the Ca^{2+}-dependent first phase response. Time-dependent potentiation does not require the continuous presence of glucose and is largely independent of calcium ions, and interestingly, it is only present in certain species such as humans and rodents (Berglund, 1987).

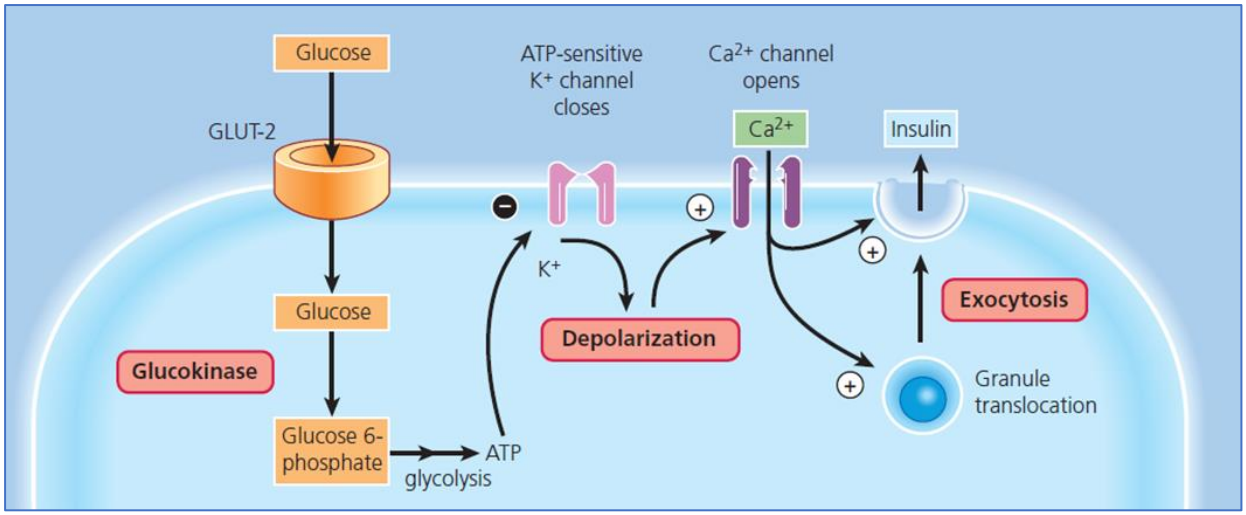

Figure 1.9. Schematic illustration of intracellular mechanisms of glucose-stimulated insulin secretion. Glucose is metabolised to generate ATP, which in turn closes ATP-sensitive K^+ channels, which prevents potassium ions from leaving the cell causing membrane depolarisation, which in turn opens VGCC in the membrane and allows calcium ions to enter the cell. The increase in intracellular calcium triggers insulin granule exocytosis (Jones and Persaud et al., 2017).

1.3.2. Regulation of insulin secretion by non-nutrients

The responses of beta cells to nutrients can be amplified or inhibited by various hormones and neurotransmitters. During normoglycaemia, these agents do not affect insulin secretion to ensure that insulin is not secreted in the absence of nutrients and to prevent hypoglycaemia. Many potentiators (e.g., acetylcholine, serotonin) and inhibitors (e.g., adrenaline; somatostatin) of glucose-stimulated insulin secretion act through GPCRs (Ahrén, 2009; Atanes and Persaud, 2019) that are composed of a single polypeptide chain that crosses the plasma membrane seven times and signals through heterotrimeric G-proteins physically associated with the receptors (Figure 1.10). Upon ligand binding, each GPCR undergoes conformational changes that allow it to act as a guanine-nucleotide exchange factor (GEF) on α-subunits of G-proteins. The exchange of GDP to GTP on α-subunits promotes dissociation of β/γ complexes, which regulate the generation of second messengers that act on effector enzymes.

There are several identified G-proteins. Gαs activates adenylyl cyclase (AC) that catalyses the conversion of ATP to cAMP, which in turn activates protein kinase A. On the other hand, activated Gi inhibits AC to decrease cAMP production, and hence inhibit PKA activity. Gαq stimulates phospholipase C activation to cleave phosphatidylinositol (4,5)-bisphosphate (PIP_2) into DAG and IP_3. IP_3 opens IP_3 - gated calcium ion channels in the endoplasmic reticulum (ER), leading to a subsequent increase in Ca^{2+} concentration in the cytosol. This allows translocation of protein kinase C to the plasma membrane, where it is activated by DAG. Therefore, the effect of an agent on insulin secretion depends on the nature of its receptors.

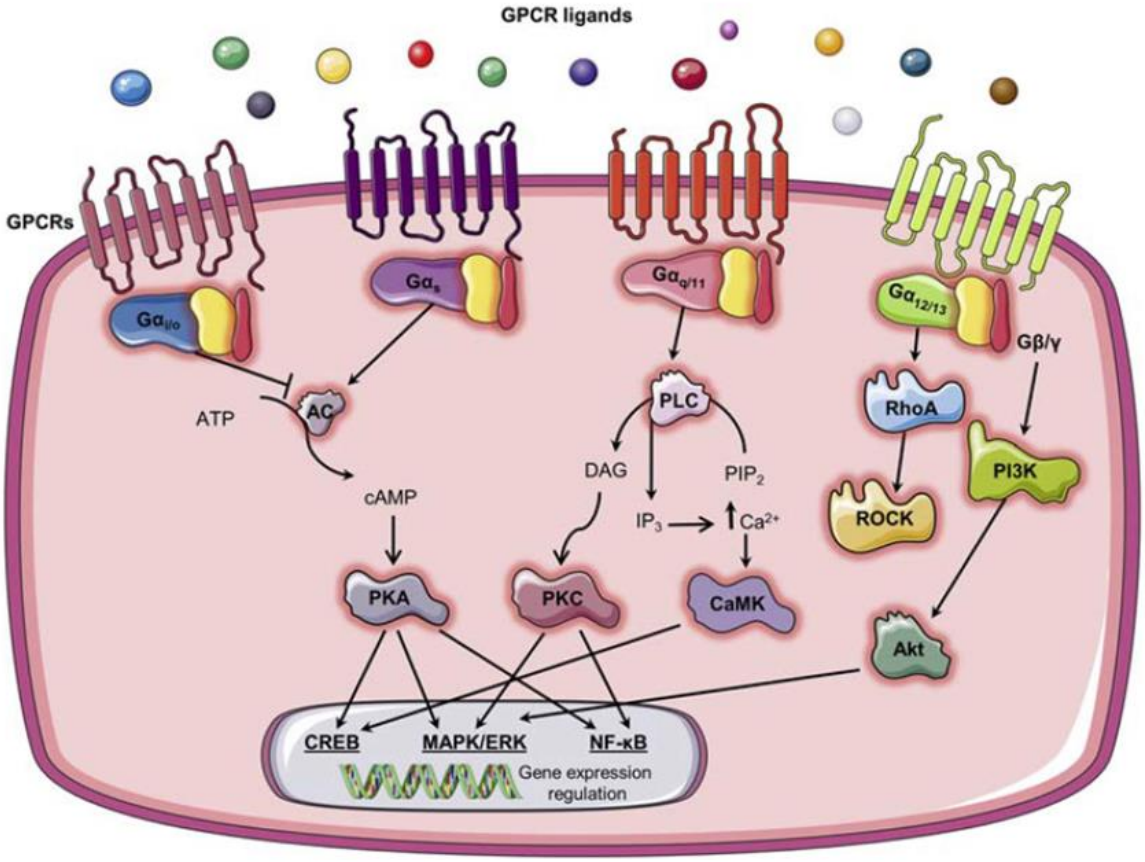

Figure 1.10. Different types of G-protein coupled receptors (GPCRs) and their downstream signalling. GPCRs are membrane-bound receptors that can be coupled to different G-proteins and have either stimulatory or inhibitory effects on the cell. GPCRs undergo conformational changes following ligand binding, which allow the Gα subunits of the heterotrimeric GTP-binding proteins to exchange GDP for GTP and dissociate their β/γ complexes. The Gαs and Gαi/o subunits activate or inhibit AC, respectively, which result in changes in cAMP levels. Gαq/11 activates PLC-mediated hydrolysis of PIP_2 to DAG and IP_3. IP_3 mobilises calcium ions from the ER. Calcium ions, in turn, activate the calcium-calmodulin-dependent protein kinases (CaMK). On the other hand, cAMP activates PKA kinase, and DAG activates PKC, resulting in phosphorylation of serine and threonine protein residues that leads to exocytosis of insulin granules from beta cells (short-term effect) or changes in gene expression (long-term effect). Activation of Gα12/13-coupled receptors regulate actin cytoskeletal remodelling. Gβ/γ can activate PI3K, which results in activation of Akt. Akt stimulates GLUT4 translocation in peripheral cells or drives fuel storage through modulation of gene expression (Atanes and Persaud, 2019).

1.4. Regulation of beta cell mass

Beta cell mass is defined as the balance between beta cell proliferation, neogenesis, hypertrophy, and apoptosis. Beta cell mass expands in response to various physiological challenges, such as pregnancy or obesity, whereas beta cell dysfunction and reductions in beta cell mass have been broadly recognised as critical determinants of the development of T2D. There is evidence that the total islet number is 30% lower in patients with T2D (Cho et al., 2010; Westermark and Wilander, 1978), individuals with T2D also have deficits in relative beta cell volumes by 63% (Butler et al., 2003), and beta cell mass is decreased by 39% in those patients when compared to healthy individuals (Rahier et al., 2008).

Reductions in beta cell number are associated with increased apoptosis rather than insufficient replication or neogenesis of beta cells (Bouwens and Rooman, 2005; Cho et al., 2010). Many cell types, such as hepatocytes, which have been damaged, can easily regenerate (Michalopoulos, 2017). However, the regenerative capacity of beta cells is very limited in the absence of a major stimulus (Docherty and Sussel, 2021). This is due to the limited capacity of beta cells to proliferate and low replication rates both in rodents and humans.

In obesity, as peripheral insulin resistance develops, beta cell mass increases through proliferation, neogenesis, and/or hypertrophy to compensate for an increased demand for insulin and to maintain normoglycaemia. Although increased insulin secretion in hyperglycaemia can have autocrine effects to reduce beta cell apoptosis and promote proliferation, sustained high demand for insulin can lead to beta cell apoptosis through glucose and lipid toxicity, chronic inflammation, and increased oxidative stress (Cho et al., 2010; Sakuraba et al., 2002). Beta cell dysfunction and reductions in beta cell mass result in an uncompensated phase and hyperglycaemia (Figure 1.11). If uncontrolled, this

uncompensated phase can further progress to an accelerating phase that is accompanied by severe beta cell loss through fibrosis, amyloidosis, and increased beta cell toxicity. What is more, with decreases in beta cell number, an increase in alpha cell mass could intensify hyperglycaemia resulting in worsening of T2D and diabetic complications (Cho et al., 2010).

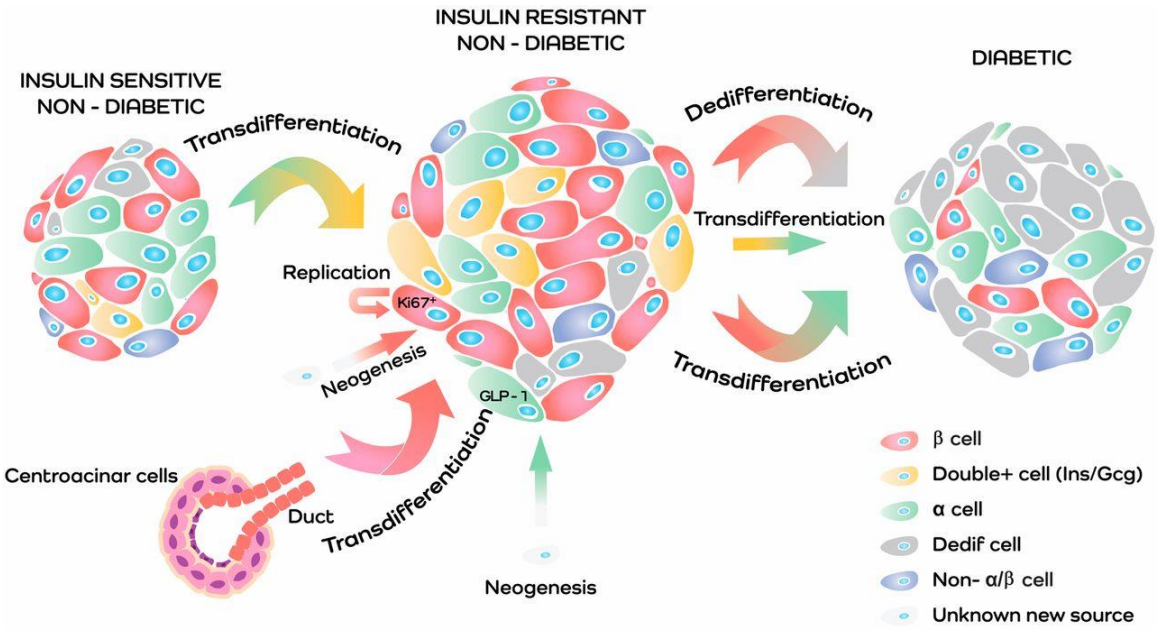

Figure 1.11. Hypothesis for morphological alterations and plasticity of islets according to different physiological conditions. In the initial phases of T2D development, as insulin resistance increases insulin demand, beta cell mass expands through beta cell replication, neogenesis, transdifferentiation (from exocrine cells or alpha cells), and hypertrophy, to maintain a compensatory phase. A sustained increase in insulin demand could lead to beta cell apoptosis through nutrient toxicity, dedifferentiation of overstressed beta cells (dedif), chronic inflammation and increased oxidative stress, resulting in reduced beta cell mass and an uncompensated phase. Severe beta cell loss may progress through increased fibrosis and amyloid formation (Mezza et al., 2019).

1.4.1. Apoptosis

Apoptosis, referred to as programmed cell death, is an important feature of diabetes (Figure 1.12). In T1D, beta cells are destroyed by an autoimmune attack, whereas abnormally elevated metabolic factors drive beta cell apoptosis in T2D. Apoptosis of beta cells can be additionally induced by several signals, such as nutrient toxicity, proinflammatory cytokines, amyloid deposition, and/or fibrotic destruction (Cnop et al., 2005).

Beta cell destruction is an important etiological factor in the progression of T2D. The main mechanism underlying reductions in beta cell mass is increased apoptosis rates of beta cells. Therefore, therapeutic approaches to inhibit apoptosis could be an important development in the treatment of T2D (Butler et al., 2003; Donath et al., 2005).

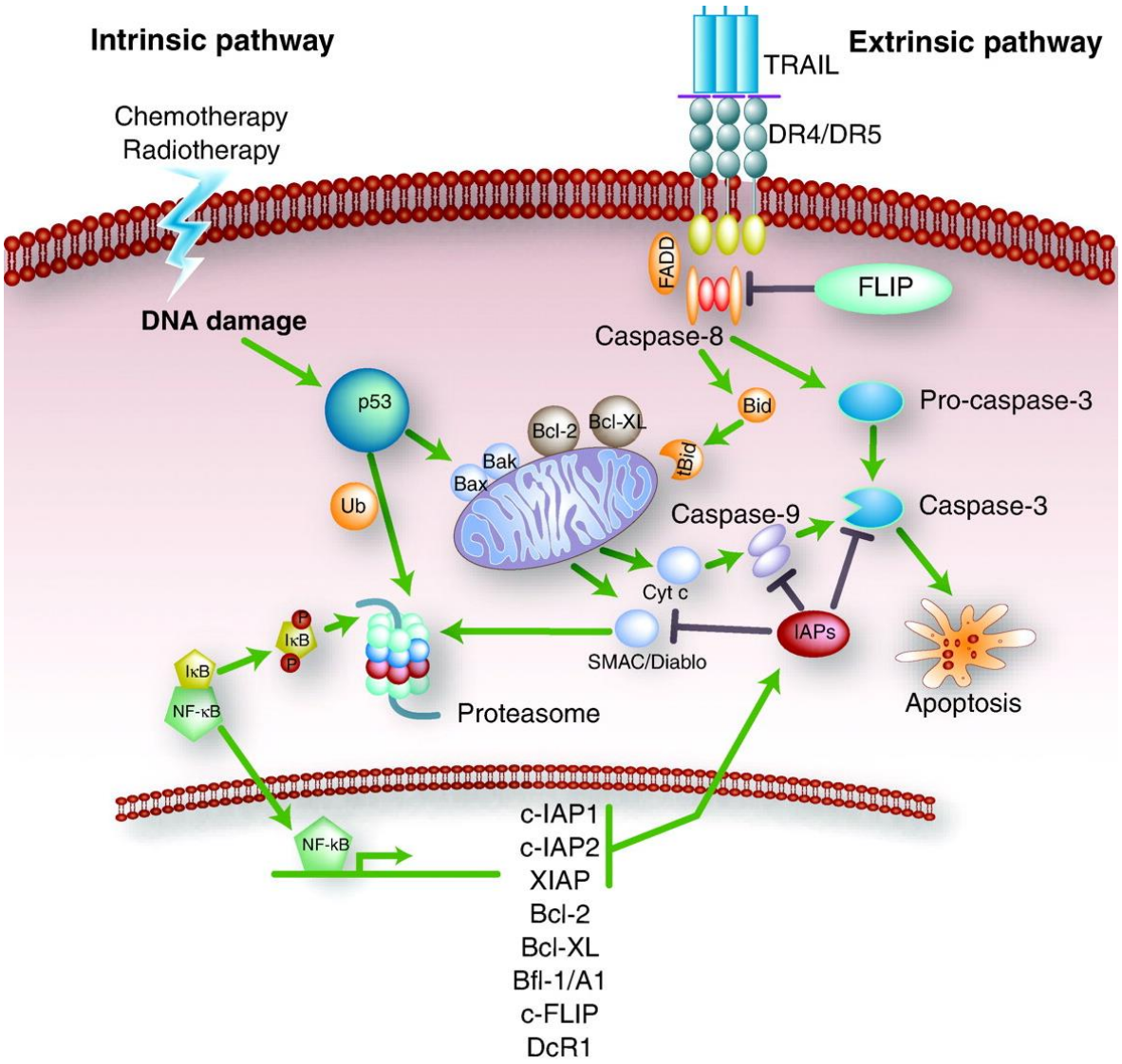

Figure 1.12. Schematic representation of the apoptotic pathway. Apoptosis is induced via the death receptor and can lead to activation of the extrinsic and intrinsic pathways. → means activation; ⊣ means inhibition (de Vries et al., 2006). The intrinsic apoptosis pathway is often triggered by p53 as a result of DNA damage. In the intrinsic pathway, the death signal reaches mitochondria, leading to release of cytochrome c from mitochondria, which binds to Apaf1 (not shown). Cytochrome c/Apaf1 forms a complex with pro-caspase 9 to activate caspase 9, which in turn promotes caspase 3 activation, leading to cell death. On the other hand, the extrinsic pathway is initiated through tumour necrosis factor receptors. These receptors activate pro-caspases 8 and 10 by recruiting the endogenous adaptor protein FADD. Pro-caspases 8 and 10 cleave themselves to form activated caspase 8 or 10. Effector enzymes, such as caspases 3, 6, 7, are activated in this cascade to facilitate apoptosis (Ghavami et al., 2014).

1.4.1.1. Chronic inflammation

Islets in obesity and T2D could be a target of inflammation leading to tissue damage and impaired beta cell function (Figure 1.13; Figure 1.14). Inflammation is characterised by the infiltration by the immune cells, activation of local tissue immune cells, and local production of cytokines and chemokines. The insulitis (inflammation of the islets) may be involved in beta cell compensation for insulin resistance, but if the inflammation becomes chronic, beta cells lose their function and undergo apoptosis leading to decreased beta cell mass (Donath et al., 2005). In contrast to T1D, the dominant immune cell type involved in islet inflammation in obesity and T2D is the macrophage. There is evidence that they play a key role in mouse and human islet inflammation that is seen in obesity and T2D (Ehses et al., 2007; Richardson et al., 2009; Ying et al., 2020), and that activation of the immune system is linked to T2D progression (Tsalamandris et al., 2019). In those cases, macrophages switch phenotype from anti-inflammatory M2-type to proinflammatory M1-type, which plays a key role in the initiation and amplification of islet inflammation (Sell et al., 2012; Tsalamandris et al., 2019). The increased macrophage accumulation in islets results from proliferation of resident macrophages and macrophage infiltration. Macrophages promote beta cell hyperplasia through signals, such as platelet-derived growth factor, and they impair beta cell function (Ying et al., 2020).

There is evidence that patients with T2D express elevated levels of IL-1β and several chemokines (Miras and le Roux, 2014), and inflammasome/IL-1β signalling is the most common high-impact pathway activated in islets (Cavelti-Weder et al., 2012; Grant and Dixit, 2013). Tumour necrosis factor α (TNF-α) also has an important role in islet inflammation (Tilg and Moschen, 2008). High levels of TNF-α produced in adipose tissue induce inflammation and insulin resistance,

as well as islet beta cell death (Rosenvinge et al., 2007; Ruan and Lodish, 2002). The inflammatory state in T2D, mediated via production of proinflammatory cytokines, is augmented by adipokines that stimulate additional inflammatory responses in obesity, and promote obesity-induced metabolic and cardiovascular diseases (Takaoka et al., 2009).

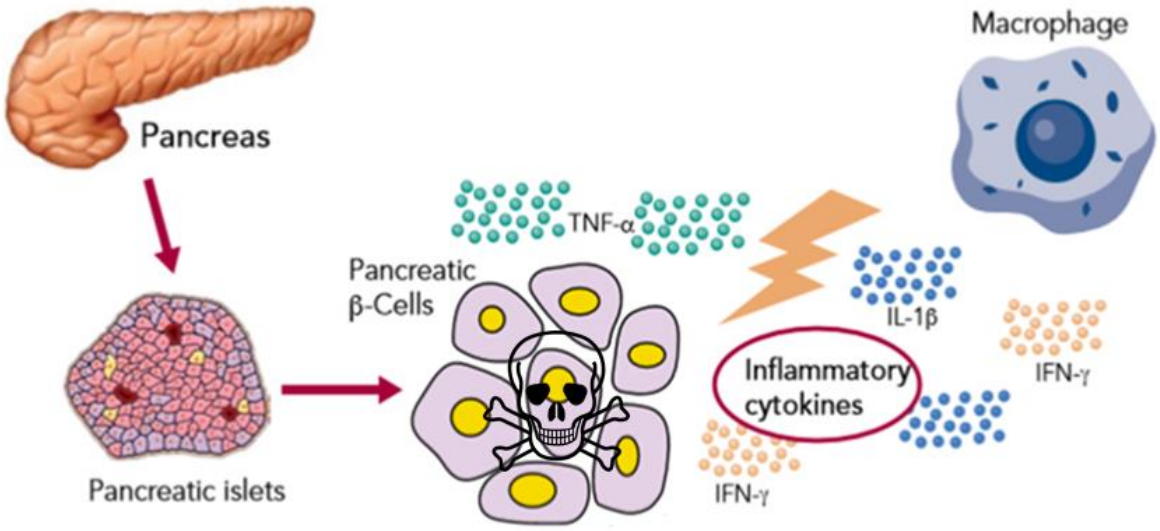

Figure 1.13. Inflammation has a key role in the pathophysiology of T2D and is linked to metabolic abnormalities. The presence of M2-type macrophages and proinflammatory cytokines, including IL-1β, TNF-α and IFN-γ, promote islet cell death and this is linked to metabolic abnormalities in T2D. Adapted from Tsalamandris et al., 2019.

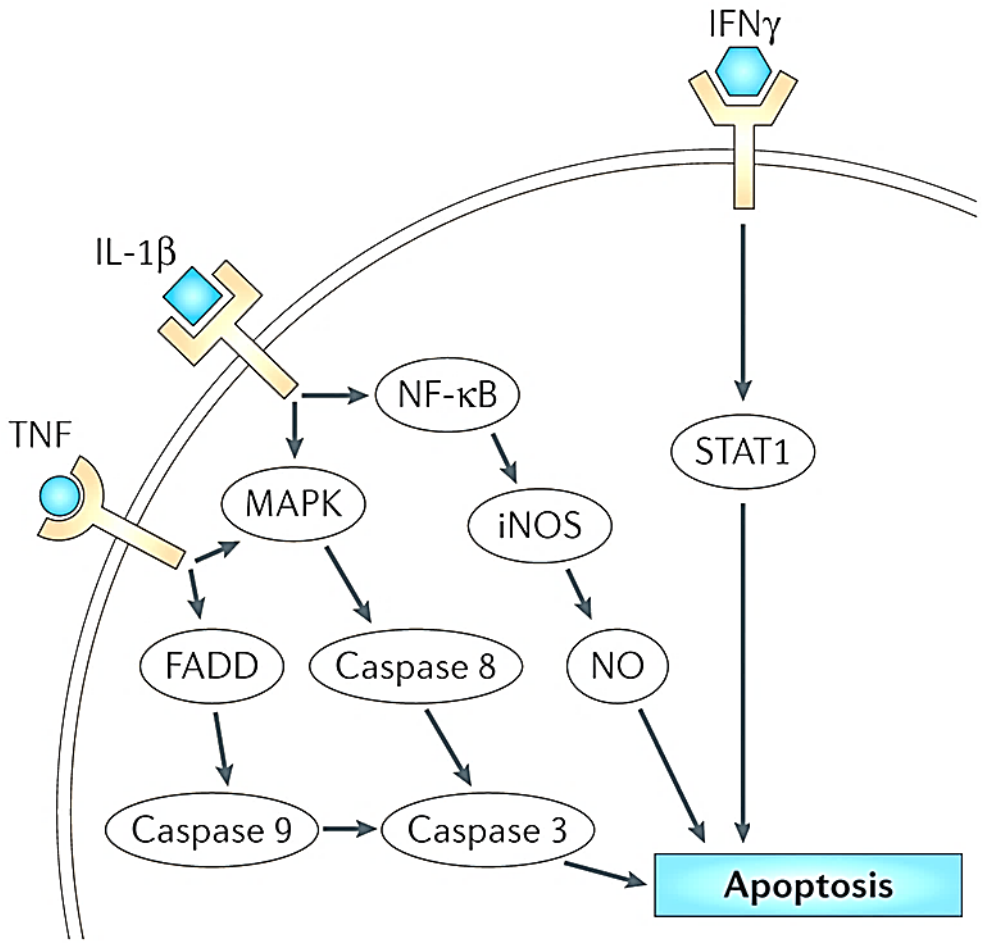

Figure 1.14. Signalling pathways involved in cytokine-induced apoptosis of beta cells. Proinflammatory cytokines, IL-1β, IFN-γ, and TNF-α induce apoptosis in beta cells via factor-κB (NF-κB) and the STAT1 pathway or by activating caspases 3, 8, and 9, which result in apoptosis (Vetere et al., 2014).

1.4.1.2. Amyloid deposition and fibrotic destruction of beta cells

Among factors that stimulate islet macrophages to secrete IL-1β is islet amyloid polypeptide (IAPP), or amylin, which is secreted by beta cells (Kamata et al., 2014). Some studies show no relationship between amyloid deposits and the duration of T2D (Sempoux et al., 2001), whereas others link IAPP deposits with beta cell apoptosis, reductions in beta cell mass, and beta cell dysfunction (Bernard-Kargar and Ktorza, 2001; Kahn et al., 1999). Moreover, human amyloid has been shown to be toxic to beta cells (Janson et al., 1999) and to contribute to reductions in beta cell mass both in rodents and humans (Lorenzo et al., 1994). Over 90% of T2D patients have amyloid deposits in their islets (Bishoyi et al., 2021; Mukherjee et al., 2015), and the degree of amyloidosis increases with the duration and severity of T2D (Hayden and Sowers, 2002). Islet amyloidosis shows a diffuse distribution in the pancreas, with a progressive reduction in endocrine mass occurring with increases in amyloid mass (Wang et al., 2001). In other words, as the amyloid deposits expand, the beta cell mass shrinks. Moreover, fibrotic destruction of beta cells is an important pathogenic mechanism underlying reductions in beta cell mass (Kim et al., 2008). The pancreatic stellate cells (PSC), which proliferate in the presence of hyperglycaemia and hyperinsulinaemia, are involved in the progression of islet fibrosis in T2D in rodents and possibly also in humans (Cho et al., 2010).

1.4.1.3. Nutrient toxicity

Apoptosis induced by nutrient toxicity is one of the most important mechanisms of beta cell loss in T2D. Glucotoxicity is when prolonged and sustained hyperglycaemia leads to impairment of beta cell function and activation of apoptosis (Kaiser et al., 2003). Excessive glucose metabolism leads to increased generation of reactive oxygen species (ROS) in the mitochondria and oxidative stress activation. Due to the low expression of antioxidant enzymes (Zraika et al., 2006), beta cells are sensitive to oxidative stress and undergo apoptosis. Moreover, chronic hyperglycaemia results in chronic stimulation of beta cells to synthesise insulin, which can induce ER stress, also resulting in beta cell death (Harding and Ron, 2002). In addition to this, beta cells are susceptible to elevated lipid levels and lipotoxicity (Ye et al., 2019) (Figure 1.15). Some free fatty acids (FFA), such as palmitate, and lipoproteins have pro-apoptotic effects on beta cells (Maedler et al., 2003). FFAs promote beta cell apoptosis by increasing caspase activities, downregulating Bcl-2 expression, and phosphorylating Akt (Lin et al., 2014). The Bcl-2 family of proteins act as an apoptosis decision point (Tsujimoto, 2001), whereas, when phosphorylated, Akt promotes cell survival and replication, and inhibits apoptosis (Chen et al., 2014). Interestingly, prolonged exposure of MIN6 beta cells to a saturated fatty acid, palmitate, leads to increased levels of p53, downregulation of Bcl-2 expression, and apoptosis (Lin et al., 2014).

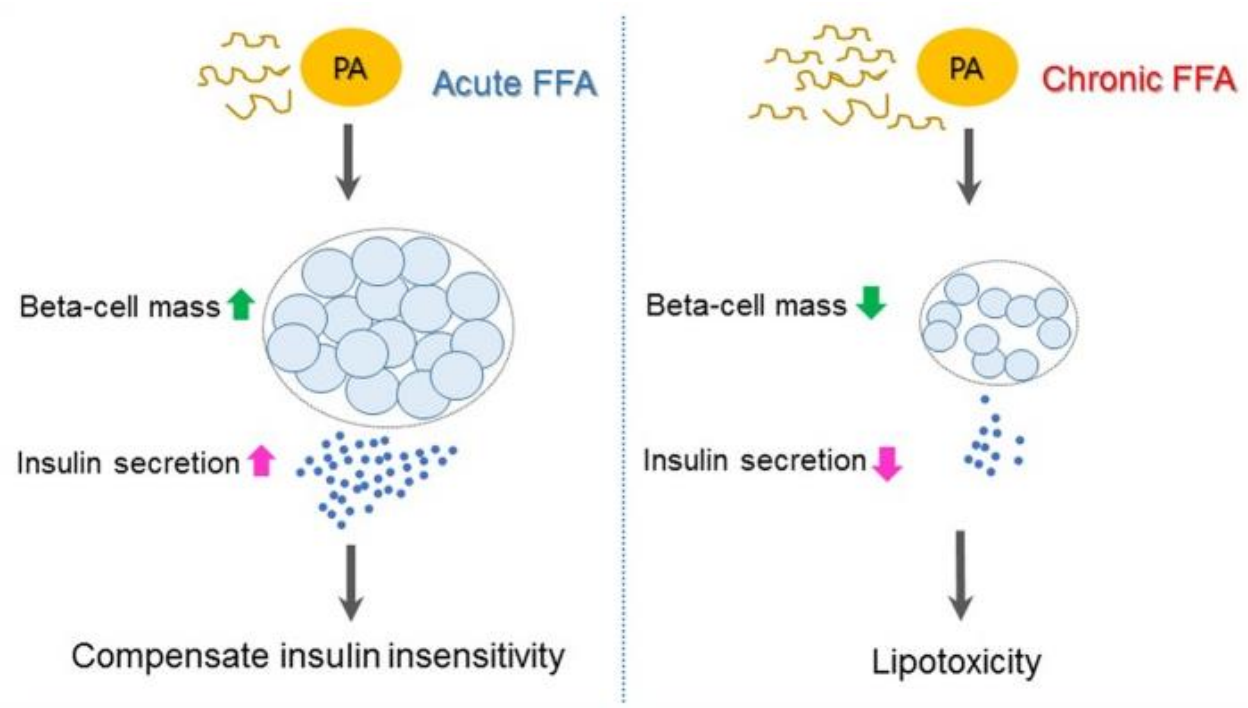

Figure 1.15. Mechanisms underlying lipotoxicity-induced failure of beta cells. In the state of insulin resistance, acutely elevated free fatty acids (FFAs), including palmitate, increase insulin secretion and beta cell mass to compensate for insulin insensitivity. However, chronic increases of FFAs in plasma result in lipotoxicity, which in turn leads to beta cell dysfunction and apoptosis (Oh et al., 2018).

1.4.2. Proliferation

Beta cell proliferation, in addition to neogenesis and hypertrophy, is an important compensatory mechanism by which beta cells cope with an increased demand for insulin during the progression of T2D (Cho et al., 2010). Many growth factors have been shown to activate beta cell replication *in vivo* or *in vitro* (Figure 1.16). These include insulin-like growth factors (IGF-I and -II), platelet-derived growth factor (PDGF), and epidermal growth factor (EGF) (Garcia-Ocana et al., 2001; Hill et al., 1999). Moreover, both insulin and glucose can control beta cell population dynamics by stimulating beta cell proliferation (Beith et al., 2008; Muller et al., 2006; Stamateris et al., 2016). For instance, transgenic mice with a beta cell-specific knockout of the insulin receptor show reductions in beta cell mass and develop T2D (Otani et al., 2004). As insulin resistance develops, beta cells respond by secreting more insulin, which in turn stimulates an increase in beta cell mass (Muller et al., 2006). Compensatory growth of beta cell mass through beta cell replication has been reported to occur following glucose infusion (Wang et al., 1996). However, chronic exposure to high glucose levels may lead to glucotoxicity and induce apoptotic pathways (Bouwens and Rooman, 2005; Cho et al., 2010).

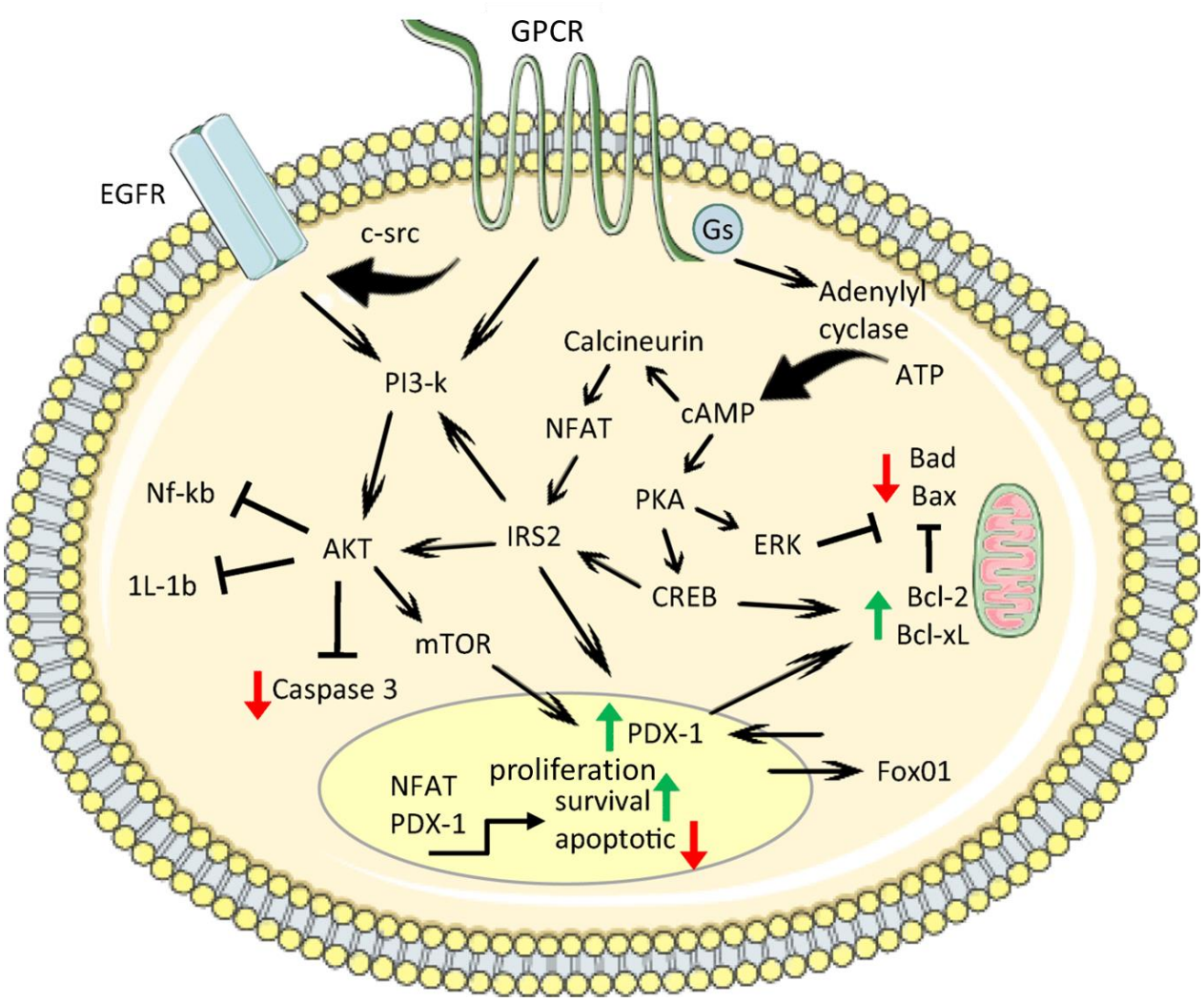

Figure 1.16. Beta cell signalling pathways associated with proliferation and survival. Pro-survival factors, including GLP-1 and EGFR ligands, activate different signalling cascades, such as PI3k/Akt and PKA/ERK, to increase expression of pro-survival factors (Bcl-1 and Bcl-xL) and decrease expression of proapoptotic factors (Bad and Bax). Activation of Akt stimulates mTOR activity and expression of the transcription factor PDX-1. NFAT, alongside with PDX-1, also regulates expression of survival genes. Adenylyl cyclase is activated downstream of the Gαs-coupled GPCR. Increased cAMP signals via calcineurin and then NFAT to increase IRS2 or through PKA, CREB and MAPK/ERK1/2 to phosphorylate and stimulate pro-proliferative and pro-survival factors (Hartig and Cox, 2020).

1.4.2.1. Pregnancy

A model for the regulation of beta cell mass during pregnancy has been proposed in which lactogenic signalling induces TPH1 expression and synthesis of serotonin in islets (Kim et al., 2010). In this model, serotonin functions in a paracrine and autocrine manner to stimulate beta cell proliferation via 5-HT2B. This is of great importance because the energy requirements of the foetus during pregnancy impose changes in mother's metabolism and increase insulin resistance. Placental lactogen (PL) and other placental hormones promote insulin resistance (Barbour et al., 2002; Ladyman et al., 2020; Sibiak et al., 2020; Yang et al., 2021), which leads to elevations in maternal blood glucose to ensure that nutrient flow to the growing foetus is maintained. On the other hand, prolactin and PL counterbalance this resistance and prevent maternal hyperglycaemia by inducing beta cell mass expansion (Huang et al., 2008; Lombardo et al., 2011; Parsons et al., 1992). Serotonin acts downstream of lactogenic signalling and activates 5-HT2B receptors to induce proliferation of beta cells (Figure 1.17). After pregnancy, when the expression of 5-HT2B decreases, the expression of an inhibitory 5-HT1D increases in islets to facilitate reductions in beta cell mass to the pre-pregnancy state (Kim et al., 2010). Other endocrine signals that play important roles in the regulation of beta cell mass and function in pregnancy include oestrogens and progestogens, kisspeptin, and leptin (Petres and Sferruzzi-Perri, 2021). During gestation, oestrogen protects beta cells against oxidative stress and apoptosis and induces glucose-stimulated insulin secretion, whereas progesterone increases beta cell proliferation, but it has no effect on insulin secretion (Alonso-Magdalena et al., 2008; Picard et al., 2002; Choi et al., 2005; Zhou et al., 2018). On the other hand, placental kisspeptin is important for normal glucose homeostasis during pregnancy, and its levels are closely correlated with the enhanced capacity of maternal beta cells to secrete insulin

(Bowe et al., 2019; Reynolds et al., 2009). What is more, there is evidence for a crosstalk involving adiponectin between adipose tissue, placenta and beta cells. Recent studies show that adiponectin promotes beta cell mass expansion in pregnancy though production of PL (Qiao et al., 2021).

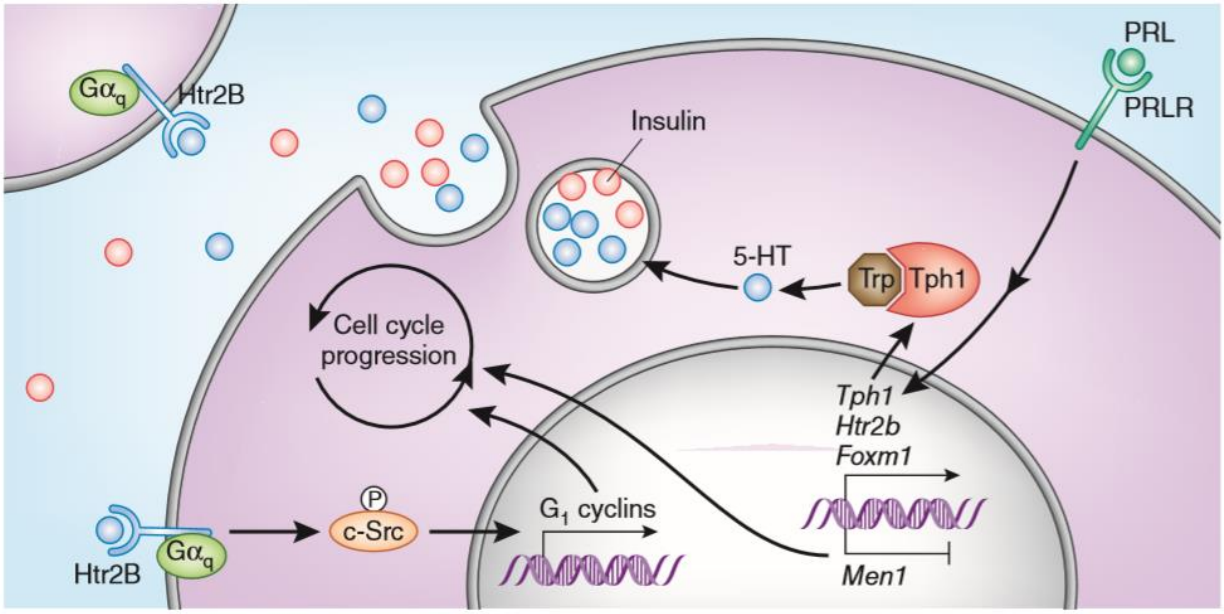

Figure 1.17. Beta cells expand during pregnancy through pathways involving lactogenic and serotonergic signalling. Prolactin and lactogenic hormones act at the prolactin receptor (PRLR), which increases the expression of serotonergic genes (TPH1 and 5-HT2B) upon activation. Elevated expression of TPH1 in turn increases serotonin (5-HT) production from tryptophan. Serotonin is secreted from the beta cell together with insulin, and once released, it activates the 5-HT2B receptor on the surface of beta cells. C-Src is phosphorylated downstream of the 5-HT2B receptor, and signals for increased expression of G1 cyclin proteins to stimulate cell cycle progression and proliferation (Georgia and Bhushan, 2010).

1.4.2.2. Obesity

Obesity is a major contributor to the development of insulin resistance, beta cell failure, and the onset of T2D. In obese people there are increases in the levels of FFA, lipoproteins (VLDL and LDL), glycerol, proinflammatory cytokines, including TNF-α, and other signals that are pro-apoptotic for beta cells and promote the development of insulin resistance (Bouwens and Rooman, 2005). Beta cells compensate for the increased demand for insulin by proliferating and increasing their mass in non-diabetic obese humans (Hudish et al., 2019). In *ob/ob* transgenic mice that present with severe obesity and hyperglycaemia due to a mutation in the leptin gene, beta cell mass is significantly increased (Bock et al., 2003). What is more, there is a linear correlation between body weight and beta cell mass (Montanya et al., 2000). However, if this transient increase in beta cell proliferation is insufficient to prevent hyperglycaemia, an increase in beta cell apoptosis and T2D will develop (Cerf, 2013). Interestingly, species-related differences do exist between human and rodent pancreas, for example, with respect to the beta-cell replicative activity; the proliferative potential of human beta cells is lower when compared to rodents and decreases with age (Tyrberg et al., 1996).

1.5. Mental illness

1.5.1 Major depressive disorder

Major depressive disorder (MDD) is a debilitating disease characterised by at least one depressive episode that lasts a minimum of 2 weeks and involves changes in cognition, mood and sleeping pattern, loss of interests and pleasure, as well as lack of motivation and energy (Otte et al., 2016). Worldwide, MDD affects 6% of the adult population per annum (Bromet et al., 2011), and women are twice as likely to develop depression than men (Seedat et al., 2009). Depression is a serious condition because depressed patients are 20-fold more likely to die by suicide when compared to the general population (Chesney et al., 2014). Despite family history, smaller hippocampal size and alterations in the main neurobiological systems that mediate the stress response are linked to the development of depression (Kupfer et al., 2012). There is no established mechanism to explain all aspects of MDD (Otte et al., 2016). Importantly, the physical illness, including diabetes, is more common in people with mental health problems, such as depression. MDD is usually treated with psychotherapy, including cognitive behavioural therapy (CBT), and/or psychopharmacology, including tricyclic antidepressants (TCAs), monoamine oxidase inhibitors (MAOIs), or selective serotonin reuptake inhibitors (SSRIs). Some of the association between antidepressants and diabetes may be confounded by illness.

1.5.2. Anxiety

MDD is often accompanied by anxiety. Anxiety disorders constitute the largest group of mental disorders (Craske et al., 2017) and include generalised anxiety disorder (GAD), obsessive-compulsive disorder (OCD), panic disorder, post-traumatic stress disorder (PTSD), and social phobia, which collectively affect over 7% of the world population each year. The most common symptoms of anxiety

include exaggerated and enduring fear, avoidance of perceived threats and, in some cases, panic attacks. The condition is linked to genetic background, disturbances in the limbic system, and/or dysfunction of the HPA (hypothalamic-pituitary-adrenocortical) axis (Craske and Stein, 2016). Anxiety is treated in a similar way to MDD, with psychotherapy and/or medications, most commonly with SSRIs. Symptoms that characterise a major depressive episode and MDD overlap with depressive symptoms in anxiety and schizophrenia.

1.5.3. Schizophrenia

Schizophrenia is a rare mental condition, and the lifetime prevalence of the disorder is approximately 1%. It is a chronic psychiatric disorder that is a combination of psychotic symptoms, including hallucinations and delusions, as well as motivational and cognitive dysfunctions (Kahn et al., 2015). Disturbances in the mesolimbic and mesocortical pathways in the brain are relevant to positive and negative symptoms of schizophrenia, respectively (Vanes et al., 2019). What is more, this cognitive and behavioural disorder is associated with abnormal processing of information. Schizophrenia is managed by psychosocial interventions, such as CBT, cognitive remediation and supported education, and antipsychotic medication.

1.5.4. Other psychiatric disorders

Other psychiatric disorders that are managed with CBT and/or medications include bipolar disorder, obsessive compulsive disorder (OCD), Tourette syndrome and eating disorders – anorexia nervosa and bulimia nervosa.

Bipolar disorder, also known as manic depression, causes extreme mood swings ranging from emotional highs, such as mania, and lows, such as depression. On the other hand, OCD is associated with repetitive obsessions and compulsions,

often including intrusive thoughts about religion and symmetry, and hygiene. Tourette syndrome is another serious psychiatric condition, and it is characterised by several motor and vocal tics that can include blinking and throat clearing, as well as coprolalia (the use of obscene words). Anxiety disorders, depression and substance abuse are very common among people with eating disorders. They are defined by abnormal eating behaviours that negatively affect mental and physical health. Psychiatric disorders can arise from many different sources and some risk factors include genetic factors, social influences, such as nutrition and social stress, and drug misuse.

1.6. Diabetes and mental illness

Several lines of evidence suggest a bidirectional link between diabetes and MDD (Alzoubi et al., 2018; Deuschle, 2013; Pan et al., 2010), meaning that both conditions are closely related (Figure 1.18). Therefore, prevention of T2D in patients with depression and management of depression in patients with diabetes are both clinically important. Having diabetes doubles the risk of developing depression, while people with depression have 65% increased risk of diabetes (Campayo et al., 2010). In addition, individuals with diabetes and depression have poorer glycaemic management than individuals with diabetes who do not have depression (Ascher-Svanum et al., 2015). It is important to note that the relationship between mood disorders (depression, anxiety, and psychotic illnesses) and diabetes vary. For mood disorders, there is clear evidence of bidirectionality, whereas for psychotic illness, diabetes frequently follows the diagnosis of the mental illness. A meta-analysis has found that people with depression are at an increased risk of diabetes when compared to people without depression, and people with diabetes are at a higher risk of depression than participants without diabetes (Zhuang et al., 2017). In addition, another meta-

analysis investigating the prevalence of T2D in participants with depression has shown that patients with MDD are at an increased risk of developing T2D than healthy control participants (Vancampfort et al., 2015). On the other hand, severe hyperglycaemia in patients with T2D is positively associated with the severity of depressive symptoms, independently of glycaemic management and treatment (Kikuchi et al., 2015). What is more, diabetes and depression are both related to increased all-cause and cardiovascular mortality (Papatheodoru et al., 2018).

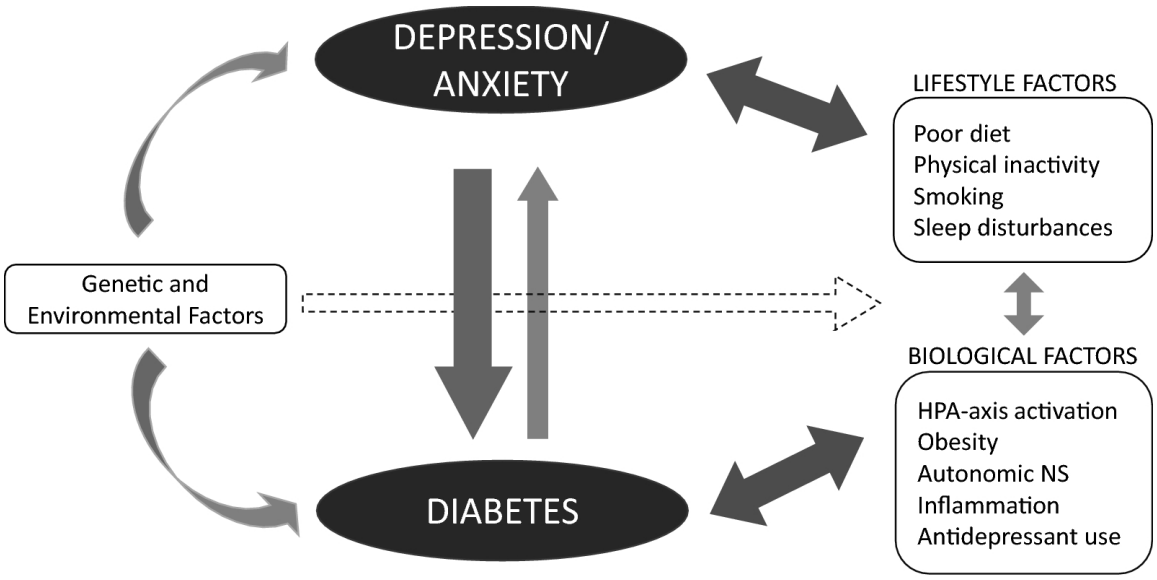

Figure 1.18. Potential behavioural and pathological mechanisms linking depression and anxiety to diabetes. Genetic, environmental, and a range of behavioural factors contribute to a bidirectional relationship between these mood disorders and diabetes. Pathophysiological mechanisms of this link include HPA axis activation that stimulates increases in glucocorticoids, which in turn contribute to insulin resistance. Obesity is linked to increases in plasma glucose and FFA levels that lead to insulin resistance. Autonomic nervous system (NS) dysfunction links to vascular and digestive dysfunction, whereas the innate inflammatory response leads to beta cell destruction (Naicker, 2018).

Evidence is growing that T2D and depression share biological origins, such as overreaction of innate immunity resulting in inflammation, and dysregulation of the hypothalamic-pituitary-adrenal axis (Moulton et al., 2015). Different environmental factors may activate common pathways that lead to the development of T2D and depression. These include a low socioeconomic status, physical inactivity, and/or unbalanced diet (Alzoubi et al., 2017; Badescu et al., 2016). On the other hand, treatment with tricyclic antidepressants is associated with weight gain and disruption of glycaemic control (Deuschle, 2013). What is more, management of diabetes can result in chronic stress that can lead to MDD. Interestingly, diabetes is associated with structural changes in the brain, such as cerebral atrophy, lacunar infarcts, changes to blood flow (van Harten et al., 2006), as well as reductions in hippocampus volumes, which are inversely related to glycaemic management and $HbA1_C$ levels (Hajek et al., 2014).

1.6.1. Mechanisms underlying the relationship between diabetes and depression

1.6.1.1. Inflammation

Inflammation has been implicated in the development of both T2D and depression. A meta-analysis has shown a significant increase in inflammatory biomarkers, including C-reactive protein (CRP) and interleukin 6 (IL-6) in depression (Haapakoski et al., 2015). Interestingly, elevated levels of IL-6 in childhood are associated with an increased risk of future depression (Ting et al., 2020), while increased levels of CRP can predict the development of T2D (Wang et al., 2013). When CRP levels and the incidence of T2D were studied, participants with elevated depressive symptoms and high CRP levels had a higher T2D risk (Au et al., 2014). Levels of proinflammatory cytokines, such as TNF-α, are also elevated in patients with MDD. In recent meta-analysis studies, higher levels of TNF-α, IL-6, IL-1RA, and chemokines have been linked to depression (Kohler et

al., 2017; Leighton et al., 2017). Moreover, there is an association between depression and plasma levels of CRP, IL-1β, IL-1RA, and MCP-1 in T2D patients. Interestingly, their levels are also elevated in depressed participants with T2D (Laake et al., 2014). Taken together, there is growing evidence that inflammation is a common factor in both T2D and MDD.

1.6.1.2. Hypothalamic-pituitary-adrenocortical axis

Evidence is growing that depression and T2D share biological origins, potentially through dysregulation of the hypothalamic-pituitary-adrenocortical axis. Both T2D and depression are associated with chronic stress that hyperactivates the hypothalamic-pituitary-adrenocortical (HPA) axis and the sympathetic nervous system (SNS), increasing the production of cortisol, adrenaline, and noradrenaline (Kyrou and Tsigos, 2009). Chronic elevations in cortisol and SNS activation promote the development of obesity and insulin resistance, lead to anxiety through the activation of the flight-or-fight response, as well as depression and increased appetite through tachyphylaxis of the reward system (Chrousos, 2009; Prestele et al., 2003). Glucocorticoids promote muscle protein breakdown, lipolysis, and gluconeogenesis, and reduce glucose utilisation. This, in turn, affects body composition leading to obesity, insulin resistance, and hyperglycaemia (Gragnoli, 2012). In addition, cortisol levels are related to the presence and severity of diabetic complications (Chiodini et al., 2007) and disturbed neurogenesis in the stress-sensitive regions of the hypothalamus (Herbert et al., 2006). In addition, T2D is associated with hippocampal atrophy and impaired hippocampal function through glucocorticoid-mediated effects on neurons (Stranahan et al., 2008), whereas MDD is associated with reductions in hippocampal volume (Roddy et al., 2019).

1.6.1.3. Genetic factors

The link between depression and diabetes has been studied by investigating a common genetic variant and specific environmental factors that predispose to both conditions (Clarke et al., 2016; Kan et al., 2016; Ji et al., 2016). Functional enrichment analysis has identified several immune response and lipid metabolism pathways to be enriched in T2D and MDD (Ji et al., 2016). Future studies should aim to investigate single nucleotide polymorphisms (SNPs) that are shared by these disorders.

1.6.2. Effect of treatment on the relationship between depression and diabetes

People with psychiatric conditions and diabetes are more likely to live in socially deprived areas, which are linked to less frequent health examinations and poorer health outcomes. Effective glycaemic management is associated with improvements in mood (Lustman and Clouse, 2005). The effect of metformin on depression has been investigated in a randomised placebo-controlled study of participants with both depression and T2D (Guo et al., in 2014). This study has shown that metformin significantly improves the cognitive performance of the patients when compared to the placebo participants. What is more, the thiazolidinedione pioglitazone has been shown to induce remission of major depressive episodes, and the GLP-1 receptor agonist liraglutide has been shown to improve cognitive function in patients with diabetes (Colle et al., 2017; Mansur et al., 2017).

On the other hand, improving mood has been shown to improve diabetes management. One meta-analysis of the effectiveness of CBT on glycaemic management in adults with diabetes has shown a marked decrease in HbA1c levels in the CBT group when compared to control groups (Uchendu and Blake, 2017). In terms of antidepressant treatment, it has been reported that some

antidepressants are more effective in the treatment of affective disorders in patients with diabetes than others, and selective serotonin reuptake inhibitors (SSRIs) are the only class of antidepressants with confirmed favourable effects on glycaemic control (Deuschle, 2013; Tharmaraja et al., 2019).

1.7. Selective serotonin reuptake inhibitors

SSRIs are the most commonly prescribed group of antidepressants used in the treatment of moderate depression, anxiety, panic attacks and obsessive-compulsive disorder. Drugs of this type include fluoxetine, sertraline and paroxetine. The SSRIs are well-absorbed and exert their effects on neurotransmission by blocking the serotonin transporters and increasing the levels of serotonin in the synaptic cleft available to bind to the post-synaptic receptors (Figure 1.19). Serotonin is an important transmitter in the central nervous system that also plays a role as a local hormone in the intestine, peripheral vascular system and endocrine pancreas (Wyler et al., 2017) (Section 1.2.4.3).

The SSRIs have been shown to be anti-inflammatory (Sachs et al., 2015), affect cytokine production (Lu et al., 2017; Sharifi et al., 2014), enhance neurogenesis in the brain (Duan et al., 2008), and there is evidence that they affect glucose regulation in people with depression and with or without diabetes (Chiwanda et al., 2016; Deuschle, 2013; Tharmaraja et al., 2019). It is possible that the improvements in glucose homeostasis in individuals being treated with SSRIs is due to direct beneficial effects of these drugs on beta cells. Thus, it has been reported that sertraline can increase glucose-stimulated insulin secretion in rats (Gomez et al., 2001), and there is evidence that insulin acts as an autocrine agent to increase beta cell proliferation and inhibit apoptosis (Muller et al., 2006). What

is more, both sertraline and fluoxetine have been shown to block K^+ channels in platelets and astrocytes, and it is possible that they also inhibit K_{ATP} channels in beta cells, decrease K^+ efflux, and cause cell depolarisation crucial for insulin secretion (Frizzo, 2017; Ohno et al., 2007). Interestingly, in the rat brain, chronic fluoxetine treatment increases the activity of the ERK-CREB signal system, which has been implicated in the neuronal mechanism of depression (Qi et al., 2008). Sertraline also increases phosphorylation of ERK, also known as MAPK, in the brain, and it has neuroprotective effects (Taler et al., 2013). In the endocrine pancreas, ERK and CREB are involved in beta cell mass expansion (Hussain et al., 2006; Liu et al., 2012; Jiang et al., 2018), and it could be that some SSRIs improve blood glucose control by inducing beta cell proliferation through similar mechanisms as they use to promote neurogenesis in the brain.

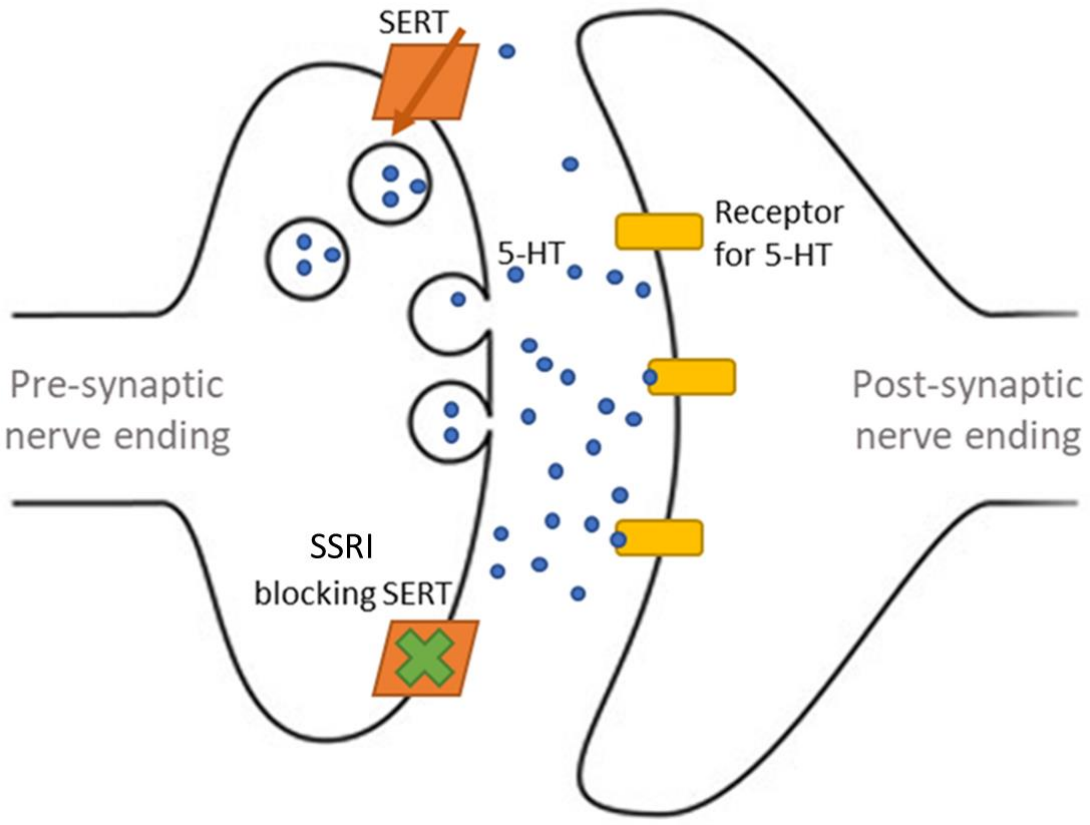

Figure 1.19. SSRIs ease depression by increasing levels of serotonin (5-HT) in the synaptic cleft available to bind to the serotonin receptors. Serotonin released by the neuron is recycled through reuptake by the SERT. SSRIs block the reuptake of serotonin and therefore make more serotonin available to bind to its receptors on the post-synaptic site.

1.7.1. Fluoxetine

Fluoxetine was discovered in 1972 and it is listed on the World Health Organization's List of Essential Medicines, as one of the most effective and safe medicines (World Health Organisation, 2019). Fluoxetine and its metabolite, norfluoxetine, are potent inhibitors of serotonin uptake by SERT, with high selectivity, and they have long plasma half-lives of 2 and 7 days, respectively (Altamura et al., 1994). Both are metabolised in the liver and excreted in the urine. It is available in tablets of 20, 40 and 60mg and its efficacy is comparable to tricyclic antidepressants, but fluoxetine has fewer or less severe side effects, of which the most common are nausea, headache, nervousness, and insomnia (Buchman et al., 2002). Most importantly, overdose seems to be rather safe (Hammen and Watkins, 2008; Wenthur et al., 2015). The chemical structure of fluoxetine lacks the three-fused ring system of tricyclic antidepressants (TCAs), with the trifluoromethyl substituent on the phenoxy ring, which is a determinant of its specificity as an SSRI. It has a mild affinity for 5-HT receptors and low affinity for α1-adrenoreceptors, histamine H1 receptors, muscarinic cholinergic receptors, and dopamine D2 receptors. What is more, fluoxetine acts as an agonist at 5-HT2B (Kim et al., 2010) and α1-adrenoreceptors (Proudman et al., 2020), while it blocks 5-HT2C (Ni et al., 1997), 5-HT1 (Beasley et al., 1992), and muscarinic receptors (García-Colunga et al., 1997; Ofek et al., 2012), and a number of ion channels, including the 5-HT3 receptor (Choi et al., 2003).

1.7.2. Sertraline

Sertraline is a potent competitive inhibitor of serotonin uptake by SERTs. It was approved for medical use in the 1990s (Lopez-Munoz and Alamo, 2009). In 2016, it was the most prescribed psychiatric medication in the United States (Grohol, 2018). It is metabolised in the liver, with N-demethylation to desmethylsertraline and deamination to desmethylsertraline ketone. The half-life of sertraline is 26-32h, and it is available in tablets of 50 and 100mg (Singh and Saadabadi, 2021). Common side effects include diarrhoea, sexual dysfunction, and insomnia, and in some cases an increased suicide risk has been observed in young users. As for fluoxetine, sertraline also has a low affinity for α1-adrenoreceptors, dopamine D2, histamine H1, 5-HT2, and muscarinic cholinergic receptors (Hammen and Watkins, 2008).

1.7.3. Paroxetine

Paroxetine is a phenylpiperidine derivative and a potent SSRI. It was introduced in 1992 to treat anxiety disorders and depression (Bourin et al., 2001). Similar to fluoxetine and sertraline, paroxetine undergoes first-pass metabolism in the liver. Its half-life varies on a number of different patient-specific and drug-specific variables, with a mean of 24h. Paroxetine is available in tablets of 5-50mg per day (Shrestha et al., 2021). The most common side effects of this medication are nausea, headache, dryness of mouth, and trouble sleeping, but its overdose appears to be relatively safe and is manifested by vomiting, ataxia, tachycardia, and seizures. Paroxetine has low affinity for α1-adrenoreceptors and dopamine D2, histamine H1, and 5-HT2, and has mild/moderate affinity for the muscarinic cholinergic receptors (Hammen and Watkins, 2008).

1.7.4. The use of antidepressants in T2D

The prevalence rate of MDD is two times higher in with diabetes with T2D (Roy and Lloyd, 2012). Antidepressant use has dramatically increased in recent years (Barnard et al., 2013) and it is associated with an increased number of co-morbid chronic disorders, such as T2D. The prevalence of antidepressant use among people with diabetes is 8.4% (Ivanova and Schmitz, 2010). Some antidepressants have been associated with hyperglycaemia, glucose intolerance and weight gain leading to obesity, and being overweight or obese accounts for 44% of the cases of diabetes in people taking antidepressants (Leitner et al., 2017). Although the mechanisms remain unclear, this increase in weight could be attributed to off target effects of antidepressants or improvements in appetite due to successful antidepressant therapy. On the other hand, a meta-analysis of 5 randomised controlled trials (RCTs) has shown that fluoxetine treatment results in over 4kg weight loss followed by improvements in fasting blood glucose, and reductions of $HbA1_C$ and triglycerides in patients with T2D (Ye et al., 2011). There is also evidence that treatment with SSRIs, such as fluoxetine and sertraline, increases insulin sensitivity independently of reductions in BMI (Chen et al., 2010; Connolly et al., 1995; Goodnick et a, 2001; Maheux et al., 1997). Furthermore, a 6-month double-blinded RCT has shown improvements in glycaemic control with another SSRI, paroxetine, in the short run (Paile-Hyvarinen et al., 2007). However, a randomised trial has reported a significant weight gain with paroxetine when compared to fluoxetine and sertraline (Fava et al., 2000).

It is possible that some antidepressants are more effective in the treatment of affective disorders in people with diabetes than others. For example, it has been demonstrated that fluoxetine and sertraline improve glucose regulation (Gomez et al., 2001), whereas some selective serotonin-noradrenaline reuptake

inhibitors (SNRIs) and TCAs exert no or untoward effects on glucose homeostasis (Chen et al., 2010; Ghaeli et al., 2004; Kauffman et al., 2005; Laimer et al., 2006; Moosa et al., 2003). The negative effect on glucose homeostasis has been reported with combination therapies and TCA use, suggesting that SSRIs might be the safest choice in the treatment of depression in people with a tendency for glucose dysregulation. Their beneficial effects on blood glucose levels and HbA_{1C} could be attributed to elevated serotonin levels, available to exert functional effects, for example, on the islets, and this will be investigated in this thesis. To investigate whether SSRIs have the same or different mechanisms of action in the endocrine pancreas, three different SSRIs were chosen and compared. Fluoxetine and sertraline were selected as the widely prescribed options, whereas paroxetine was chosen as a less commonly prescribed SSRI.

1.8. Antipsychotic drugs

Antipsychotics are a class of medication used to manage psychosis in schizophrenia and bipolar disorder or as an add-on therapy of major depressive disorder. They revolutionised the management of psychosis that had been previously limited to admission to psychiatric hospitals, sedation or insulin-induced coma. Antipsychotic drugs fall into two categories: first- and second-generation drugs. First-generation antipsychotics (FGAs), known as typical, were discovered in the 1940s and include haloperidol and loxapine (Solmi et al., 2017). On the other hand, second-generation antipsychotics (SGAs), known as atypical (AAPs), have been developed more recently (Ramachandraiah et al., 2009) and include aripiprazole and clozapine. The AAPs have transformed the treatment of psychotic conditions as they have a lower propensity to cause extrapyramidal side effects, including akathisia, parkinsonism, and tardive dyskinesia, when compared to the FGAs. These properties of AAPs are aligned with their

differentiating receptor profiles (Ginovart and Kapur, 2012). Although exact modes of action of antipsychotic medications remain unknown, it is known that they act on receptors in the brain's dopamine pathways, as well as on serotonin receptors, and histamine and muscarinic receptors. Affinities for histamine H1 and 5-HT2C receptors could explain why antipsychotic drugs are associated with obesity, since these receptors are coupled to regulation of food intake. Thus, blockade of H1 receptors by some antipsychotics leads to reduction of adenosine monophosphate-activated protein kinase (AMPK) that activates appetite, whereas antagonism of 5-HT2C on anorexigenic proopiomelanocortin neurons increases appetite (He et al., 2014). Almost all currently available AAPs, with a few exceptions, are 5-HT2A, 5-HT1A and 5-HT1D receptor agonists, and they antagonise 5-HT6 and 5-HT7. 5-HT2A and 5-H1D are both expressed by islet cells, and they have stimulatory and inhibitory functions, respectively (Sullivan et al., 2015; Meltzer and Massey, 2011). Interestingly, the expression of these receptors is significantly increased in islets of patients with T2D (Bennet et al., 2015).

As outlined above, the prevalence of T2D is increased among people suffering from mental illnesses, including schizophrenia (Mamakou et al., 2018; Yang et al., 2020), and there are concerns that antipsychotic therapy increases the risk of developing T2D (Liao et al., 2011; Smith et al., 2008). However, AAPs vary in side effects related to glucose dysregulation (Yood et al., 2009) and the direct effects of individual AAPs at beta cells are not well understood. Importantly, there is a hierarchy of weight gain and risk of metabolic side effects caused by different types of antipsychotics: the highest risk is associated with olanzapine and clozapine treatment, whereas the lowest risk is with aripiprazole and lurasidone treatment. There is evidence that some antipsychotic drugs, including clozapine, induce insulin and glucagon secretion from human islets at therapeutically

relevant concentrations (Aslanoglou et al., 2021). Moreover, it has been shown that islets express components of the dopaminergic system (Ustione et al., 2013) and that D2 receptor blockade with domperidone, a D2 receptor antagonist, promotes proliferation and prevents apoptosis of mouse beta cells through increases in intracellular cAMP (Sakano et al., 2016). On the other hand, treatment with first- and second-generation antipsychotics has been associated with diabetic ketoacidosis, the uncontrolled production of ketone bodies that leads to potentially life-threatening reductions in blood pH. What is more, rates of ketoacidosis are significantly increased in people with comorbid mental illness and diabetes (Polcwiartek et al., 2016; Vuk et al., 2017). This suggests that some antipsychotic medications could decrease insulin secretion, but the underlying mechanisms remain to be further investigated. Therefore, one of the aims of this thesis was to investigate the effects of two commonly prescribed AAPs, aripiprazole and clozapine, on mouse and human beta cell mass and function.

1.8.1. Aripiprazole

Aripiprazole, sold under the brand name Abilify, is a novel antipsychotic drug. It was approved for medical use in 2002 to treat schizophrenia, depression, autistic disorder, and Tourette's syndrome (Citrome, 2006; Hirsch and Pringsheim, 2016; Padala et al., 2005). Aripiprazole is metabolised in the liver by CYP3A4 and CYP2D6, forming its active metabolite dehydroaripiprazole. Pharmacokinetics studies show that serum levels of aripiprazole are 110-500ng/ml, which corresponds to 0.24-1.12μM in blood (Eryilmaz et al., 2014; Gründer et al., 2009; Kirschbaum et al., 2008; Sparshatt et al., 2010). Interestingly, coadministration of aripiprazole with fluvoxamine (100mg/day) or paroxetine (20mg/day) inhibits CYP3A4 and CYP2D6, and therefore increases plasma levels of aripiprazole. Fluvoxamine and paroxetine are CYP3A4 and CYP2D6 inhibitors, respectively, and

they markedly decrease systemic clearance of aripiprazole (Azuma et al., 2011). The half-life of aripiprazole is 72h, and it is available in tablets of 10-20mg (Winans, 2003). Common side effects include agitation, erectile dysfunction and hypotension.

Aripiprazole acts by modulating neurotransmission overactivity of dopamine, which improves symptoms of schizophrenia (Mailman et al., 2010). Mechanisms of action of aripiprazole differ from those of other AAPs (Starrenburg and Bogers, 2009). It has antagonist activity on postsynaptic D2 receptors and partial agonist activity on presynaptic D2 receptors (Wood and Reavill, 2007), D3 (Kegeles Et al., 2009), and partially D4 (Shapiro et al., 2003). Aripiprazole also affects serotonin signalling through partial agonism at the 5-HT1A (Jordan et al., 2002), by acting as a partial agonist of 5-HT2A and 5-HT2C, an inverse agonist of 5-HT2B, an antagonist of 5-HT6, and a partial agonist of 5-HT7 (de Bartolomeis et al., 2015; Schwartz, 2018; Shapiro et al., 2003). In addition, aripiprazole has an effect on histamine (H_1) and adrenergic (α), and, as SSRIs, it blocks SERT (Keck and McElroy, 2003). Aripiprazole has a unique partial agonist property at the D2 and some serotonin receptors, including 5-HT2C, and this therefore offers some functional selectivity (Bolonna and Kerwin, 2005; Tuplin and Holahan, 2017), which could explain why it is highly effective in the management of both positive and negative symptoms of schizophrenia (Tuplin and Holahan, 2017). Aripiprazole, as a partial agonist, activates the D2 receptor, but provokes a fraction of the response relative to a full agonist. In the mesolimbic pathway that is associated with positive symptoms of schizophrenia, aripiprazole has a lower intrinsic effect when compared to dopamine, and hence it decreases dopaminergic transmission. In the mesocortical pathway, aripiprazole increases dopaminergic activity and reduces negative symptoms of schizophrenia (Guzman, 2021; Mailman and Murthy, 2010).

The atypical antipsychotic medications have become stigmatised by metabolic side effects, such as obesity, T2D, and cardiovascular disease (Allison et al., 1999; Basu and Brar, 2006; Bischoff et al., 2020; Gianfrancesco et al., 2006). It has been suggested that the initiating pathophysiology is weight gain, secondary to centrally mediated surges in appetite (Allison et al., 1999). Aripiprazole is associated with less weight gain than other AAPs, such as olanzapine (McEvoy et al., 2005), and it is considered to be metabolically neutral (Nielsen et al., 2010; Wang et al., 2013). However, when it is used in monotherapy, it is associated with weight gain, and this is one of the reasons that it was not licensed for use as an antidepressant. In addition, there is conflicting data on the effect of aripiprazole treatment on glycaemic control and the risk of T2D. Aripiprazole has been shown to modestly increase insulin resistance following short-term administration (Teff et al., 2013), but it has not been directly associated with an increased risk of T2D (Yood et al., 2009). Interestingly, aripiprazole is effective in correcting adverse effects, such as metabolic syndrome, caused by some antipsychotic drugs or in refractory cases (Fleischhacker et al., 2014; Silva et al., 2019). In adjunctive therapy in schizophrenia patients treated with clozapine, it has some metabolic benefits, including improved glucose clearance and weight loss, (Fan et al., 2012).

1.8.2. Clozapine

Clozapine is unique among antipsychotic drugs, as it is the only antipsychotic medication with effectiveness in treatment-resistant schizophrenia (TRS) (Farooq et al., 2019). However, the mechanism of this superior effectiveness of clozapine in TRS remains unclear. Clozapine is sold as Clozaril and it was discovered in 1956 and approved for medical use in 1972 (Haidary and Padhy, 2020). Clozapine is metabolised in the liver by several cytochrome P450 (CYP) isozymes. Therapeutic

plasma levels of clozapine are 200-1,000ng/ml, which corresponds to 0.61-2.66µM (Funderburg et al., 1994; Keshavarzi et al., 2020; Schulte, 2003; Varma et al., 2011; Yada et al., 2021; Yusufiet al., 2007). The estimated half-life of clozapine is 10.2-29.2h (Fang and Mosier, 2014; McEvoy et al., 1996; Jann et al., 1993). The initial dose of clozapine is 12.5mg and the maximum dose can be as high as 900mg depending on the patient's age and medical history, with a usual dose ranging between 149-600mg/day (Subramanian et al., 2017). Common side effects of clozapine treatment include agitation, constipation, drowsiness, erectile dysfunction, insomnia and increased weight (De Fazio et al., 2015). Some SSRIs inhibit the metabolism of clozapine leading to significantly increased plasma levels of this AAP (Sproule et al., 1997).

Pharmacologically, clozapine has antagonist activity at several receptors. These receptors include dopamine (D1, D2, D3, D4, D5), serotonin (5-HT1A, 5-HT2A, 5-HT2C), muscarinic (M1, M2, M3, M5), α1- and α2-adrenergic, as well as histamine (H1) receptors (Chathoth et al., 2018; Cikánková et al., 2019; Meltzer, 1994; Numata et al., 2018). Additionally, clozapine is associated with improvements in depression, anxiety, and the negative cognitive symptoms associated with schizophrenia due to its action at serotonin receptors. Interestingly, a direct interaction of clozapine with the $GABA_B$ receptor has been demonstrated, suggesting that potentiation of $GABA_B$ could be a novel mechanism that is involved in the pathophysiology and treatment of schizophrenia (Wu et al., 2011). Clozapine has been shown to stimulate nerve cell proliferation in the hippocampus of adult rats and mice, and to have a neural stem cell-protective activity, which suggests it has a neurogenic-promoting activity (Chikama et al., 2017; Halim et al., 2004; Lewis et al., 2006; Lundberg et al., 2020). As for fluoxetine, clozapine promotes neural stem cell viability, increases levels of the

anti-apoptotic protein Bcl-2 and decreases caspase-3 activity (Todorovic et al., 2019). What is more, it has been suggested that clozapine inhibits accumulation of toxic protein aggregates and defective organelles induced by ketamine, a non-competitive N-methyl-D-aspartate receptor antagonist used in rodents to mimic symptoms similar to those associated with schizophrenia in humans (Becker et al., 2004; Lundberg et al., 2020). Despite its beneficial effects in the brain, clozapine has been linked to metabolic adverse effects (Grover et al., 2016) and increased risk of T2D and dyslipidemia (Holt, 2019; Ingimarsson et al., 2017; Yood et al., 2009), and there is tentative evidence that clozapine is associated with a small increased risk for T2D compared with first generation antipsychotics in schizophrenia patients (Smith et al., 2008). However, patients with schizophrenia often have features of metabolic syndrome before the initiation of treatment (Chathoth et al., 2018). A large number of patients with schizophrenia are obese and have glucose dysregulation by the time clozapine is initiated, but the relationship between clozapine treatment and hyperglycaemia are incompletely understood. It has been suggested that clozapine may inhibit glucose transporters responsible for glucose uptake by the brain and peripheral tissues (Tovey et al., 2005). In addition, there is evidence for a causal connection between clozapine and acute hyperglycaemia that could be reversed with clozapine withdrawal (Kumar et al., 2019), but the underlying mechanisms are unclear. Clozapine does not alter the levels of growth hormone (GH) or insulin-like growth factor-1 (IGF-1) within three months of treatment, indicating that changes in glucose tolerance due to clozapine treatment involve other mechanisms that are yet to be elucidated (Howes et al., 2004).

At the receptor level, blockade of H1 and 5-HT2C receptors by clozapine could be associated with the metabolic risks of the drug (Nasrallah, 2008). Antagonism of the histamine receptor is linked to antipsychotic-induced weight gain (Kroeze et al., 2003). What is more, *in vivo* studies have shown that clozapine activated the enzyme AMPK in the hypothalamus, which reverses the action of leptin (Kim et al., 2007). In addition to this, blockade of 5-HT2C is associated with antipsychotic-induced weight gain and diabetes (Matsui-Sakata et al., 2005), as 5-HT2C knockout mice develop insulin resistance and impaired glucose tolerance (Nonogaki et al., 1998).

Even though the use of atypical antipsychotic drugs, including clozapine, has been linked to metabolic disturbances (Koro et al., 2002; Teff et al., 2013), the direct effects of individual drugs on beta cell mass and function have not been fully investigated, and it remains unclear whether some of these drugs produce metabolic disturbances by promoting insulin resistance in the periphery or through increasing beta cell death and/or dysfunction. Therefore, clozapine, which is associated with severe metabolic side effects, and aripiprazole, which has less deleterious impact on glycaemic management, were chosen for this study and experiments were carried out to address the direct effects of these drugs at beta cells.

1.9. Aims

Antidepressants and antipsychotics are widely used for the treatment of mood and psychotic illnesses, commonly in people with diabetes, and it is important to unravel their modes of action, including their direct effects at beta cells.

The principal aim of this thesis is to determine the direct effects of selective serotonin reuptake inhibitors (fluoxetine, sertraline and paroxetine) and atypical antipsychotics (aripiprazole and clozapine) on beta cell mass and function using a beta cell line (MIN6 cells), primary mouse and human islets, and pseudoislets.

Specifically, the objectives are to:

- Investigate the expression of SERT by beta cells and islets using standard PCR and Western blotting analyses.
- Investigate the expression of D2 and 5-HT receptors by beta cells and islets using quantitative PCR and fluorescence immunohistochemistry.
- Determine the direct effects of selective serotonin reuptake inhibitors (fluoxetine, sertraline and paroxetine) on beta cell viability, insulin secretion, proliferation and apoptosis.
- Study the effects of fluoxetine delivery to *ob/ob* mice on beta cell proliferation *in vivo*.
- Determine the direct effects of atypical antipsychotic drugs (aripiprazole and clozapine) on beta cell viability, insulin secretion, proliferation, and apoptosis.
- Study the effect of fluoxetine, aripiprazole and clozapine on infiltration of islet-derived pseudoislets by macrophages using invasion and migration assays.

Chapter 2. Materials and Methods

2.1. MIN6 beta cell culture

Cell culture is a technique of maintaining live cells that are separated from their original tissue. Therefore, cells are grown under carefully controlled conditions. These conditions typically consist of essential nutrients, such as amino acids, glucose, vitamins, and minerals that are provided in culture media. Additionally, cells require serum that contains growth factors stimulating cell proliferation, and antibiotics used to prevent bacterial contamination.

Insulin secreting cell lines have been generated to provide a valuable complement to primary islets, which are not readily available and have low rates of proliferation. Furthermore, cell culture studies allow for a controlled manipulation of cellular processes, such as cell division. One of the cell lines that functionally resemble primary beta cells is the MIN6 beta cell line. It is derived from a mouse insulinoma tumour and generated by targeted oncogenesis in mouse beta cells to drive simian virus 40 large T antigen (SV40LT) expression using the insulin promoter (Miyazaki et al., 1990). MIN6 cells display characteristics of primary beta cells, including glucose transport and phosphorylation via GLUT2 and glucokinase, respectively. Although they have less secretory granules than beta cells and concomitantly lower insulin content, MIN6 cells are glucose-responsive and capable of secreting insulin (Miyazaki et al., 1990), and they are therefore a good *in vitro* model to study beta cell function. The ability of MIN6 cells to secrete insulin declines with a higher passage number (usually over 50) due to gene expression changes, including downregulation of phospholipase D1, an important regulator of glucose-stimulated insulin secretion (GSIS) (Hughes et al., 2004) and glucokinase, as well as upregulation of hexokinase with lower Km and Vmax, meaning that high passage cells are less

sensitive to changes in glucose concentrations (Ishihara et al., 1994). Therefore, in this thesis, MIN6 cell passages between 30-50 were used to study insulin secretion.

2.1.1. Cryopreservation and thawing of MIN6 beta cells from frozen storage

It is important that healthy cells in the log phase of growth are frozen down and preserved for long-term storage to maintain frozen cell stocks. Cryopreservation of cells requires aseptic harvesting close to 90% confluency, as described in Section 2.1.2 below, and the use of a cryoprotective agent to prevent cell damage from ice crystal formation at low temperatures. A controlled freezing rate of 1°C/min is essential to preserve optimal viability of the recovered cells.

MIN6 cells were trypsinised (Section 2.1.2) and re-suspended in 10ml of fresh Dulbecco's Modified Eagle's Medium (DMEM). The cell suspension was then centrifuged, and the pellet was re-suspended in DMEM containing 10% (v/v) cryoprotectant dimethyl sulfoxide (DMSO), at a concentration 1 x 10^6 cells/ ml. 1ml aliquots were transferred into labelled cryoprotective Nunc® vials, which were then placed inside a passive freezer Nalgene® Mr Frosty at -80 °C overnight. An outer compartment of the container was filled with 100% isopropyl alcohol to allow the reproducible freezing rate of between –1°C and –3°C. Frozen vials containing cells were transferred long-term into a liquid nitrogen vessel at -196°C.

Once frozen, cells may be retrieved from liquid nitrogen and reconstituted by thawing. The thawing procedure is stressful to cells, therefore working quickly ensures that a high number of cells survive. Vials containing frozen MIN6 cells were placed into a 37°C water bath for 1min, and their contents were transferred into sterile 15ml centrifuge tubes. The thawed cells were diluted in 10ml pre-

warmed DMEM and centrifuged at 1000rpm for 5min. Cell pellets were re-suspended in fresh DMEM and transferred into T25 flasks and into the incubator at 37°C (95%air/5%CO_2) overnight. The medium was then changed to remove non-adherent cells and the cells were maintained in culture as described in Section 2.1.2.

2.1.2. Maintaining MIN6 beta cells in culture

The MIN6 cells used in this study were provided from Professor J. I. Miyazaki's laboratory at Tokyo University in Japan. MIN6 cells were maintained in culture at 37°C (95%air/5%CO_2) in DMEM containing 25mM glucose and supplemented with 10% (v/v) foetal bovine serum (FBS), 100U/ml penicillin and 100µg/ml streptomycin, and 2mM L-glutamine, which can be presented as 10% (v/v) FBS, 1% (v/v) penicillin and streptomycin, and 1% (v/v) L-glutamine. Phenol red served as a pH indicator to measure nutrient depletion.

MIN6 cells (Passages 30–50) were maintained in DMEM as monolayers in T25 or T75 flasks (the number indicating surface area in cm^2) containing 8 or 15ml DMEM under aseptic conditions to avoid contamination with bacteria or yeast. The medium was changed every 3-6 days. When cell confluency reached 70–90%, cells were sub-cultured or harvested by trypsinisation and used in experiments. For adherent cultures, cells need to be detached: this is commonly achieved by trypsinisation, which is a process of cell detachment and separation using 0.1% trypsin/0.02% EDTA. Trypsin digests the attachment sites to the flask surface, whereas EDTA binds to calcium ions required for cell-to-cell calcium-dependent adhesion (Figure 2.1). MIN6 cells were exposed to 1.5ml trypsin/EDTA at 37°C for 3-5 min to avoid over-digestion due to proteolytic activity of trypsin. To help cells detach, the flask was tapped against the palm then medium containing serum was added to the flask to inactivate trypsin. The cell suspension was centrifuged

at 1300rpm for 3min, the supernatant was aspirated, and the cell pellet was resuspended in 1ml of DMEM for cell counting.

Figure 2.1. Light microscopy images of MIN6 cells (P35) in culture at magnifications x20 (A) and x40 (B). MIN6 cells disassociated with trypsin and EDTA at magnification x40 (C).

2.1.3. Cell counting

The cell concentration is calculated for seeding cells into plates and to adjust the amount of the reagents required for each experiment. There are several methods for cell counting. Two methods used in this thesis are manual and automated counting.

Manual counting uses a counting chamber to visualise and count cells. The haemocytometer is a type of counting chamber carved into a piece of thick glass with a depth of 0.1mm and etched squares of $0.1mm^2$. It is commonly used to calculate the density of cells in suspensions based on these chamber dimensions. The cell suspension was mixed with 0.4% (w/v) Trypan blue dye in equal volumes. Trypan blue is a vital stain that allows visualisation of the dead cells with compromised cell membrane integrity, as it is normally excluded from cells with intact plasma membranes. 10µl of the cell suspension-Trypan blue mixture was placed in the space between the chamber and the glass coverslip, filling it by capillarity (Absher, 1973; Cadena-Herrera et al., 2015). The grid visualised under

the light microscope was used to manually count the number of cells within the areas of known volume (Figure 2.2). The distance between the chamber and the coverslip is 0.1mm and the counting squares are $0.1mm^2$, giving a volume of $0.1mm^3$, therefore the concentrations of the cells in suspension can be calculated. The total number of cells was calculated using a formula: *total cell number/ml = average cell number of the four corner squares x* 10^4 *x 2*, which takes into account the dilution in Trypan blue. Cell viability was determined by Trypan blue staining and non-viable cells, which were usually less than 5%, were excluded from the final count. Although manual counting is cheap, it has several disadvantages due to human perception, definition of cells, and counting enough cells. Human interference can be avoided by using automated methods, which are faster and allow higher precision. Automated counting was performed using an Invitrogen Countess Automated Cell Counter, with the image analysis software for assessment of cells in suspension. 10µl of cell suspension-Trypan blue mixture was added to the cell counting chamber slide that resembles a haemocytometer. The slide was inserted into the allotted slot on the machine for cells to be counted. Although both methods rely on the same principle, the automated cell counter can provide accurate cell counts for a wider cell concentration range than a haemocytometer and it is less time consuming and more reproducible. However, using a haemocytometer is a cheaper method for measuring cell viability of multiple cell suspensions that allows for a better visualisation and examination of the cells.

Calculation of the number of cells in suspension was used for seeding cells for experimental use by using the formula: *desired cell number per well x total volume / cell concentration.* For experiments in this thesis, MIN6 cells were plated onto 96-well plates at densities of 15,000-20,000 cells/well.

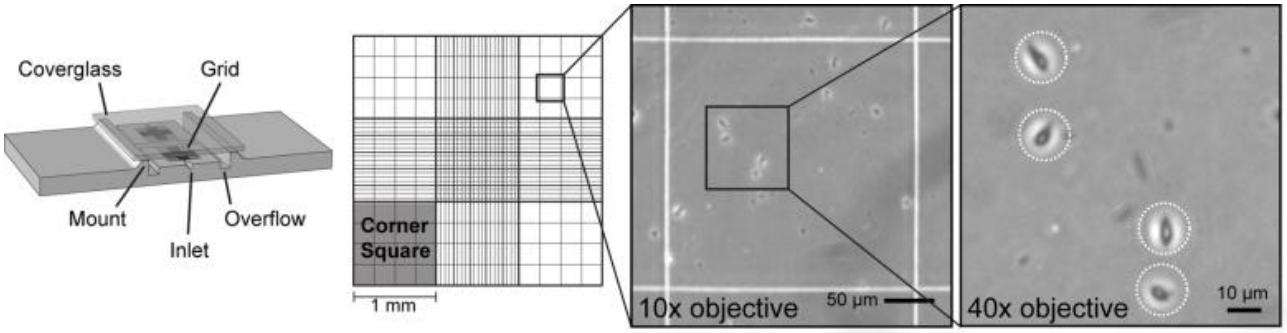

Figure 2.2. Counting cells using a haemocytometer and Trypan blue. 10µl of cell suspension was mixed in equal volumes with Trypan blue and pipetted into the space between the haemocytometer and the coverslip. Four corner squares (1mm by 1mm) were localised, and the average number of cells was calculated. Cells outside the square lines were omitted (Zhang and Kuhn, 2005).

2.2. Islet isolation

Islets of Langerhans secrete hormones that regulate blood glucose and are therefore a key focus of diabetes research. The process of purifying viable and functional islets from mouse or human pancreas is complex and requires several steps. The primary goal of isolating islets is to obtain glucose-responsive, viable islets that can be used for functional analyses. Islet isolation procedure involves pancreas retrieval, enzymatic digestion of the exocrine tissue, and maintenance of isolated islets in culture.

2.2.1. Mouse islet isolation

Mouse islets were isolated from male CD-1 mice (≥20g) aged 8-18 weeks via pancreatic digestion with collagenase (1mg/ml in serum-free Minimal Essential Medium (MEM)). Mice were culled by cervical dislocation or asphyxiation with CO_2. The abdominal cavity was opened following confirmation of death. The ampulla of Vater was clamped, and 2.5ml collagenase solution (1mg/ml collagenase in MEM) was injected into the common bile duct (CBD) (Figure 2.3).

The distended pancreas was separated from the tissues, dissected out, transferred into a 50ml-Eppendorf tube, and placed on ice. The pancreas was then incubated in the water bath at 37°C for 10min to allow enzymatic digestion of the exocrine tissue. 25ml of MEM supplemented with 10% (v/v) newborn calf serum (NCS) was added to stop the reaction, and the remaining tissue pellets were sieved following steps of centrifugation (1400rpm, 10 °C, 1.5min; 1500rpm, 10°C, 1.5min) and passed through a sieve to separate islets from fat and poorly digested exocrine tissue. Islets were further purified by centrifugation (3510rpm, 10 °C, 24min) with MEM and histopaque, which is a polysucrose solution that serves as a density gradient cell separation medium. Islets were then gently removed from the gradient, washed in MEM, hand-picked into the Petri dishes with RPMI medium containing 11mM glucose and supplemented with 10% (v/v) FBS, 1% (v/v) penicillin and streptomycin, and 1% (v/v) L-glutamine, and incubated at 37°C (95%air/5%CO_2).

2.2.1.1. Animal maintenance

Male CD-1 or *ob/ob* mice were housed under controlled conditions (1400 h light:1000 h darkness; lights on at 0700 h; temperature at 22±2 °C) and provided with food and water *ad libitum*. All animal procedures were undertaken in accordance with the United Kingdom Home Office Regulations.

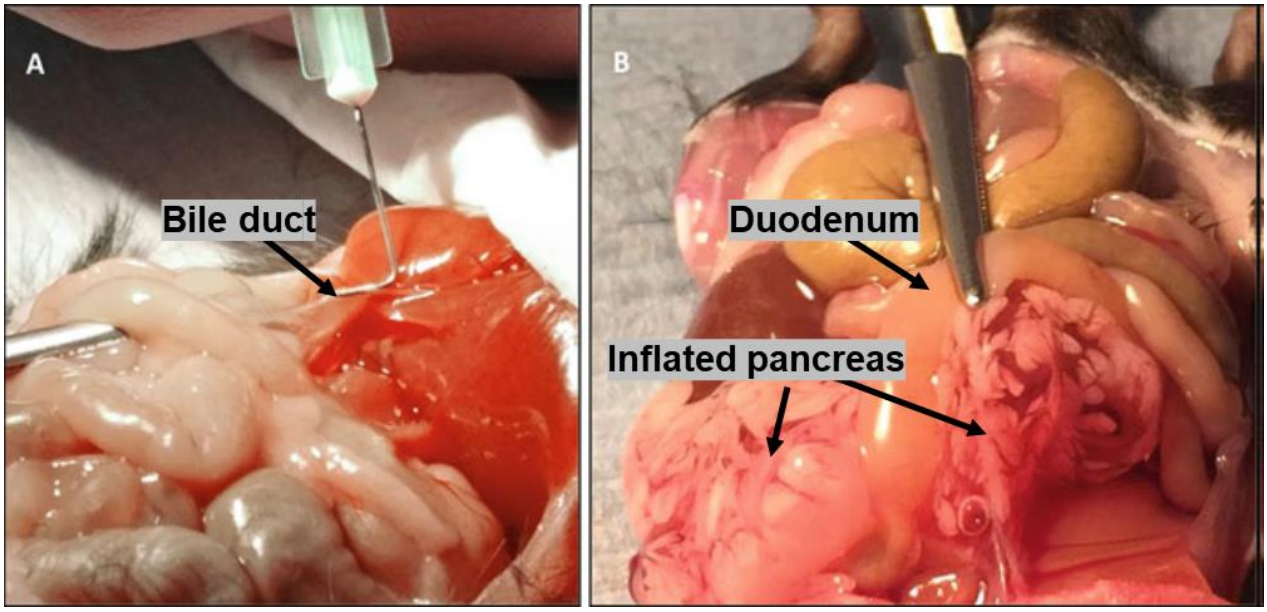

Figure 2.3. Mouse pancreas digestion. Bile duct cannulation (A) and distension of the pancreas by perfusion with collagenase solution (B) (Atanes et al., 2020).

2.2.2. Human islet isolation

Human islets were retrieved from non-diabetic, heart-beating, and brain-dead donors, and isolated through Liberase digestion by the Islet Transplantation Unit at King's College Hospital. The process consists of four major steps: pancreas preparation, perfusion with Liberase, pancreas digestion in the specially designed chamber, and islet purification (Figure 2.4). Islets were then maintained in culture in CMRL medium containing 5.5mM glucose and supplemented with 10% (v/v) FBS, 1% (v/v) penicillin and streptomycin at 37°C (95%air/5%CO_2).

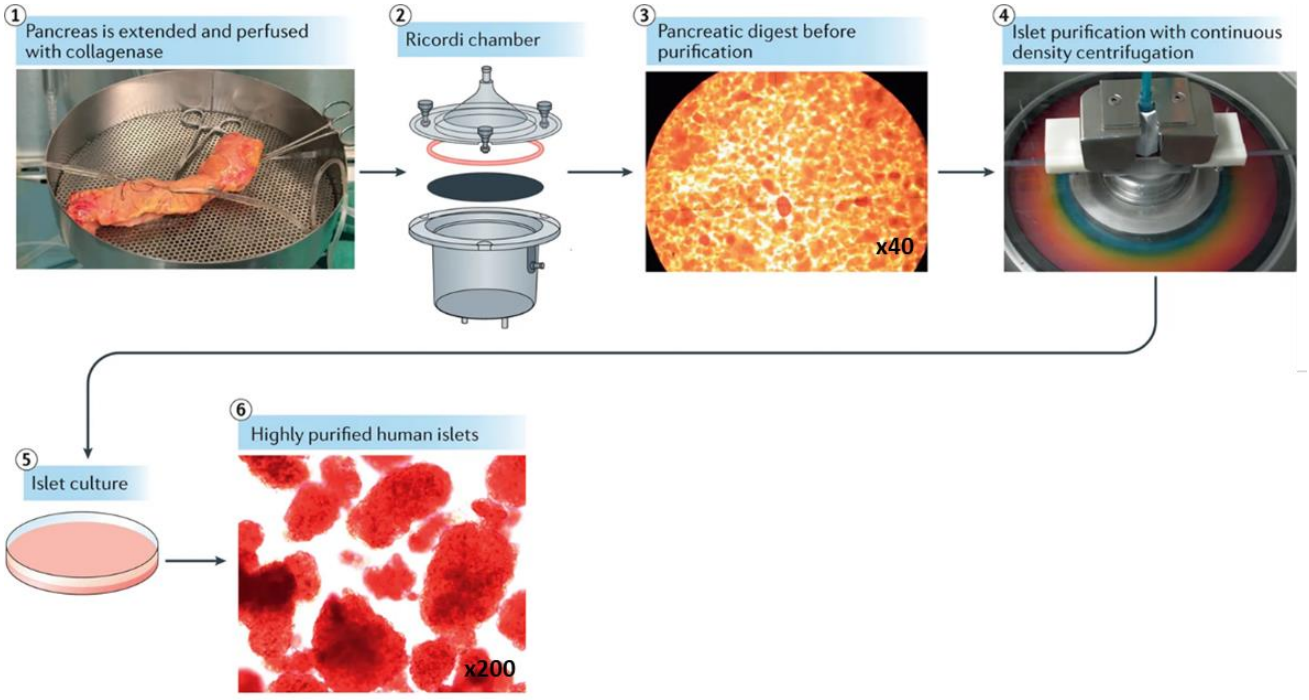

Figure 2.4. The main steps of human islet isolation. Perfusion of the distended pancreas with collagenase solution (1). Schematic of Ricordi chamber (2). Pancreatic digest with islets stained red with dithizone (3). COBE 2991 cell apheresis system with continuous Biochrom osmotic gradients (4). Islet culture prior to experimental use (5). Purified human islets (red) (6) (Shapiro et al., 2017).

2.2.3. Maintaining islets in culture

Mouse or human islets were maintained in culture at 37°C (95%air/5%CO_2) in RPMI medium containing 11mM glucose and supplemented with 10% (v/v) FBS, 1% (v/v) penicillin and streptomycin, and 1% (v/v) L-glutamine for 48h. The medium was changed every 24-48h.

2.3. Monolayer primary islet cell culture

High resolution imaging studies of islet biology have been limited by insufficient techniques to culture monolayers of primary islet cells. The culture of islet cells on glass surfaces is a novel method that allows high resolution imaging (Phelps et al., 2017). Beta cell lines, including MIN6 cells, can also be cultured on glass, but they lack the signalling input of non-beta endocrine cells (Skelin et al., 2010). Although two-dimensional culture of dispersed islet cells is possible on plastic surfaces, it requires coating with cell-derived extracellular matrices, including extracellular matrix secreted from human carcinoma cells or bovine corneal epithelial cell matrix, which have high batch-to-batch variability and they are linked to beta cell redifferentiation (Kaido et al., 2006; Phelps et al., 2017; Weinberg et al., 2007). Therefore, for monolayer primary islet cell culture, the glass coverslips were coated with a defined surface coating of laminin in the presence of neurobasal media GlutaMAX (Gibco) containing the B-27 neuronal growth supplement to promote cell adhesion and spreading. B-27 contains growth factors, antioxidants, and retinoic acid (Brun et al., 2015), as well as insulin that supports islet cell function and survival (Johnson et al., 2006). The neurobasal media was chosen over RPMI as RPMI contains high levels of neuroactive amino acids that potentially decrease viability of dispersed rat and human islet cells, whereas neurobasal medium is associated with higher viability of islet cell cultures in a monolayer when compared to RPMI (Phelps et al., 2017).

This method enables adhesion and formation of monolayers of well-connected and fully differentiated mouse and human islet endocrine cells.

2.3.1. Preparation of matrix-coated coverslips

Round borosilicate glass coverslips (12mm diameter and 0.17mm thickness) were transferred to 24-well plates and coated with laminin from Engelbreth-Holm-Swarm murine sarcoma basement membrane at 50µg/ml in Ca^{2+}/Mg^{2+}-supplemented Hanks Balanced Salt Solution (HBSS) overnight at 37°C. The coverslips were washed in Ca^{2+}/Mg^{2+}-supplemented HBSS and left to dry for 10min prior to seeding.

2.3.2. Preparation of mouse and human islet cell monolayer cultures

Mouse islets were isolated from pancreases of CD-1 male mice (8-12 weeks) as previously described in Section 2.2.1. Human islets were obtained from the Islet Transplantation Unit at King's College Hospital (Section 2.2.2). Groups of 500 hand-picked islets were cultured at 37°C in 10cm non-adherent cell culture dishes in MEM supplemented with 5.5mM glucose, 10% (v/v) FBS, 1% (v/v) penicillin and streptomycin, and 1% (v/v) L-glutamine. Mouse or human islets were hand-picked from suspension cultures after 24h, collected in 15ml tubes, and washed in PBS. Islets were dissociated into a suspension of single cells through trypsin digestion. 300µl 0.05% trypsin-EDTA was added to 1.5ml Eppendorf tubes containing 500 islets and pipetted continuously for 3min at 37°C using a heat block. Trypsin digestion was stopped by adding neurobasal media supplemented with 5% (v/v) FBS, 1x B-27, 1% (v/v) penicillin and streptomycin, and 10mM Hepes buffer to a total volume of 15ml. Islet cells were pelleted by centrifugation for 5min at 1400rpm, resuspended in neurobasal media, then seeded at a density of

35,000 cells/cm^2 on laminin-coated glass coverslips. Islet cells required 3-4 days of culture to adhere and spread on the glass surfaces, and 10-14 days to form pseudoislets, which were used experimentally. Culture medium was changed every 2 days.

2.4. Gene expression

Gene expression studies rely on polymerase chain reaction (PCR), a common technique that allows amplification of DNA fragments rapidly by several orders of magnitude. Using PCR, copies of a very small amount of DNA sequences are exponentially amplified in cycles of temperature changes. PCR is performed following two steps: total RNA extraction and cDNA synthesis.

2.4.1. RNA extraction

Total RNA was isolated from 1 x 10^6 MIN6 cells, 200 isolated mouse islets and 200 human islets using the Qiagen RNeasy Spin Column kit. MIN6 cell and islet pellets were lysed in 700µl RTL buffer, which contains a high concentration of guanidine isothiocycanate to support the binding of RNA to the column membrane. RLT buffer was supplemented with 1% (v/v) of a reducing agent β-mercaptoethanol (β-ME), which is important for effective inactivation of RNAses in the lysate. The lysate was then passed through the QIAshredder homogeniser, and each column was centrifuged at 12,000rpm for 2min. Homogenisation allows disruption of the cells and prevents sample degradation. One volume of 70% ethanol was added to the homogenised lysates, mixed by pipetting, and transferred into the RNeasy spin columns. The columns were centrifuged at 12,000rpm for 2min and the flow-through was discarded. 350µl of buffer RW1, containing guanidine salt and ethanol, was added to the column to wash the membrane-bound RNA from biomolecules, the columns were then centrifuged at 12,000rpm for 2min, and

the flow-through was discarded. The presence of genomic DNA in RNA samples can lead to false positive results. Therefore, DNA digestion was carried out by adding 80µl of DNase incubation mix (10µl DNase I solution and 70µl buffer RDD) to ensure that only RNA remains bound to the column. After 15 min, the columns were washed with buffer RW1, centrifuged at 12,000rpm for 2min, and the flow-through was discarded. The columns were exposed to 500µl of a mild washing buffer called buffer RPE, centrifuged again, and the flow-through was discarded. Empty columns were spun for 1min to dry, and total RNA was eluted with 30µl RNase-free water (Figure 2.5). Total RNA purity and concentration were assessed using a Nanodrop Microvolume spectrometer that measures 260/280 and 260/230 ratios. Values lower than 2 may indicate protein, phenol, or carbohydrate contamination. RNA samples were then stored at -80°C.

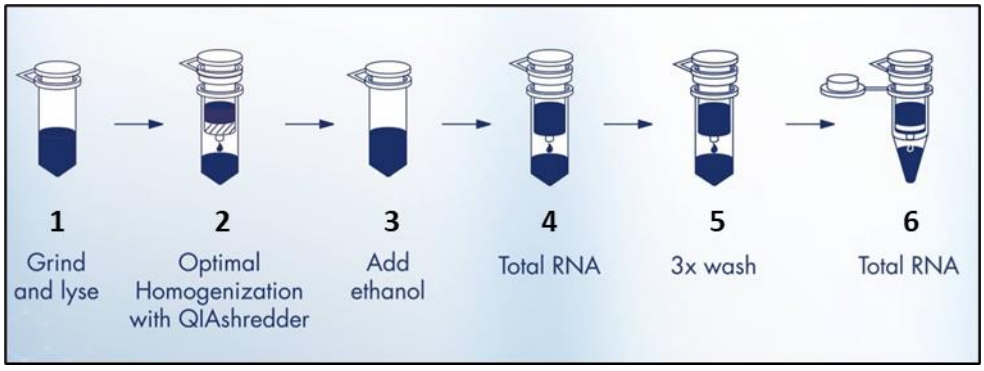

Figure 2.5. Major steps of RNA extraction using RNeasy and QIAshredder. The sample was lysed with RLT buffer (1) and homogenised to shear genomic DNA and reduce viscosity of lysate (2). 70% ethanol was added to adjust binding conditions and inactivate RNases to ensure purification of highly intact RNA (3). After that, the protocol followed the standard bind-wash-elute steps. The sample was applied to RNeasy spin column for RNA adsorption to the membrane (4), RW1 and RPE buffers were used to wash off possible contaminants (5), and total RNA was eluted in water (QIAGEN GmbH, 2013).

2.4.2. Reverse Transcription

Reverse transcription is a process of cDNA synthesis from an RNA template using a reverse transcriptase enzyme (RT). The synthesis of the first cDNA strand is directed by the RNA template and short random primers complementary to the 3' end. The dNTP mix serves as building blocks for DNA synthesis. The Applied Biosystems High-Capacity cDNA Reverse Transcription Kit contains all components necessary for the quantitative conversion of RNA to single-stranded cDNA (Table 2.1). The 0.2ml Eppendorf tubes containing cDNA (10-50ng/µl) and master mix were loaded onto a PCR Thermal Cycler, and the thermal cycling conditions were: 25^{o}C for 10min, 37^{o}C for 2h, 85^{o}C for 5min, and 4^{o}C. The kit was used to synthesise cDNA from the collected RNA, and its downstream applications included standard PCR and real-time PCR.

Table 2.1. Components of the High-Capacity cDNA Reverse Transcription Kit.

Component	Volume (µl) /Reaction	Final concentration
10x RT buffer	2	1x
25x dNTP mix (100mM)	0.8	4mM
10x RT random primers	2	1x
MultiScribe Reverse Transcriptase (50U/µl)	1	2.5U/µl
Nuclease-free water	3.2	-

2.4.3. Polymerase chain reaction (PCR)

PCR is an invitro method of DNA replication, and a single cycle consists of denaturation, annealing and elongation steps. During denaturation (94–98°C for 20–30 seconds), double-stranded DNA is broken into two single-stranded DNA

molecules. When the temperature is lowered (50–65°C for 20–40 seconds) primers anneal to each of a single stranded DNA template. The primers are single-stranded sequences that complement short regions at the 3' end of each DNA strand. Annealing is followed by elongation (72-80°C). In this step, the DNA polymerase synthesises a new DNA strand complementary to the DNA template strand by adding free dNTPs from the master mix to the template in the 5'-3' direction (Rychlik et al., 1990). With each cycle, the original template strands and all newly generated strands become template strands for the next round of elongation, leading to exponential amplification of the specific DNA region, making it possible to obtain a large quantity of DNA for analysis or further experiments.

Standard PCR was used to amplify MIN6 cell and islet cDNAs and identify gene products of interest. A master mix was prepared (Table 2.2), and the reaction volume was set to 20µl: 19µl master mix and 1µl cDNA was mixed in a 0.2ml PCR tube and loaded onto a RT-PCR Thermal Cycler. The cycling conditions were 94^{o}C for 30 sec, 58^{o}C for 30 sec, 72^{o}C for 1 min.

Agarose gel electrophoresis was used to determine sizes of the reaction products. A 1.8% gel was prepared by adding 50ml of 1x TBE buffer (Table 2.3) to 900mg of agarose. Ethidium bromide (5µl) was then used as a fluorescent tag to stain nucleic acids. The cDNA molecules and a molecular weight marker (ladder) were loaded onto the agarose gel and run at 100V. After 30 min, DNA was visualised using the UV light. DNA molecules were separated by size within a gel, the distance travelled was compared to the DNA ladder bands, and the approximate sizes of cDNA molecules were identified.

Table 2.2. Master mix used for the standard PCR.

Component	Volume (µl) /20µl Reaction	Final concentration
10X Buffer	2	1x
$MgCl_2$ (25mM)	1.2	2.5mM
dNTPs (40mM)	0.8	1.6mM
10x Qiagen QuantiTect primer	2	1x
Taq polymerase (5U/µl)	0.2	-
Nuclease-free water	12.8	-

Table 2.3. Components of 10x TBE buffer. 1x TBE buffer (gel running buffer) was prepared with RNase-free H_2O by diluting 100ml to 1l.

Component	Amount (g) /1l dH_2O	Final concentration
Tris base	121.1	1M
Boric acid	61.8	1M
EDTA	7.4	0.02M

2.4.4. Quantitative PCR

While standard PCR uses gel electrophoresis to visualise the amplified reaction products, real-time quantitative PCR (RT-qPCR) can detect amplifications during the early phases of the reaction. The advantage of this method is that it is quantitative. Data are collected during the exponential growth phase when the amount of the product is directly proportional to the amount of the template (Kralik and Ricchi, 2017).

There are two types of methods used to detect PCR products using real-time PCR: SYBR Green–based detection and TaqMan-based detection. The SYBR Green-based method uses a dsDNA binding dye to detect PCR products as it accumulates during PCR, while TaqMan uses a fluorogenic probe specific to the target gene.

A master mix for the SYBR green-based method was prepared (Table 2.4) and 9µl of this was pipetted into wells of a 96-well plate. 1µl of cDNA sample (1000ng/20µl reaction) or water (blank) was then added to the appropriate wells. RT-qPCR was performed using a LightCycler 480 thermal cycler. Specificity of the PCR products were determined by the melting curve analysis followed by agarose gel electrophoresis to determine sizes of amplicons.

Table 2.4. Components of the SYBR Green master mix used for the RT-qPCR.

Component	Volume (µl) /Reaction
SYBR Green master mix	5
Qiagen QuantiTect primer (Table 2.5)	2
cDNA	1
Nuclease-free water	2

Table 2.5. Qiagen QuantiTect primers.

Protein	Gene	Catalogue number (Mouse)	Catalogue number (Human)
SERT	SLC6A4	QT00058380	QT00058380
5-HT2B	HTR2B	QT00060368	QT00144704
5-HT3A	HTR3A	QT01039885	QT01002687
5-HT1F	HTR1F	QT00102242	QT01002673
D2	DRD2	QT01169063	QT00012558

2.5. Protein expression

Protein expression is a functional read-out of gene expression that gives indication of how much protein is present in a sample. Protein quantification was performed by Western blotting and fluorescent immunohistochemistry (IHC). The two methods rely on the principle of antibody-antigen interactions. Western blotting allows detection of a specific protein, whereas IHC additionally visualizes the presence of a protein within a cell.

2.5.1. Protein extraction and quantification

Proteins were extracted from MIN6 cells, mouse islets and human islets by using the radioimmunoprecipitation assay (RIPA) lysis buffer (Table 2.6). The buffer enables protein extraction from the membrane, cytoplasm, and nucleus without initiating protein degradation. 500µl of RIPA buffer was added to the 1.5ml Eppendorf tube containing 300,000 MIN6 cells or 200 islets pre-washed in PBS. The samples were incubated for 5-15min on ice, sonicated to facilitate lysis, and centrifuged at 8000rpm for 10min at 4°C. For the measurement of MAPK, CREB and Akt phosphorylation following fluoxetine treatment, MIN6 beta cells were seeded into 6-well plates, and they were incubated in DMEM in the absence or presence of fluoxetine (1µM) for 24h. Parallel groups of MIN6 cells were treated with 10µM forskolin (FSK) for the final 10min as a positive control. 100µl of RIPA buffer with phosphatase and protease inhibitors (1 tablet each; Pierce™ Protease Inhibitor Mini Tablets and PhosSTOP EASYpack) was used to lysate the cells. The samples were incubated for 30min on ice, sonicated every 10min to facilitate lysis, and centrifuged at 8000rpm for 10min at 4°C.

Protein contents were quantified using the BCA method.

Table 2.6. Components of RIPA buffer.

Component	Volume (ml) / 100ml dH_2O	Final concentration
Sodium chloride (5 M)	3	150mM
Tris-HCl (1 M, pH 8.0)	5	50mM
Nonidet P-40	1	1% (v/v)
Sodium deoxycholate (10 %)	5	0.5% (v/v)
SDS (10 %)	1	0.1 (v/v)

Sample volume and total protein concentration were measured using the Pierce BCA Protein Assay kit, which is based on bicinchoninic acid having high specificity for cuprous (Cu^{+}) ions, which are formed when proteins reduce cupric (Cu^{2+}) ions in the copper sulphate of the assay reagent. The purple-coloured product of the reaction exhibits absorbance at 562nm, which is linear with increasing protein concentrations. A set of protein standards was prepared by diluting bovine serum albumin (Table 7). Samples, standards, and BCA working solution were added to a 96-well plate and incubated for 30 min at 37°C. Absorbance was read using a microplate reader, and the protein concentrations were calculated using a standard curve generated by plotting absorbance against BSA concentrations (mg/ml) as shown in Figure 2.6.

Table 2.7. Preparation of diluted albumin (BSA) standards.

Vial	Volume of diluent (RIPA buffer)	Volume and Source of BSA (µl)	Final BCA concentration (µg/ml)
A	0	300 of Stock	2,000
B	125	375 of Stock	1,500
C	325	325 of Stock	1,000
D	175	175 of B dilution	750
E	325	325 of C dilution	500
F	325	325 of E dilution	250
G	325	325 of F dilution	125
H	400	100 of G dilution	25
I	400	0	0 (Blank)

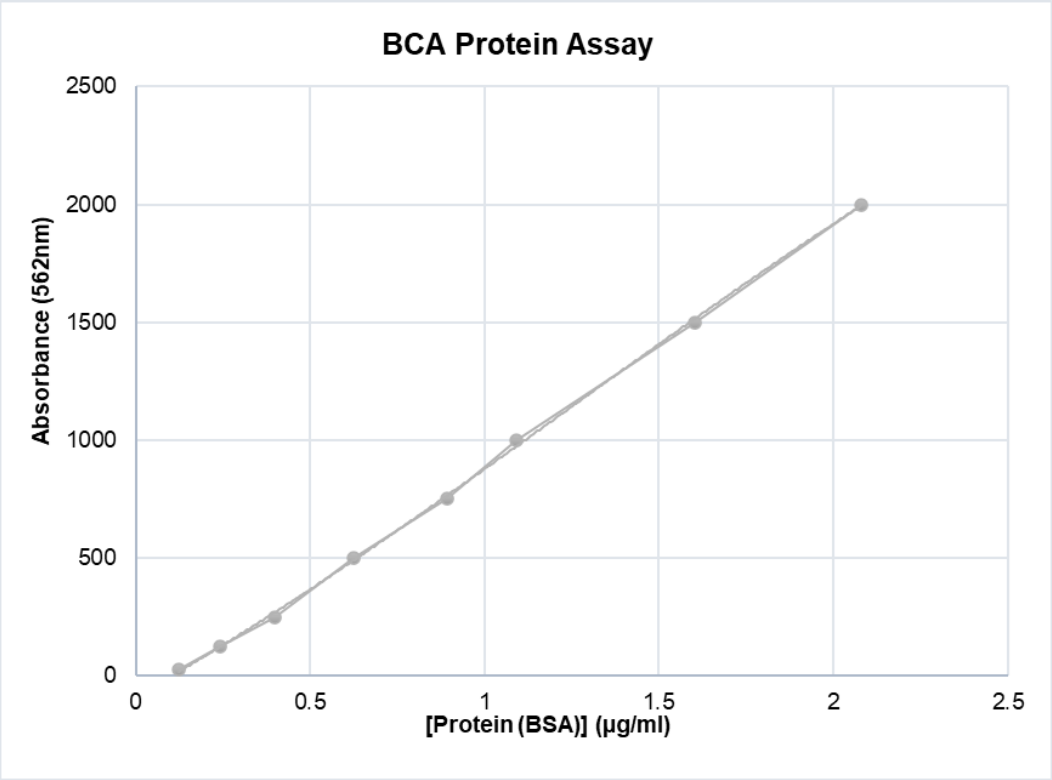

Figure 2.6. Typical standard curve for bovine serum albumin (BSA) in the BCA Protein Assay.

2.5.2. Western Blotting

Western blotting, also called protein immunoblotting, is an analytical technique used to detect specific proteins in a sample of tissue homogenate. In this technique, proteins are separated based on molecular weight through polyacrylamide gel electrophoresis and immunostained with antibodies directed against antigens of interest.

Proteins in MIN6 cell and islet lysates were separated by their molecular masses in an electric field using sodium dodecyl sulphate polyacrylamide gel electrophoresis (SDS-PAGE). For the Western blotting experiments in this thesis, proteins were separated using commercially available 4-12% NuPAGE gels. The gel was placed in a mini cell apparatus filled with the running buffer (Table 2.8). 1.5% SDS dye was added to the protein lysates obtained from MIN6 cells and islets, and a molecular weight marker, before heating up to boiling and loading onto the gel. The gel was run at 200V constant voltage for 1h. Proteins were then transferred onto the polyvinylidene fluoride (PDVF) membrane to later identify target proteins based on the specificity of the antibody-antigen interaction. A cassette containing the gel, membrane, and filters, was soaked in the transfer buffer (Table 2.9) and run at 30V for 2h. The presence of the proteins on membrane was then confirmed with Ponceau S staining. The membrane was washed in PBS to wash off the stain and incubated in the blocking buffer (5% w/v milk-TBST) (Table 2.10) for 1h at room temperature to prevent the non-specific binding of antibodies (including both primary antibody and secondary antibody) to the membrane. After blocking, the membrane was incubated overnight at 4°C with the appropriate primary antibody (Table 2.11). Following five washes in TBST, the membrane was incubated for 1h at room temperature with the correct secondary antibody diluted in TBST (Table 2.12). Secondary antibody was washed

off with TBST, and the immunoreactive proteins were identified by exposing the membrane to ECL reagent (0.1ml/1cm^3). In the dark, photographic film visualised light emission produced by the reagent substrate, and the protein sizes were extrapolated from the marker.

Table 2.8. Reagents required to prepare 20x MOPS running buffer. This was diluted to 1x for western blotting.

Components	Amount (g) /500ml distilled water	Final concentration
MOPS	104.6	1M
Tris Base	66.6	1M
EDTA	10	20mM
SDS	3	69.3mM

Table 2.9. Preparation of the 1x transfer buffer used for Western blotting.

Components	Volume (ml)
Distilled water	749
10x NuPAGE Transfer buffer	100
Antioxidant	1
Methanol	100

Table 2.10. Preparation of 10x TBST. The pH was set to 7.6 with 12N HCl.

Components	Amount (g)/250ml distilled water	Final concentration
Tris base	749	20mM
NaCl	100	150mM

Table 2.11. Primary antibodies used in the Western blotting experiments.

Primary antibody against	Description	Dilution	Catalogue number
SERT	Rabbit polyclonal anti-SERT	1:10,000	Ab130130
P-MAPK	Rabbit polyclonal anti-phospho-MAPK	1:1,000	9211S
P-CREB	Rabbit monoclonal anti-phospho-CREB	1:1,000	9198
P-Akt	Rabbit polyclonal anti-phospho-Akt	1:1,000	9271
Beta ACTIN	Mouse monoclonal anti-beta actin	1:5,000	A2228

Table 2.12. Secondary antibodies used in the Western blotting experiments.

Secondary antibody	Dilution	Catalogue number
HRP-conjugated anti-rabbit	1:10,000	A17345
HRP-conjugated anti-mouse	1:100	31430

2.5.3. Fluorescent immunohistochemistry

Fluorescent immunohistochemistry is used to quantify cellular localisation and abundance of specific proteins in a tissue section. The process consists of four main steps: fixation, antigen retrieval to increase availability of proteins for detection, blocking to minimise background staining, antibody labelling, and visualisation by fluorescent microscopy.

Freshly dissected mouse pancreases were fixed in paraformaldehyde (4%) for 3h to prevent protein degradation. Fixed pancreases were passed through xylene and graded ethanol (100%-70%) to remove water from the tissues prior to embedding in paraffin. Wax blocks were cut to 5µm slices with the microtome Leica RM2255, treated with 90% ethanol and water (40°C), then mounted onto microscope slides and kept at room temperature.

The paraffin was removed from sections by heating the slides at 60°C for approximately 1min to gain access to the pancreatic tissue. The remaining paraffin was removed by submersion into 100% xylene, followed by gradual rehydration in ethanol (100%, 95%, 70%). Tissue sections then underwent an antigen retrieval process to expose the antigenic sites masked during the tissue fixation process. Sections were placed in a pressure cooker filled with a citric acid working solution (10mM, 0.05% Tween-20, pH 6) at 175°C, and heated in the microwave for 15min. Slides were then exposed to running water for 10min for cooling. These steps were omitted for the staining of pseudoislets on glass coverslips that had been fixed with 4% PFA because paraffin was not used in these experiments. After the antigen retrieval step, sections prepared for anti-BrdU antibody incubation were additionally exposed to 2N HCl for 10min at 37°C to denature DNA and 0.1M borate buffer (pH 8.5) for 10min to neutralise. Individual sections on slides were incubated in the blocking buffer (1%BSA +

10%goat serum in 0.1% PBST) for 1h at room temperature to eliminate non-specific binding of the antibodies. Sections were incubated with the primary antibodies (Table 2.13) overnight at 4°C and washed in PBS. The slides were subsequently exposed to the secondary antibodies (Table 2.14) for 1h at room temperature, washed in PBS, and incubated with DAPI (1:500) for 5min. Fluoromount aqueous mounting medium was then used for mounting. Images of the sections were taken with the Nikon eclipse TE2000U fluorescent microscope or Eclipse Ti-E Inverted A1 inverted confocal microscope. The images were analysed using ImageJ software.

Table 2.13. Primary antibodies used for immunostaining.

Primary antibody against	Description	Dilution	Catalogue number
Insulin	Guinea pig polyclonal anti-insulin	1:100	Dako A0564
BrdU	Rat monoclonal anti-BrdU	1:100	Bio-Rad OBT0030S
SERT	Rabbit polyclonal anti-SERT	1:200	Abcam 130130
Ki67	Rabbit polyclonal anti-Ki67	1:200	Abcam 15580
CD80	Rabbit monoclonal anti-CD80	1:200	Ab238648
Glucagon	Mouse monoclonal anti-glucagon	1:1000	MilliporeSigma G2654
Somatostatin	Rat monoclonal anti-somatostatin	1:50	Abcam 30788
Serotonin	Rat monoclonal anti-serotonin	1:200	sc-58031
D2	Goat polyclonal anti-D2	1:200	Abcam 30743

Table 2.14. Secondary antibodies used for immunostaining.

Secondary antibody	Dilution	Catalogue number
Alexa-fluor 594 anti-guinea pig IgG	1:100	Jackson immunolab 706-585-148
Alexa fluor 594 donkey anti-rat IgG	1:100	Jackson immunolab 712-585-150
Alexa fluor 594 donkey anti-mouse IgG	1:100	Jackson immunolab 715-585-150
Alexa fluor 488 donkey guinea pig IgG	1:100	Jackson immunolab 706-545-148
Alexa fluor 488 donkey anti-rabbit IgG	1:100	Jackson immunolab 711-545-152
Alexa fluor 488 goat anti-rabbit IgG	1:1000	Invitrogen A11070
Alexa fluor 488 goat anti-mouse IgG	1:1000	Invitrogen A11029
Alexa fluor 488 goat anti-rat IgG	1:1000	Invitrogen A11006
Alexa fluor 488 goat anti-guinea pig IgG	1:1000	Invitrogen A11074
Alexa fluor 488 goat anti-rabbit IgG	1:1000	Invitrogen A21428

2.6. Cell proliferation

Beta cell mass is determined by the overall cell number and size, and since control of blood glucose levels depends on appropriate insulin secretion, it is important to maintain adequate beta cell mass. Beta cell mass may adapt in response to increased physiological demands for insulin, such as increased body mass, pregnancy, or during development of T2D (Section 1.4.2). Therapeutics that act on beta cells to promote insulin secretion have been in use to treat T2D for years. However, with the increasing incidence of diabetes comes a requirement for new treatments that can both increase beta cell mass and insulin secretion.

2.6.1. BrdU ELISA proliferation assay

Proliferation of MIN6 cells was investigated using the Cell Proliferation ELISA, BrdU (colorimetric) Kit. MIN6 cells were seeded into 96-well plate at a density of 20,000/well. Cells were incubated with FBS-free DMEM supplemented with 5.5mM glucose and in the absence or presence of a drug of interest for 48-96h. 10% FBS served a s a positive control, as it provides growth factors that stimulate cell division. MIN6 cells were then labelled with a BrdU labelling reagent and incubated for 2h at 37°C (95%air/5%CO_2). The cells were subsequently fixed and denatured for 30min using a FixDenat solution, and then incubated with an antibody directed against BrdU for 90min. Substrate solution was added to the wells following a washing step. The reaction was stopped with 1M H_2SO_4, and absorbance was determined at 450nm using a microplate reader.

2.6.2. Ki67 staining of mouse and human pseudoislets

Proliferation of mouse and human pseudoislet cells that formed three-dimensional clusters on laminin-coated coverslips was assessed by immunohistochemistry. Pseudoislets were stained with an antibody that detected the proliferative marker Ki67, as described in Section 2.5.3. Ki67 was chosen over BrdU because the islet BrdU treatment protocol requires minimum 5 days of culture, and extended culture of pseudoislets could lead to significant changes in gene expression of pseudoislet cells when compared to primary islets and newly formed pseudoislets (Figure 2.7).

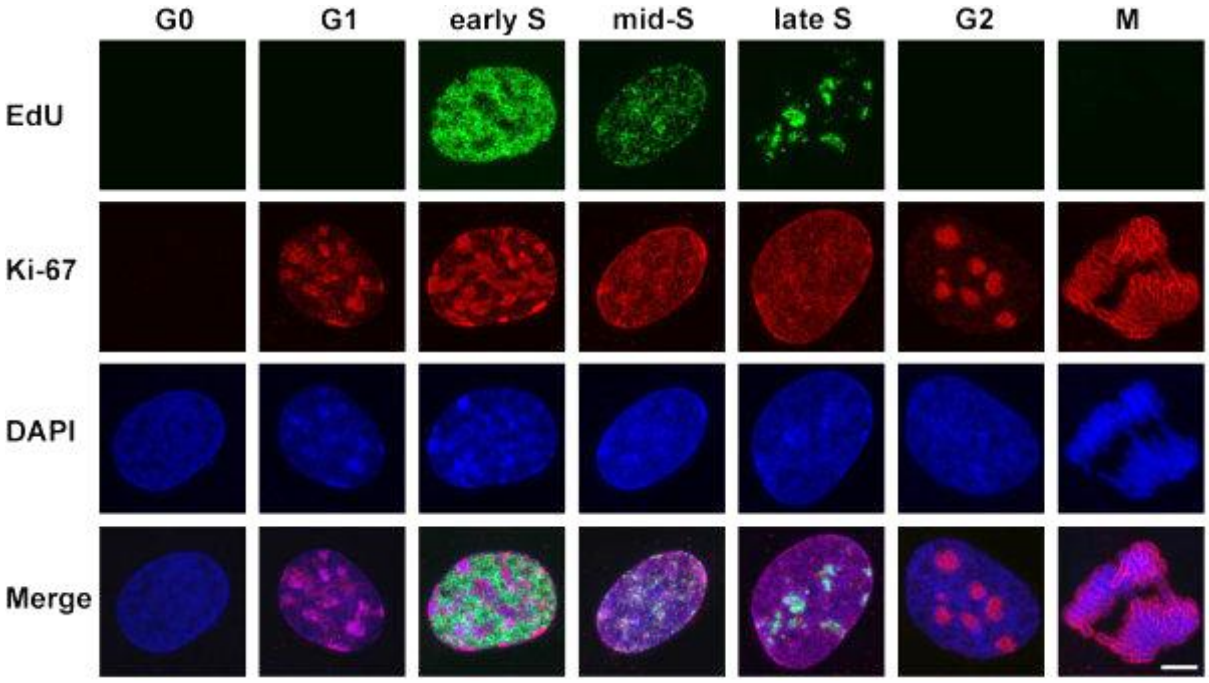

Figure 2.7. Staining patterns of Ki67 and EdU (thymidine analogue, similar to BrdU) in Syrian hamster nuclei at different phases of the cell cycle (G0, G1, S, G2 and M). The images were split into green, red and blue channels that show Ki67, EdU and DAPI staining, respectively. Scale bar = 5µm. (Solovjeva et al., 2012).

2.7. Cell viability and ATP production

Cell viability assays are usually based on quantifying the ratio of live to dead cells and used for evaluating *in vitro* effects of drug candidates, such as cytotoxicity, to optimize experimental conditions. Methods involved in assessing cell viability in this thesis were the Trypan blue exclusion assay and Cell-Titer Glo assay.

2.7.1. Trypan blue exclusion assay

Cell membrane integrity following incubation with a drug of interest was measured using the Trypan blue staining. Trypan blue is routinely used as a cell stain to assess cell viability using the dye exclusion test. Dead cells have a compromised cell membrane that is permeable to the dye and appear blue by light microscopy (Strober, 2015). This test is often performed while counting cells with the haemocytometer, as described in Section 2.1.3.

MIN6 cells were seeded into 6-well plates at a density of 300,000 cells per well and left to adhere overnight at 37°C (95%air/5%CO_2) in DMEM (25mM glucose). The cells were incubated in the culture media in the absence or presence of drugs of interest for 48h. Cell viability was assessed by incubation of MIN6 cells in a Trypan blue solution (0.2% w/v) for 15min. Cells were visualised using a Nikon TMS phase contrast microscope and photographs were obtained with a Canon EOS 4000D camera (Tokyo, Japan). Stained and non-stained cells were also counted using a haemocytometer, and percentage viability was calculated as percentage of non-stained cells over total cell number.

Mouse or human islets were incubated in RPMI (11mM glucose) supplemented with 10% (v/v) FBS, 1% (v/v) penicillin and streptomycin, and 1% (v/v) L-glutamine without or with a drug of interest for 48h, and islet cell membrane integrity was investigated by Trypan blue (0.2% w/v) staining for 15 min. The islets were visualised with an Olympus KL300 LED microscope and photographs were taken with a Canon EOS 4000D camera (Tokyo, Japan).

2.7.2. CellTiter-Glo assay

The CellTiter-Glo Luminescent Cell Viability Assay is used to determine the number of metabolically active cells based on quantification of ATP. The use of assay working solution results in cell lysis, followed by generation of a luminescent signal, which is proportional to the amount of ATP present.

MIN6 cells were seeded into opaque-walled 96-well plates at a density of 15,000 cells/well. The cells were incubated with 50µl of DMEM supplemented with 5.5mM glucose and in the absence or presence of a drug for 48h. Equal volumes of the working solution of the reagent (mix of CellTiter Glo buffer and substrate) was added to each well for 15min, and the luminescence was measured by the Turner Biosystems Veritas Microplate Luminometer.

Mouse or human islets were incubated with RPMI and with or without a drug for 48h. Groups of 5 islets were transferred in 50µl appropriate medium to white 96-well plate, and 50µl of the working solution of the reagent was added to the wells for 15min prior to the measurement of luminescence.

2.8. Cell apoptosis

Apoptosis is a type of programmed cell death that helps regulate cell numbers. This intracellular death program is tightly regulated by suicide proteases called caspases. Usually, in adult tissues, apoptosis balances cell division. Rates of apoptosis and proliferation are very low in the adult pancreas. However, apoptosis is a common pathophysiological feature of diabetes, and in T2D, glucose toxicity promotes beta cell death and leads to decreased beta cell mass (Section 1.4.1.). Therefore, apoptosis plays an important role in the pathophysiology of T2D, and there is a great interest in therapeutics that are protective against beta cell death.

2.8.1. Caspase-Glo 3/7 assay

The activation of caspases 3 and 7 that are associated with an apoptotic cascade was detected using the Promega Caspase-Glo 3/7 assay. MIN6 cell and islet apoptosis was induced by exposure to proinflammatory cytokines (0.05U/µl IL-1β, 1U/µl TNF-α and 1U/µl IFN-γ) or 500µM palmitate (Table 2.15). MIN6 cells (15,000/well) were incubated with DMEM containing 5.5mM glucose, while groups of 200 mouse or human islets were incubated with 11mM glucose-supplemented RPMI, with or without a drug of interest for 48h. Cytokines or palmitate were then added to the MIN6 cells or islets for 24h, after which groups of 5 islets in 50µl of medium were transferred to opaque-walled 96-well plates. An equal volume of the working solution of the reagent (mix of Caspase3/7 Glo buffer and luminescent substrate) was added to the wells containing MIN6 cells or islets prior to detection of luminescence by the Turner Biosystems Veritas Microplate Luminometer.

Table 2.15. Preparation of palmitate-containing media for the Caspase-Glo 3/7 assay. Palmitate (13.9mg/ml) was dissolved in 50%EtOH/50%H_2O at 70°C and diluted in 10% BSA (fatty acid-free). In control groups, 50%EtOH/50%H_2O without palmitate was used. Following 1h incubation at 37°C, palmitate or control media were further diluted in DMEM (MIN6 cells; 25mM glucose) or RPMI (islets; 11mM glucose) supplemented with 2% (v/v) FBS, 1% (v/v) penicillin and streptomycin, and 1% (v/v) L-glutamine. The drugs of interest were diluted in either control or palmitate-containing media.

Palmitate concentration	Palmitate	Palmitate control
50mM	13.9mg/ml palmitate + 50%EtOH/50%H_2O (heat at 70°C for 10min)	Only 50%EtOH/50%H_2O
5mM	Dilute 1/10 in 10% fatty acid-free BSA	Dilute 1/10 in 10% fatty acid-free BSA
	Incubate at 37°C for 1h	Incubate at 37°C for 1h
500µM	Dilute 1/10 in DMEM/RPMI+2%FBS	Dilute 1/10 in DMEM/RPMI+2%FBS
	Add the drug and treat the cells for 24h	Add the drug and treat the cells for 24h

2.8.2. Apoptosis assay by flow cytometry

Apoptotic cells demonstrate many morphological and biochemical characteristics. Flow cytometry allows for the measurement of individual cells in solution as they pass by the instrument's laser.

MIN6 cells were seeded into 6-well plate at a density of 100,000cells/well. After overnight culture, cells were incubated with DMEM (5.5mM glucose) in a presence or absence of a drug. Cells were incubated at 37°C (95%air/5%CO_2) for 48 hours, and the cytokines (0.05U/µl IL-1β, 1U/µl TNF-α and 1U/µl IFN-γ) were added 24h prior to flow cytometry assay.

Staining was performed using the Alexa Fluor® 488 annexin V/Dead Cell Apoptosis kit. MIN6 cells were trypsinised, centrifuged at 1600rpm for 3 min, and washed in PBS. Cell pellets were resuspended in 100µl of 1X Binding Buffer and moved to the FACS tubes. 5µl FITC annexin V and 5µl propidium iodide (PI) were added to each tube except controls (unstained cells, cells stained with FITC annexin V alone, and cells stained with PI alone). The tubes were vortexed and incubated in the dark at room temperature for 15 min. 400µl Binding Buffer (red-fluorescent PI nucleic acid binding dye) was added to each tube to stop the reaction, and the samples were analysed using the BD Canto II analyser. After staining the cells with Alexa Fluor 488 annexin V and PI in the provided binding buffer, apoptotic cells showed green fluorescence, dead cells showed red and green fluorescence, whereas live cells did not fluoresce (Figure 2.8).

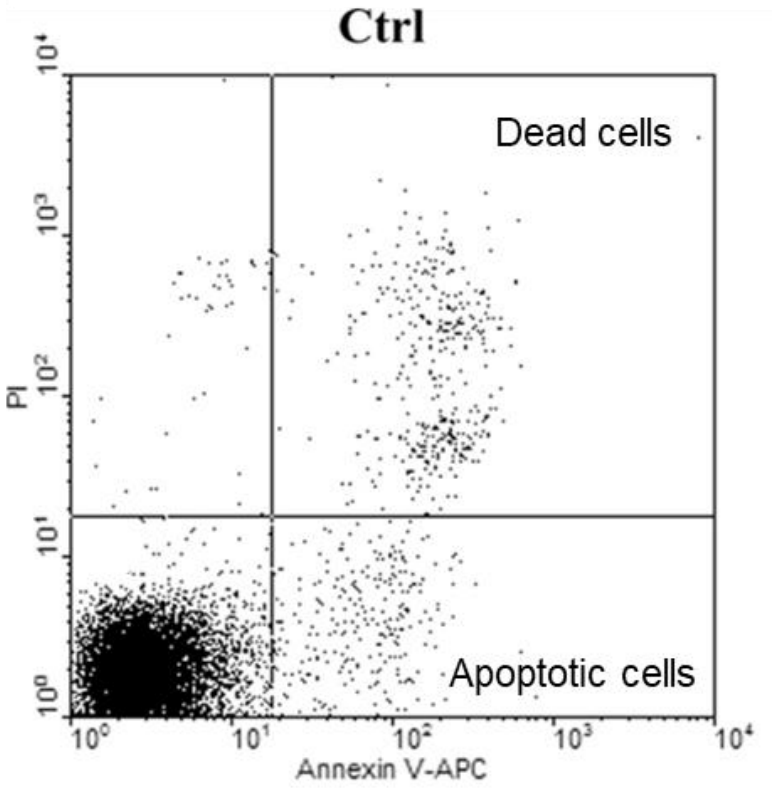

Figure 2.8. Example visualisation of the annexin V FITC and PI staining to measure apoptosis. Apoptotic cells (annexin V-positive) can be seen in the bottom right quadrant, and dead cells (annexin V- and PI-positive) are in the top right quadrant. Viable cells are negative for both stains (Wlodkowic et al., 2013).

2.9. Measurements of insulin secretion

Measurement of insulin secretion is important to detect and understand the changes in beta cell function. There are two common methods to assess insulin secretion from beta cells: static insulin secretion method and perifusion.

2.9.1. Static insulin secretion experiment

The acute and chronic effects of the drugs of interest on insulin secretion from MIN6 cells, mouse islets and human islets were investigated in static insulin secretion experiments.

2.9.1.1. Static insulin secretion experiment using MIN6 beta cells

MIN6 cells (P30-40) were seeded into 96-well plate at a density of 20,000 cells/well. After overnight culture, the cells were washed with PBS and pre-incubated for 2h with DMEM supplemented with 2.5mM glucose. The cells were incubated with DMEM supplemented with either 2.5 or 25mM glucose and in the presence or absence of the appropriate drug for 30min. Muscarinic agonist carbachol at 500µM served as a positive control. The supernatants were kept at -20°C prior to radioimmunoassay.

For chronic exposure, MIN6 cells were incubated with DMEM supplemented with 5.5mM glucose to mimic blood glucose levels in mice and without or with addition of a drug of interest for 48h. Cells were then incubated with DMEM supplemented with either 2.5 or 25mM glucose (without a drug) at 37°C (95%air/5%CO_2) for 30 min to test the responsiveness of beta cells to glucose following drug exposure. Carbachol (500µM) was used as a positive control. The supernatants were kept at -20°C until assay for insulin content.

2.9.1.2. Static insulin secretion experiment using mouse or human islets

In acute experiments, islets were pre-incubated for 1h in a physiological salt solution (Gey and Gey, 1936) (Table 2.16 and 2.17) supplemented with 2mM glucose, and three islets per replicate were transferred to 1.5ml Eppendorf tubes containing 600µl buffer supplemented with either 2mM or 20mM glucose, and in the presence or absence of a drug. Carbachol (500µM) served as a positive control. Islets were then incubated in appropriate buffers with or without a drug for 1h at 37°C (95%air/5%CO_2). 500µl of supernatant was transferred to new tubes and stored at -20°C prior to radioimmunoassay.

In chronic experiments, islets were incubated with RPMI, and without or with addition of a drug for 48-96h. Islets were then pre-incubated for 1h in the physiological salt solution (Gey and Gey, 1936) (2mM glucose). Groups of three islets were transferred to the 1.5ml Eppendorf tubes containing 600µl buffer with either 2mM or 20mM glucose. Carbachol (500µM) served as a positive control. Islets were incubated in appropriate buffers for 1h at 37°C (95%air/5%CO_2), then centrifuged at 2000rpm for 2min at 4°C. 500µl of supernatant was transferred to new tubes and stored at -20°C until insulin content was measured by radioimmunoassay.

Table 2.16. Preparation of 2x Gey and Gey stock solution. The volume was made up to 2l with distilled water.

Components	Amount (g)/ 2l	Final concentration (mM)
NaCl	26	111
KCl	1.48	5
$NaHCO_3$	9.08	27
$MgCl_2$-$6H_2O$	0.84	1
KH_2PO_4	0.12	0.22
$MgSO_4$-$7H_2O$	0.28	0.28

Table 2.17. Preparation of the ready-to-use physiological salt solution (2mM glucose). The pH was set to 7.4 with 95%air /5%CO_2. Physiological salt solution (20mM glucose) was prepared by adding 0.648g glucose to 200ml 2mM glucose-solution.

Components	Amount	Final concentration
2x Gey and Gey stock solution	200ml	1x
Distilled water	200ml	-
Glucose	0.144g	2mM
$CaCl_2$ (1M)	0.8ml	2mM
BSA	0.2g	0.05% (w/v)

2.9.2. Perifusion

Dynamic insulin secretory profile of mouse or human islets to release insulin in response to changes in glucose levels and in the presence of drugs of interest was investigated using a perifusion system (Figure 2.9). Islets were perifused with a physiological salt solution (supplemented with either 2mM or 20mM glucose) and a drug (Table 2.16). Groups of 50 islets were picked into perifusion chambers and exposed to a constant flow (0.5ml/minute) of the physiological buffer with or without a drug for 60 minutes, with perifusates collected every 2 minutes. Samples were stored at -20°C until insulin content was assessed by radioimmunoassay.

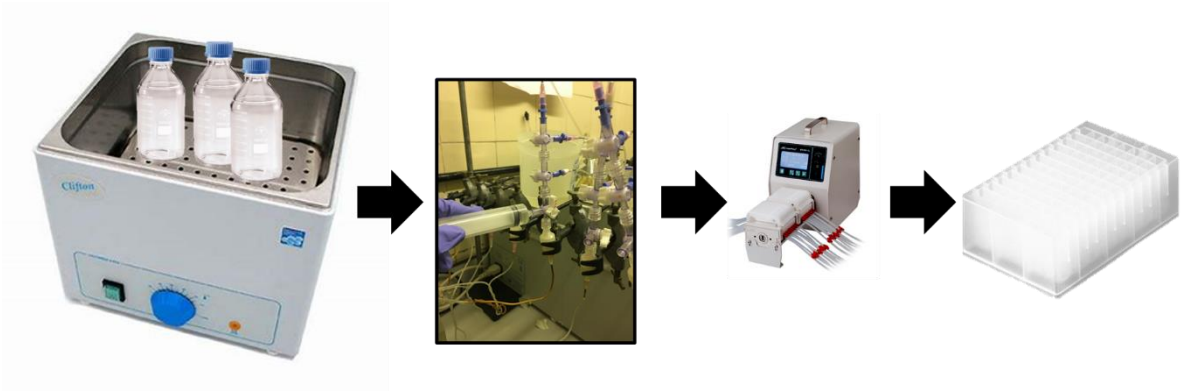

Figure 2.9. The perifusion system consists of a water bath set to 37°C, bottles containing the appropriate buffers, PVC tubes, stopcocks, islet chambers, peristaltic pump, and collection blocks. Direction of the flow of buffers through the tubes is indicated by the arrows.

2.9.3. Radioimmunoassay

The concentration of insulin secreted from MIN6 cells, mouse islets and human islets under experimental conditions was quantified using a radioimmunoassay method, which is based on competitive binding of unlabelled (AG) and radiolabelled insulin (AG*) for limiting antibody (AB) concentrations. AG, standard concentrations of insulin and insulin to be measured, and its corresponding AG* in the tracer compete for the limited number of binding sites on the AB, and achieve an equilibrium as in the following equation:

$$AB + AG + AG^* \leftrightarrow AB{:}AG + AB{:}AG^* + AG + AG^*$$

The concentrations of AG vary over a known range, while AG* and AB concentrations remain constant, which allows for a generation of values of AB:AG* that correspond to the AG values, which are in turn used to generate a standard curve. The standard curve is used to translate AB:AG* values from the supernatant samples and calculate AG concentrations (the amount of insulin secreted under experimental conditions).

Radioimmunoassay relies on radiolabelled antigen (AG*) as a tracer that can be recognised by a specific antibody. The anti-insulin antibody was generated in a guinea pig because guinea pig insulin is considerably different from its mouse and human equivalents, thus allowing antibodies to be generated when the guinea pigs were injected with bovine insulin. I^{125} isotope was used for radioisotopic labelling because it is predominantly a γ-emitter, and γ-radiation is a very penetrative type of radiation, and therefore easy to detect. To generate iodinated insulin for the immunoassay the I^- ion is oxidised to the reactive I^+ ion using a strong oxidising reagent, and at neutral pH those reactive ions are covalently bound to tyrosine residues in insulin. One of the most commonly used oxidising agents in radioionation of tyrosine residues is iodogen (1,3,4,6-

tetrachloro-3α,6α-diphenyl glycoluril), which was used for iodination of insulin used in our assay. The iodinated insulin was subsequently purified by gel filtration chromatography (Grange et al., 2014; Jafri et al., 2011).

Borate buffer (Table 2.18) was used for dilutions of all radioimmunoassay components. The final anti-insulin antibody dilution was 1:60,000, I^{125}insulin tracer was diluted to give ~12,000 counts per minute/100μl, insulin standard (10ng/ml) was diluted in series (10-0.04ng/ml) in triplicates (Table 2.19), and test samples were diluted in duplicates to stay in a range over which the assay is sensitive (0.06-3ng/ml). Reference tubes, in triplicates, were prepared to measure non-specific binding, maximum antibody binding, and total γ-emission. The antibody and tracer were added to the samples, and standards and assay tubes were left at 4°C for 48h to equilibrate. After 48h, 1ml of precipitant (Table 2.20) was added to each tube (except the totals) to precipitate antibody-antigen complexes, and tubes were centrifuged at 3,000rpm at 4°C for 15 min. The γ-emission was then measured using a Packard Cobra II γ counter.

Table 2.18. Preparation of borate buffer. The pH was adjusted to 8 with 12N HCl. The volume was made up to 2l with distilled water.

Components	Amount (g)/ 2l	Final concentration (mM)
Boric acid	16.5	133
NaOH	5.4	10
EDTA	7.4	67.5

Table 2.19. Preparation of standards and reference tubes for RIA. T: totals (total count tubes containing 100µl of radiotracer to indicate the amount of radioactivity), NSB: non-specific binding (non-specific binding tubes containing 200µl buffer and 100µl tracer to determine the binding of the antigen in the absence of the antibody), B_0: maximum binding (maximum binding tubes containing 100µl borate buffer, 100µl anti-insulin antibody and 100µl tracer to indicate how much tracer binding will take place in the absence of unlabelled insulin), standards (0.04-10ng/ml).

	Buffer	Antibody (AB)	Tracer	Standard	Sample
Non-specific binding (NSB)	200µl	-	100µl	-	-
Maximum binding (B0)	100µl	100µl	100µl	-	-
Totals (T)	-		100µl	-	-
Standards (0.04-10ng/ml)	-	100µl	100µl	100µl	
Samples	-	100µl	100µl		100µl

Table 2.20. Preparation of precipitant for RIA. The volume was made up to 1l with PBS.

Components	Amount / 1l	Final concentration
30% PEG	500ml	15% (v/v)
Gammaglobulin	100mg	1% (w/v)
PBS	500ml	-

2.10. Macrophage migration and invasion

Activation of the innate immune system in obesity is a risk factor for the development of T2D (Ehses et al., 2007). The resident macrophages in islets have been intensively studied with respect to inflammation and T2D, and there is evidence that those macrophages accumulate in the islets during disease progression (Zirpel and Roep, 2021), and that they display a proinflammatory phenotype at the early stages of T2D (Cucak et al., 2013). Cell migration is a highly integrated multistep process. The macrophages polarise and extend protrusions towards the attractant. These protrusions are driven by actin polymerisation and can be stabilised by extracellular matrix adhesion or cell-to-cell interactions (Rougerie et al., 2013). Cell Biolabs' CytoSelect™ cell migration assay and EZCell™ cell migration/chemotaxis assay kits utilise polycarbonate membrane inserts that serve as a barrier to distinguishing migratory from nonmigratory cells, and therefore quantify their migratory properties. Migratory cells extend protrusions via actin cytoskeleton reorganistion towards the attractant to pass through the 5µm pores of the membrane or cling to the outer layer of the inserts, and they are then stained and quantified.

To study the effect of drugs of interest on macrophage invasion and migration into islets, Raw 264.7 thymic cells (Taciak et al., 2018) were seeded into inserts that were later placed over mouse or human pseudoislets cultured on glass coverslips. A cytokine mix (0.05U/µl IL-1β, 1U/µl TNF-α and 1U/µl IFN-γ) was added for 24h and macrophage migration into mouse and human islets was measured using CytoSelect™ cell migration assay and EZCell™ cell migration/chemotaxis assay, respectively, as described below.

2.10.1. CytoSelect™ Cell Migration Assay

Mouse pseudoislets were cultured on glass coverslips as described in Section 2.3, transferred to a 24-well plate, and incubated for 24h in DMEM containing 5.5mM glucose without or with a drug of interest. Raw 264.7 cells were thawed and seeded into a T75 flask in RPMI supplemented with 10% (v/v) FBS, 1% (v/v) penicillin and streptomycin, and 1% (v/v) L-glutamine. When the cells were confluent, they were starved overnight and activated with 100ng/ml LPS (lipopolysaccharide) in serum-free RPMI (Figure 2.10). 100µl of cell suspension (1×10^5 cell/ml) was added to each 5µm insert. After 3h of cell activation, the inserts with cell suspension were placed over glass coverslips with mouse pseudoislets and treated with 5.5mM glucose DMEM containing 0.05U/µl IL-1β, 1U/µl TNF-α and 1U/µl IFN-γ, in the absence or presence of a drug of interest, for 24h at 37°C (95%air/5%CO_2). After 24h of cytokine treatment, the media from the inside of the inserts were aspirated and the inserts were transferred to clean wells containing 400µl of cell detachment solution and incubated for 30min at 37°C (Figure 2.11). The cells were dislodged from the membrane by immersing the inserts in the 400µl detachment solution. 400µl of the medium solution was added to the detachment solution and mixed to combine thymic cells that had migrated through the membrane, and the cells detached from the bottom side of the membrane. 180µl of this mixture was added to a 96-well plate and 60µl of lysis buffer/CyQuant® GR dye solution (1:75) was added to each well of the 96-well plate containing migratory cells. Following a 20min incubation at room temperature, 200µL of the mixture was transferred to a 96-well plate suitable for fluorescence measurement, and the fluorescence was read at Ex/Em of 480nm/520nm using the plate reader.

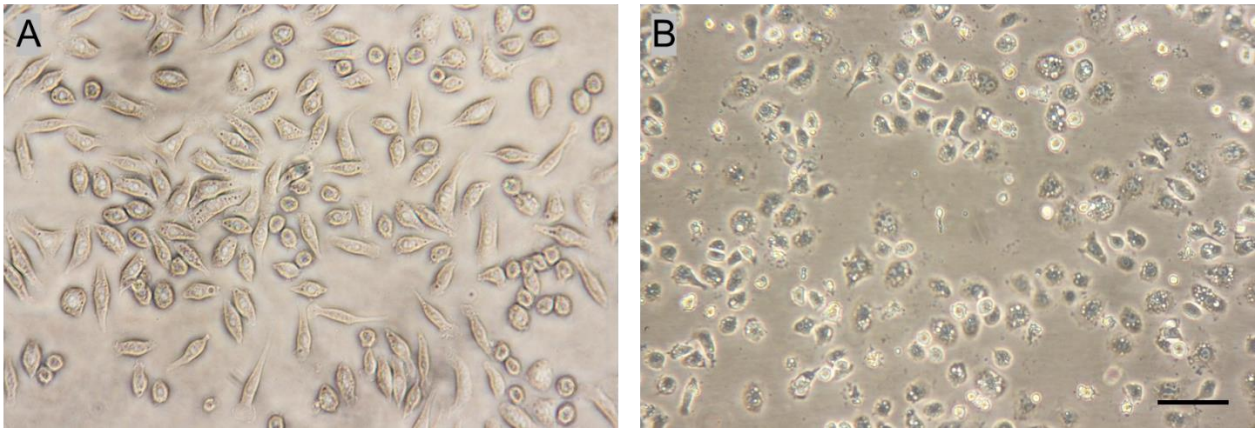

Figure 2.10. Raw 264.7 cells before (A) and after activation with LPS (B). LPS stimulates the formation of spindle-shaped pseudopodia and differentiation of macrophages into dendritic-like cells. (Dai et al., 2018; Saxena et al., 2003). Scale bar = 100µm.

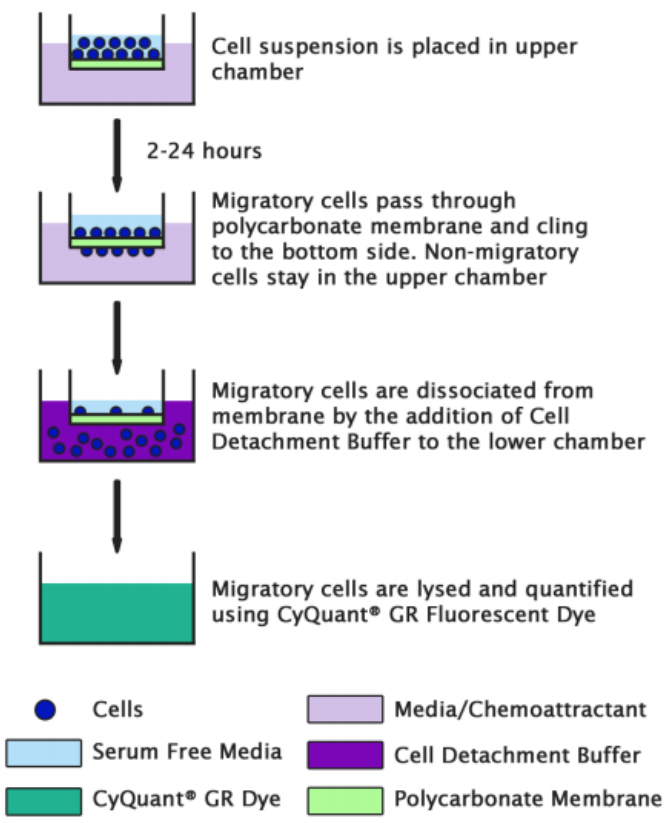

Figure 2.11. Principle of the migration assay. The assay utilises the polycarbonate membrane inserts (5µm pore size) in a 24-well plate. The membrane provides a barrier to distinguish migratory cells from nonmigratory cells. The migratory cells are removed from the top of the membrane, stained, and quantified (Cell Biolabs, 2016).

2.10.2. EZCell™ Cell Migration/Chemotaxis Assay

Human pseudoislets were cultured on glass coverslips as described in chapter 2.3.3, transferred to a 24-well plate, and incubated for 24h in 5.5mM glucose DMEM, without or with a drug of interest. Raw 264.7 cells were thawed and seeded into a T75 flask in RPMI supplemented with 10% (v/v) FBS, 1% (v/v) penicillin and streptomycin, and 1% (v/v) L-glutamine. Thymic cells were starved in serum-free RPMI media for 24h prior to the experiment. After starvation, the cells were resuspended at 3 x 10^5/ml in serum free RPMI, activated with 100ng/ml LPS, and 200µl of cell suspension was added to each insert. After 3h of cell activation, 600µl of 5.5mM glucose DMEM supplemented with 2% (v/v) FBS, 1% (v/v) penicillin and streptomycin, and 1% (v/v) L-glutamine were added to each well containing coverslips with human pseudoislets. The inserts were placed over coverslips containing human pseudoislets and incubated for 24h in the absence or presence of 0.05U/µl IL-1β, 1U/µl TNF-α and 1U/µl IFN-γ and a drug of interest at 37°C (95%air/5%CO_2). A standard curve was prepared by adding 50µl cell suspension (1 x 10^6 cells/ml) per well in a clear 96-well plate, with serial dilution (1:1) in wash buffer to give 100µl total volume. Wash buffer was used as a blank. 10µl of cell dye was added to each well, and the plate was incubated at 37°C for 1h. The fluorescence was read at Ex/Em of 530/590nm. Following a 24h incubation for cell migration, the media from the inside of the inserts were aspirated and the remaining cells were removed from the membrane using a cotton swab. The inserts were removed from the plate, inverted, and set aside. The plate was centrifuged at 1,000 x g for 5min at room temperature. The media were aspirated, and the cells washed with 500µl washing buffer. The plate was centrifuged again, and the washing buffer was aspirated. The cell dye solution was prepared by mixing cell dye and cell dissociation solution 1:10. 550µl of the mix was added to each well and the inserts were placed back in the plate and

incubated for 1h at 37°C. The plate was tapped on the side to dissociate migratory cells attached to the outer side of the inserts, and the inserts were removed and discarded. 110µl of the mix was transferred to a 96-well plate suitable for fluorescence measurement and the fluorescence was read at Ex/Em of 530nm/590using the plate reader.

2.10.3. Invasion assay

Mouse and human pseudoislets were cultured on glass coverslips in 6-well plates, as described in chapter 2.3.3, and incubated in 2.5mM glucose DMEM supplemented with 2% (v/v) FBS, 1% (v/v) penicillin and streptomycin, and 1% (v/v) L-glutamine, in the absence or presence of a drug of interest. Raw 264.7 cells were seeded on inserts at a density of 1 x 10^5 cells/insert in serum-free RPMI supplemented with 1% (v/v) penicillin and streptomycin. The cells were activated by adding LPS at 100ng/ml. The inserts were placed over the glass coverslips with pseudoislets in a 6-well plate, and the media were replaced for 2.5mM DMEM containing a mix of proinflammatory cytokines and a drug of interest. The pseudoislets were visualised and examined by light microscopy. After completion of 48h experiments, coverslips with islets were fixed in 4% paraformaldehyde (PFA) for analysis of macrophage infiltration by immunohistochemistry.

2.11. *In vivo* studies

In vivo experiments were performed using male *ob/ob* mice, which are a model of hyperglycaemia and insulin resistance. These animals carry mutations in the gene responsible for leptin production, and therefore they have increased hunger and become profoundly obese (Lindström, 2007). *Ob/ob* mice have enlarged islets due to sustained hyperglycaemia and insulin resistance, hence they are often used as an animal model of T2D, and they are ideal for the investigation of the role of potential therapies for T2D.

The effects of fluoxetine injections on beta cell proliferation and glucose tolerance in *ob/ob* mice were investigated in the *in vivo* experiments.

2.11.1. Fluoxetine injections and BrdU delivery

In *in vivo* experiments, two groups of five *ob/ob* mice (56.0±0.8g), aged 29 weeks, were either injected with DMSO (vehicle) or fluoxetine (10mg/kg body weight in a volume of 0.4ml DMSO/kg) intraperitoneally 4 times over 14 days. The thymidine analogue and proliferation marker BrdU (1mg/ml) was introduced in drinking water for 7 days prior to sacrifice to allow its incorporation into dividing cells (Figure 2.12). The pancreases were dissected out and embedded in paraffin. Wax-embedded pancreases were cut into 5µm sections using the microtome Leica RM2255. Beta cell proliferation was identified in pancreas sections by immunohistochemistry using antibodies against BrdU and insulin.

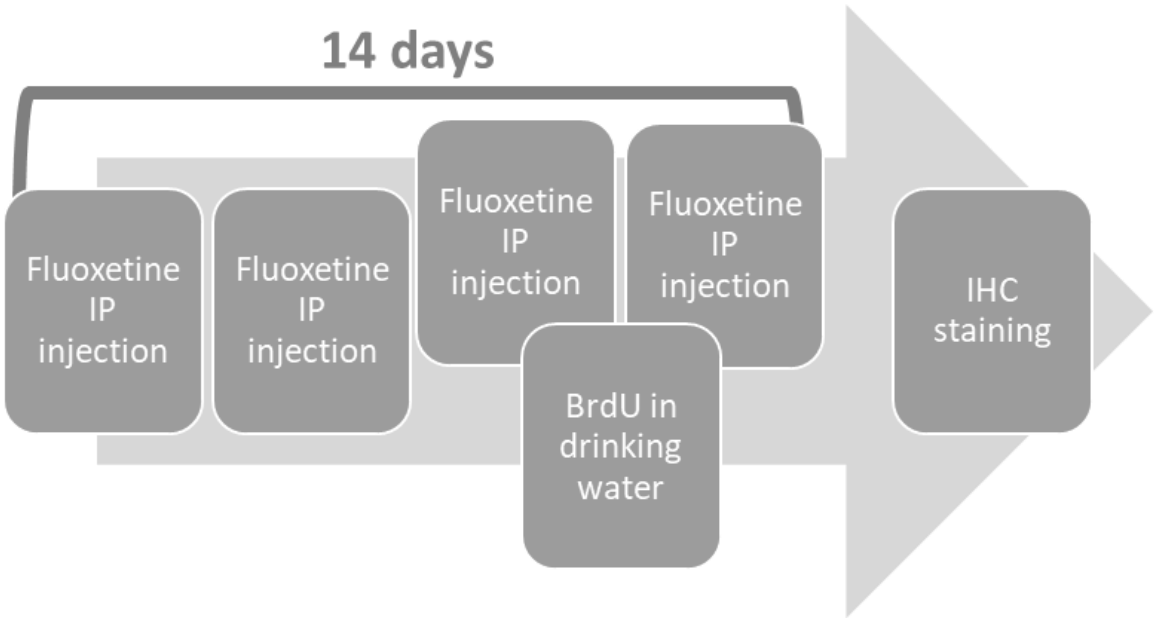

Figure 2.12. Steps of delivery of fluoxetine and BrdU *in vivo*.

2.11.2. Glucose tolerance tests

Intraperitoneal glucose tolerance tests were performed on overnight fasted *ob/ob* mice. Mice were fasted for 16h by removing food from the cages. Basal glucose concentration was measured from tail blood using the Acc-Chek glucose meter. Glucose (30%) at 2g/kg, in the presence of fluoxetine/DMSO or DMSO only, was administered by intraperitoneal injection, and blood was collected from the pinpricks on the tails. Plasma glucose concentrations were measured at 15, 30, 60, 90, 120, 150min after glucose delivery.

2.12. Statistical analysis

Data are expressed as mean + SEM, with the number of repeats or animals stated as n. Data were analysed using a two-tailed Student's t-test with Welch's correction or one-way ANOVA with a recommended multiple comparisons test (Dunnett's multiple comparisons test). Statistical analyses were performed using GraphPad Prism 9 or Excel in order to determine the significance for indicated comparisons – *p<0.05; **p<0.01; ***p<0.001. Immunohistochemistry images were analysed using ImageJ software.

200 islets per pancreas are routinely isolated from CD-1 mice, and statistical power analysis was carried out for each *in vitro* method based on data generated in similar experiments. The following sample sizes are required for 90% power with a confidence level of 5% to detect significant differences between treatment groups:

- Static incubations experiments require 8 replicates
- Dynamic insulin secretion (perifusion) experiments require 4 replicates
- Islet apoptosis assays require 8 replicates

Power calculations using data generated from previous experiments indicated that 5 mice per treatment group are required for 90% power with a confidence level of 5% to detect significant differences in glucose tolerance tests.

Chapter 3. Expression of serotonin signalling elements and the D2 receptor by islets and beta cells

3.1. Introduction

Serotonin, also known as 5-HT, is best known as a neurotransmitter in the central nervous system, where it regulates several physiological processes, such as behaviour and appetite. However, the serotonin synthesised in the brainstem accounts for only a small percentage of total body serotonin. Approximately 95% of serotonin is produced in the periphery, for example by enterochromaffin cells of the gut and adipocytes, where it acts as a local hormone or enters the circulation (Gershon, 2013). Serotonin signalling is mediated by serotonin receptors, including 5-HT2B and 5-HT3A that have been linked to changes in islet beta cell mass and insulin secretion (Bennet et al., 2015; Kim et al., 2010). Interestingly, beta cells share common developmental features with serotonergic neurons (Devaskar et al., 1994; Ohta et al., 2011; Wilson et al., 2003). Secreted serotonin is reabsorbed from the extracellular space by the plasma membrane serotonin transporter (SERT). Selective serotonin reuptake inhibitors (SSRIs) stop serotonin reuptake by blocking SERT, and there is a growing body of evidence suggesting that different types of islet cells express the machinery to generate, store, respond to, and/or transport serotonin (Almaca et al., 2016; Kim et al., 2010; Ohta et al., 2011). Therefore, in this chapter, standard and quantitative PCRs, Western blotting, and fluorescence immunohistochemistry were used to determine the expression of SERT, tryptophan hydroxylase (an enzyme involved in the synthesis of serotonin; TPH), serotonin, and serotonin receptors (5-HT2B, 5-HT3A, and 5-HT1F) in MIN6 beta cells, mouse islets and human islets.

In addition to measuring the expression of the serotonin signalling elements, the presence of the dopamine D2 receptor was also investigated by quantitative PCR

analysis and fluorescence IHC, since it is a common target for atypical antipsychotics (AAPs): for example, clozapine acts as a D2 antagonist, whereas aripiprazole is a partial agonist at D2 receptors.

3.2. Methods

3.2.1. PCR

Total RNAs were isolated from MIN6 cells, mouse islets and human islets using RNeasy kits according to the manufacturer's protocol, and they were reverse-transcribed into cDNAs as described in Sections 2.4.1. and 2.4.2. Standard and quantitative PCR analyses were used to identify expression of genes encoding SERT, 5-HT2B, 5-HT3A, and D2 receptors, using bioinformatically validated primers as listed in Table 2.6. In standard PCR, the SERT amplicons were separated using agarose gel electrophoresis and visualised under UV light. In quantitative PCR experiments, expression levels of serotonin receptor genes were normalised to beta actin (ACTB) mRNA expression in the same samples as an internal reference.

3.2.2. Western blotting

Proteins were extracted from MIN6 cells, mouse islets and human islets, and they were quantified by the BCA protein assay (Section 2.5.1). Thereafter, immunoreactive SERT proteins were detected in Western blots as described in Section 2.5.2.

3.2.3. Fluorescence immunohistochemistry

Fluorescence immunohistochemistry was performed using brain and pancreas sections from wild type and *ob/ob* mice according to the protocol in Section 2.5.3.

The tissue sections were stained with antibodies against serotonin, TPH, D2 receptor, insulin, or TUJ (class III beta tubulin, a marker of neurons in the central and peripheral nervous system).

3.3. Results

3.3.1. Expression of SERT mRNAs by MIN6 beta cells and islets

PCR amplification with primers for mouse and human SERT produced single amplicons of the expected sizes (187 and 207bp, respectively) using cDNA templates derived from human islets (lane 1), mouse islets (lane 2), and MIN6 cells (lane 3). As expected, no products were amplified using non-reverse-transcribed RNAs as negative controls (lane 4). These observations revealed that SERT mRNA was expressed by human islets, mouse islets and MIN6 cells (Figure 3.1).

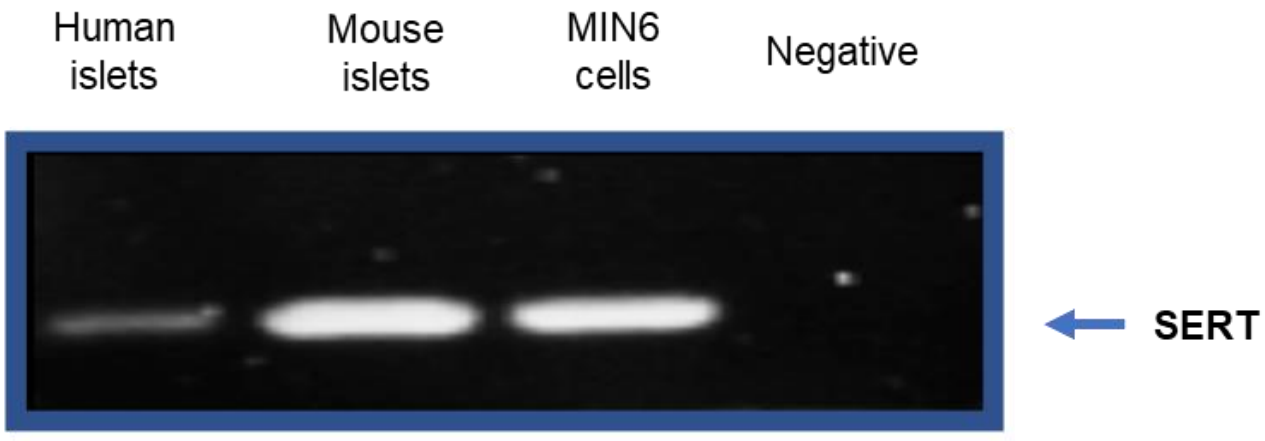

Figure 3.1. Detection of SERT mRNA in human islets, mouse islets and MIN6 cells. Products of PCR using primers for mouse and human SERT were electrophoretically separated on a 1.8% agarose gel. Amplicons of appropriate sizes were obtained after amplification of human and mouse cDNAs, using appropriate, species-specific primers for SERT.

3.3.2. SERT mRNAs are translated into SERT proteins in MIN6 beta cells and islets

Western blotting was used to determine whether SERT mRNAs were translated to proteins in islets and MIN6 cells. Protein extracts from MIN6 cells, mouse islets and human islets were separated by gel electrophoresis, blotted onto a PVDF membrane, and immunoprobed with an antibody against SERT (Section 2.5.2). As shown in Figure 3.2, immunoreactive proteins of 71kDa were detected in all samples, which is consistent with the predicted molecular weight of full-length SERT protein in mouse and human tissues. Thus, as expected, SERT expression at the protein level was detected in human islets, mouse islets and MIN6 cells.

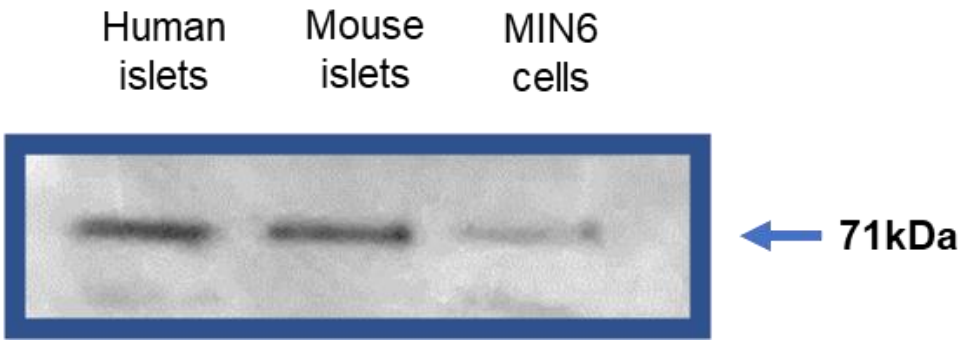

Figure 3.2. Protein expression of SERT in human islets, mouse islets and MIN6 cells. 50µg islet and MIN6 cell protein lysates were separated on a 10% polyacrylamide gel, and SERT expression in these samples was detected by Western blot analysis using an antibody directed against both mouse and human SERT. Immunoreactive proteins for SERT were seen at 71kDa in islet (lanes 1 and 2) and MIN6 cell lysates (lane 3).

3.3.3. Expression and localisation of serotonin and tryptophan hydroxylase in mouse pancreas

The expression and localisation of serotonin and TPH, an enzyme involved in serotonin synthesis, in mouse pancreas were also determined by fluorescence immunohistochemistry. Analysis of immunohistochemical staining of adult mouse pancreases showed that serotonin was expressed mainly within the islet capillaries and TPH was expressed at negligible levels. In addition, co-staining with an anti-insulin antibody indicated that serotonin was expressed only by occasional beta cells (Figure 3.3, panel C). Fluorescence was not visible when sections were incubated with secondary antibodies alone (Figure 3.3, panels G-I). Staining reliability with the primary antibodies was confirmed by the detection of serotonin and TPH in brain tissue sections (Figure 3.3, panels J and K).

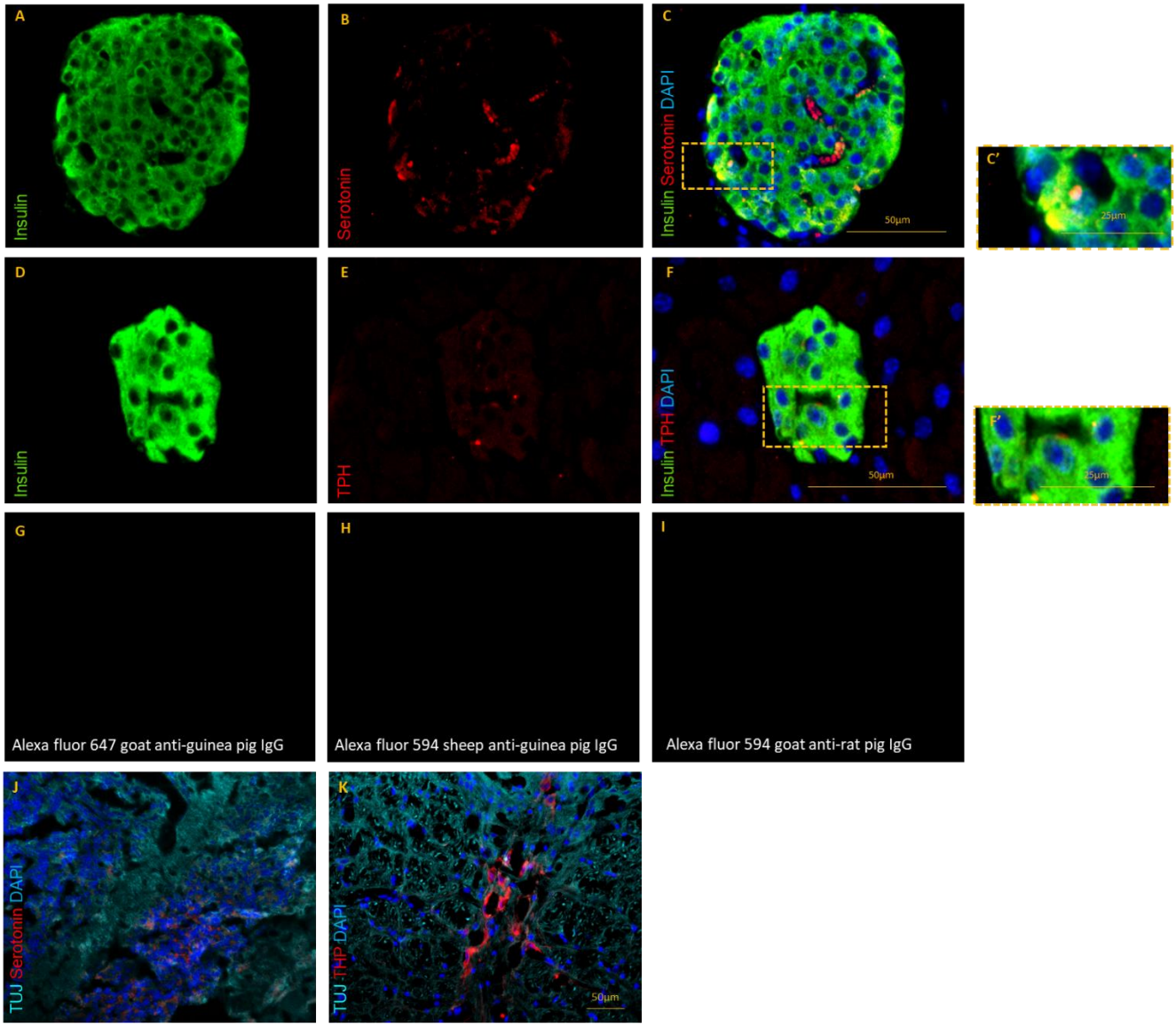

Figure 3.3. Detection of serotonin and TPH expression by fluorescence immunohistochemistry in paraffin-embedded mouse pancreas sections. Pancreatic sections from a lean adult mouse were immunoprobed with antibodies directed against serotonin (B) or TPH (E) (red), and insulin (green). DAPI nuclear staining is shown in blue. Higher magnifications of the islet region are delimited by a box (C-C' and F-F'). Scale bars are 50µm (C, F, I) or 25µm (C', F', I'). No immunoreactivity was detected in the negative control sections where the primary antibody against serotonin, TPH or insulin (G, H, I) was omitted. Immunostaining of mouse brain sections using the antibodies directed against serotonin or TPH, and TUJ served as positive controls (J, K).

3.3.4. Expression of serotonin receptor mRNAs by MIN6 beta cells and human islets

Quantitative PCR was used to investigate whether human islets express the serotonin receptors 5-HT2B and 5HT3A, which have been previously implicated in serotonin signalling in beta cells (Kim et al., 2010; Moon et al., 2020), and 5-HT1F, whose activation reduces glucagon secretion from alpha cells (Almaca et al., 2016). Quantitative PCR revealed that all three serotonin receptors were expressed by MIN6 cells and human islets, with 5-HT3A being the most abundant subtype in MIN6 cells, and 5-HT1F showing highest expression in human islets (Figures 3.4).

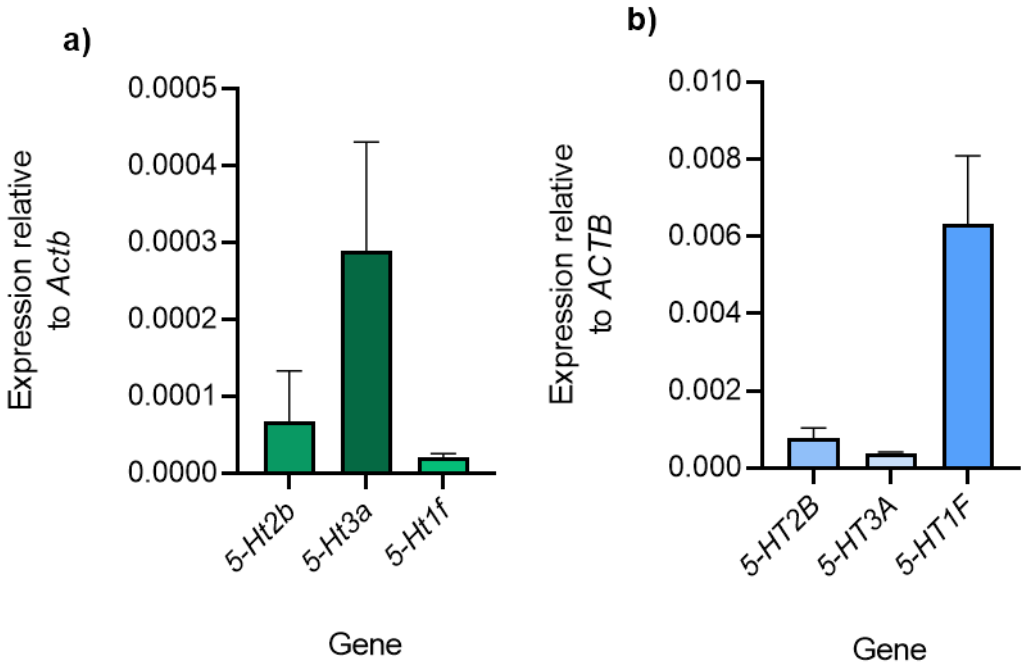

Figure 3.4. Quantification of 5-HT2B, 5-HT3A and 5-HT1F mRNAs in MIN6 cells (A) and human islets (B) using quantitative PCR. Mouse and human gene names are written in lower case and capital letters, respectively. Data are expressed as mean + SEM relative to beta actin (ACTB) mRNA levels in the same samples, from 3-4 biological replicates.

3.3.5. Expression of D2 receptor mRNAs in MIN6 beta cells and human islets, and localisation of D2 protein in mouse pancreas

Quantitative PCR confirmed the expression of the dopamine D2 receptor in MIN6 cells and human islets (Figure 3.5). In addition, the expression and localisation of D2 in mouse pancreas and brain were determined by fluorescence IHC according to the protocol in Section 2.5.3 using antibodies against D2 and insulin. Analysis of immunohistochemical staining of pancreatic sections revealed that D2 was expressed at low levels by occasional beta cells of lean and *ob/ob* mice (Figure 3.6). Only few beta cells expressed D2, and D2 immunoreactivity was not identified in the majority of the beta cells. D2 staining in the brain tissue was used as a positive control because D2 receptors are widely expressed by nerve cells in the brain (Levey et al., 1993).

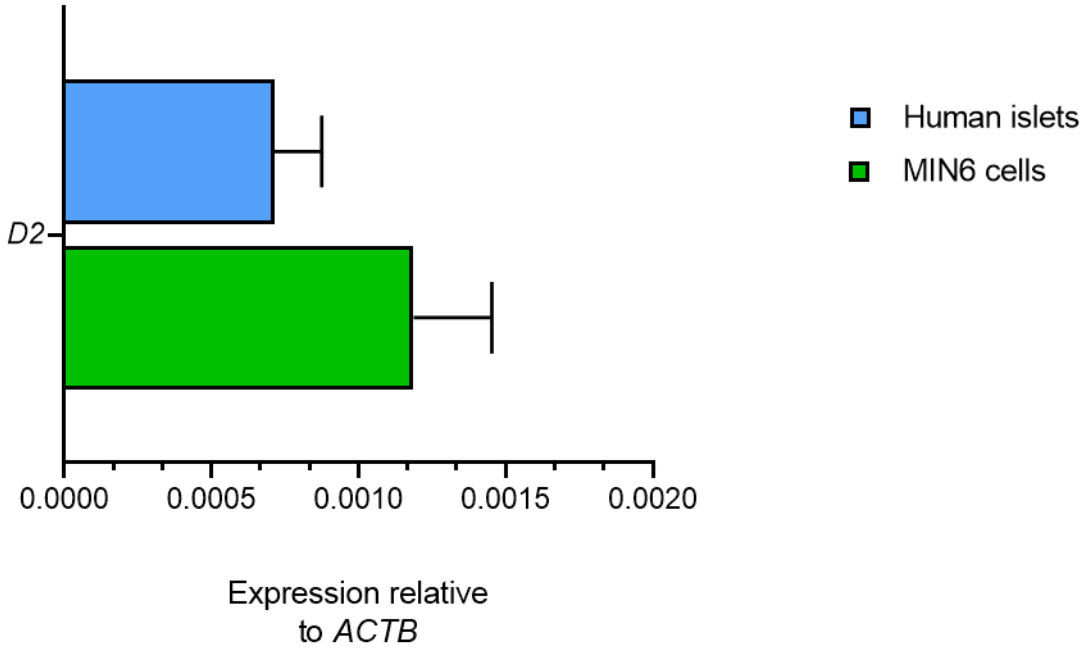

Figure 3.5. Detection of D2 receptor mRNA in MIN6 cells (green) and human islets (blue) using quantitative PCR. Data are expressed as mean + SEM relative to beta actin (ACTB) expression in the same samples, n = 3-4 biological replicates.

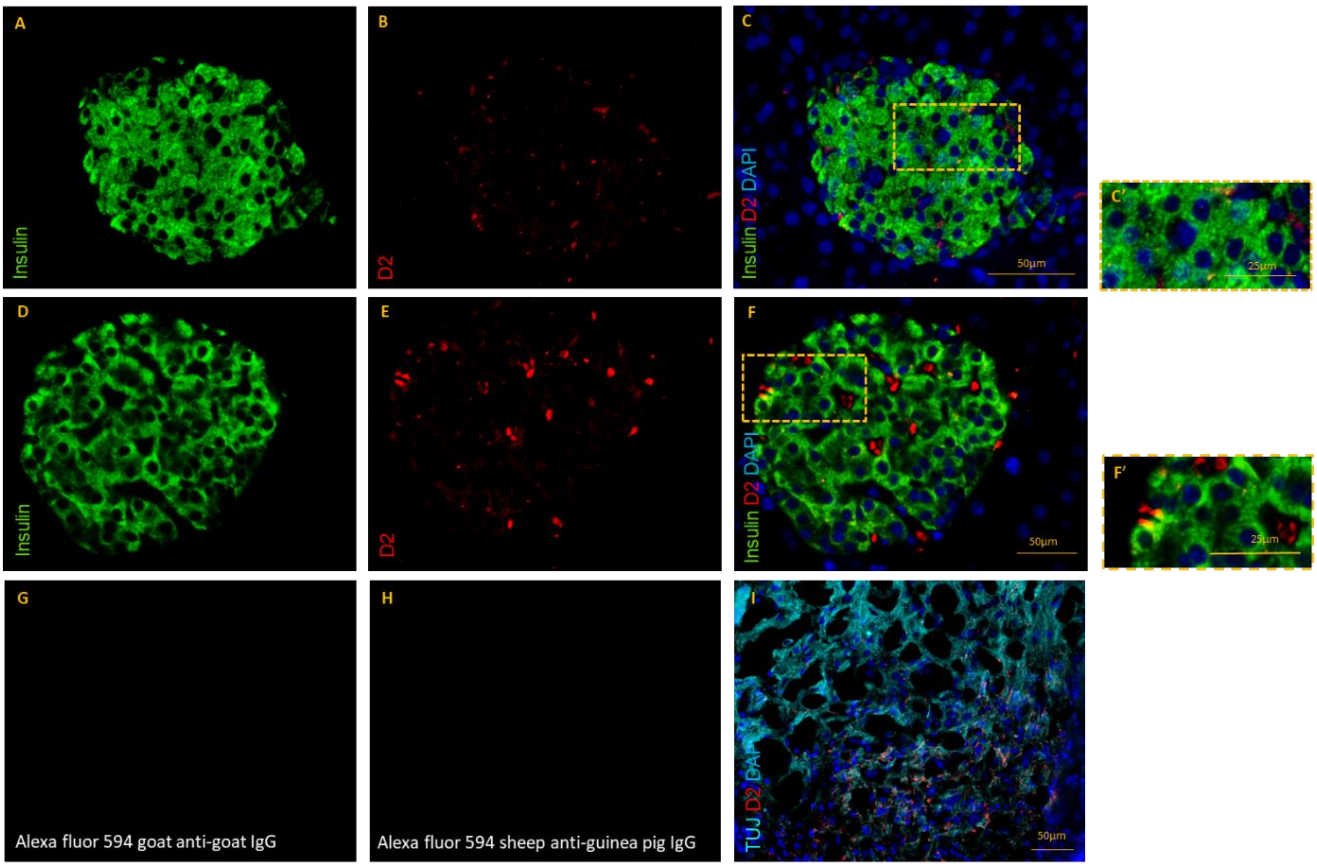

Figure 3.6. Detection of D2 receptor by fluorescence immunohistochemistry in paraffin-embedded adult mouse pancreas sections. Images of islets in a pancreatic section from a lean mouse (A-C) and an *ob/ob* mouse (D-F) immunoprobed with antibodies directed against D2 (red) and insulin (green). The blue colour in the nucleus shows DAPI staining. Higher magnifications of the islet region are delimited by a box (C-C' and F-F'). Scale bars are 50µm (C, F) or 25µm (C', F'). No immunoreactivity was detected in the negative control sections where the primary antibody against D2 or insulin (G, H) was omitted. Immunostaining of a brain section using antibodies directed against D2 and TUJ was performed as a positive control (I).

3.4. Discussion

SERT is an important serotonin signalling element and the major target of SSRIs, since the spatio-temporal aspects of serotonin action are limited by its uptake from the extracellular space by SERT (Claassen et al., 1977). The data presented in this chapter demonstrate that SERT is expressed by MIN6 cells, mouse islets and human islets at mRNA and protein levels. Nevertheless, TPH and serotonin are absent or expressed by mouse beta cells at low levels. This is consistent with reports that they are expressed by beta cells at trace levels in adult mice pancreases (Moon et al., 2020; Takahashi et al., 2020; Kim et al., 2010). This could suggest a novel mechanism of action of SSRIs on mouse beta cells, independent from increases in local serotonin. However, levels of expression of serotonin and TPH, and serotonin sources should be compared between mouse and human beta cells in future experiments. In addition, experiments using human islets are consistent with previous reports that 5-HT1F mRNA is highly expressed in human islets, whereas mRNAs encoding the remaining islet serotonin receptors, including 5-HT2A and 5-HT2B, are present only at trace levels (Amisten et al., 2013; Amisten et al., 2017). The low expression of 5-HT2B mRNA in MIN6 cells shown in this chapter agrees with the report that this mRNA is low in non-pregnant adult mice and it only significantly increases in pregnancy (Kim et al., 2010).

As well as serotonin receptors, including the 5-HT2 subfamily, the D2 receptor is a common target for AAPs. D2 receptor expression has been previously identified by immunodetection in INS-1E cells, as well as in rat and human islets (Rubi et al., 2005), and by quantitative PCR in human islets (Amisten et al., 2013). Consistent with these earlier observations, the presence of D2 mRNA and protein was identified in MIN6 cells, mouse islets and human islets in this chapter.

However, TPH and serotonin expression was only detected in occasional mouse beta cells, which is consistent with the report that not all human beta cells express serotonin (Almaca et al., 2016). The levels of D2 receptor expression were also low, and this observation differs from a previous report that D2 receptors are abundantly expressed by human beta cells (Rubi et al., 2005), suggesting species-related differences in dopamine signalling in mouse and human islets. Pharmacological blockade of D2 receptors with AAPs in human islets markedly increases insulin and glucagon secretion (Aslanoglou et al., 2021), indicating that AAPs can act directly on human islet alpha and beta cells to affect hormone secretion, which is of great importance in understanding the effects of antipsychotic therapy on islet function.

Chapter 4. Direct effects of the selective serotonin reuptake inhibitors, fluoxetine, sertraline and paroxetine, on beta cell mass and function

4.1. Introduction

Type 2 diabetes (T2D) is characterised by insulin resistance and loss of functional beta cells. Therapeutics that act on beta cells to promote insulin secretion have been in use to treat T2D for decades. However, with an increasing incidence of T2D, there is an emerging need for effective therapies that also target beta cell mass so that more functional beta cells are available to secrete insulin. Meanwhile, there is a great interest in repurposing drugs that have an established safety profile for the treatment of other conditions. It is possible that such drugs could be used to improve beta cell function and/or to promote beta cell expansion.

Selective serotonin reuptake inhibitors are commonly used for the treatment of mental disorders as they increase serotonin neurotransmission by binding to SERT, and thereby block the reuptake of serotonin at the synaptic clefts. However, the therapeutic potential of targeting a peripheral serotonin system has not been fully explored. There is evidence that serotonin acts as a local hormone in the endocrine pancreas (Kim et al., 2010; Robinson, 2009), and it is secreted at detectable levels from human islets (Bennet et al., 2015). Therefore, SSRIs play a direct role in regulating beta cell mass and function by increasing local serotonin levels. However, the exact mechanism of action of SSRIs on beta cells is not yet understood. The peripheral effects of three commonly prescribed SSRIs - fluoxetine, sertraline and paroxetine - on beta cell function were therefore investigated in this chapter. Magnetic resonance spectroscopy experiments have revealed that fluoxetine and sertraline reach steady state concentrations in plasma of 0.3-2.6µM and 0.2-0.8µM, respectively (Bolo et al., 2000; Bosch et al.,

2008), and gas chromatography/mass spectrometry has shown that mean plasma levels of paroxetine are 0.09µM (Lima et al., 2008; Tomita et al., 2014). Therefore, concentrations between 0.01-1µM were used in the functional experiments described in this chapter to determine the effects of these SSRIs in the endocrine pancreas.

MIN6 beta cells and mouse islet beta cells share functional and morphological similarities (Miyazaki et al., 2021; Schulze et al., 2016), so the readily available MIN6 cell line offers a valuable model for preliminary functional experiments. Although primary mouse and human islets are more difficult to isolate and use experimentally, it is important to also carry out experiments using primary islets as they better reflect the capacity for intra-islet cellular crosstalk that occurs in situ. Therefore, in the current chapter, experiments were carried out with MIN6 cells, as well as with mouse and human islets, to investigate changes in beta cell function and mass in response to exposure to SSRIs.

4.2. Methods

4.2.1. ATP generation in MIN6 beta cells: CellTiter-Glo assay

The CellTiter-Glo assay was used to quantify ATP generation by MIN6 cells growing in monolayers. In these experiments, MIN6 cells were seeded into 96-well white plates at a density of 15,000 cells/well. The cells were incubated in DMEM supplemented with 5.5mM glucose, 10% (v/v) FBS, 1% (v/v) penicillin and streptomycin, and 1% (v/v) L-glutamine in the absence or presence of fluoxetine, sertraline or paroxetine (0.01-10µM) for 48h. The CellTiter-Glo reagent was added to the wells for 15min, and luminescence was measured as described in Section 2.7.2.

4.2.2. ATP generation in islets: CellTiter-Glo 3D assay

ATP generation by mouse and human islets was quantified using a CellTiter-Glo 3D assay designed for 3D cell aggregates. The islets were incubated in RPMI (11.1mM glucose) supplemented with 10% (v/v) FBS, 1% (v/v) penicillin and streptomycin, and 1% (v/v) L-glutamine in the absence or presence of fluoxetine, sertraline or paroxetine (0.01-1μM) for 48h. Groups of 3 mouse islets or 5 human islets of similar sizes were then transferred to white-walled 96-well plates, and the CellTiter-Glo 3D reagent was added to each well 15min prior to the measurement of luminescence as described in Section 2.7.2.

4.2.3. Cell viability: Trypan blue exclusion assay

The Trypan blue exclusion assay was used to assess viability of MIN6 cells and mouse islets. MIN6 cells were seeded into 6-well plates at a density of 300,000 cells/well and incubated in DMEM supplemented with 25mM glucose, 10% (v/v) FBS, 1% (v/v) penicillin and streptomycin, and 1% (v/v) L-glutamine in the absence or presence of fluoxetine, sertraline or paroxetine (0.1-10μM). Trypan blue uptake by MIN6 cells after a 48h exposure to SSRIs was assessed following their incubation in Trypan blue (0.2% w/v) for 15min. Cells to which the dye had gained access (blue; dead) and non-stained (viable) cells were visualised by light microscopy (Section 2.7.1).

Mouse islets were cultured in 10cm Petri dishes in RPMI supplemented with 11.1mM glucose, 10% (v/v) FBS, 1% (v/v) penicillin and streptomycin, and 1% (v/v) L-glutamine in the absence or presence of fluoxetine, sertraline or paroxetine (0.1-10μM) for 48h. Cell membrane integrity was assessed by light microscopy after incubation of islets in Trypan blue (0.2% w/v) for 15min (Section 2.7.1).

4.2.4. Insulin secretion from MIN6 beta cells

Insulin release was assessed in static insulin secretion experiments, where MIN6 cells were seeded into 96-well plates at a density of 20,000 cells/well.

In acute experiments, MIN6 cells were pre-incubated in DMEM supplemented with 2.5mM glucose, 10% (v/v) FBS, 1% (v/v) penicillin and streptomycin, and 1% (v/v) L-glutamine for 2h at 37°C, and then incubated with DMEM supplemented with 2.5mM or 25mM glucose in the absence or presence of fluoxetine, sertraline or paroxetine (0.01-1µM) for 30min (Section 2.9.1.1.). 500µM carbachol was used as a positive control to potentiate insulin secretion through activation of the M3 muscarinic receptor coupled to phospholipase-C (Yamazaki et al., 2006). The supernatants were collected and kept at -20°C until radioimmunoassay for insulin was performed (Section 2.9.3).

In chronic static incubation experiments, MIN6 cells were incubated in DMEM supplemented with 5.5mM glucose (to mimic plasma glucose levels in mice) in the absence or presence of fluoxetine, sertraline or paroxetine (0.01-1µM) for 48h. The cells were then pre-incubated in DMEM (2.5mM glucose) for 2h, and then incubated in DMEM supplemented with either 2.5mM glucose, 25mM glucose or 25mM glucose + 500µM carbachol for 30min without SSRIs. The supernatants were collected and kept at -20°C until assayed for insulin.

4.2.5. Insulin secretion from mouse and human islets

Insulin secretion from mouse and human islets was measured by static and dynamic experiments.

In acute static incubation experiments, islets were pre-incubated for 1h in a physiological salt solution (Gey & Gey buffer) supplemented with 2mM glucose, as described in Section 2.9.1.2, and groups of 3 mouse islets or 5 human islets were incubated with buffer supplemented with either 2mM or 20mM glucose in the presence or absence of fluoxetine, sertraline or paroxetine (0.01-1μM) for 1h. Carbachol (500μM) was used as a positive control. The supernatants were collected and stored at -20°C prior to insulin radioimmunoassay.

In chronic static incubation experiments, islets were incubated in RPMI (11.1mM glucose) supplemented with 10% (v/v) FBS, 1% (v/v) penicillin and streptomycin, and 1% (v/v) L-glutamine without or with fluoxetine, sertraline or paroxetine (0.01-1μM) for 48h. Following a 1h pre-incubation, groups of 3-5 islets were then incubated in Gey & Gey buffer supplemented with either 2mM or 20mM glucose (without a drug) for 1h at 37°C. Carbachol (500μM), which is a muscarinic M3 receptor agonist, served as a positive control. The supernatants were kept at -20°C until assayed for insulin.

In dynamic secretion experiments, groups of 50 mouse or human islets were perifused at a constant temperature of 37°C with a physiological salt solution containing 2mM or 20mM glucose in the absence or presence of 1μM fluoxetine, 1μM sertraline or 0.1μM paroxetine as described in Section 2.9.2. Perifusate fractions were collected at 2 min intervals and secreted insulin was quantified by radioimmunoassay.

4.2.6. MIN6 beta cell proliferation: BrdU ELISA

Proliferation of MIN6 cells was quantified using a BrdU ELISA kit. MIN6 cells were plated into 96-well plates at a density of 20,000 cells/well and cultured in DMEM supplemented with 5.5mM glucose, 1% (v/v) penicillin and streptomycin, and 1% (v/v) L-glutamine, but no FBS, and in the absence or presence of fluoxetine or sertraline (0.1-1µM) or paroxetine (0.01-1µM) for 48h. 10% (v/v) FBS containing growth factors was used as a positive control. Thereafter, the cells were labelled with 100µM BrdU labelling reagent for 2h at 37°C, and MIN6 cell proliferation was determined by colorimetric quantification of BrdU incorporation into cellular DNA as described in section 2.6.1.

4.2.7. MIN6 beta cell and islet apoptosis: Caspase-Glo 3/7 assay

The caspase-Glo 3/7 apoptosis assay was used to detect apoptosis in MIN6 cells, mouse islets and human islets.

Groups of 15,000 MIN6 cells were seeded into 96-well white plates then cultured in DMEM supplemented with 5.5mM glucose, 10% (v/v) FBS, 1% (v/v) penicillin and streptomycin, and 1% (v/v) L-glutamine in the absence or presence of fluoxetine, sertraline or paroxetine (0.01-1µM) for 48h. The cells were exposed to a proinflammatory cytokine cocktail (0.05U/µl IL-1β, 1U/µl TNF-α and 1U/µl IFN-γ) or 500µM palmitate 24h before the quantification of caspase3/7 activities, as described in Section 2.8.1.

Groups of 3 mouse islets or 5 human islets were maintained in culture in RPMI (11.1mM glucose) supplemented with 10% (v/v) FBS, 1% (v/v) penicillin and streptomycin, and 1% (v/v) L-glutamine and without or with fluoxetine or sertraline (0.1-1µM) or paroxetine (0.01-0.1µM) for 48h, in the absence or presence of the same proinflammatory cytokine cocktail that was used for MIN6

cell experiments, or palmitate (500µM). Apoptosis was determined by measuring caspase3/7 activities using a Caspase-Glo 3/7 assay following the manufacturer's instructions as described in Section 2.8.1.

4.2.8. MIN6 beta cell apoptosis: Flow cytometry

Apoptosis of individual MIN6 cells was determined by flow cytometry. MIN6 cells were seeded into 6-well plates at a density of 100,000cells/well and incubated with DMEM supplemented with 5.5mM glucose, 10% (v/v) FBS, 1% (v/v) penicillin and streptomycin, and 1% (v/v) L-glutamine in the absence or presence of fluoxetine, sertraline or paroxetine (0.01-1µM) for 48h. The proinflammatory cytokine cocktail was added 24h prior to the flow cytometry assay to induce apoptosis in MIN6 cells. Staining was performed using an Alexa Fluor® 488 annexin V/Dead Cell Apoptosis kit as described in Section 2.8.2 and the samples were analysed using a BD Canto II analyser.

4.2.9. Beta cell signalling: Western blotting

Proteins were extracted from MIN6 cells following a 24h treatment with fluoxetine and they were quantified by the BCA protein assay (Section 2.5.1). Thereafter, immunoreactive beta actin (loading control) and phosphorylated MAPK (p42/44 MAPK), CREB and Akt were detected in Western blots as described in Section 2.5.2.

4.3. Results

4.3.1. Fluoxetine

4.3.1.1. Effects of fluoxetine on ATP generation by beta cells

ATP plays an important role in insulin release, and it is an indicator of cellular metabolic activity and cell numbers. ATP generation by MIN6 cells, mouse islets and human islets was quantified using the CellTiter-Glo assay following a 48h incubation with fluoxetine (0.1-10µM). Figure 4.1a shows that 0.1-1µM fluoxetine significantly increased ATP production by MIN6 cells, whereas 10µM fluoxetine had cytotoxic effects on MIN6 cells that led to them lifting from the wells, which subsequently led to virtually undetectable luminescence. Experiments with mouse (Figure 4.1b) and human (Figure 4.1c) islets indicated that 0.1-1µM fluoxetine also significantly elevated ATP production after 48 hours exposure. 10µM fluoxetine had no significant effect on ATP synthesis in islets, indicating that it was better tolerated by three-dimensional islets than MIN6 cell monolayers.

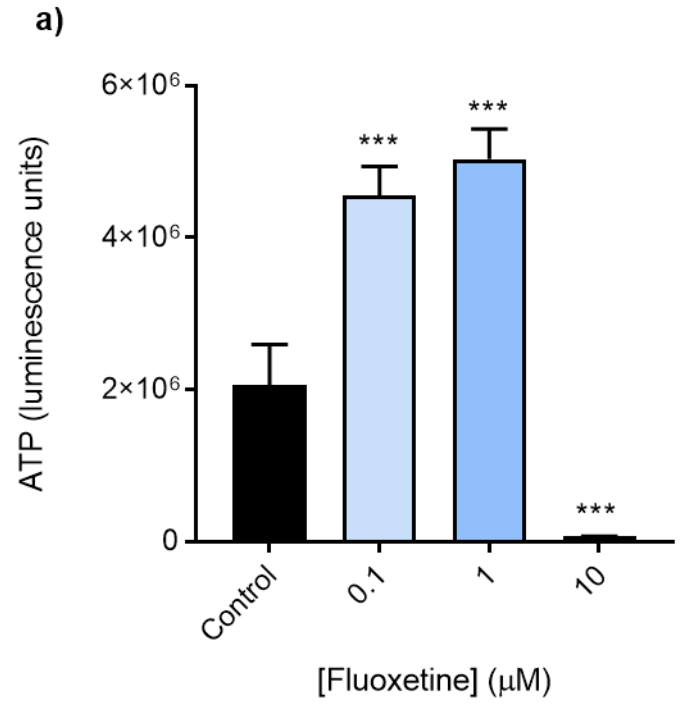
a)
6×10^6
4×10^6
2×10^6
0
ATP (luminescence units)
***
***
***
Control
0.1
1
10
[Fluoxetine] (μM)

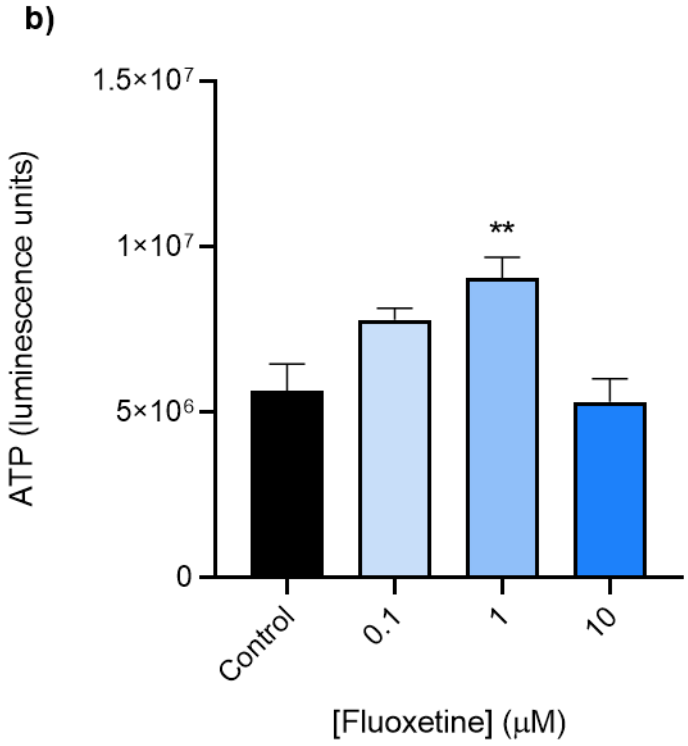
b)
1.5×10^7
1×10^7
5×10^6
0
ATP (luminescence units)
**
Control
0.1
1
10
[Fluoxetine] (μM)

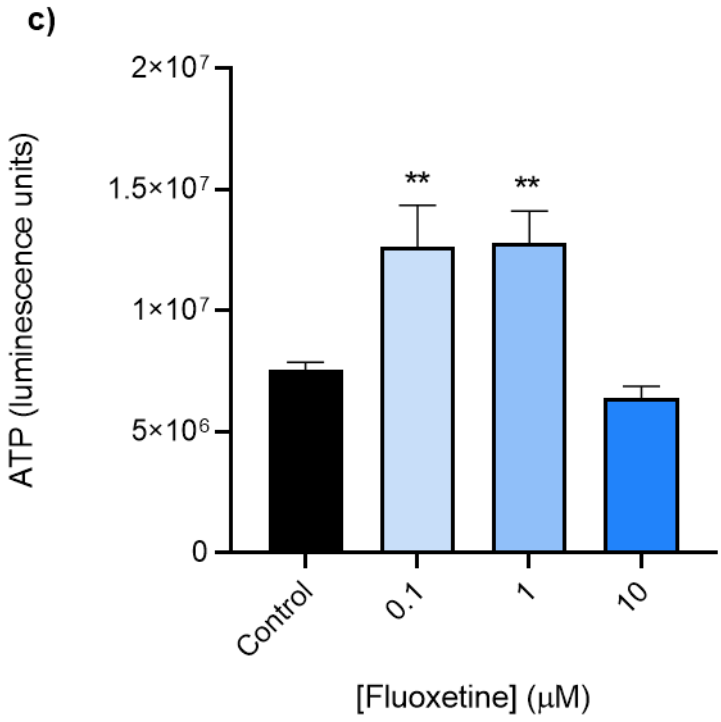

Figure 4.1. Effects of fluoxetine on ATP generation by MIN6 cells (a), mouse islets (b) and human islets (c). The cells or islets were incubated without (control) or with fluoxetine (0.1-10μM) for 48h, and ATP production was measured using the luminescent CellTiter-Glo assay. Data are mean + SEM, n=8 observations representative of 2-5 separate experiments. **p<0.01, ***p<0.001 relative to the control samples, One-way ANOVA, Dunnett's multiple comparisons test.

4.3.1.2. Effects of fluoxetine on beta cell viability

The Trypan blue uptake assay was used to investigate whether fluoxetine is well tolerated by MIN6 cells and mouse islets, and whether it affects cell viability. After 48h culture in the absence or presence of fluoxetine (0.1-10μM), staining with Trypan blue was performed and visualised by light microscopy. MIN6 cells and islets pre-exposed to concentrations of fluoxetine of 1μM or lower did not show noticeable Trypan blue uptake, while excessive dye uptake was evident in cells and islets that had been exposed to 10μM fluoxetine (Figure 4.2a, c). MIN6 cells that had been incubated with 10μM fluoxetine for 48h detached from the well surface and appeared blue, and the islets showed excessive dye uptake by the cells in the centre of the islets where beta cells are present. Haemocytometer quantification of MIN6 cells retrieved after exposure to 0.1-10μM for 48h, and incubated in the presence of 0.2% (w/v) Trypan blue for 15min, also indicated that 10μM fluoxetine significantly reduced cell viability (Figure 4.2b). These experiments suggest that low and therapeutically relevant concentrations of fluoxetine (0.1-1μM) are well tolerated by MIN6 cells and islets, and they do not compromise cell viability, whereas 10μM of this SSRI is cytotoxic to beta cells, and hence it was not used in the functional experiments described in this chapter.

a)

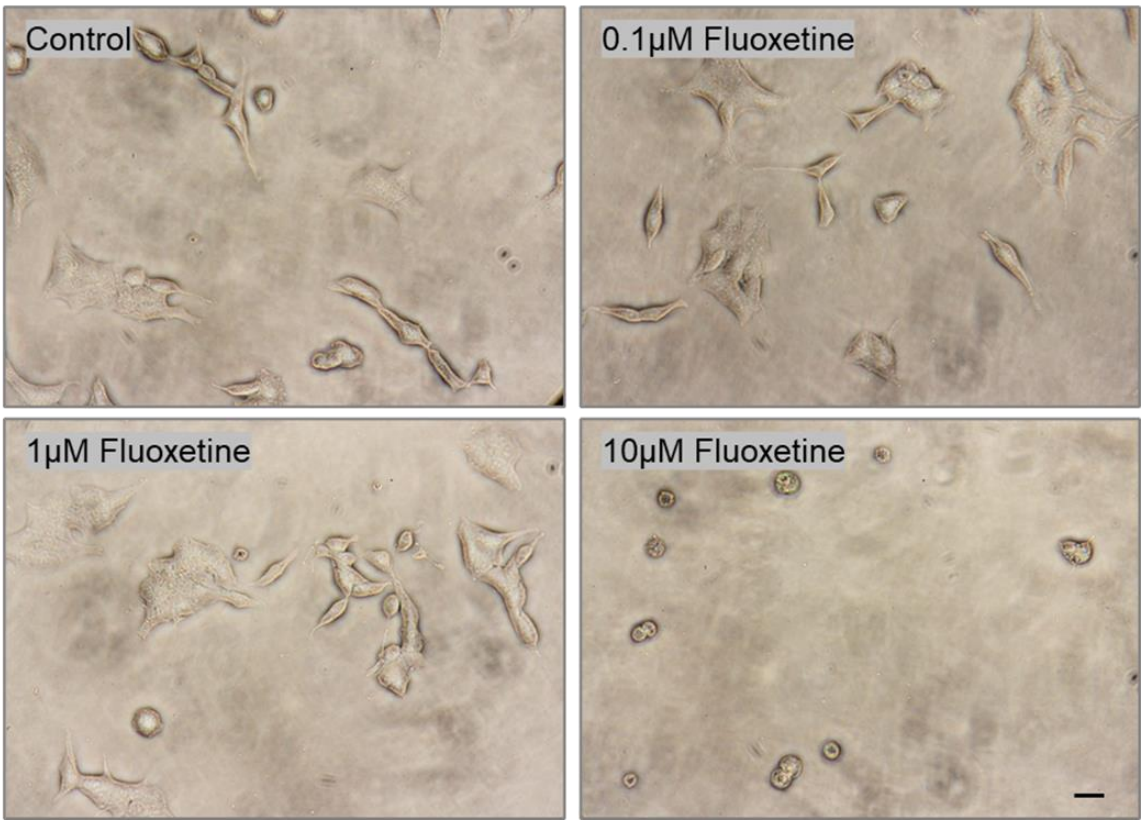
Control
0.1µM Fluoxetine
1µM Fluoxetine
10µM Fluoxetine

b)

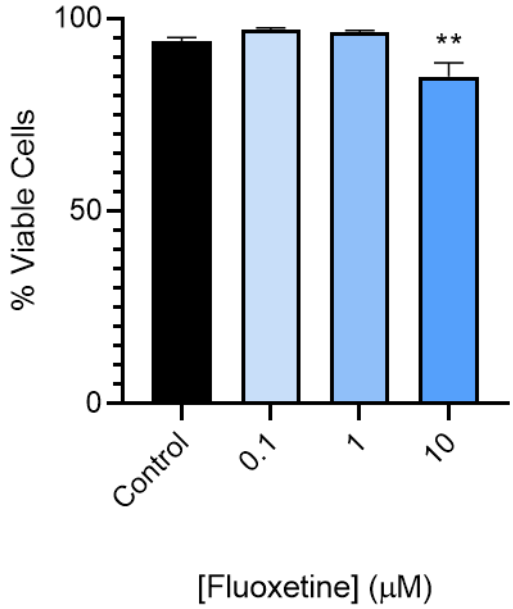
100
50
0
% Viable Cells
**
Control
0.1
1
10
[Fluoxetine] (µM)

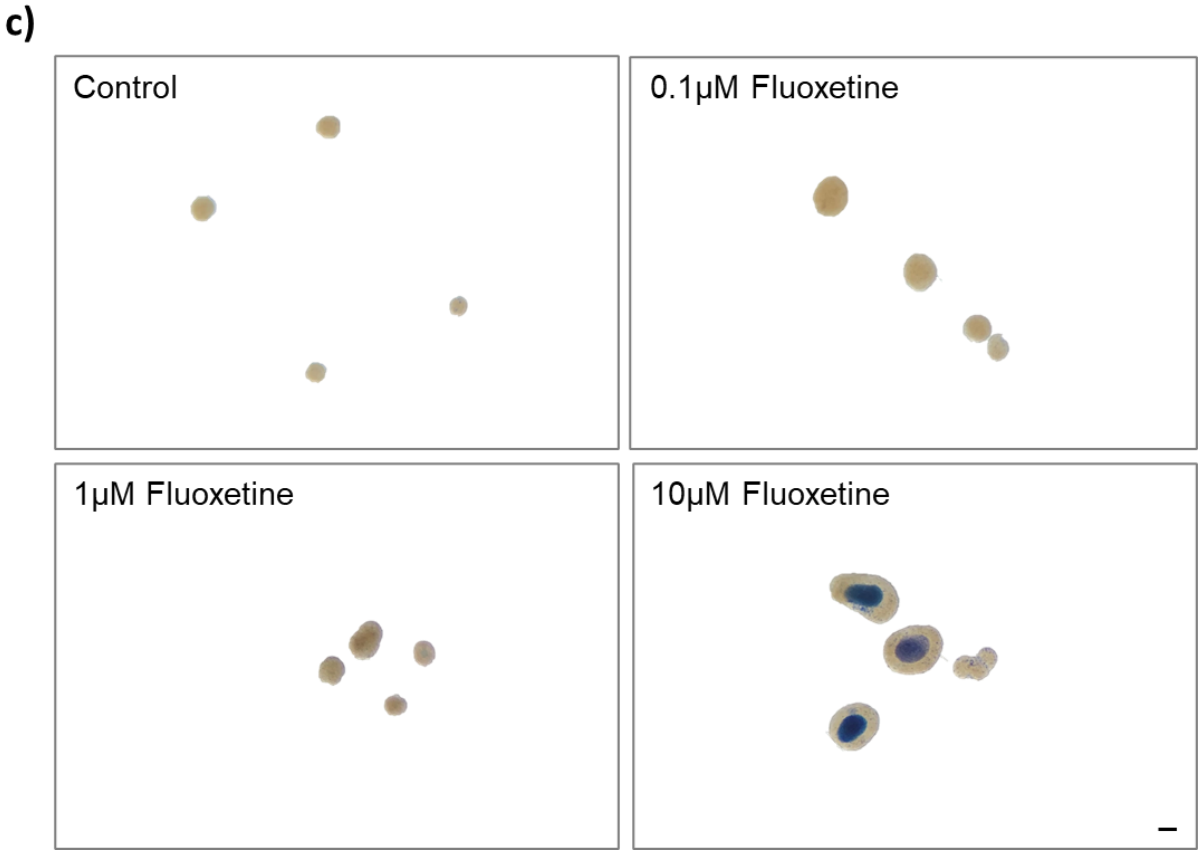

Figure 4.2. Effects of fluoxetine on MIN6 cell and mouse islet viability. Micrographs of Trypan blue-stained MIN6 cells (a) and mouse islets (c) after incubation for 48h in DMEM in the absence (control) or presence of fluoxetine (0.1-10µM). Scale bars show 50µm. Percentage viability of MIN6 cells was calculated by counting the numbers of viable and dead cells using a haemocytometer (b). Data are mean + SEM, n =5 technical repeats. **p<0.01 relative to the controls, One-way ANOVA, Dunnett's multiple comparisons test.

4.3.1.3. Effects of fluoxetine on insulin secretion

Having established that fluoxetine at 0.1µM and 1µM was well tolerated by MIN6 cells and mouse islets, the effects of these low and therapeutic concentrations of fluoxetine on insulin secretion by MIN6 cells and islets were investigated in acute and chronic static incubation experiments. Acute and chronic exposure of MIN6 cells to 1µM fluoxetine led to significantly increased insulin secretion at high, 25mM glucose (Figure 4.3a, b). In addition, 1µM fluoxetine significantly potentiated glucose-induced insulin secretion from mouse (Figure 4.3c, d) and human (Figure 4.3g, h) islets. However, it had no effect on basal insulin secretion at 2-2.5mM glucose, which is clinically important because drugs that increase insulin secretion at low glucose levels may cause hypoglycaemia in the fasting state. 1µM fluoxetine also further potentiated insulin secretion from mouse islets in the presence of the muscarinic M3 receptor agonist carbachol at high, 20mM glucose (Figure 4.3 e, f). Cholinergic activation of insulin secretion is mediated through muscarinic M3 receptors (Duttaroy et al., 2004; Gautam et al., 2006; Kong and Tobin, 2011; Yamazaki et al., 2006), and fluoxetine may activate other receptors on beta cells in order to maximise hormone secretion. In contrast to the effects seen with 1µM fluoxetine, 0.1µM fluoxetine had no significant effect on glucose-induced insulin release from MIN6 cells and islets, and it also did not modify basal insulin secretion.

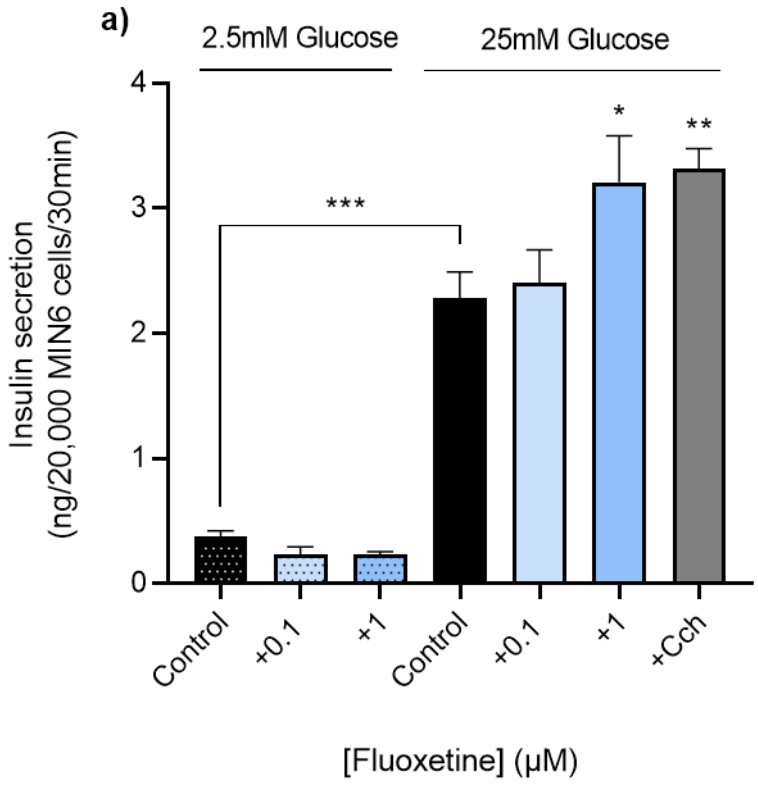
a)
2.5mM Glucose
25mM Glucose
Insulin secretion
(ng/20,000 MIN6 cells/30min)
0
1
2
3
4
***
*
**
Control
+0.1
+1
Control
+0.1
+1
+Cch
[Fluoxetine] (μM)

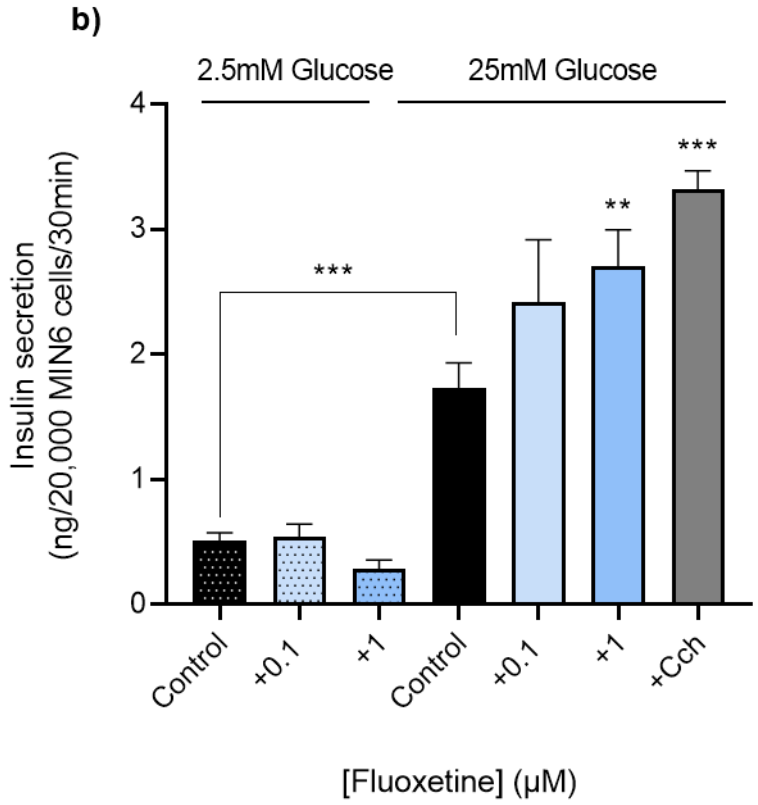
b)
2.5mM Glucose
25mM Glucose
Insulin secretion
(ng/20,000 MIN6 cells/30min)
0
1
2
3
4
***
**
***
Control
+0.1
+1
Control
+0.1
+1
+Cch
[Fluoxetine] (μM)

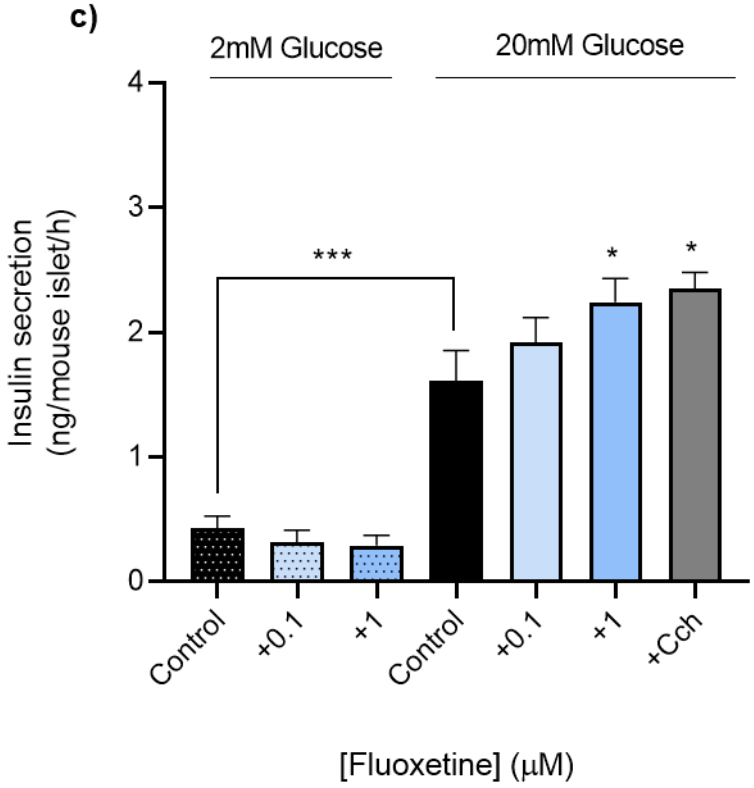
c)
2mM Glucose
20mM Glucose
Insulin secretion (ng/mouse islet/h)
0
1
2
3
4
***
*
*
Control
+0.1
+1
Control
+0.1
+1
+Cch
[Fluoxetine] (μM)

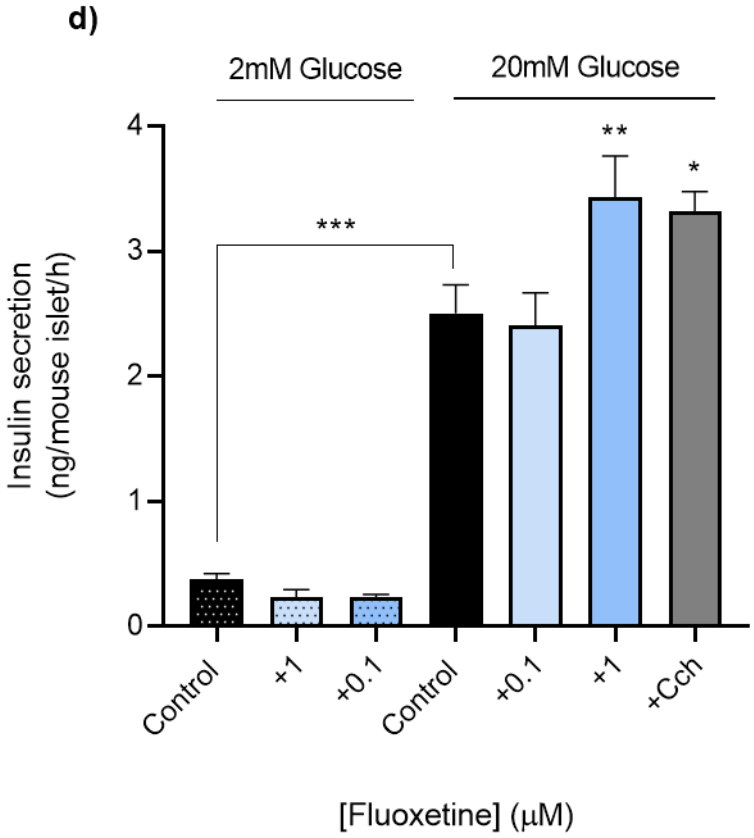
d)
2mM Glucose
20mM Glucose
Insulin secretion (ng/mouse islet/h)
0
1
2
3
4
***
**
*
Control
+1
+0.1
Control
+0.1
+1
+Cch
[Fluoxetine] (μM)

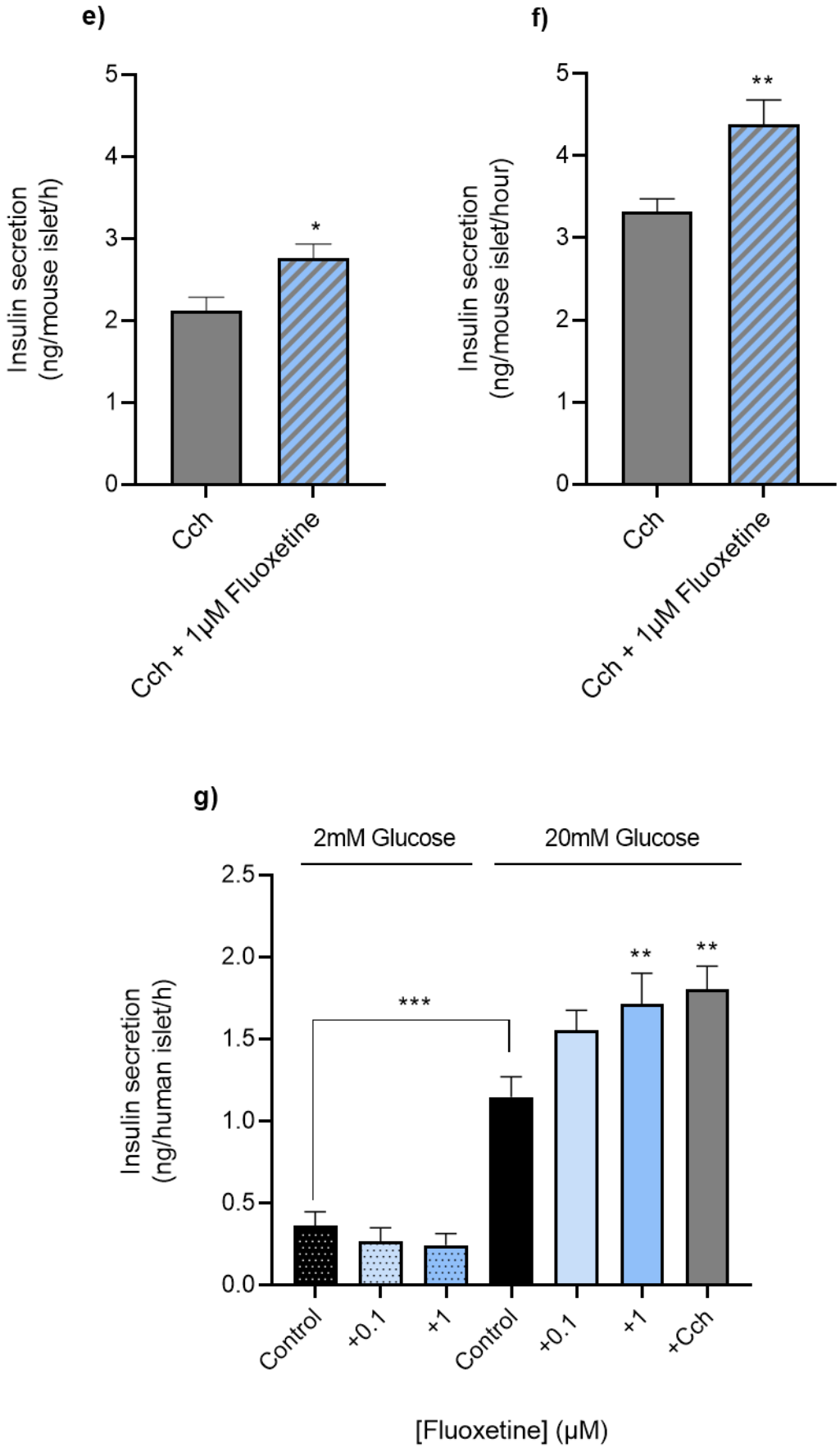
e)
Insulin secretion (ng/mouse islet/h)
5
4
3
2
1
0
*
Cch
Cch + 1μM Fluoxetine
f)
Insulin secretion (ng/mouse islet/hour)
5
4
3
2
1
0
**
Cch
Cch + 1μM Fluoxetine
g)
2mM Glucose
20mM Glucose
Insulin secretion (ng/human islet/h)
2.5
2.0
1.5
1.0
0.5
0.0
***
**
**
Control
+0.1
+1
Control
+0.1
+1
+Cch
[Fluoxetine] (μM)

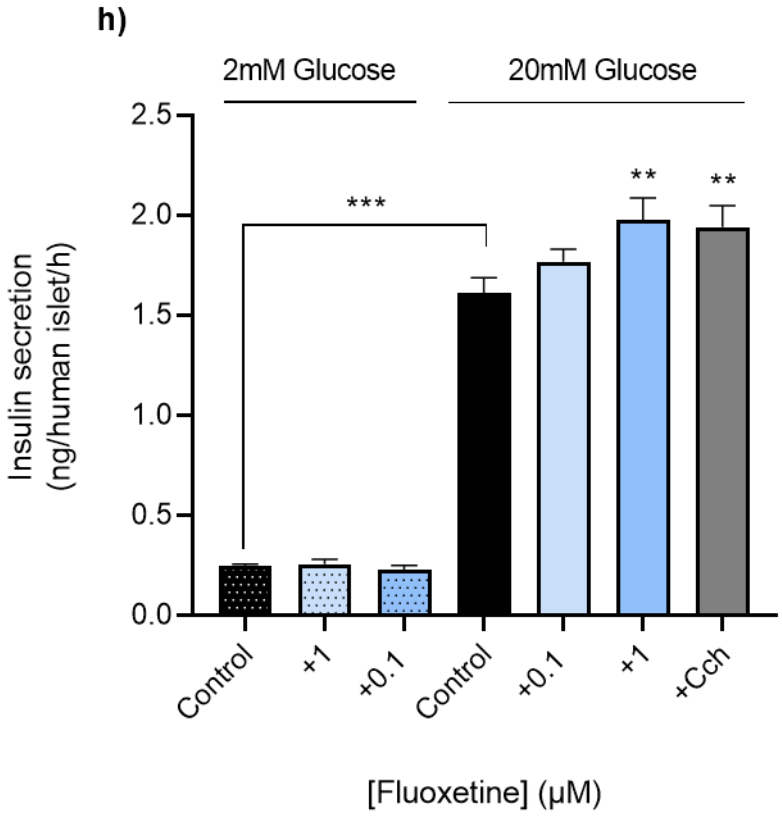

Figure 4.3. Effects of fluoxetine on insulin secretion from MIN6 cells (a – acute; b - chronic), mouse islets (c, e – acute; d, f - chronic) and human islets (g – acute; h -chronic), and on insulin secretion from mouse islets in the presence of 20mM glucose and 500μM carbachol in acute (e) and chronic experiments (f). MIN6 cells or islets were incubated without or with fluoxetine for 30min (MIN6 cells) or 1h (islets) without pre-treatment with fluoxetine (acute experiments) or following a 48h incubation in the absence or presence of fluoxetine (chronic experiments). All data shown are mean + SEM, n=8 observations representative of 2-4 separate experiments, One-way ANOVA, Dunnett's multiple comparisons test. *p<0.05; **p<0.1; ***p <0.001 relative to the control samples at 20-25mM glucose.

Dynamic insulin secretion was determined by perifusion of mouse and human islets, which allows more detailed information than can be obtained in static incubation experiments. These experiments indicated that acute exposure to 1μM fluoxetine caused a small but significant potentiation of glucose-stimulated insulin secretion (GSIS) from both perifused mouse (Figure 4.4a, b) and human (Figure 4.4c, d) islets, indicating that fluoxetine acts acutely to improve the dynamic insulin secretory output in response to glucose.

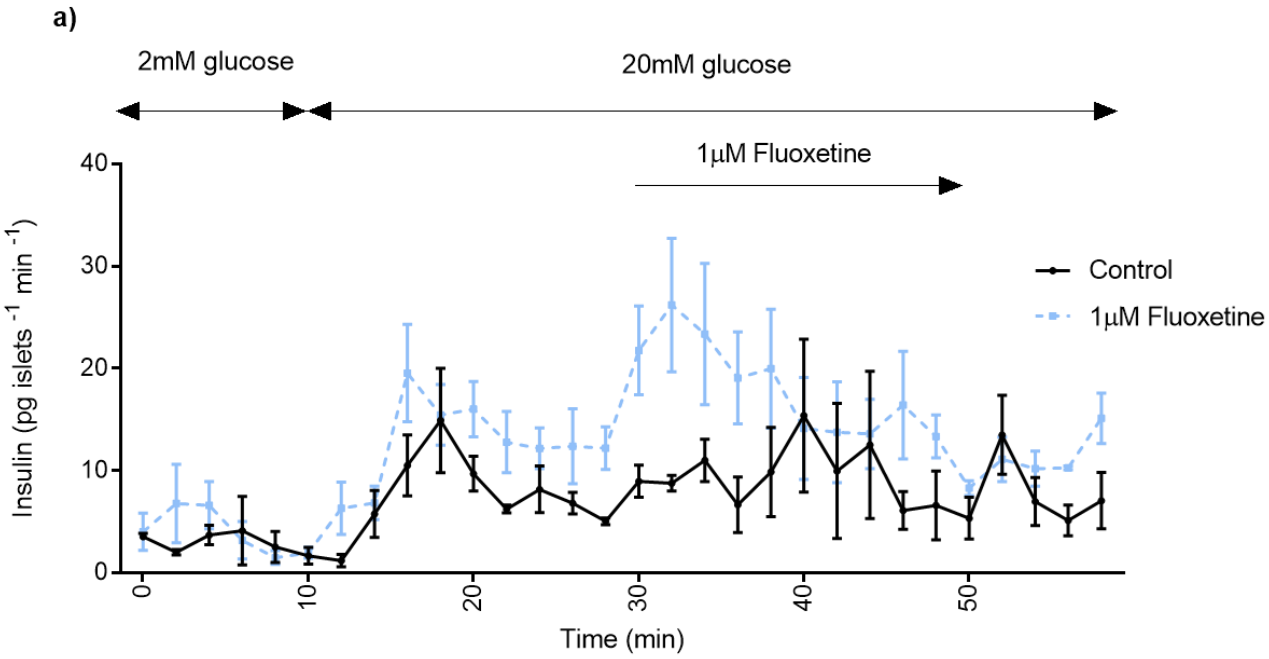

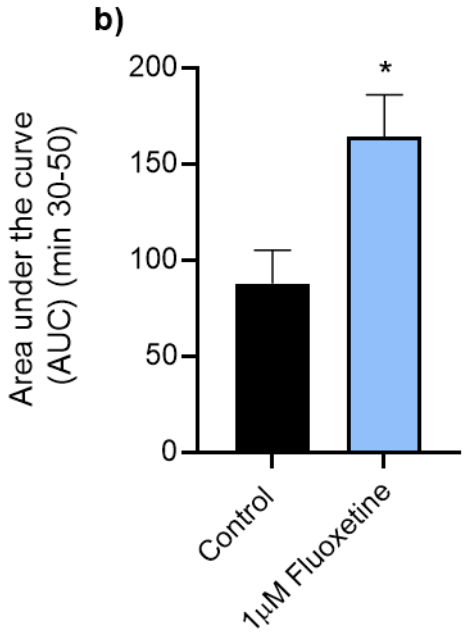
b)
Area under the curve (AUC) (min 30-50)
200
150
100
50
0
*
Control
1μM Fluoxetine

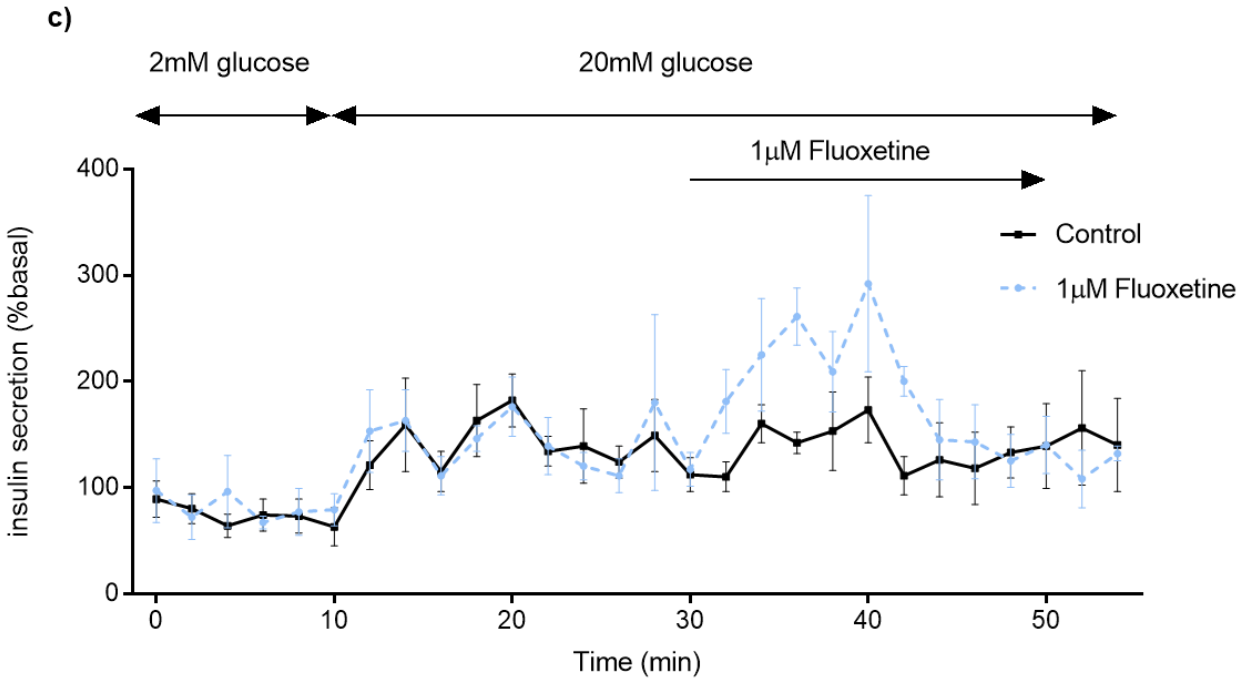
c)
2mM glucose
20mM glucose
1μM Fluoxetine
Control
1μM Fluoxetine
insulin secretion (%basal)
400
300
200
100
0
0
10
20
30
40
50
Time (min)

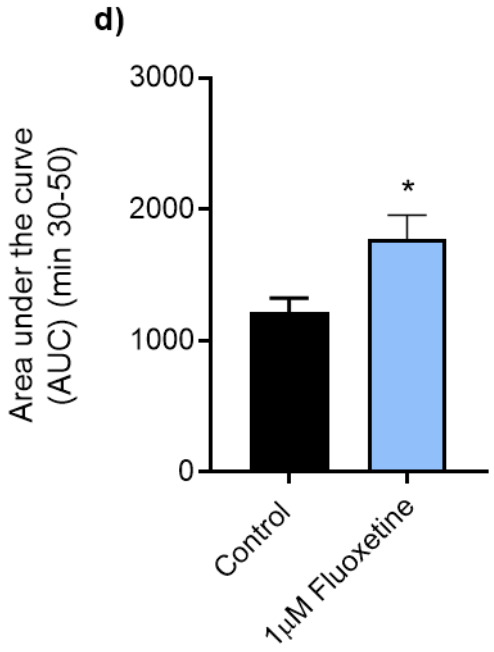

Figure 4.4. Effects of 1μM fluoxetine on dynamic insulin secretion from mouse islets (a, b) and human islets (c, d). Insulin secretion was stimulated by 20mM glucose, and the potentiating effects of fluoxetine on glucose-induced insulin secretion from islets are represented by the area under the curve (AUC) data for the 20min period of exposure to fluoxetine (b - mouse islets; d – human islets). Data are expressed as mean ± SEM; n=4 groups of islets per treatment, each containing 50 mouse or human islets; unpaired t-test. *$p<0.05$ versus control (black).

4.3.1.4. Effects of fluoxetine on beta cell proliferation

Increased ATP generation in response to 48h exposure of fluoxetine could be a consequence of fluoxetine increasing beta cell number through increased proliferation. The direct effects of fluoxetine on MIN6 cell proliferation were therefore determined by quantifying the incorporation of the synthetic nucleoside BrdU into the DNA of proliferating MIN6 cells. 48h exposure to therapeutically relevant concentrations of fluoxetine (0.1-1μM) led to significantly increased BrdU incorporation when compared to control MIN6 cells maintained in the absence of fluoxetine (Figure 4.5). 10% FBS, rich in growth factors that stimulate cell division, served as a positive control, and this caused an approximately 3-fold elevation in BrdU incorporation. In this experiment, fluoxetine acted directly on MIN6 cells to increase their proliferative rate *in vitro*.

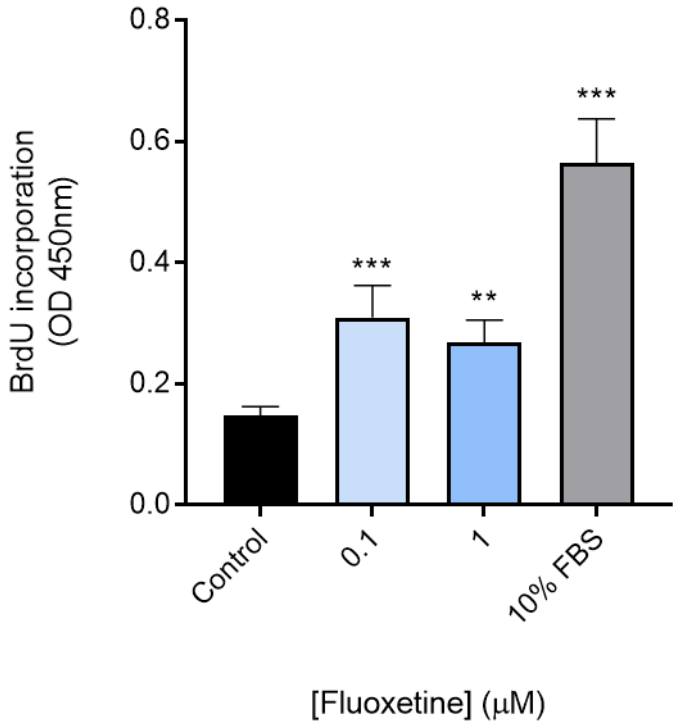

Figure 4.5. Effects of fluoxetine on MIN6 cell proliferation. MIN6 cells were exposed to fluoxetine for 48h and BrdU incorporation was measured by quantifying absorbance at 450nm. Data are mean + SEM, n=8 observations representative of 3 separate experiments, **p<0.01,

***p<0.001 relative to the control samples, One-way ANOVA, Dunnett's multiple comparisons test.

4.3.1.5. Effects of fluoxetine on beta cell apoptosis

Beta cell mass is increased by proliferation and decreased by beta cell death, which occurs primarily through apoptosis. MIN6 cell, mouse islet and human islet apoptosis was evaluated by measuring caspase3/7 activities that play an essential role in driving apoptosis. The effects of exposure to fluoxetine on caspase3/7 activities were quantified in the absence and presence of proinflammatory cytokines or the saturated free fatty acid palmitate, as beta cells have relatively low basal rates of apoptosis (Hayes et al., 2017). These experiments indicated that treatment with 0.1-1µM fluoxetine had no effect on basal or cytokine-induced caspase3/7 activities in MIN6 cells (Figure 4.6a), whereas 0.1-1µM fluoxetine had a protective effect against cytokine-induced apoptosis of mouse and human islets (Figure 4.6b, c). Fluoxetine also protected mouse and human islets (Figure 4.6e, f), as well as MIN6 cells (Figure 4.6d), from apoptosis induced by palmitate. Both inflammation and high levels of circulating free fatty acids contribute to the pathophysiology of T2D, therefore the ability of the drug to protect beta cells against cytokine- and palmitate-induced apoptosis would be an advantage in the treatment of diabetes.

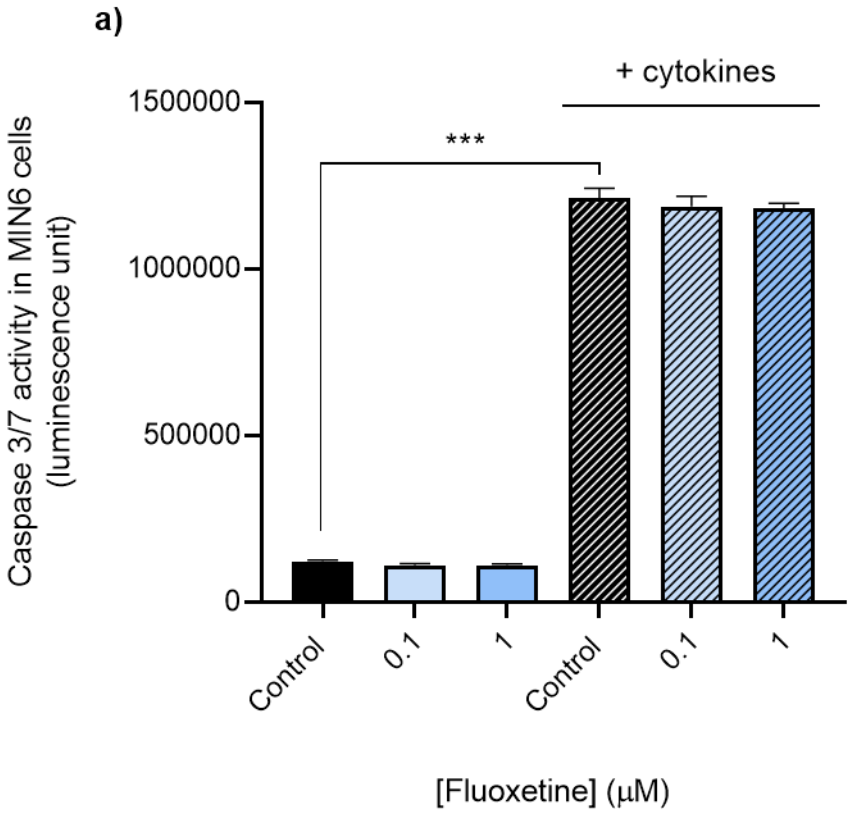
a)
+ cytokines
***
1500000
1000000
500000
0
Caspase 3/7 activity in MIN6 cells
(luminescence unit)
Control
0.1
1
Control
0.1
1
[Fluoxetine] (µM)

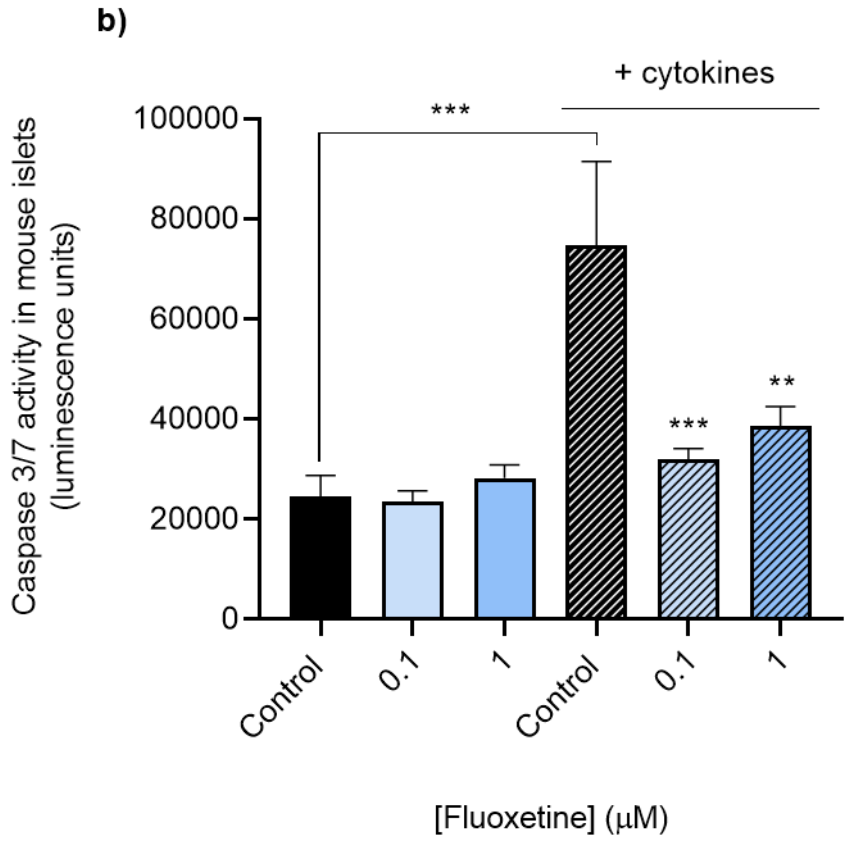
b)
+ cytokines
***
100000
80000
60000
40000
20000
0
***
**
Caspase 3/7 activity in mouse islets
(luminescence units)
Control
0.1
1
Control
0.1
1
[Fluoxetine] (µM)

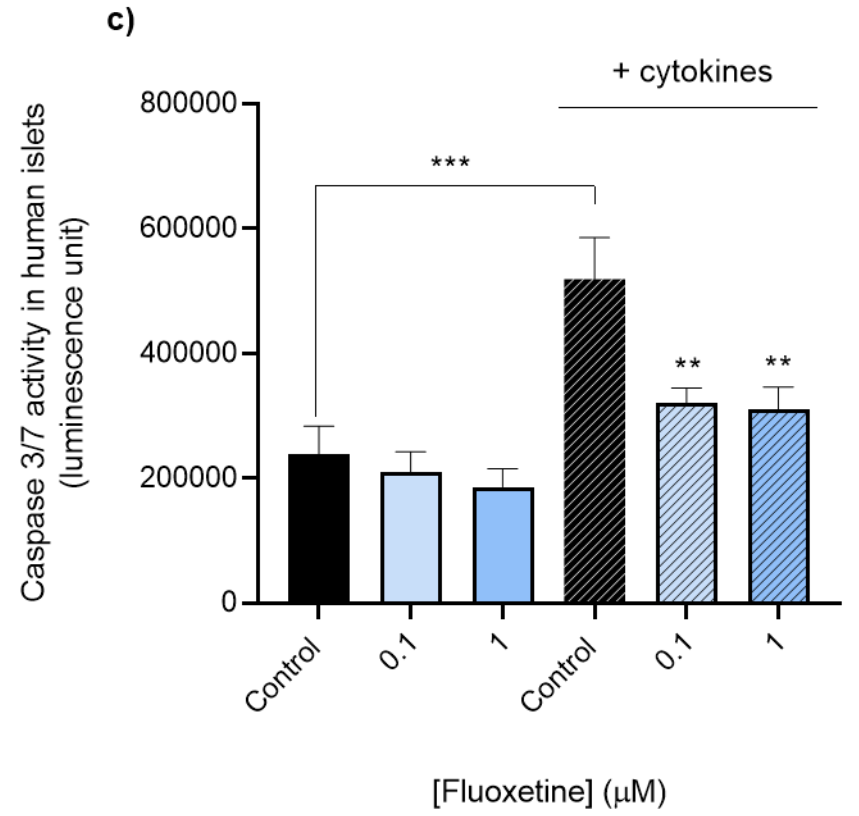
c)
+ cytokines
800000
600000
400000
200000
0
***
**
**
Caspase 3/7 activity in human islets
(luminescence unit)
Control
0.1
1
Control
0.1
1
[Fluoxetine] (µM)

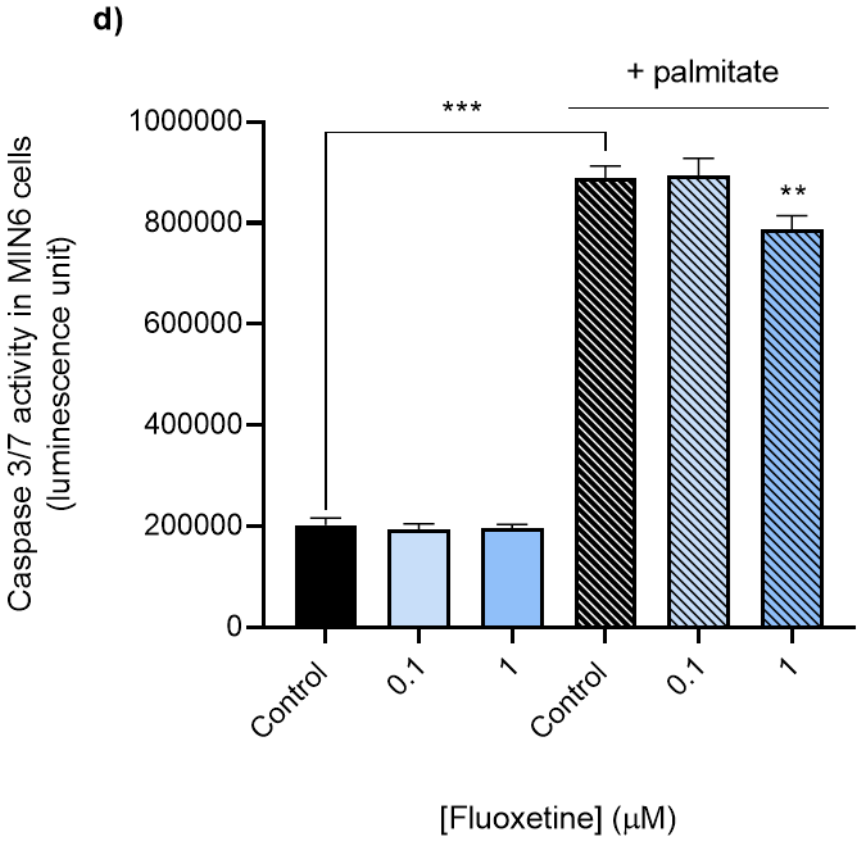
d)
+ palmitate
1000000
800000
600000
400000
200000
0
***
**
Caspase 3/7 activity in MIN6 cells
(luminescence unit)
Control
0.1
1
Control
0.1
1
[Fluoxetine] (µM)

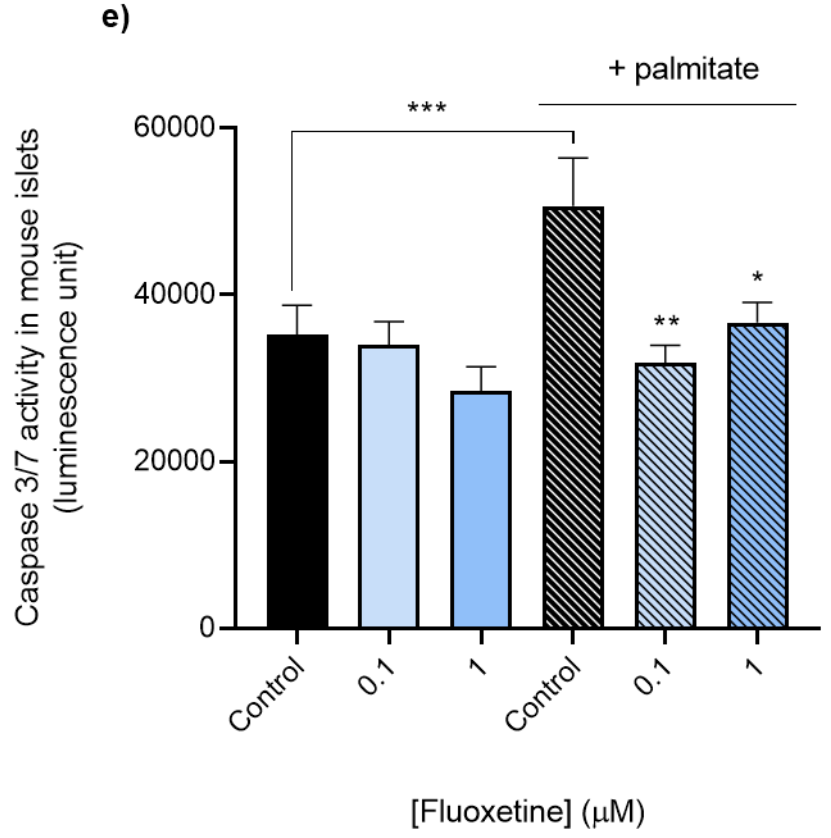
e)
+ palmitate
***
60000
40000
20000
0
Caspase 3/7 activity in mouse islets (luminescence unit)
**
*
Control
0.1
1
Control
0.1
1
[Fluoxetine] (μM)

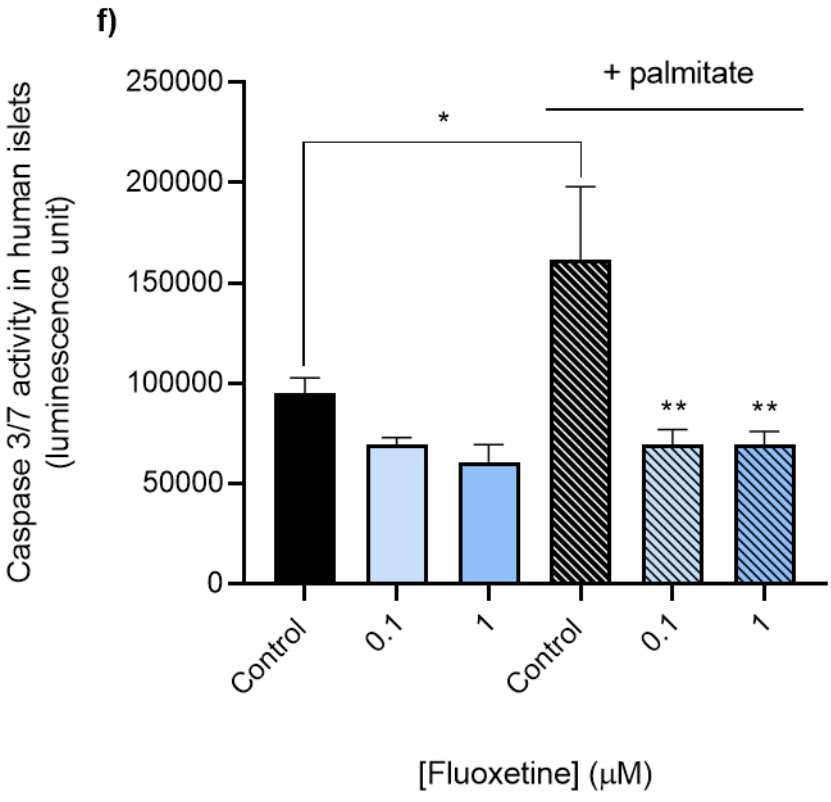
f)
+ palmitate
*
250000
200000
150000
100000
50000
0
Caspase 3/7 activity in human islets (luminescence unit)
**
**
Control
0.1
1
Control
0.1
1
[Fluoxetine] (μM)

Figure 4.6. Effects of fluoxetine on apoptosis of MIN6 cells (a, d), mouse islets (b, e) and human islets (c, f) assessed by luminescence quantification of caspase3/7 activities. MIN6 cells or islets were cultured in the absence or presence of fluoxetine for 48h. A proinflammatory cytokine mix or palmitate were added 24h before quantification of luminescence. Data are expressed as mean + SEM; n=8 observations representative of 4, 3 and 2 experiments using MIN6 cells, mouse islets and human islets, respectively. *p<0.05; **p<0.01; ***p<0.001 versus appropriate control in the absence (black) or presence (striped line) of cytokines; One-way ANOVA, Dunnett's multiple comparisons test.

The protective effect of fluoxetine against cytokine-induced apoptosis in mouse and human islets (Figure 4.6b-c) was not observed in MIN6 cells (Fig 4.6a). As demonstrated in Sections 4.3.1.2. and 4.3.1.4, 0.1 and 1µM fluoxetine increase ATP generation and proliferation of MIN6 cells. It is therefore possible that protective effects of fluoxetine against cytokine induced MIN6 cell apoptosis is masked by an increased number of cells, and therefore increased caspase3/7 luminescence. To determine whether that was the case, MIN6 cell apoptosis was also measured by flow cytometry, which allows measurement of apoptosis in single cells. For these experiments, MIN6 cells were stained with annexin V, and apoptosis was induced using the same proinflammatory cytokine mix that had been used for quantification of caspase3/7 luminescence. In contrast to the data obtained in the caspase3/7 experiments (Figure 4.6a), exposure of MIN6 cells for 48h to 0.1-1µM fluoxetine resulted in significantly decreased annexin V binding, and hence reduced apoptosis (Figure 4.7).

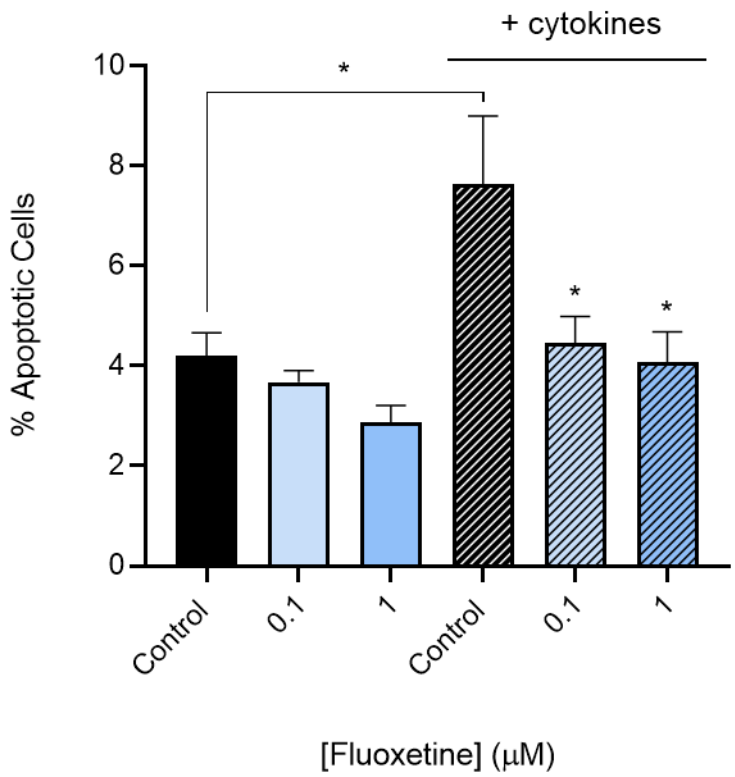

Figure 4.7. Effects of fluoxetine on apoptosis of MIN6 cells assessed by analysis of annexin V staining. Data are mean + SEM, n=3 separate experiments, *p<0.05 relative to the control samples (black striped), One-way ANOVA, Dunnett's multiple comparisons test.

4.3.1.6. Effects of fluoxetine on phosphorylation of MAPK, CREB and Akt

The effects of fluoxetine on beta cell intracellular signalling were investigated in Western blotting experiments. MAPK, CREB and Akt are involved in proliferation and survival of beta cells (Daziano et al., 2021), and Figure 4.8 shows that 1µM fluoxetine stimulated their phosphorylation, and hence activation. Phosphorylation of MAPK, CREB and Akt was also increased by 10µM forskolin, an activator of adenylyl cyclase, which served as a positive control. These experiments indicate that fluoxetine could exert its effects on beta cell proliferation through the ERK2/CaMK4/CREB/Irs2 cascade.

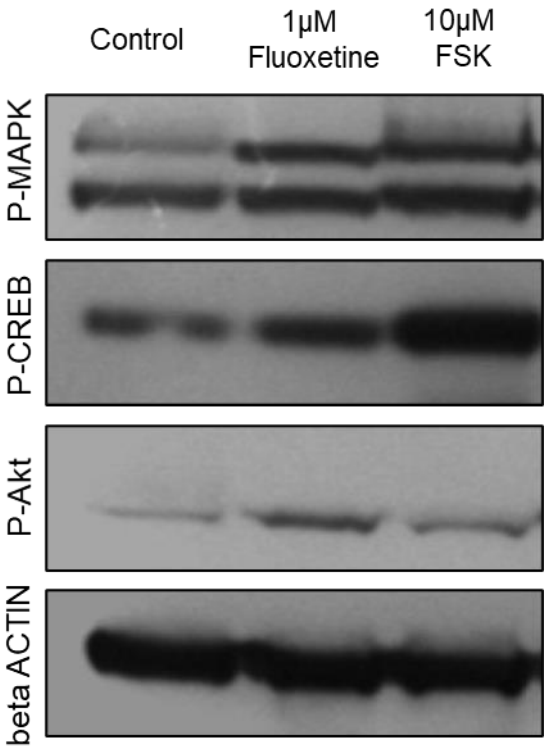

Figure 4.8. Effects of fluoxetine on phosphorylation of MAPK, CREB and Akt in MIN6 cells. MIN6 cells were incubated without or with 1µM fluoxetine for 24h before Western blotting for phosphorylation of MAPK (P-MAPK), CREB (P-CREB) and Akt (P-Akt) using appropriate antibodies. 10µM forskolin (FSK) was used as a positive control. Beta actin expression was used as loading control. Data are representative of 2-3 individual experiments.

4.3.2. Sertraline

4.3.2.1. Effects of sertraline on ATP generation by beta cells

Similar to the data obtained with fluoxetine (Figure 4.1), 48h incubation of MIN6 cells with the related SSRI, sertraline (0.1-1µM), also significantly increased ATP generation in MIN6 cells, as it did in mouse and human islets (Figure 4.9). As with fluoxetine, MIN6 cells that had been exposed to 10µM sertraline for 48h did not provide a luminescent signal, which indicates that this concentration was cytotoxic to MIN6 cells. There was no difference between ATP production by islets that had been treated with 10µM sertraline and controls, meaning that MIN6 cells are more sensitive to high concentrations of sertraline than mouse and human islets, which could be due differences in proliferative rates and cell arrangement.

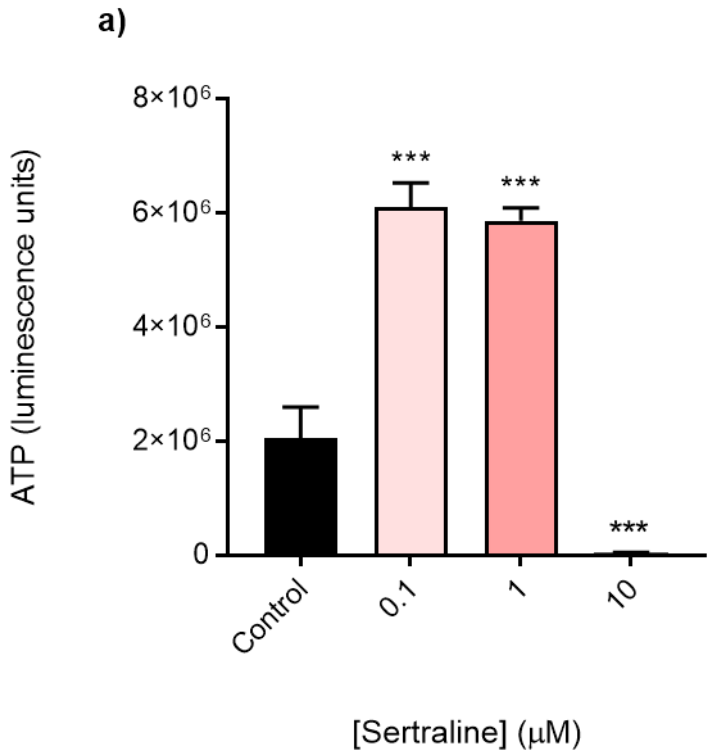

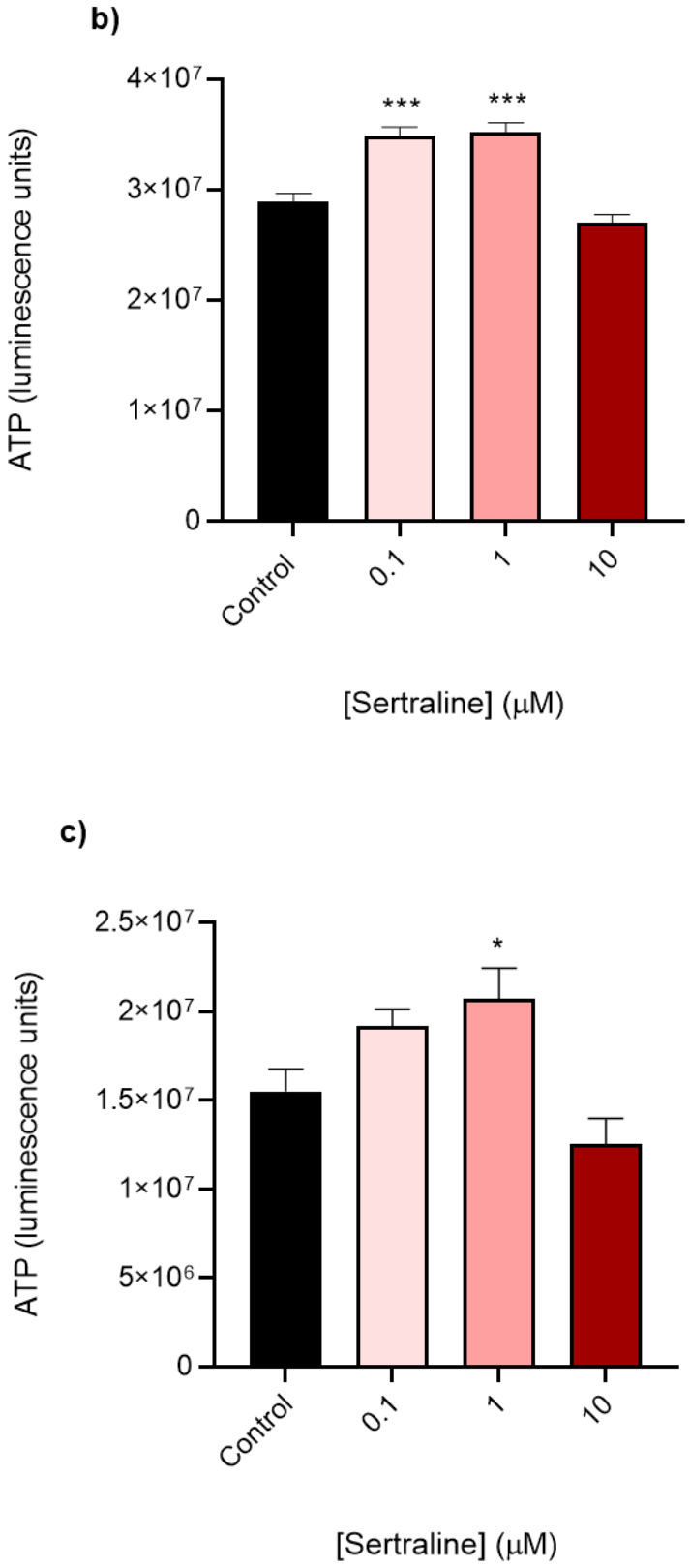

Figure 4.9. Effects of sertraline on ATP production by MIN6 cells (a), mouse islets (b) and human islets (c). The cells were incubated without or with sertraline for 48h, and ATP generation was

measured using a luminescent CellTiter-Glo assay. Data are mean + SEM, n=8 observations representative of 2-5 separate experiments. *p<0.05, ***p<0.001 relative to the control samples, One-way ANOVA, Dunnett's multiple comparisons test.

4.3.2.2. Effects of sertraline on beta cell viability

The Trypan blue test was used to determine the effects of sertraline on MIN6 cell and mouse islet viability. Following a 48h incubation in the absence or presence of sertraline (0.1-10µM), MIN6 cells were stained with Trypan blue, and the dye uptake was visualised by light microscopy. Consistent with the ATP generation data, Trypan blue uptake was only evident in MIN6 cells or islets that had been treated with 10µM sertraline, meaning that this concentration was cytotoxic to the cells, while lower concentrations did not compromise the plasma membrane nor allowed dye entry (Figure 4.10). Therefore, only concentrations of 0.1-1µM of sertraline were used in functional experiments presented in this chapter.

a)

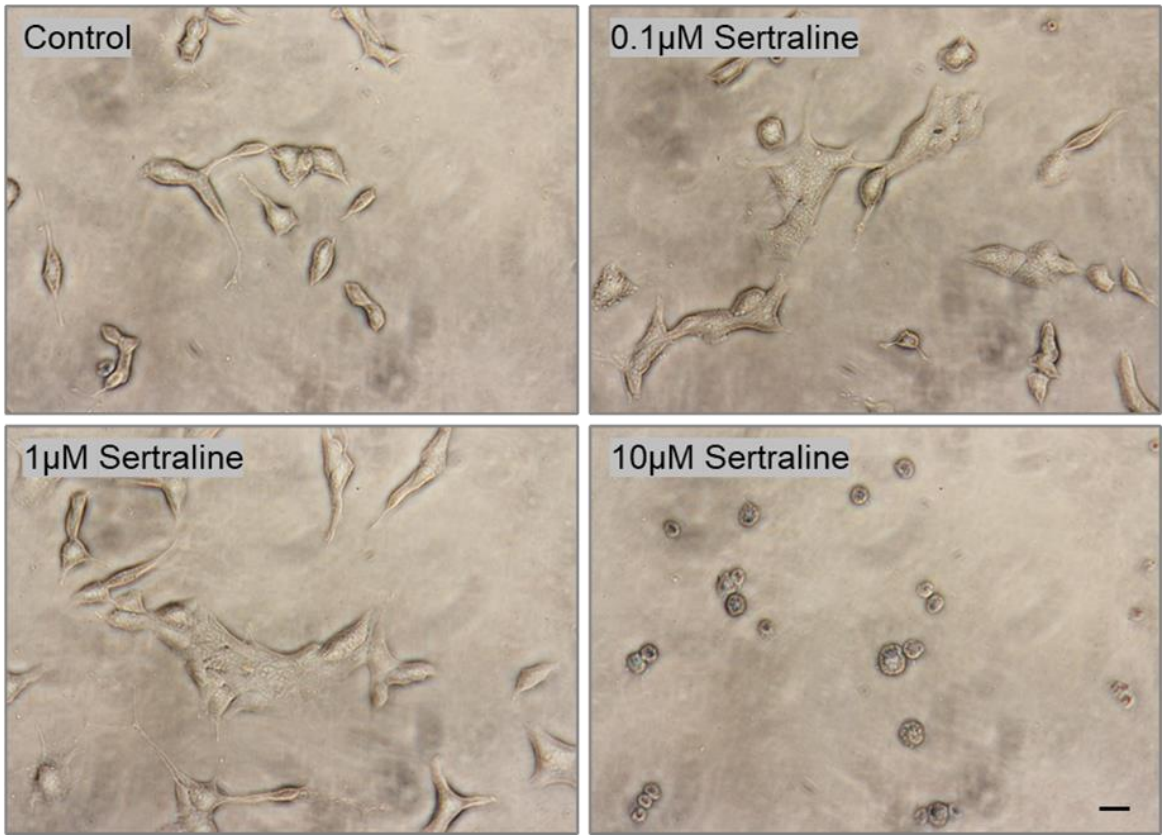
Control
0.1µM Sertraline
1µM Sertraline
10µM Sertraline

b)

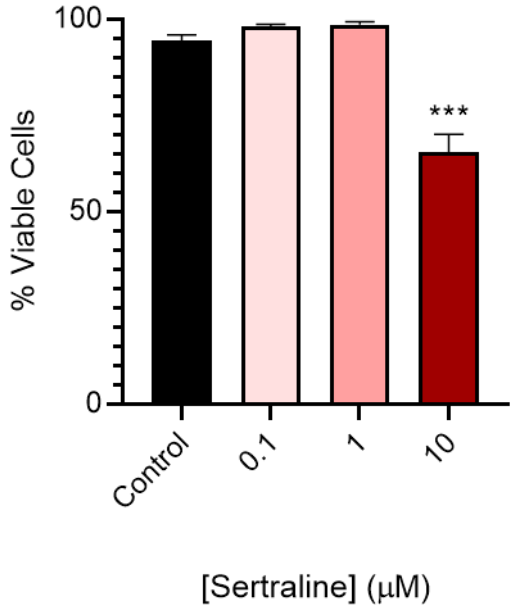
100
50
0
% Viable Cells
***
Control
0.1
1
10
[Sertraline] (µM)

c)

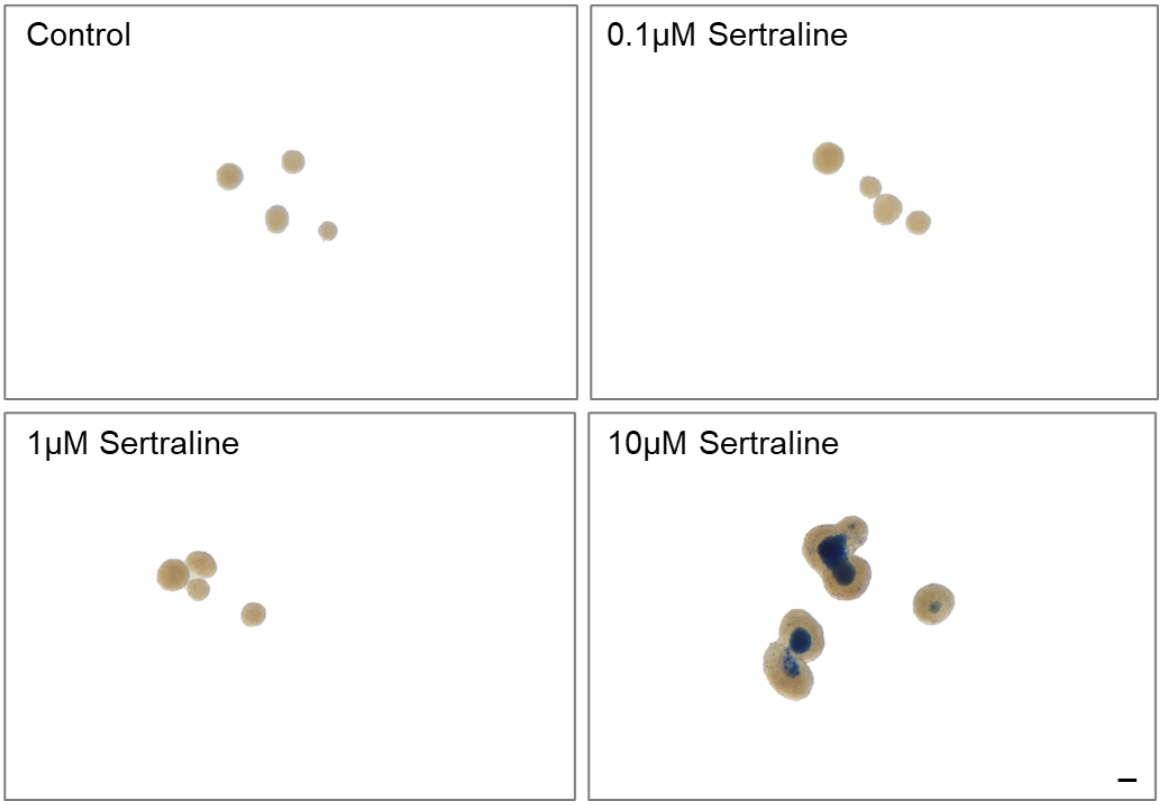

Figure 4.10. Effects of sertraline on MIN6 cell and mouse islet viability. Micrographs of Trypan blue-stained MIN6 cells (a) and mouse islets (c) after incubation for 48h in DMEM/RPMI in the absence (control) or presence of sertraline (0.1-10µM). Scale bars show 50µm. % Viability of MIN6 cells was calculated by counting the numbers of viable and dead cells using the haemocytometer (b). Data are mean + SEM, n =5 technical repeats. ***p<0.001 relative to the controls, One-way ANOVA, Dunnett's multiple comparisons test.

4.3.2.3. Effects of sertraline on insulin secretion

Given that sertraline is well tolerated by MIN6 cells and mouse islets at 0.1-1µM, static incubation experiments and perifusions were performed to investigate the effects of sertraline on insulin secretion by MIN6 cells, mouse islets and human islets. In acute and chronic static incubation experiments, sertraline (0.1-1µM) enhanced insulin secretion from MIN6 cells and mouse islets at supraphysiological glucose levels (20-25mM) (Figure 4.11). In these experiments, sertraline at 1µM had the greatest effect on GSIS from both mouse and human beta cells. However, it did not induce insulin secretion from beta cells at low glucose concentrations (2-2.5mM), which is an advantage when considering this drug for the treatment of T2D. In the similar way as fluoxetine, sertraline further enhanced insulin secretion from mouse islets in the presence of carbachol, indicating a mechanism of action of SSRIs on beta cells different to activation of a muscarinic M3 receptors that are expected to be occupied by carbachol (Figure 4.11 e, f).

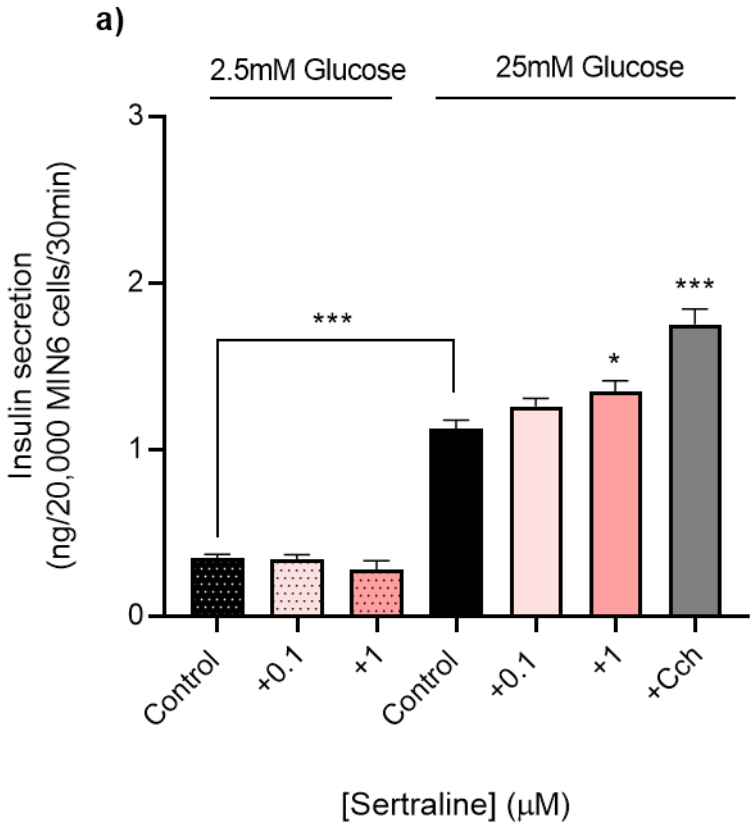
a)
2.5mM Glucose
25mM Glucose
Insulin secretion
(ng/20,000 MIN6 cells/30min)
3
2
1
0
***
*
***
Control
+0.1
+1
Control
+0.1
+1
+Cch
[Sertraline] (μM)

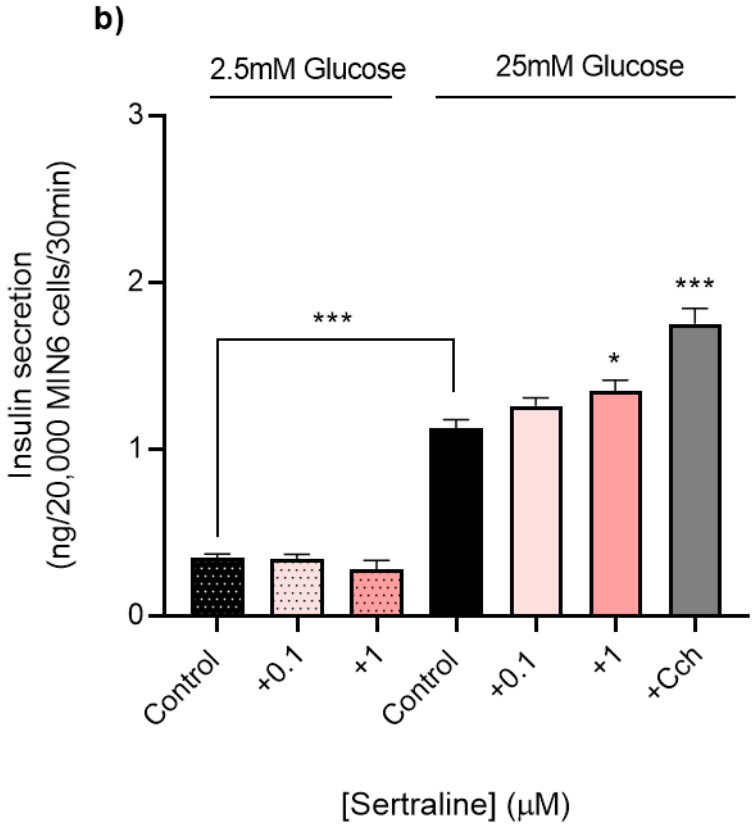
b)
2.5mM Glucose
25mM Glucose
Insulin secretion
(ng/20,000 MIN6 cells/30min)
3
2
1
0
***
*
***
Control
+0.1
+1
Control
+0.1
+1
+Cch
[Sertraline] (μM)

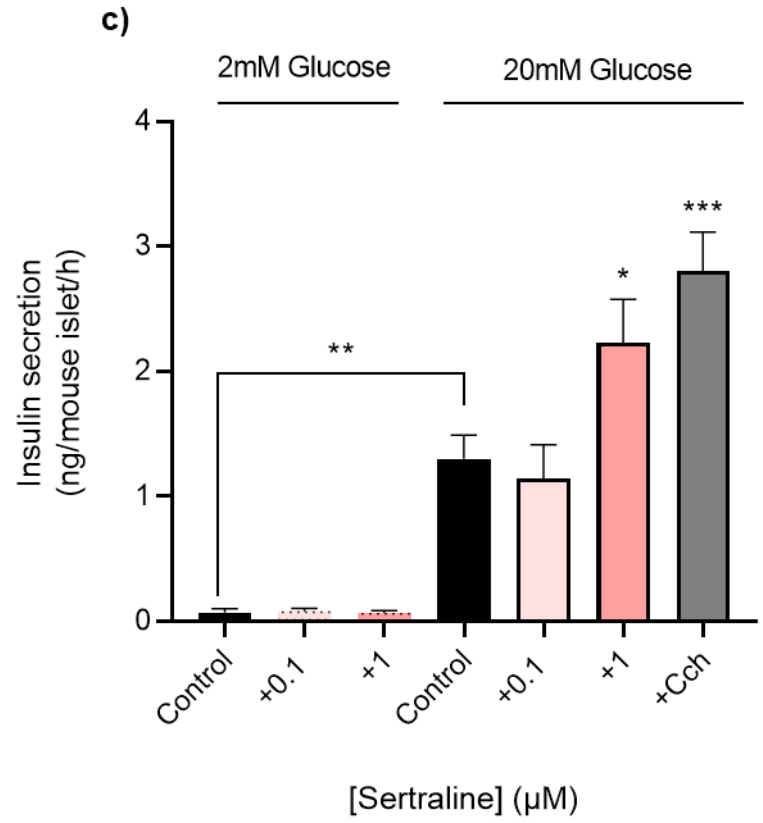
c)
2mM Glucose
20mM Glucose
Insulin secretion (ng/mouse islet/h)
4
3
2
1
0
**
*
***
Control
+0.1
+1
Control
+0.1
+1
+Cch
[Sertraline] (µM)

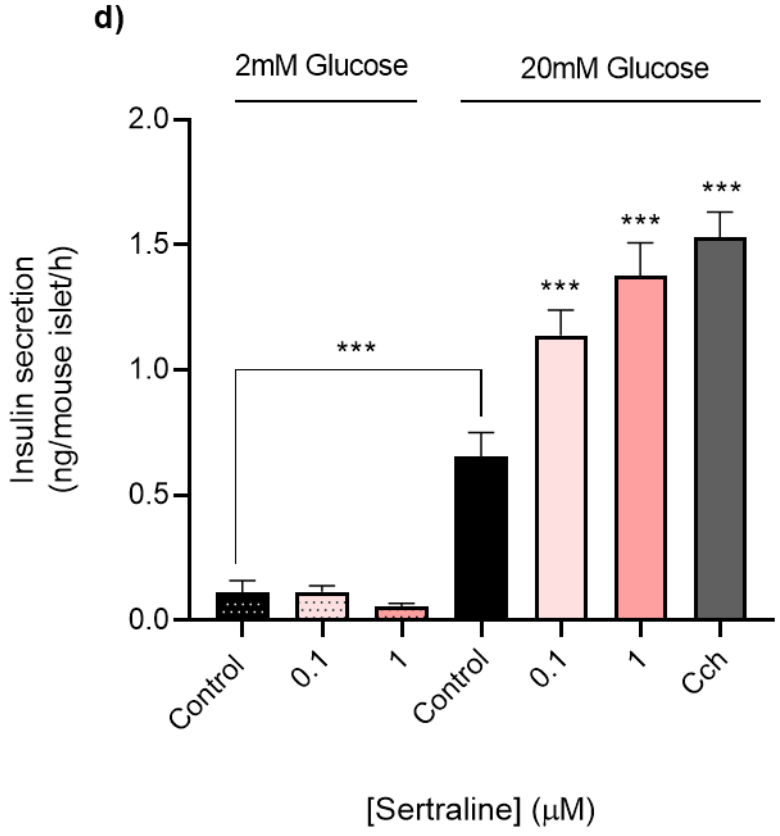
d)
2mM Glucose
20mM Glucose
Insulin secretion (ng/mouse islet/h)
2.0
1.5
1.0
0.5
0.0
***
***
***
***
Control
0.1
1
Control
0.1
1
Cch
[Sertraline] (µM)

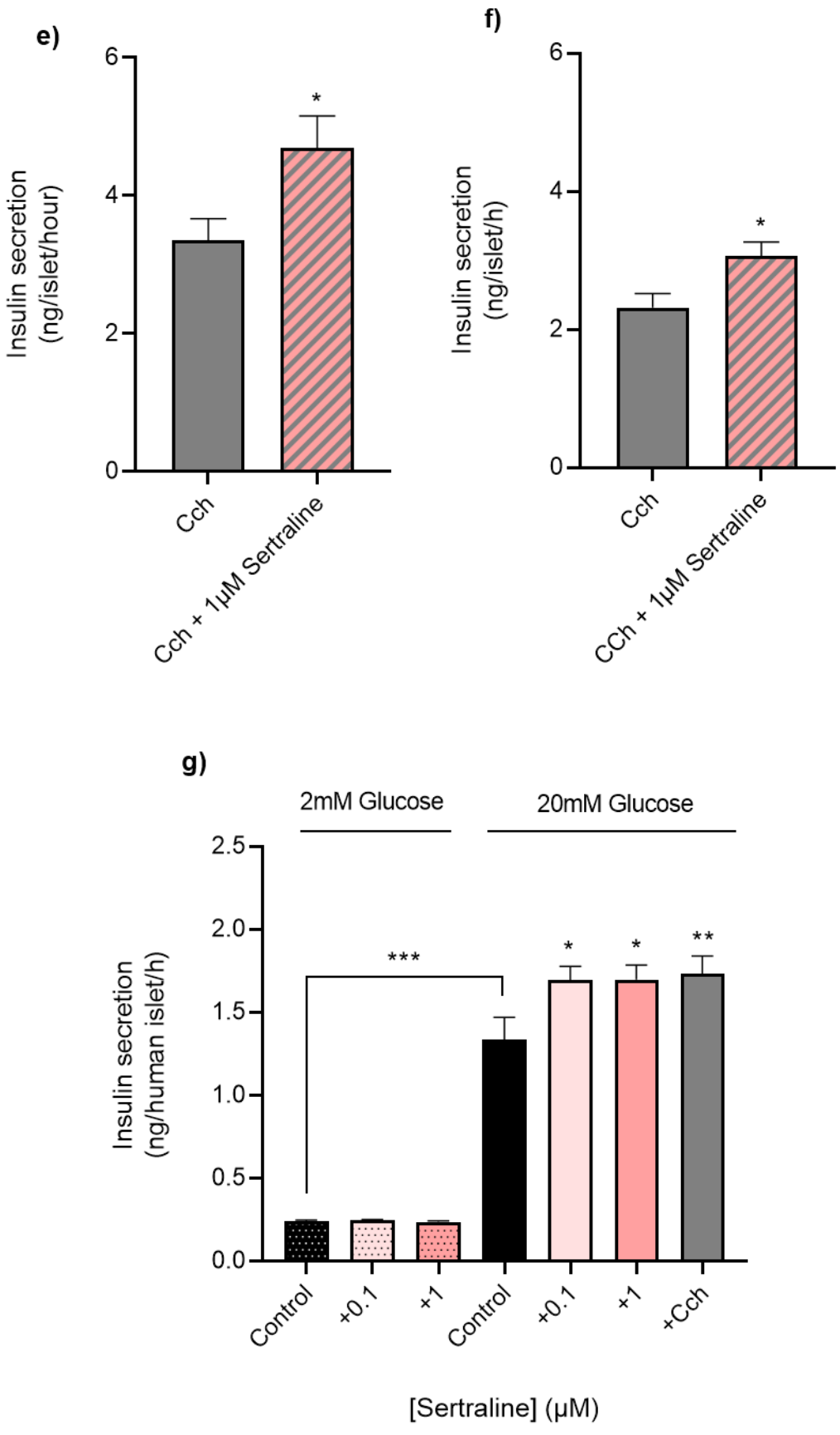
e)
Insulin secretion (ng/islet/hour)
6
4
2
0
*
Cch
Cch + 1μM Sertraline
f)
Insulin secretion (ng/islet/h)
6
4
2
0
*
Cch
CCh + 1μM Sertraline
g)
2mM Glucose
20mM Glucose
Insulin secretion (ng/human islet/h)
2.5
2.0
1.5
1.0
0.5
0.0
***
*
*
**
Control
+0.1
+1
Control
+0.1
+1
+Cch
[Sertraline] (μM)

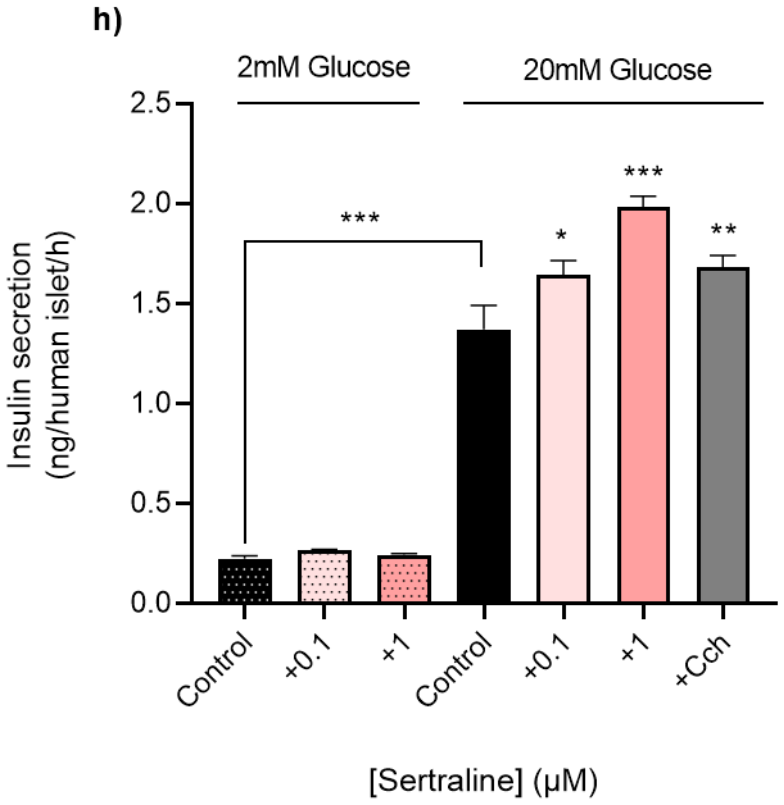

Figure 4.11. Effects of sertraline on insulin secretion from MIN6 cells (a, b), mouse islets (c, d) and human islets (g, h), and on GSIS from mouse islets in the presence of 500μM carbachol in acute (e) and chronic experiments (f). In static secretion experiments, MIN6 cells or islets were incubated in the absence or presence of sertraline for 30min (MIN6 cells), 1h (islets) (acute) (a, c, e) or 48h (chronic) (b, d, h). All data shown are mean + SEM, n=8 observations representative of 2-4 experiments. *p < 0.05; **p<0.1; ***p<0.001 relative to the control samples at 20mM glucose (islets) or 25mM glucose (MIN6 cells). One-way ANOVA, Dunnett's multiple comparisons test.

To investigate the effects of sertraline on dynamic insulin secretory profile, perifusions were performed using mouse and human islets. In these experiments, 1μM sertraline markedly increased dynamic insulin secretion from perifused islets (Figure 4.12), meaning that acute exposure to sertraline is sufficient to increase GSIS from the islets. These increases in insulin secretion were sustained for a short period of time (>10min) in the absence of the drug.

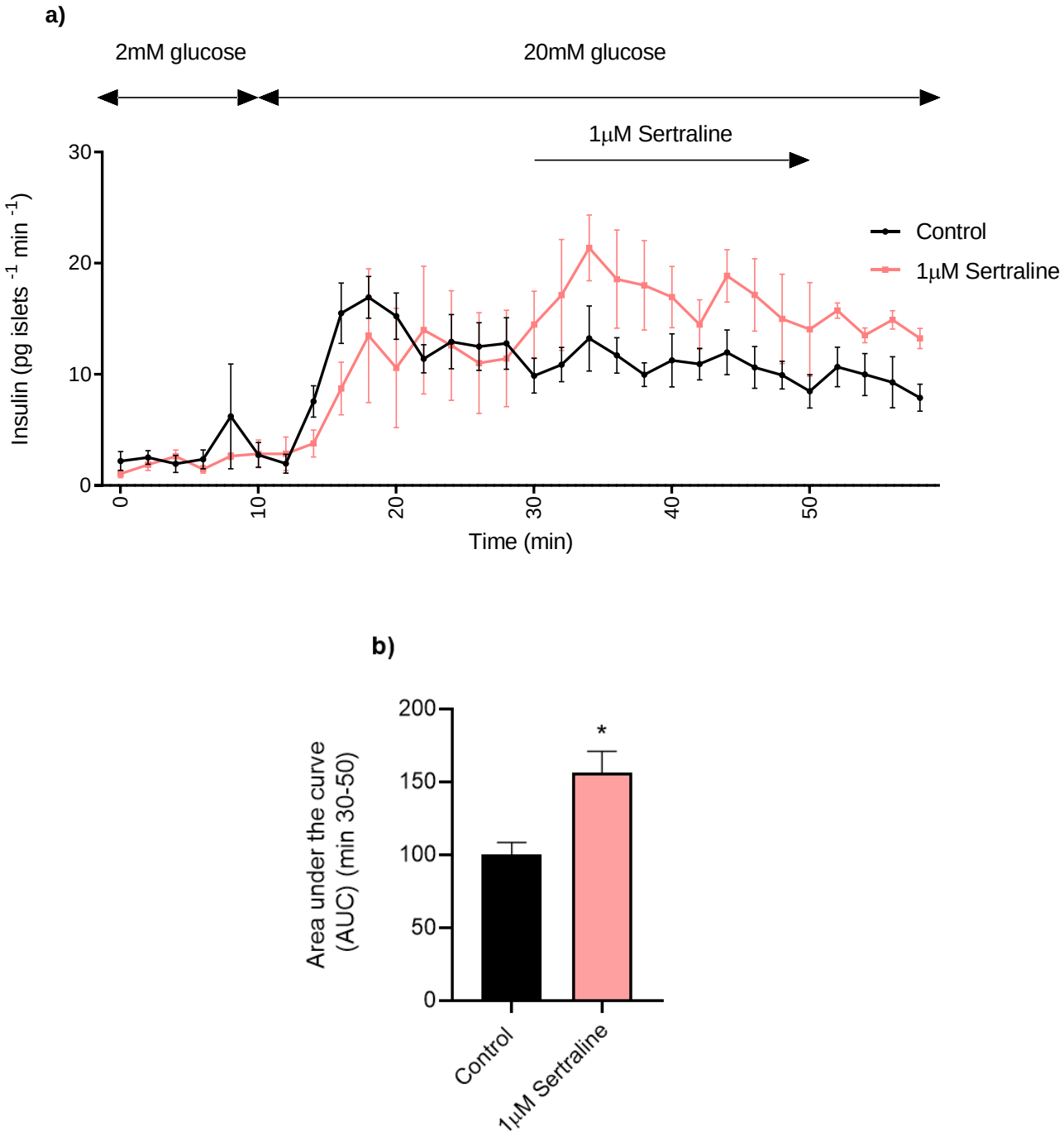

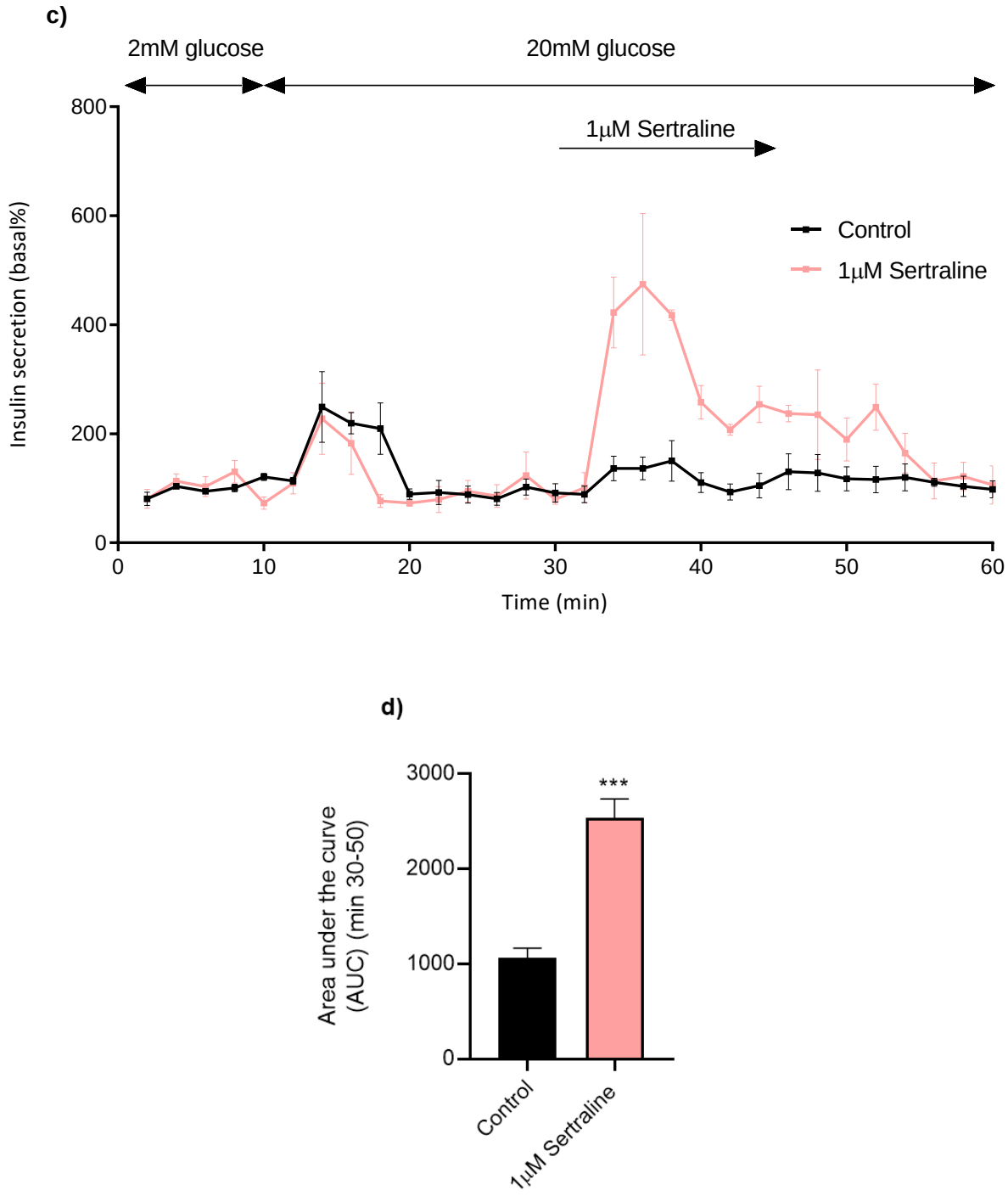

Figure 4.12. Dynamic insulin secretory profile of mouse islets (a, b) and human islets (c, d) in the absence or presence of 1μM sertraline. The effects of sertraline on glucose-induced insulin secretion from islets are represented by the area under the curve (AUC) (b- mouse islets; d – human islets). Data are expressed as mean ± SEM; n=4 groups of islets per treatment, each containing approximately 50 islets. *p < 0.05; ***p<0.001 versus control (black), unpaired t-test.

4.3.2.4. Effects of sertraline on beta cell proliferation

The favourable effects of sertraline to increase insulin secretion could be attributed to increased proliferation of beta cells. Therefore, proliferation of MIN6 cells was quantified following a 48h culture without or with sertraline (0.1-1µM). MIN6 cells were labelled with BrdU, and DNA replication was quantified using a BrdU ELISA kit. Similar to the fluoxetine data (Figure 4.6), low and therapeutically relevant concentrations of sertraline markedly increased BrdU incorporation into the DNA of dividing cells when compared to controls (Figure 4.13), indicating its direct effects on proliferation. 10% FBS containing growth factors that stimulate cell division served as a positive control, and it markedly increased BrdU readings.

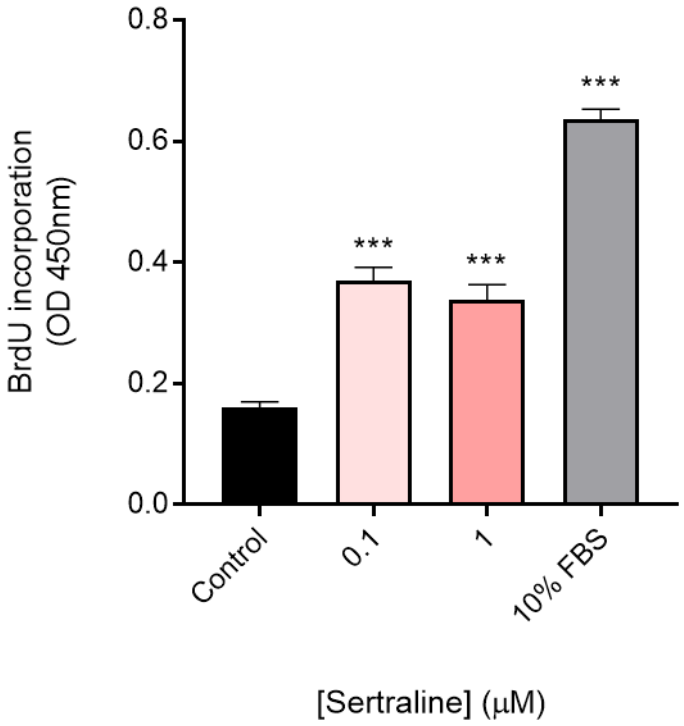

Figure 4.13. Effects of sertraline on MIN6 cell proliferation. MIN6 cells were exposed to sertraline at 0.1-1µM for 48h, and BrdU incorporation into the DNA of proliferating cells was measured using a BrdU ELISA. Data are mean + SEM, n=8 observations representative of 3

experiments. ***p<0.001 relative to the control samples, One-way ANOVA, Dunnett's multiple comparisons test.

4.3.2.5. Effects of sertraline on beta cell apoptosis

Decreased functional beta cell mass, mainly due to increased apoptosis, is the hallmark of both type 1 and type 2 diabetes (Donath and Halban, 2004). Apoptosis of MIN6 cells, mouse islets and human islets was quantified by measuring caspase3/7 activities that are increased in apoptosis. Following a 48h culture in the absence or presence of sertraline (0.1-1µM), caspase3/7 activities were quantified in MIN6 cells and islets. Apoptosis was induced using a proinflammatory cytokine mix or palmitate added for the final 24h. Levels of cytokines and circulating palmitate are increased during T2D, and as expected, they markedly elevated apoptosis rates when compared to non-treated controls in apoptosis experiments. 48h exposure to sertraline had no effect on caspase3/7 activities in MIN6 cells. However, sertraline had a protective effect against cytokine-induced apoptosis of mouse islets and human islets, as well as palmitate-induced apoptosis of MIN6 cells, mouse islets and human islets (Figure 4.14). There was no significant difference in basal apoptosis levels between controls and sertraline-treated islets where cytokines or palmitate were absent.

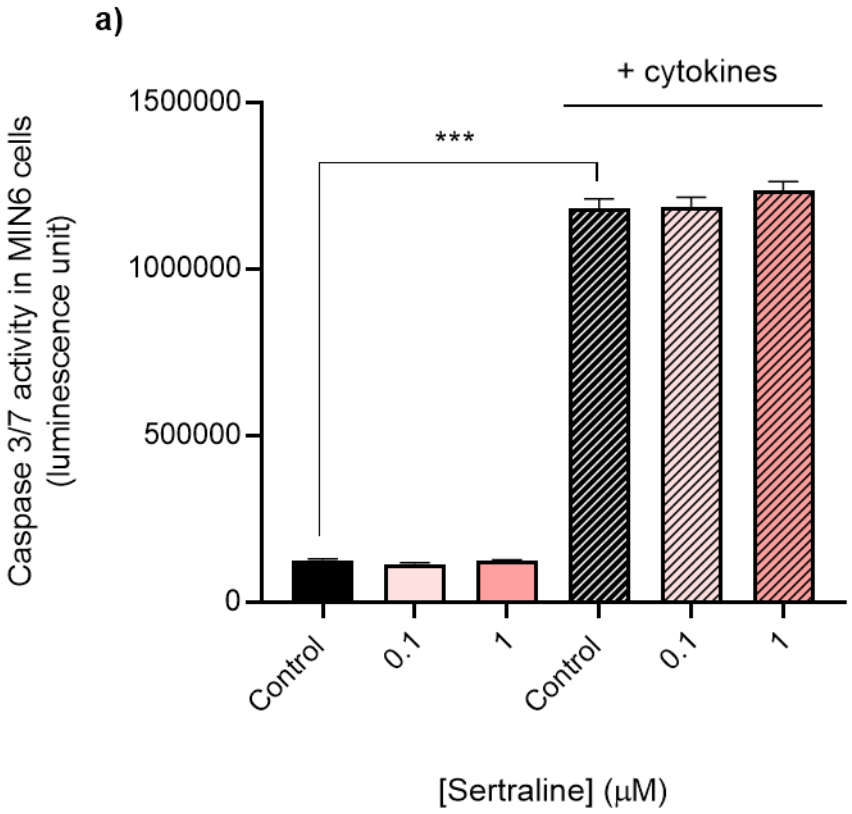
a)
+ cytokines
1500000
1000000
500000
0
***
Caspase 3/7 activity in MIN6 cells
(luminescence unit)
Control
0.1
1
Control
0.1
1
[Sertraline] (µM)

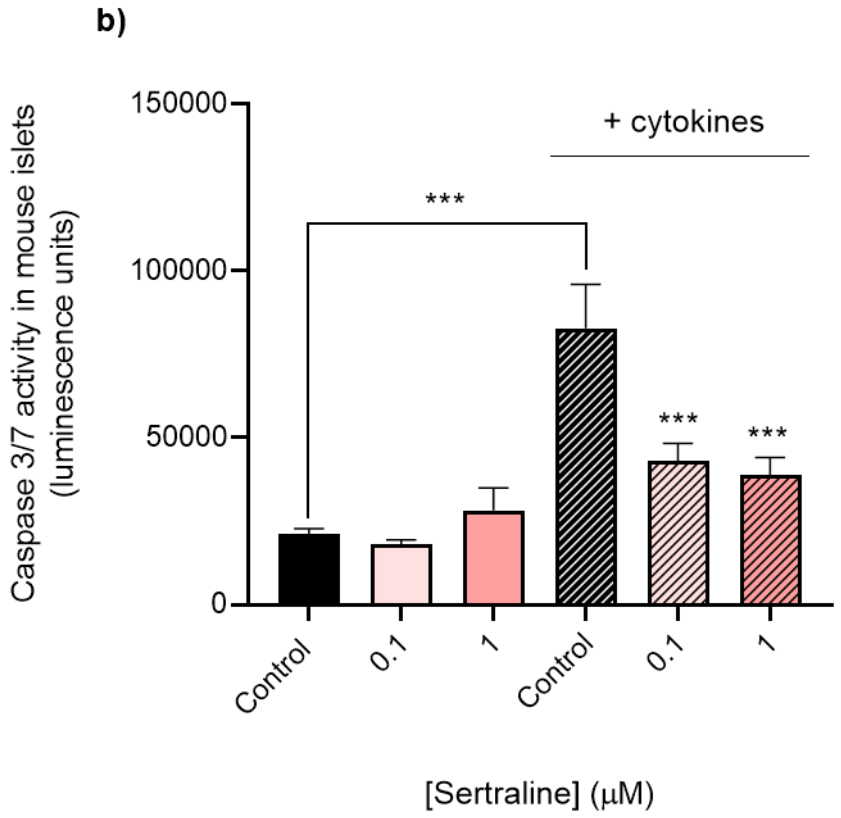
b)
+ cytokines
150000
100000
50000
0
***
***
***
Caspase 3/7 activity in mouse islets
(luminescence units)
Control
0.1
1
Control
0.1
1
[Sertraline] (µM)

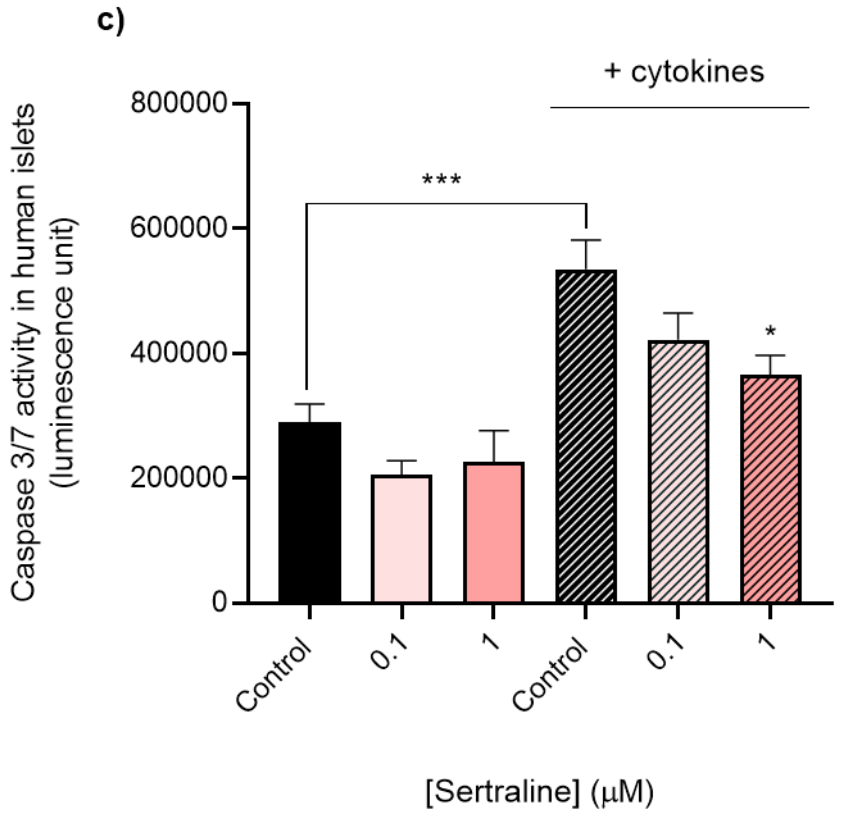
c)
+ cytokines
800000
600000
400000
200000
0
***
*
Caspase 3/7 activity in human islets
(luminescence unit)
Control
0.1
1
Control
0.1
1
[Sertraline] (µM)

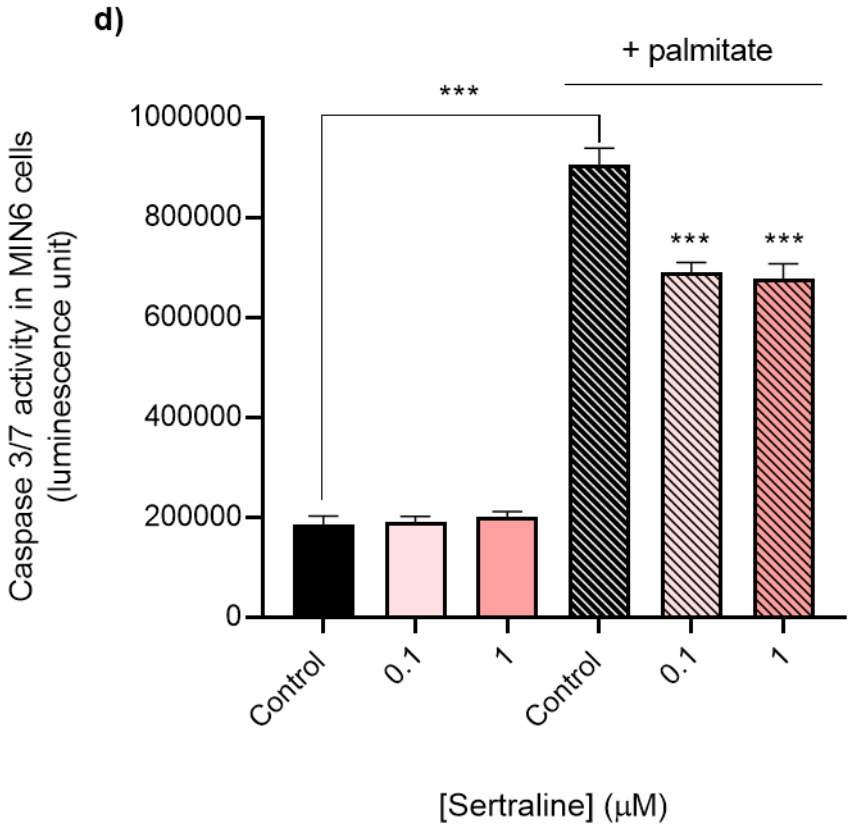
d)
+ palmitate
1000000
800000
600000
400000
200000
0
***
***
***
Caspase 3/7 activity in MIN6 cells
(luminescence unit)
Control
0.1
1
Control
0.1
1
[Sertraline] (µM)

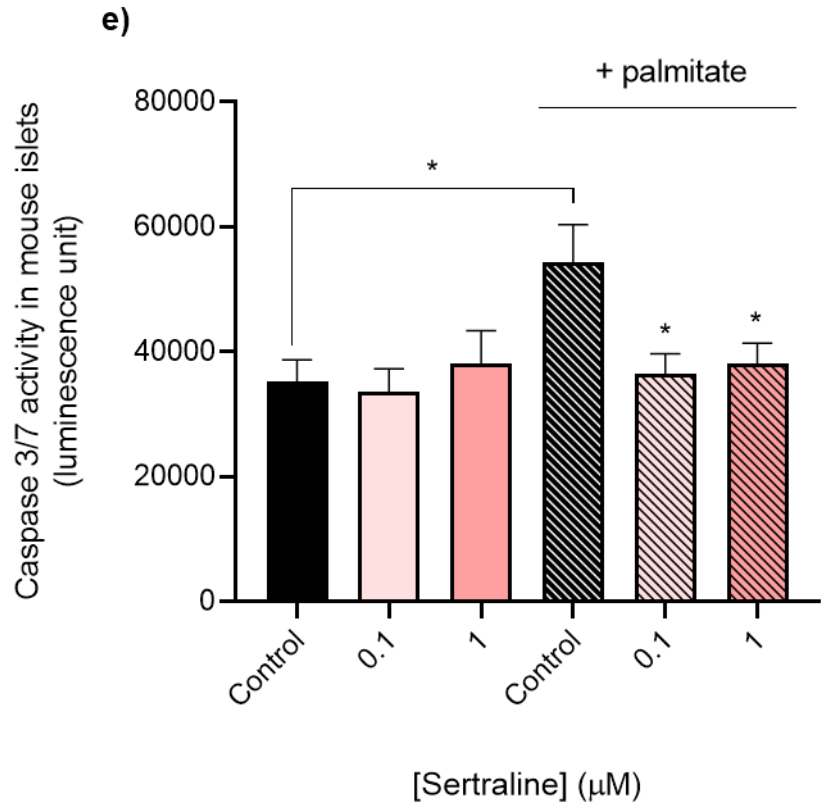
e)
+ palmitate
80000
60000
40000
20000
0
*
*
*
Caspase 3/7 activity in mouse islets
(luminescence unit)
Control
0.1
1
Control
0.1
1
[Sertraline] (μM)

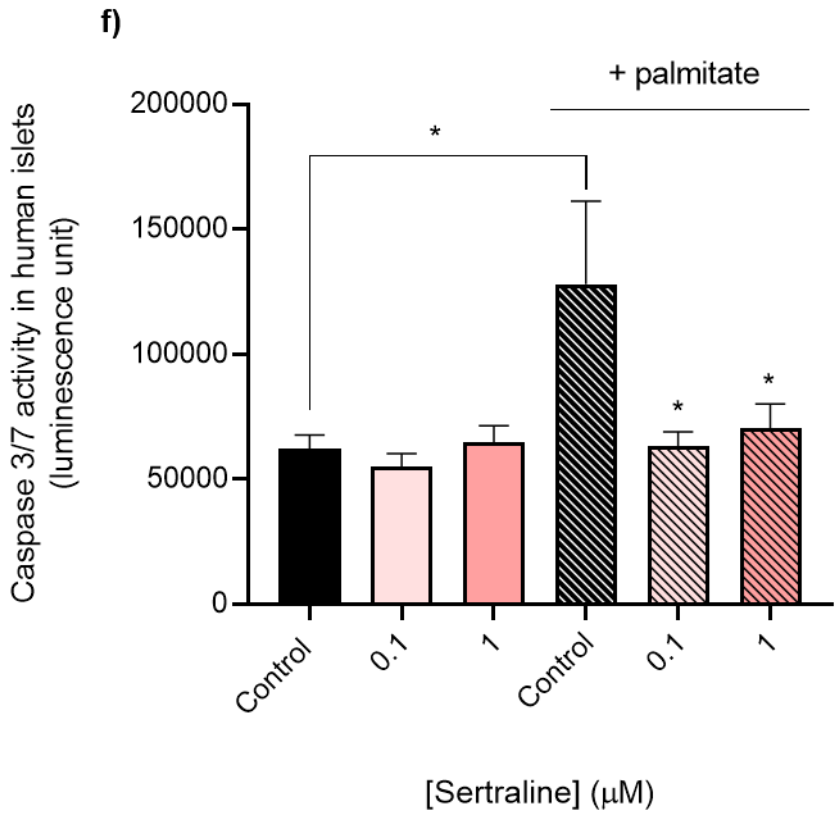
f)
+ palmitate
200000
150000
100000
50000
0
*
*
*
Caspase 3/7 activity in human islets
(luminescence unit)
Control
0.1
1
Control
0.1
1
[Sertraline] (μM)

Figure 4.14. Effects of sertraline on apoptosis of MIN6 cells (a, d), mouse islets (b, e) and human islet (c, f). MIN6 cells or islets were cultured in the absence or presence of sertraline (0.1-1μM) for 48h. Proinflammatory cytokines or palmitate (500μM) were added 24h before the staining. Data are expressed as mean + SEM; n=8 observations representative of 4, 3, and 2 experiments using MIN6 cells, mouse islets and human islets, respectively; *p<0.05; **p <0.01; ***p<0.001 versus appropriate control in the absence (black) or presence (black; striped lines) of cytokines; One-way ANOVA, Dunnett's multiple comparisons test.

Cytokine-induced MIN6 cell death was additionally determined by flow cytometry as this method allows for the measurement of apoptosis in single cells. This is to ensure that the protective effects of sertraline against apoptosis were not masked by increased proliferation of MIN6 cells in the presence of this SSRI. Staining with annexin V revealed that MIN6 cells that had been treated with 1µM sertraline showed reduced annexin V binding when compared with controls, which is indicative of decreased apoptosis (Figure 4.15).

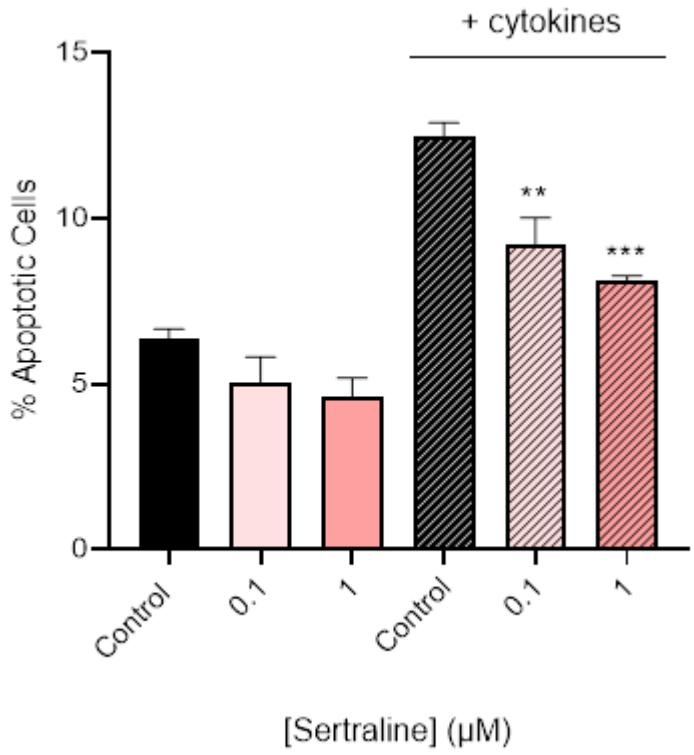

Figure 4.15. Effects of sertraline on apoptosis of MIN6 cells determined by analysis of annexin V staining. Data are mean + SEM, n=3 separate experiments. **p<0.01, ***p<0.001 relative to the control samples, One-way ANOVA, Dunnett's multiple comparisons test.

4.3.3. Paroxetine

4.3.3.1. Effects of paroxetine on ATP generation by beta cells

ATP production was measured as an indicator of metabolic activity following a treatment with paroxetine, another SSRI. After 48h incubation with paroxetine (0.01-1µM), ATP generation by MIN6 cells, mouse islets and human islets was measured using a CellTiter-Glo assay. Low therapeutically relevant concentrations of paroxetine (0.01-0.1µM), as for 0.1-1µM fluoxetine and sertraline, significantly increased ATP generation by MIN6 cells, as well as mouse and human islets (Figure 4.16), indicating increased numbers of beta cells and hence increased ATP readings. Only 1µM paroxetine had no significant effect on ATP levels, and because it exceeds the therapeutic reference range for concentrations of paroxetine in plasma in patients with depression (Lima et al., 2008; Tomita et al., 2014), this concentration was not used in functional experiments.

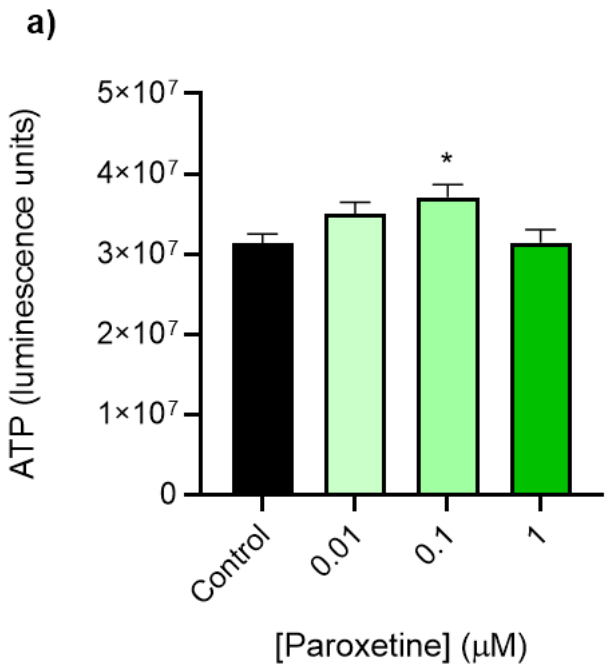

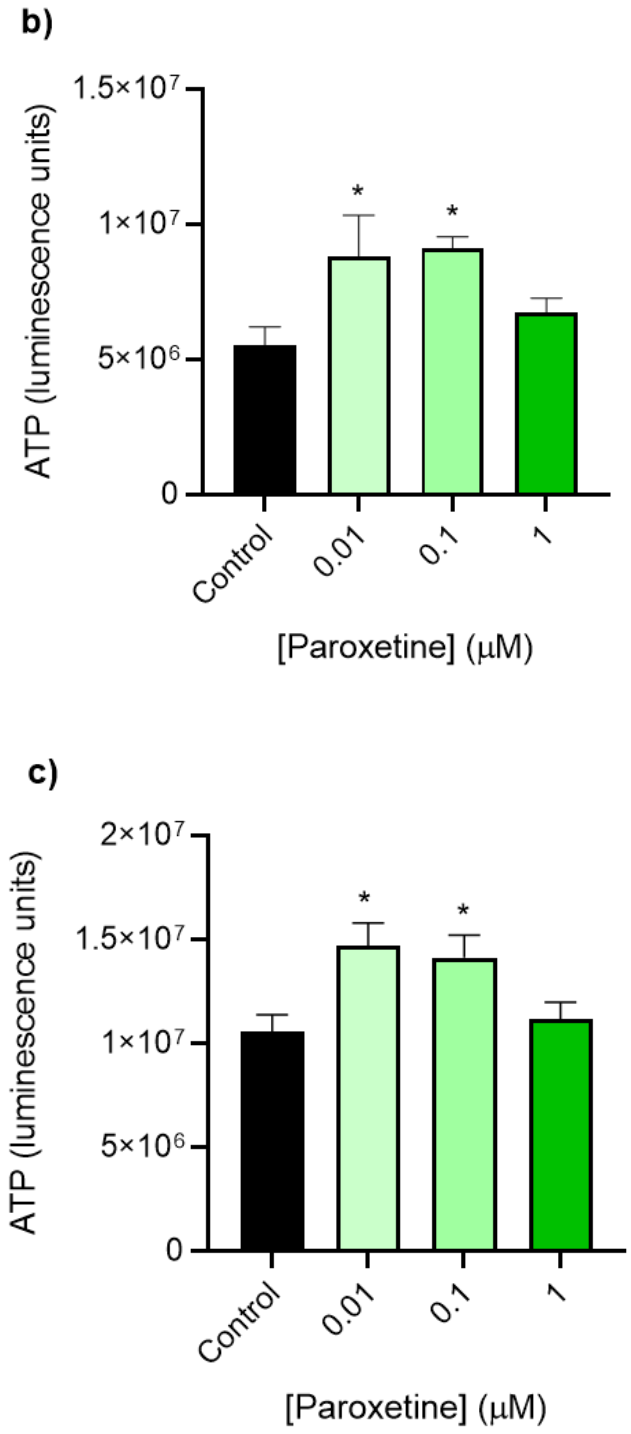

Figure 4.16. Effects of paroxetine (0.01-1μM) on ATP generation by MIN6 cells (a), mouse islets (b) and human islets (c). The cells were incubated in the absence or presence of paroxetine for 48h, and ATP levels were measured using a luminescent CellTiter-Glo assay. Data are mean + SEM, n=8 observations representative of 2-5 separate experiments. *p<0.05 relative to the control samples, One-way ANOVA, Dunnett's multiple comparisons test.

4.3.3.2. Effects of paroxetine on beta cell viability

Trypan blue exclusion test was performed to investigate the effects of paroxetine on viability of MIN6 cells and mouse islets. After 48h incubation in the absence or presence of paroxetine (0.01-10µM), MIN6 cells and islets were stained with Trypan blue, and the dye entry inside the cells was visualised by light microscopy. MIN6 cells that had been exposed to 0.01-0.1µM paroxetine showed no evident dye uptake, whereas 1µM paroxetine led to apparent dye uptake by MIN6 cells and islet cells, especially in the centre of the islets where beta cells are the most abundant (Figure 4.17). However, it was not as evident as with high concentrations of fluoxetine and sertraline. Paroxetine at 10µM paroxetine markedly increased numbers of dead cells, which are indicative of decreased percentage viability. Therefore, paroxetine only at concentrations 0.01-0.1µM was used in proliferation, apoptosis, and insulin secretion experiments.

a)

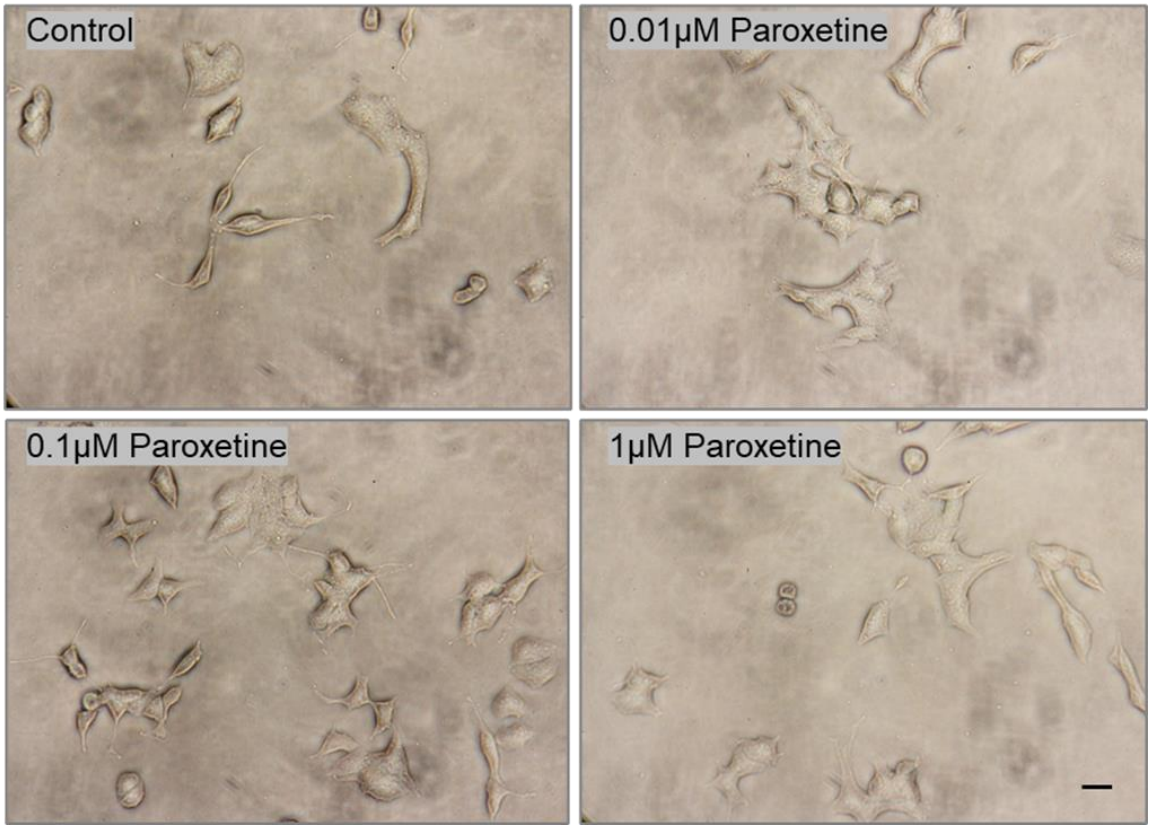
Control
0.01μM Paroxetine
0.1μM Paroxetine
1μM Paroxetine

b)

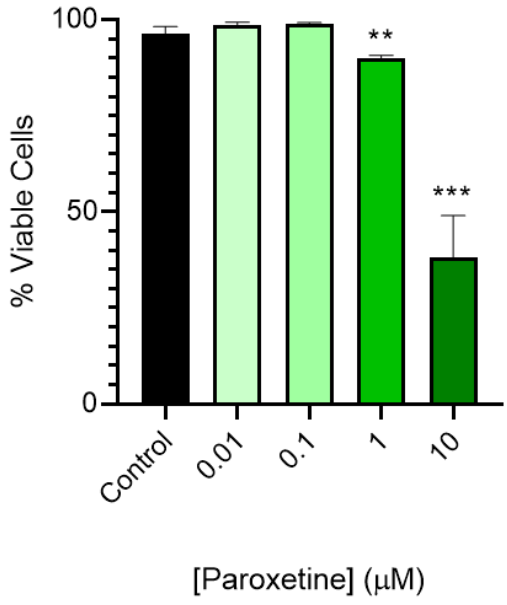
100
50
0
% Viable Cells
**
***
Control
0.01
0.1
1
10
[Paroxetine] (μM)

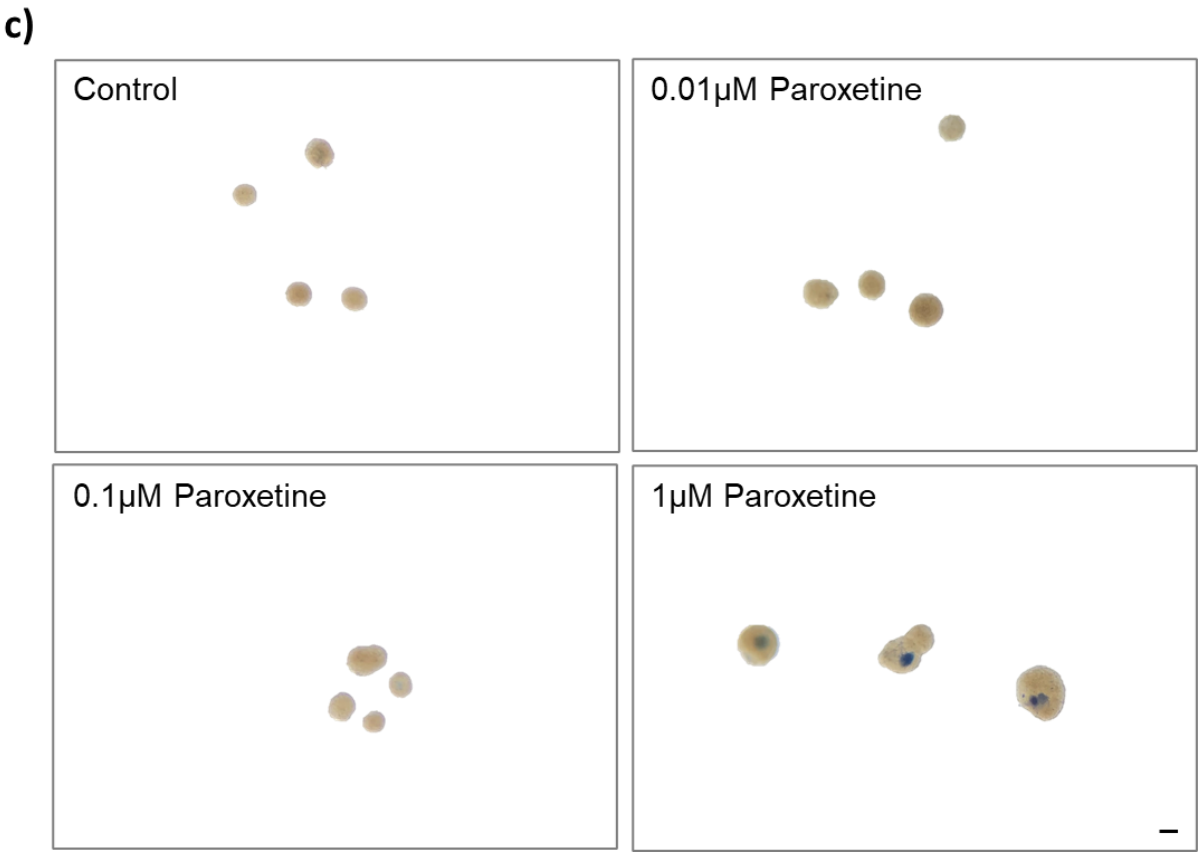

Figure 4.17. Effects of paroxetine on MIN6 cell and mouse islet viability. Micrographs of Trypan blue-stained MIN6 cells (a) and mouse islets (c) after incubation for 48h in DMEM in the absence (control) or presence of paroxetine (0.01-1µM). Scale bars = 50µm. % Viability of MIN6 cells was calculated by counting the numbers of viable and dead cells using the haemocytometer (b). Data are mean + SEM, n =5 technical repeats. **p<0.01; ***p<0.001 relative to the controls, One-way ANOVA, Dunnett's multiple comparisons test.

4.3.3.3. Effects of paroxetine on insulin secretion

The effects of paroxetine on insulin secretion by MIN6 cells, mouse islets and human islets were determined in static incubation experiments and perifusions. Figure 4.18 shows that exposure to paroxetine at 0.01µM and 0.1µM resulted in significantly increased insulin secretion at 25mM glucose from MIN6 cells in acute and chronic static incubation experiments, respectively. Additionally, paroxetine elevated insulin release from mouse and human islets at supraphysiological glucose levels (20mM glucose), and it maximised GSIS in the presence of a muscarinic M3 agonist carbachol. As other SSRIs described in this thesis, paroxetine had no significant effect on basal insulin secretion from MIN6 cells at 2.5mM glucose nor islets at 2mM glucose, which means that it is unlikely to induce hypoglycaemia when used therapeutically.

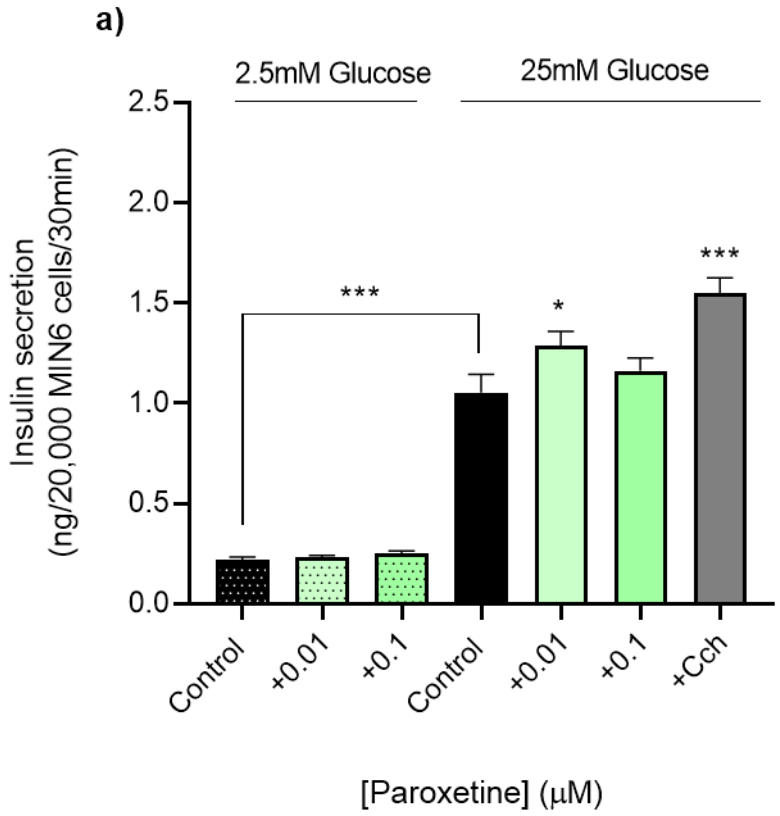

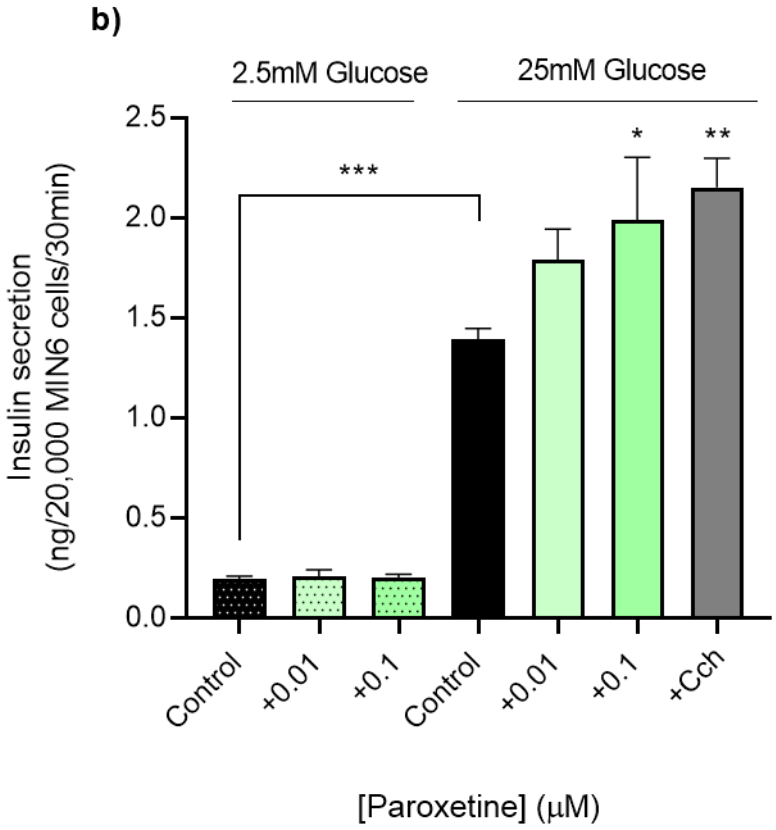
b)
2.5mM Glucose
25mM Glucose
Insulin secretion
(ng/20,000 MIN6 cells/30min)
2.5
2.0
1.5
1.0
0.5
0.0
***
*
**
Control
+0.01
+0.1
Control
+0.01
+0.1
+Cch
[Paroxetine] (μM)

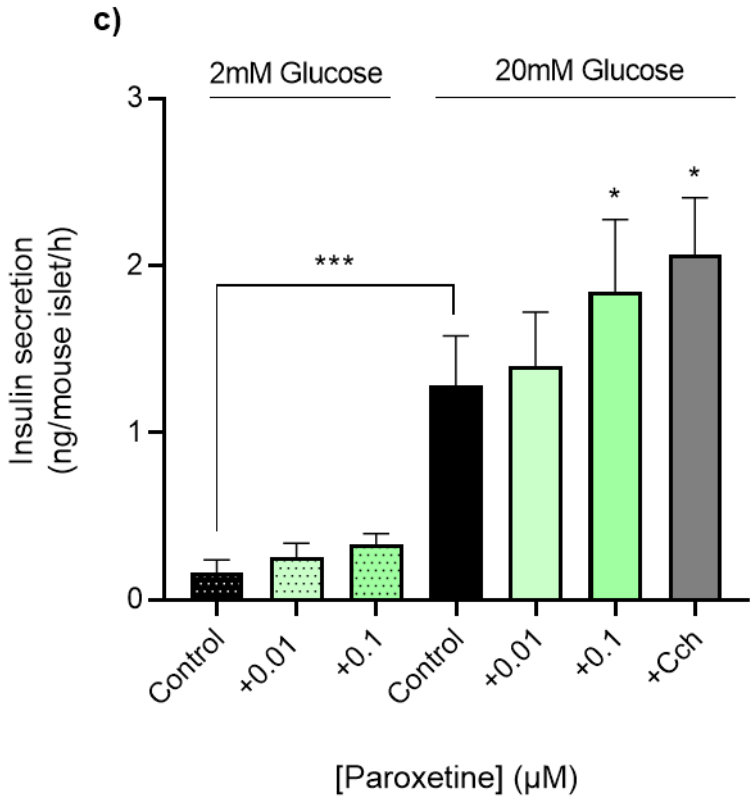
c)
2mM Glucose
20mM Glucose
Insulin secretion
(ng/mouse islet/h)
3
2
1
0
***
*
*
Control
+0.01
+0.1
Control
+0.01
+0.1
+Cch
[Paroxetine] (μM)

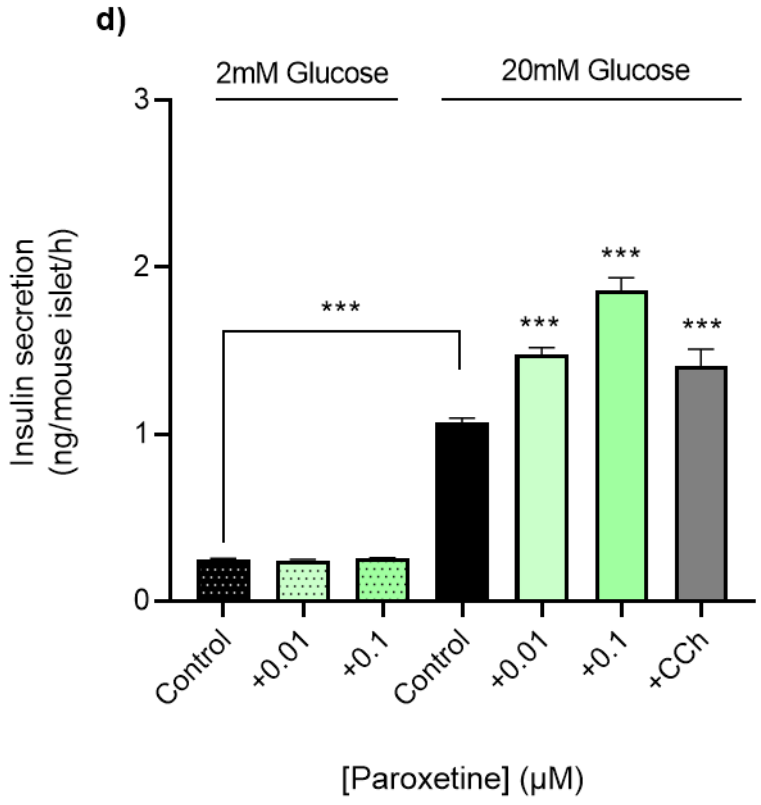
d)
2mM Glucose
20mM Glucose
Insulin secretion (ng/mouse islet/h)
3
2
1
0
***
***
***
***
Control
+0.01
+0.1
Control
+0.01
+0.1
+CCh
[Paroxetine] (μM)

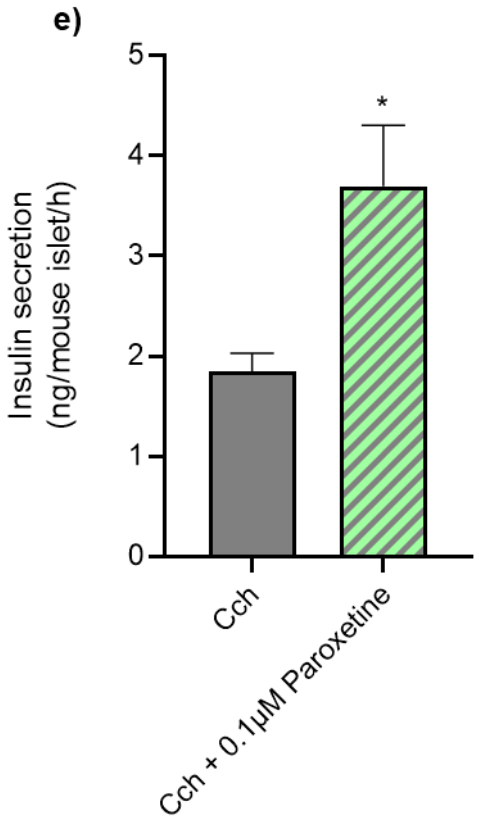
e)
Insulin secretion (ng/mouse islet/h)
5
4
3
2
1
0
*
Cch
Cch + 0.1μM Paroxetine

f)

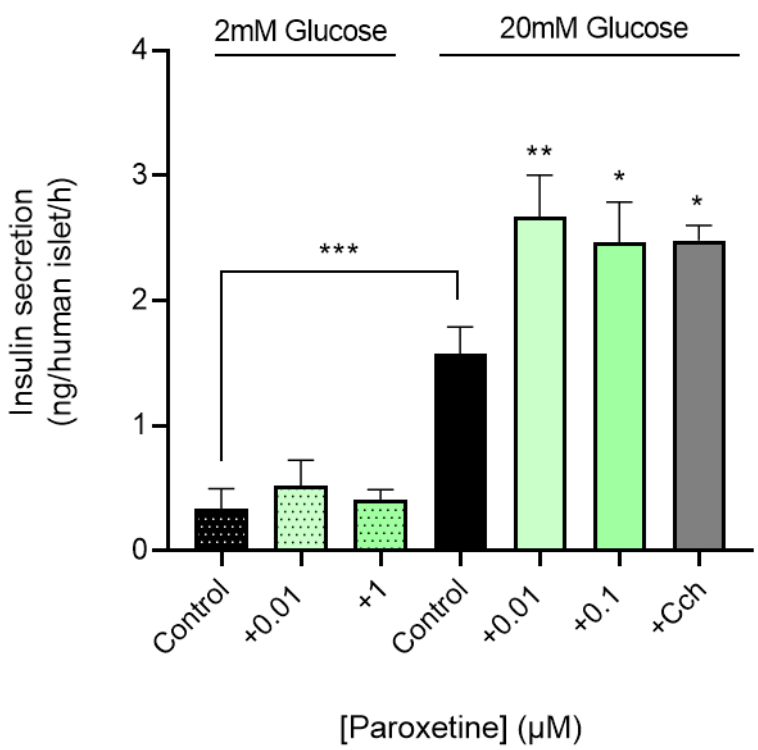
2mM Glucose
20mM Glucose
Insulin secretion (ng/human islet/h)
0
1
2
3
4
***
**
*
*
Control
+0.01
+1
Control
+0.01
+0.1
+Cch
[Paroxetine] (µM)

g)

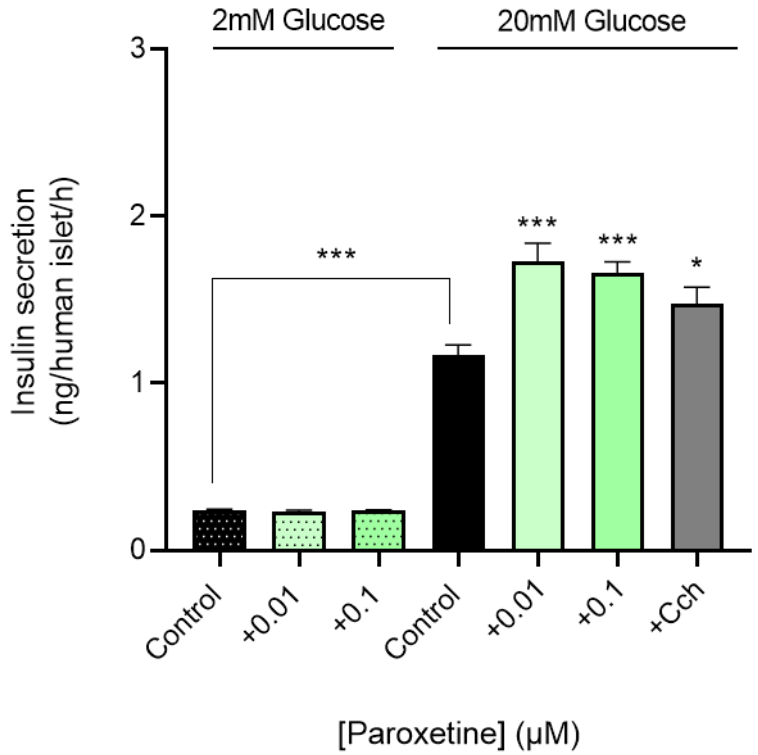
2mM Glucose
20mM Glucose
Insulin secretion (ng/human islet/h)
0
1
2
3
***
***
***
*
Control
+0.01
+0.1
Control
+0.01
+0.1
+Cch
[Paroxetine] (µM)

Figure 4.18. Effects of paroxetine on insulin secretion from MIN6 cells (a - acute, b - chronic), mouse islets (c – acute, d - chronic) and human islets (f - acute, g -chronic), and on GSIS from mouse islets in the presence of 500μM carbachol in acute experiments (e). In static secretion experiments, MIN6 cells or islets were incubated in the absence or presence of paroxetine (0.01-0.1μM) for 30min (MIN6 cells) or 1h (islets) without pre-treatment with paroxetine (acute experiments) or following a 48h incubation in the absence or presence of paroxetine (chronic experiments). All data shown are mean + SEM, n=8 observations representative of 2-4 separate experiments, One-way ANOVA, Dunnett's multiple comparisons test. *p<0.05; **p<0.1; ***p<0.001 relative to the control samples at 25mM (MIN6 cells) or 20mM glucose (islets).

In dynamic insulin secretion experiments, 0.1μM paroxetine significantly potentiated GSIS from perifused mouse (Figure 4.19a) and human (Figure 4.19c) islets. These experiments demonstrate that paroxetine shared a similar mechanism of action at beta cells as fluoxetine and sertraline to induce insulin secretion in dynamic experiments, and as sertraline it sustained insulin release for approximately 10min after the drug was cleared up with a 20mM glucose buffer.

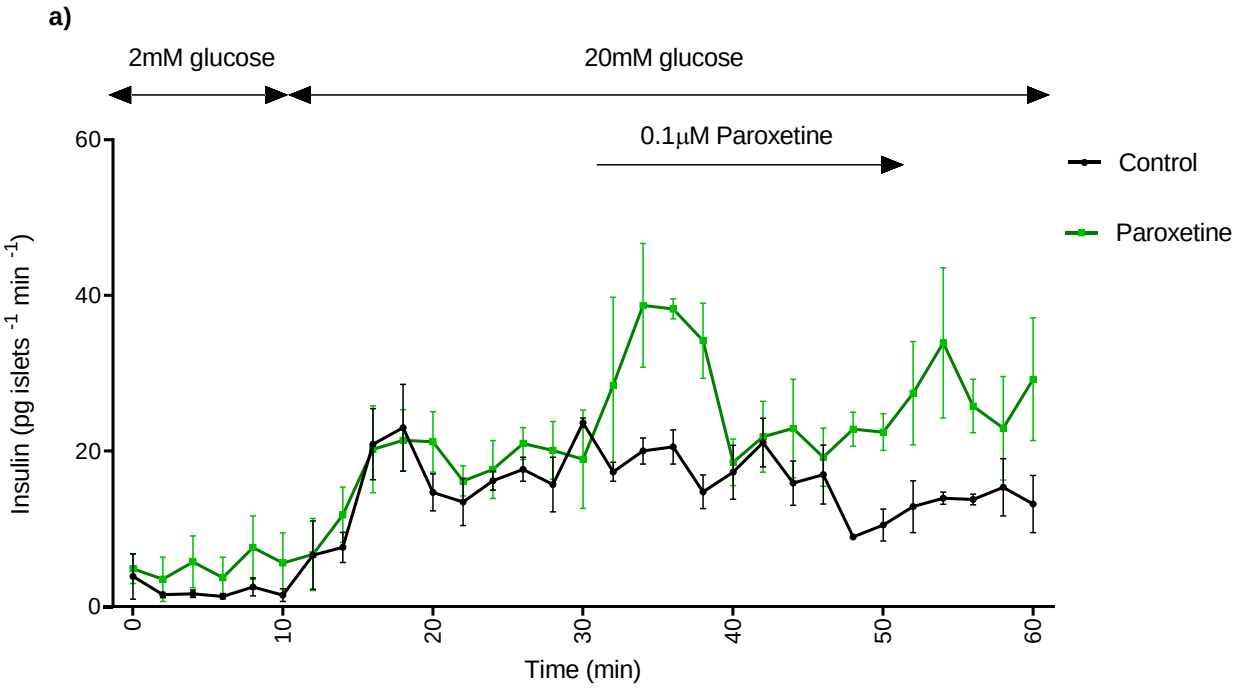
a)
2mM glucose
20mM glucose
0.1μM Paroxetine
Control
Paroxetine
Insulin (pg islets -1 min -1)
60
40
20
0
0
10
20
30
40
50
60
Time (min)

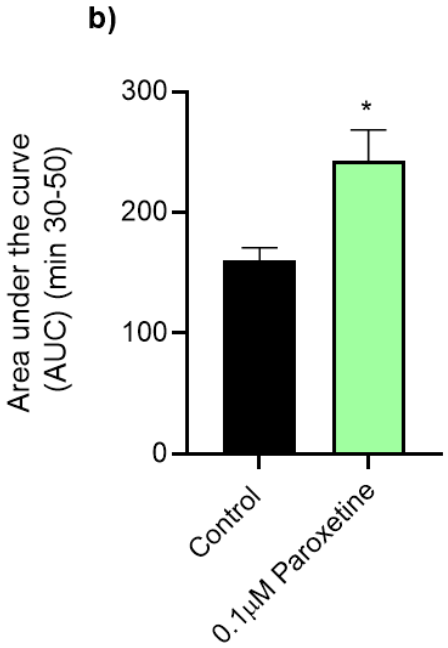
b)
Area under the curve (AUC) (min 30-50)
300
200
100
0
*
Control
0.1μM Paroxetine

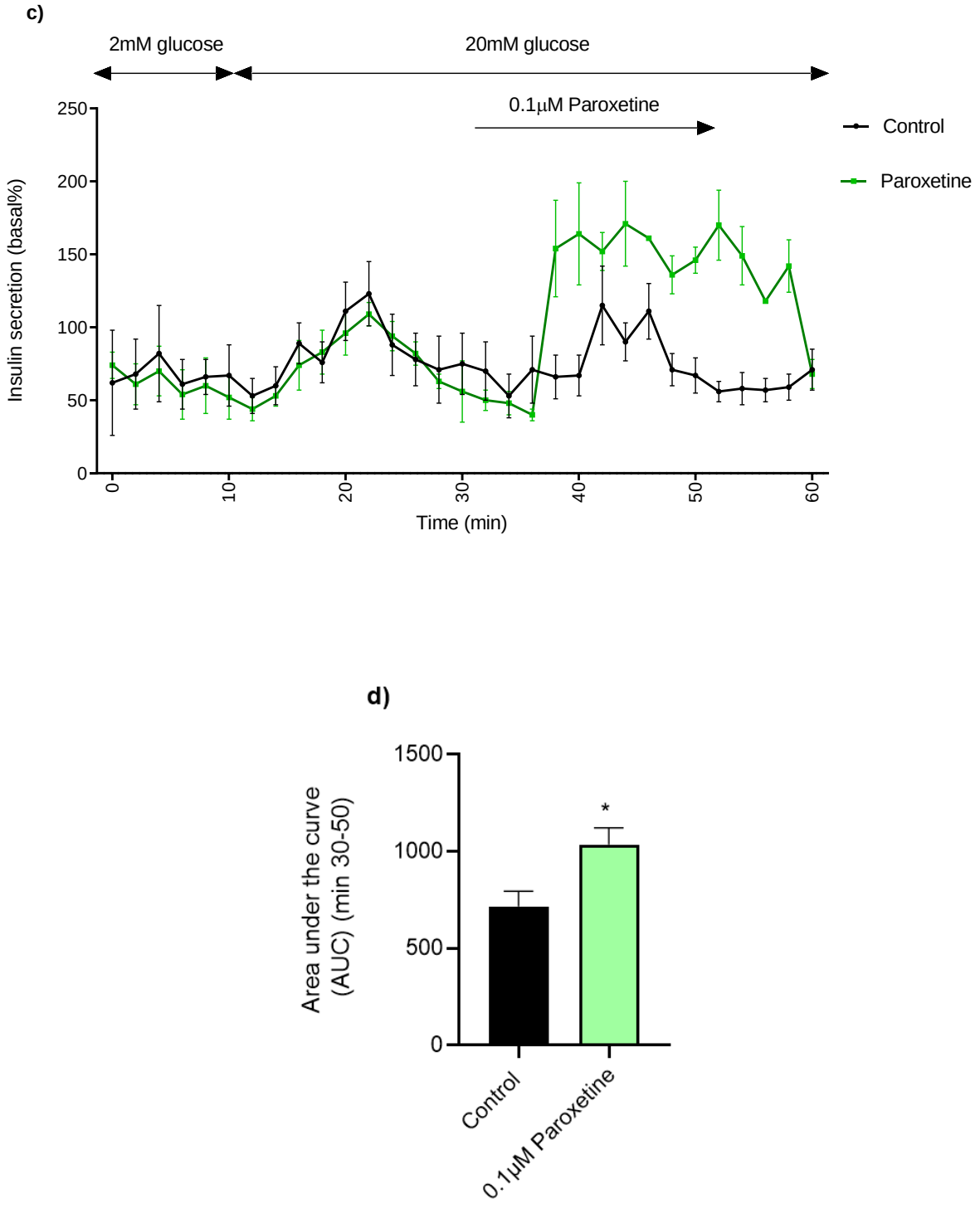

Figure 4.19. Effects of 0.1μM paroxetine on dynamic insulin secretory profile of mouse islets (a, b) and human islets (c. d). The effects of paroxetine on glucose-induced insulin secretion from islets are represented by the area under the curve (AUC). Data are expressed as mean ± SEM; n=4 groups of islets per treatment, each containing approximately 50 islets. *p<0.05 versus control (black), unpaired t-test.

4.3.3.4. Effects of paroxetine on beta cell proliferation

In order to determine the effects of paroxetine on beta cell mass, proliferation of MIN6 cells was measured after a chronic exposure to paroxetine (0.01-0.1µM). Following a 48h incubation without or with paroxetine, MIN6 cells were labelled with BrdU for the quantification of DNA replication. Low and therapeutically relevant concentrations of paroxetine significantly enhanced BrdU incorporation into the DNA of dividing MIN6 cells (Figure 4.20). 10% FBS served as a positive control, and it significantly increased MIN6 cell proliferation to similar levels as paroxetine.

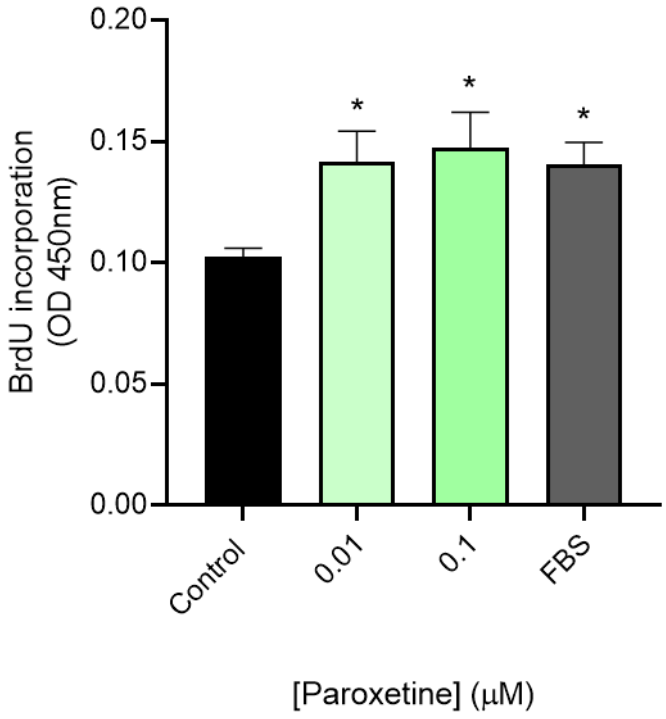

Figure 4.20. Effects of paroxetine on the proliferation of MIN6 cells. MIN6 cells were exposed to paroxetine at 0.01-0.1µM for 48h, and BrdU incorporation into the DNA of dividing cells was measured using a BrdU ELISA. Data are mean + SEM, n=8 observations representative of 3 separate experiments. *p<0.05 relative to the control samples, One-way ANOVA, Dunnett's multiple comparisons test.

4.3.3.5. Effect of paroxetine on beta cell apoptosis

Apoptosis of MIN6 cell, mouse islets and human islets was investigated by quantifying caspase3/7 activities. Similar to experiments using other SSRIs, MIN6 cells and islets were incubated for 48h in the absence or presence of paroxetine (0.01-0.1μM), and caspase3/7 activities were measured using a luminometer. Apoptosis was induced by a mix of proinflammatory cytokines or by palmitate being added for the final 24h. Paroxetine (0.01-0.1μM) had no effect on caspase3/7 activities in MIN6 cells nor on the basal apoptosis levels in the absence of apoptosis stimulator (cytokines or palmitate) in MIN6 cells, mouse islets and human islets. In addition, 0.01-0.1μM paroxetine had a protective effect against cytokine-induced apoptosis of mouse and human islets, and against palmitate-induced apoptosis of MIN6 cells and the islets (Figure 4.21).

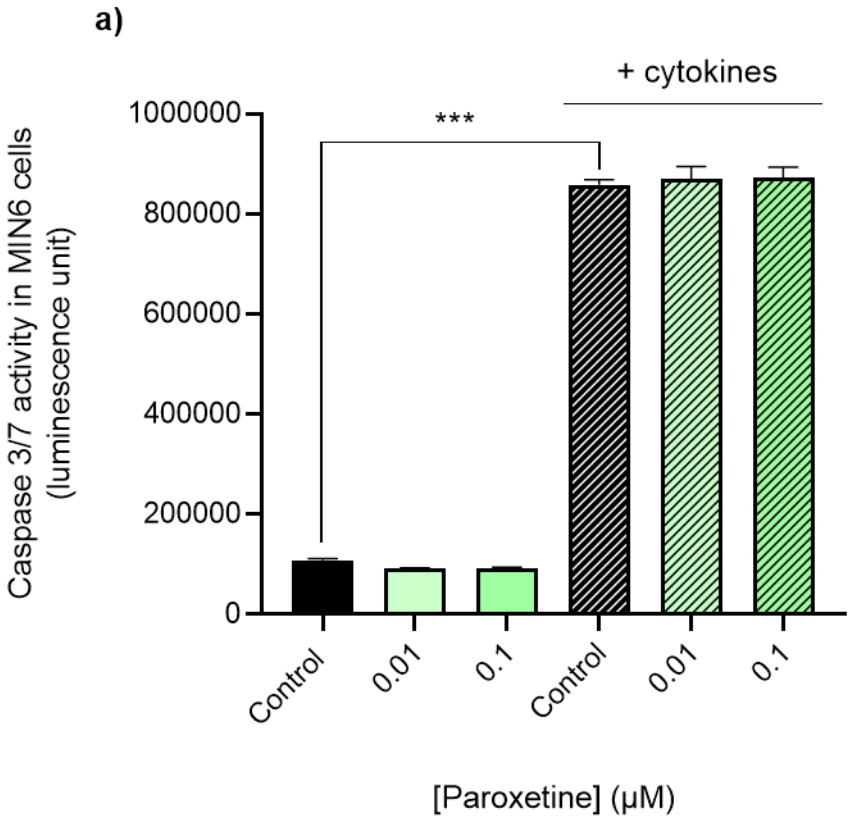
a)
+ cytokines
***
1000000
800000
600000
400000
200000
0
Caspase 3/7 activity in MIN6 cells
(luminescence unit)
Control
0.01
0.1
Control
0.01
0.1
[Paroxetine] (µM)

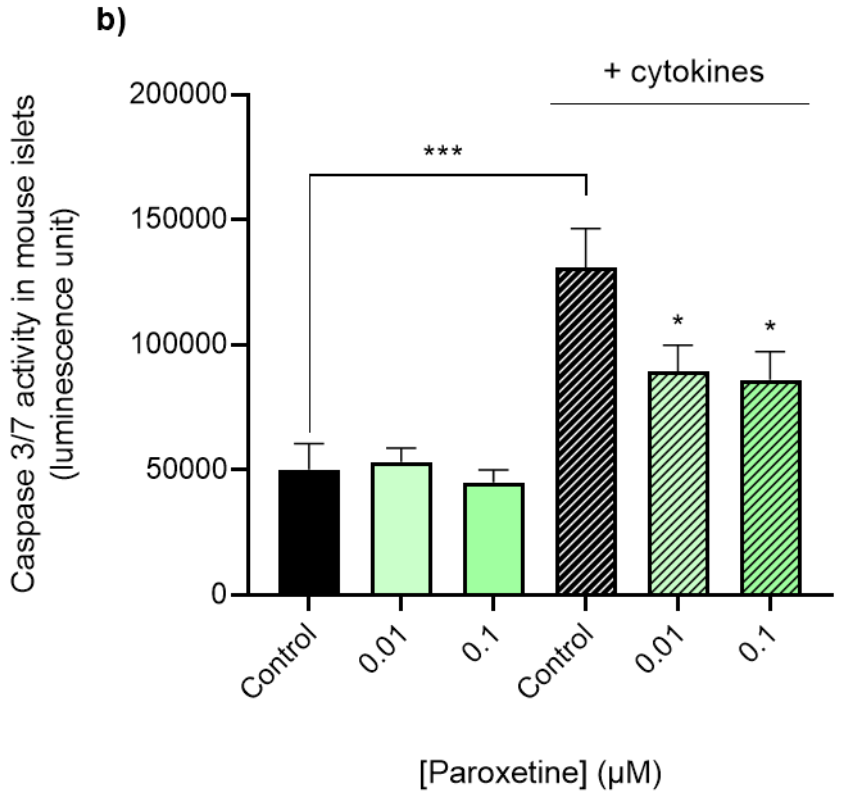
b)
+ cytokines
***
*
*
200000
150000
100000
50000
0
Caspase 3/7 activity in mouse islets
(luminescence unit)
Control
0.01
0.1
Control
0.01
0.1
[Paroxetine] (µM)

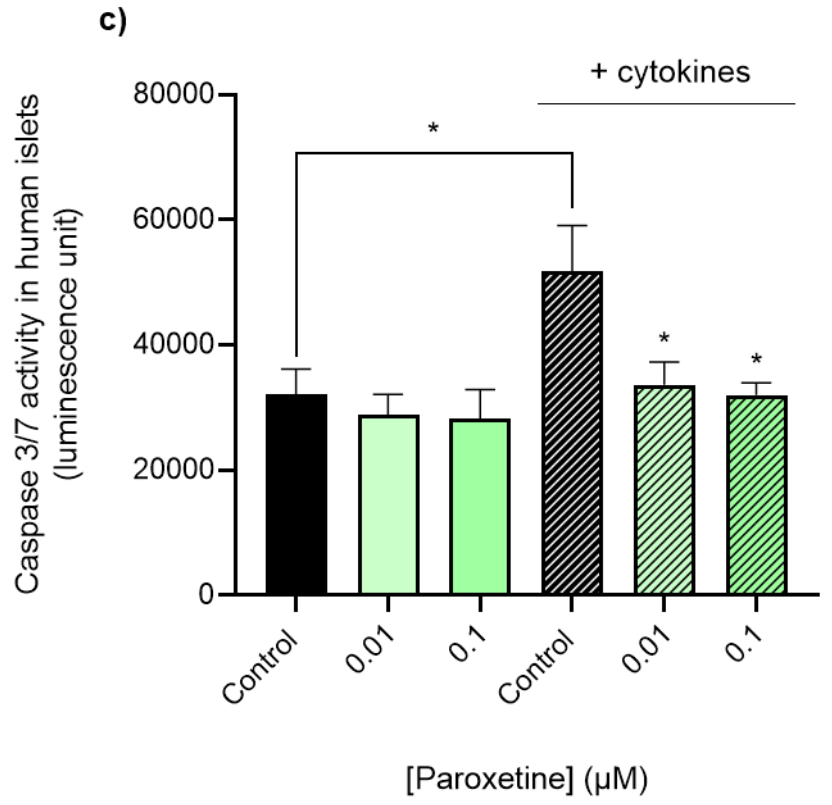
c)
+ cytokines
Caspase 3/7 activity in human islets (luminescence unit)
80000
60000
40000
20000
0
*
*
*
Control
0.01
0.1
Control
0.01
0.1
[Paroxetine] (µM)

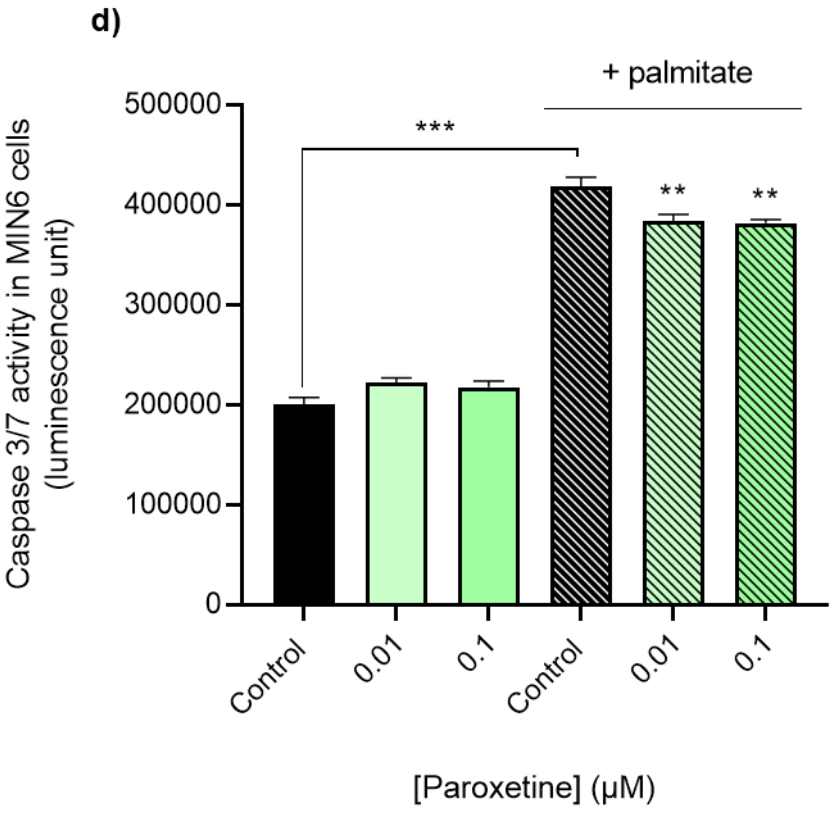
d)
+ palmitate
Caspase 3/7 activity in MIN6 cells (luminescence unit)
500000
400000
300000
200000
100000
0
***
**
**
Control
0.01
0.1
Control
0.01
0.1
[Paroxetine] (µM)

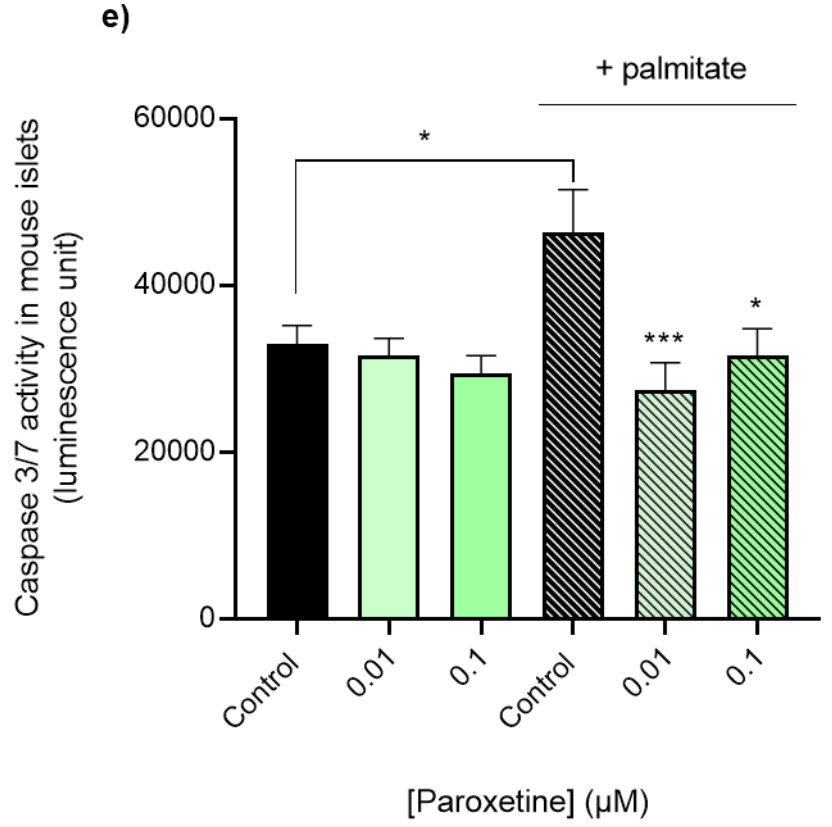
e)
+ palmitate
60000
40000
20000
0
*
***
*
Caspase 3/7 activity in mouse islets (luminescence unit)
Control
0.01
0.1
Control
0.01
0.1
[Paroxetine] (µM)

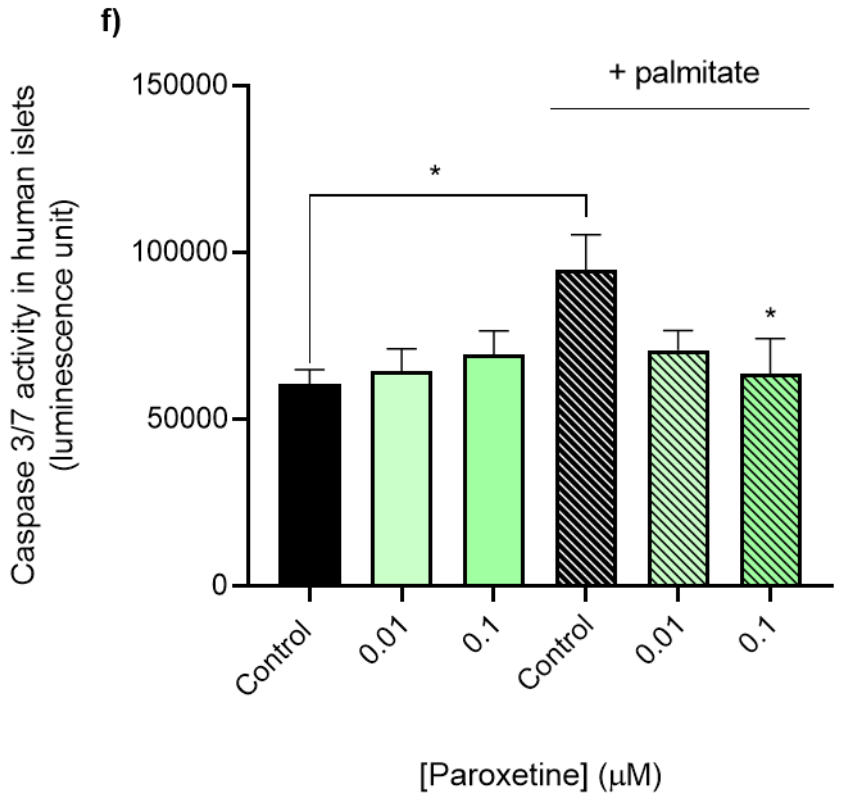
f)
+ palmitate
150000
100000
50000
0
*
*
Caspase 3/7 activity in human islets (luminescence unit)
Control
0.01
0.1
Control
0.01
0.1
[Paroxetine] (µM)

Figure 4.21. Effects of paroxetine on apoptosis of MIN6 cells (a, d), mouse islets (b, e) and human islets (c, f) assessed by luminescence reading of caspase3/7 activities. MIN6 cells or islets were cultured in the absence or presence of paroxetine for 48h. A proinflammatory cytokine mix or palmitate were added 24h before quantification of luminescence. Data are expressed as mean + SEM; n=8 observations representative of 2-4 experiments. *p<0.05; **p<0.01; ***p<0.001versus appropriate control in the absence (black) or presence (striped line) of cytokines; One-way ANOVA, Dunnett's multiple comparisons test.

As discussed in Sections 4.3.1.5 and 4.3.2.5, apoptosis of MIN6 cells was additionally measured in flow cytometry experiments, a more sensitive method to measure cell death, where MIN6 cells were stained with annexin V, and apoptosis was induced by proinflammatory cytokines 24h prior to the staining. Figure 4.22 shows that MIN6 cells that had been treated with paroxetine at 0.01µM and 0.1µM showed reduced annexin V binding when compared to controls, meaning that paroxetine at these therapeutically relevant concentrations protected beta cells against apoptosis induced by cytokines.

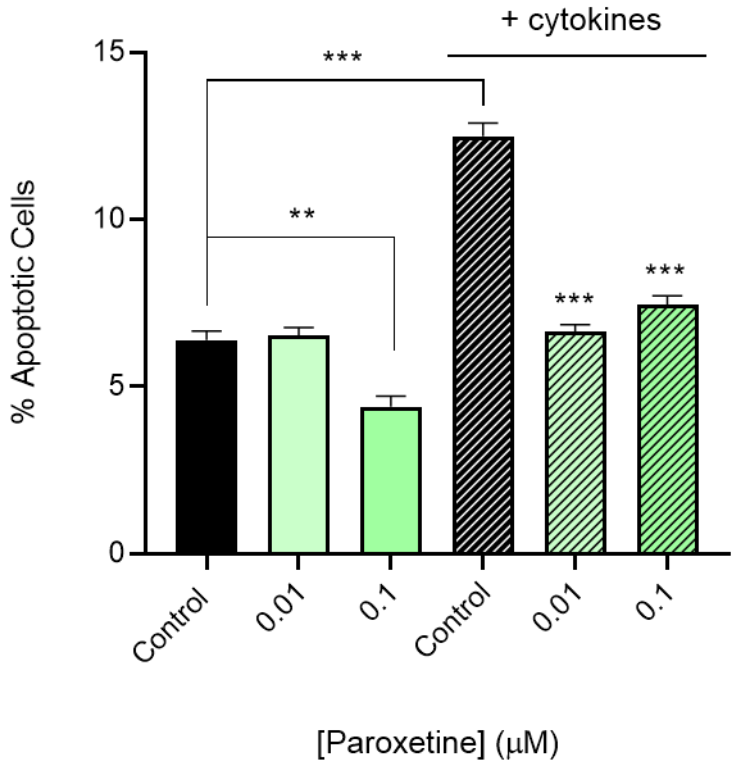

Figure 4.22. Effects of paroxetine on apoptosis of MIN6 cells assessed by flow cytometry analysis of annexin V staining. Data are mean + SEM, n=3 separate experiments. *p<0.05; **p<0.01; ***p<0.001 versus appropriate control in the absence (black) or presence (striped line) of cytokines; One-way ANOVA, Dunnett's multiple comparisons test.

4.4. Discussion

Most people with diabetes and affective disorders require long-term antidepressant treatment (Deuschle, 2013), and there have been arguments about whether the use of SSRIs could lead to metabolic disturbances and increased risk of T2D (Khoza et al., 2011). It has been reported that fluoxetine and sertraline improve glycaemic control and increase insulin sensitivity independently of reductions in body weight (Breum et al., 1995; Connolly et al., 1995; Goodnick et al., 1997; Maheux et al., 1997; Tharmaraja et a., 2019; Ye et al., 2011). On the other hand, some *in vitro* studies have linked fluoxetine to reduced insulin secretion (Isaac et al., 2013; De Long et al., 2014), impaired Ca^{2+} signalling, and ER stress in beta cells (Chang et al., 2017; Elmorsy et al., 2017). In addition, sertraline and paroxetine have been implicated in mitochondrial damage-mediated apoptosis (Then et al., 2017). However, in these earlier studies, SSRIs were used at concentrations of up to 30-70µM, which are considerably higher than the therapeutic concentrations of fluoxetine and sertraline (0.2-2.6µM) and paroxetine (0.06-0.18µM) in plasma (Bolo et al., 2000; Bosch et al., 2008; Lima et al., 2006; Tomita et al., 2014). Interstitial concentrations of these drugs within the pancreas have not been measured yet. However, there is an extensive intra-islet capillary network, and it is expected that the concentrations in the general circulation would reflect interstitial concentrations within the pancreas. In addition, the data presented in this chapter show that these SSRIs at 10µM are cytotoxic to beta cells and suggest that high concentrations that exceed the therapeutic range should not be used to assess the effects of these drugs on beta cell function. Moreover, when administered at low and therapeutic concentrations, fluoxetine, sertraline and paroxetine exerted favourable effects on the function of MIN6 beta cell, mouse islets and human islets.

4.4.1. Fluoxetine, sertraline and paroxetine increase ATP generation and viability of MIN6 beta cells and islets

Low and therapeutic concentrations of fluoxetine, sertraline and paroxetine (0.1-1µM) were well tolerated by beta cells and did not disturb plasma membrane integrity of MIN6 cells and islet cells, as determined by Trypan blue uptake analysis. ATP production is also a good indicator of cell viability and the increased ATP generation that was observed in MIN6 cells and islets that had been treated with therapeutic concentrations of SSRIs could be a consequence of increased beta cell proliferation. However, beta cells within primary islets have a limited proliferative capacity, so the increased ATP levels may reflect generally improved cell viability, and therefore increased metabolic activity. This is supported by the observation that high concentrations of SSRIs did not alter ATP levels in mouse and human islets. On the other hand, SSRIs could directly alter mitochondrial function to increase ATP synthesis. It has been shown that fluoxetine penetrates cells by crossing plasma membranes and can be found in the mitochondria (Mukherjee et al., 1998). Mitochondria are responsible for over 95% of cellular ATP production (Bernardi and Di Lisa, 2015), and ATP plays an important role in insulin secretion. However, the underlying mechanisms of how SSRIs affect cell metabolism remain to be discovered.

4.4.2. Fluoxetine, sertraline and paroxetine potentiate glucose-stimulated insulin secretion from beta cells

The data presented in this chapter show that fluoxetine, sertraline and paroxetine potentiated glucose-induced insulin secretion from beta cells in acute experiments and following chronic treatment with these SSRIs. This is of great importance therapeutically because drugs that enhance insulin secretion lower hyperglycaemia, a major determinant of diabetes, and reduce the risk of long-term diabetic complications. Moreover, these SSRIs did not induce insulin secretion at basal glucose concentrations (2-2.5mM), suggesting that they do not favour the occurrence of hypoglycaemia in the fasting state, but only increase insulin secretion at high glucose concentrations when it is required. The ability of SSRIs to augment GSIS could explain the improvements in glycaemic control seen in clinical studies (Tharmaraja et a., 2019; Ye et al., 2011). Therefore, these drugs could be beneficial in the treatment of depression in people with diabetes through ensuring that sufficient insulin is secreted to normalise blood glucose levels.

It remains unclear how SSRIs improve GSIS. The beneficial effects of SSRIs on beta cell function presented in this chapter and improvements in plasma glucose levels and HbA_{1C} reported in clinical studies could be attributed to elevated serotonin levels, which is available to exert functional effects on the pancreatic islets, increased beta cell mass or other unknown mechanism. Indeed, there is evidence that serotonin acts to potentiate GSIS from beta cells during pregnancy via 5-HT3A receptor, and that is promotes proliferation of beta cells via 5-HT2B receptor stimulation (Kim et al., 2010; Ohara-Imaizumi et al., 2013).

4.4.3. Fluoxetine, sertraline and paroxetine promote beta cell mass expansion

Beta cell mass is determined by a balance between beta cell proliferation and death (Doyle and Egan, 2007). Proliferation is an important compensatory mechanism of beta cells to cope with an increased demand for insulin during the progression of T2D (Cho et al., 2010) and during pregnancy, but under normal circumstances, the rate of primary beta cell proliferation is very low (Teta et al., 2005). Nevertheless, MIN6 cells are driven to proliferate by the presence of the SV40 large T antigen coupled to the insulin promoter (Ishihara et al., 1993), and when they are induced into a quiescent state by the withdrawal of serum, they can be used to quantify effects of exogenous agents on their proliferative capacity. In the experiments presented in this chapter, fluoxetine, sertraline and paroxetine, at low and therapeutically relevant concentrations, significantly increased BrdU incorporation into dividing MIN6 cells, which is indicative of increased proliferation. It is possible that fluoxetine and other SSRIs exert their regulatory role on beta cell mass by activating the ERK2/CaMK4/CREB/Irs2 signalling cascade. Nevertheless, more experiments are required to identify the exact molecular mechanisms of individual SSRIs on mouse and human beta cell mass and function.

On the other hand, the main mechanism underlying reductions in beta cell mass is increased beta cell apoptosis. The rates of beta cell apoptosis are normally very low (Scagila et al., 1997), which makes it difficult to identify potential protective effects of SSRIs. Therefore, in addition to quantifying basal apoptosis, cell death was induced by proinflammatory cytokines (IL-1β, TNF-α and IFN-γ) or the free saturated fatty acid palmitate, whose circulating levels are increased in T2D (Sobczak et al., 2019). Apoptosis levels in the presence of cytokines or palmitate were then determined by measuring caspase3/7 activities, which increase during

the process of programmed cell death. What is more, the caspase-dependent intrinsic apoptosis pathway has been shown to be the prime effector of inflammatory beta cell apoptosis (Brechtold et al., 2016). In the current investigation, pre-treatment with SSRIs protected mouse and human islets against cytokine- and palmitate-induced death, without having significant effects on basal rates of apoptosis. However, there was no significant effects of therapeutic SSRI concentrations on MIN6 cell apoptosis rates in the presence of cytokines. The reasons for this are not entirely clear, but since MIN6 cells proliferate faster than primary beta cells, the high apoptosis rates in the presence of fluoxetine, sertraline or paroxetine could be a reflection of the favourable effects of these SSRIs on proliferation and viability: by increasing the total number of cells over the 48h incubation period, SSRIs could lead to increased readings of caspase3/7 activities thus obscuring any potential protective effect of SSRIs against cytokine-induced apoptosis. Therefore, apoptosis of single MIN6 cells was measured by a more sensitive method, flow cytometry, and it revealed that SSRIs did have a protective effect on apoptosis in these experiments. The ability of SSRIs to promote beta cell proliferation and decrease apoptosis in a pathophysiological state of inflammation and obesity is key in considering these drugs as a possible treatment for T2D. Nevertheless, more research is required to investigate the effects of these drugs on insulin sensitivity in peripheral tissues.

Chapter 5. Evaluation of the effects of fluoxetine administration on glycaemic control and beta cell mass in *ob/ob* mice *in vivo*

5.1 Introduction

In vitro studies permit a detailed analysis of the effects of pharmacological substances on isolated cells and tissues in the absence of vascular and nervous input, in the controlled laboratory environment. Although *in vitro* experiments give a good indication of what might be expected to happen *in vivo*, results obtained from *in vitro* experiments cannot usually be transposed to predict the reaction of an entire organism *in vivo*.

Glucose homeostasis is tightly controlled by insulin and glucagon, which act in an opposing manner to maintain fasting glucose levels within a narrow range of approximately 4 to 6mM. Insulin is often called a "storage hormone" because it is released during the absorptive state when it plays a key role on its target tissues to promote glucose uptake, utilisation, and storage. One of the key causes of impaired blood glucose control is obesity, in which adipocyte-derived mediators induce insulin resistance, and this reduced capacity of peripheral tissues to respond to insulin results in hyperglycaemia. Insulin resistance drives beta cells to increase insulin secretion as a compensatory mechanism to overcome reduced insulin sensitivity, and this increased beta cell workload can lead to beta cell failure and the development of T2D. The main aim of existing therapies to treat T2D is to reduce hyperglycaemia by promoting insulin secretion or insulin utilisation, and therefore minimise the risk of diabetic complications. As the incidence of this condition is continuously increasing and many individuals with T2D require insulin therapy within 10 years of diagnosis, new drugs are necessary to effectively manage T2D by maintaining both beta cell function and mass.

SSRI drugs, such as fluoxetine, have been previously linked to improvements in glucose regulation in T2D patients (Deusche, 2013; Tharmaraja et al., 2019). In this chapter, the effects of fluoxetine on glycaemic control and beta cell mass were investigated in a mouse model of obesity. $Lep^{ob/ob}$ (*ob/ob*) mice carry mutations in the gene responsible for leptin production, and therefore they have increased hunger, become profoundly obese, and develop hyperglycaemia at around 4 weeks (Lindström, 2007).

5.2 Methods

5.2.1. Fluoxetine injections to *ob/ob* mice

Two groups of 5 male *ob/ob* mice, aged 29 weeks, were subjected to 4 intraperitoneal injections of DMSO (vehicle control; 0.4ml/kg body weight) or fluoxetine (10mg/kg body weight in a volume of 0.4ml DMSO/kg) over 14 days before being subjected to a glucose tolerance test. Mean weight of mice in groups 1 and 2 were 58.6±2.2g and 57.9±1.2g, respectively. The dose of fluoxetine administered into animals was adjusted to achieve serum concentrations in the therapeutic range. Thus, it has been previously shown that serum fluoxetine levels for the 10 mg/kg/day dose (170.3±57.8ng/ml) were towards the bottom of the range of plasma levels found in patients treated with fluoxetine tablets 20–80 mg/day (100–700 ng/ml) (Dulawa et al., 2004; Koran et al, 1996), hence this dose was chosen for this study.

5.2.2 Glucose tolerance tests after fluoxetine delivery

On day 14, after fluoxetine delivery, mice were weighed, and glucose tolerance was evaluated following a single intraperitoneal injection of glucose (2g/kg body weight) supplemented with DMSO (0.4ml/kg) or fluoxetine (10mg/kg in 0.4ml) to mice that had been fasted overnight (16h). Blood glucose was measured from a tail vein using an Accu-Check blood glucose meter immediately before glucose administration and 15, 30, 60, 90, 120, 150, and 210min post-injection.

5.2.3 Assessment of islet mass and beta cell proliferation after fluoxetine delivery

BrdU (1mg/ml) was administered in drinking water to DMSO- and fluoxetine-treated *ob/ob* mice for 7 days prior to their sacrifice. The pancreases were dissected out, fixed in paraformaldehyde (4%), embedded in paraffin, and cut into 5µm sections. The pancreatic sections were dewaxed and underwent antigen retrieval before immunohistochemical staining with antibodies directed against BrdU and insulin as described in Section 2.5.3. The microscope images were analysed using ImageJ software.

5.3 Results

5.3.1 Effect of fluoxetine on glucose tolerance in *ob/ob* mice

Two groups of 5 male *ob/ob* mice received 4 intraperitoneal administrations of DMSO or fluoxetine over the course of 14 days and were subjected to ipGTTs in the presence of DMSO or fluoxetine on day 14. No significant differences between control and fluoxetine treated mice in body weight (control: 58.6±2.2g vs. fluoxetine: 57.9±1.2g; $p>0.2$) or fasting blood glucose (7.5±0.6mM vs.6.7±0.5mM; $p>0.1$) were observed after the 14-day treatment period. The maximum glucose concentrations reached in control and fluoxetine-treated mice after glucose delivery were 42.5mM and 42mM, respectively (Figure 5.1). Despite

a drop in blood glucose concentration in fluoxetine-treated mice at 150min, there was a lack of significant difference between the two groups in the first 150min. However, fluoxetine-treated mice showed significantly improved glucose clearance at 210min when compared to the control mice (Figure 5.1).

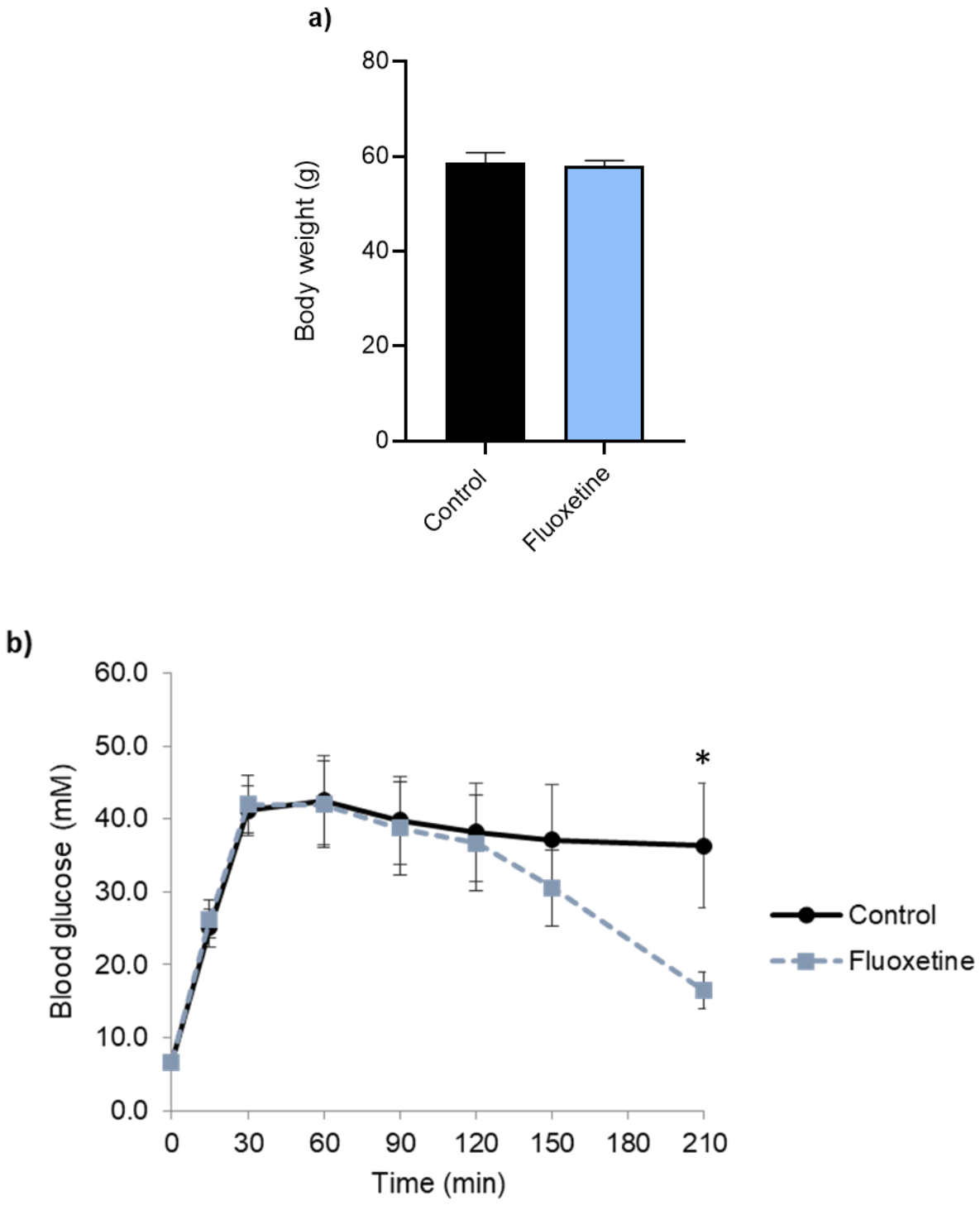

Figure 5.1. Effect of fluoxetine on glucose tolerance. Animals' body weights were measured prior to the ipGTT. Data are expressed as mean + SEM; n=5 per group; *p>0.2; unpaired t-test (a). Two groups of *ob/ob* mice were administered 4 doses of DMSO (vehicle control; 0.4ml/kg) or fluoxetine (10mg/kg in 0.4ml) intraperitoneally during a 14-day treatment period before being subjected to ipGTTs following a single injection of glucose (2g/kg) in the presence of DMSO or fluoxetine. Glucose concentrations were measured at 0, 15, 30, 60, 90, 120, 150, and 210min following glucose administration (b). Data are expressed as mean ± SEM; n=5 for control and fluoxetine-treated mice. *p<0.05, Two-way ANOVA with repeated measures.

5.3.2 Effect of fluoxetine on BrdU incorporation into beta cells

To investigate the effect of fluoxetine administration on beta cell proliferation, BrdU (1mg/ml) was administered in drinking water to *ob/ob* mice that had been treated with DMSO or fluoxetine for 7 days prior to the termination of the *in vivo* study. The number of BrdU-positive beta cells was determined by immunohistochemistry. Figure 5.2 shows that *ob/ob* mice that had been treated with fluoxetine (panels D, E, F) had a significantly increased numbers of BrdU-positive beta cells when compared to the control animals (A, B, C), as well as significantly increased overall islet size.

a)

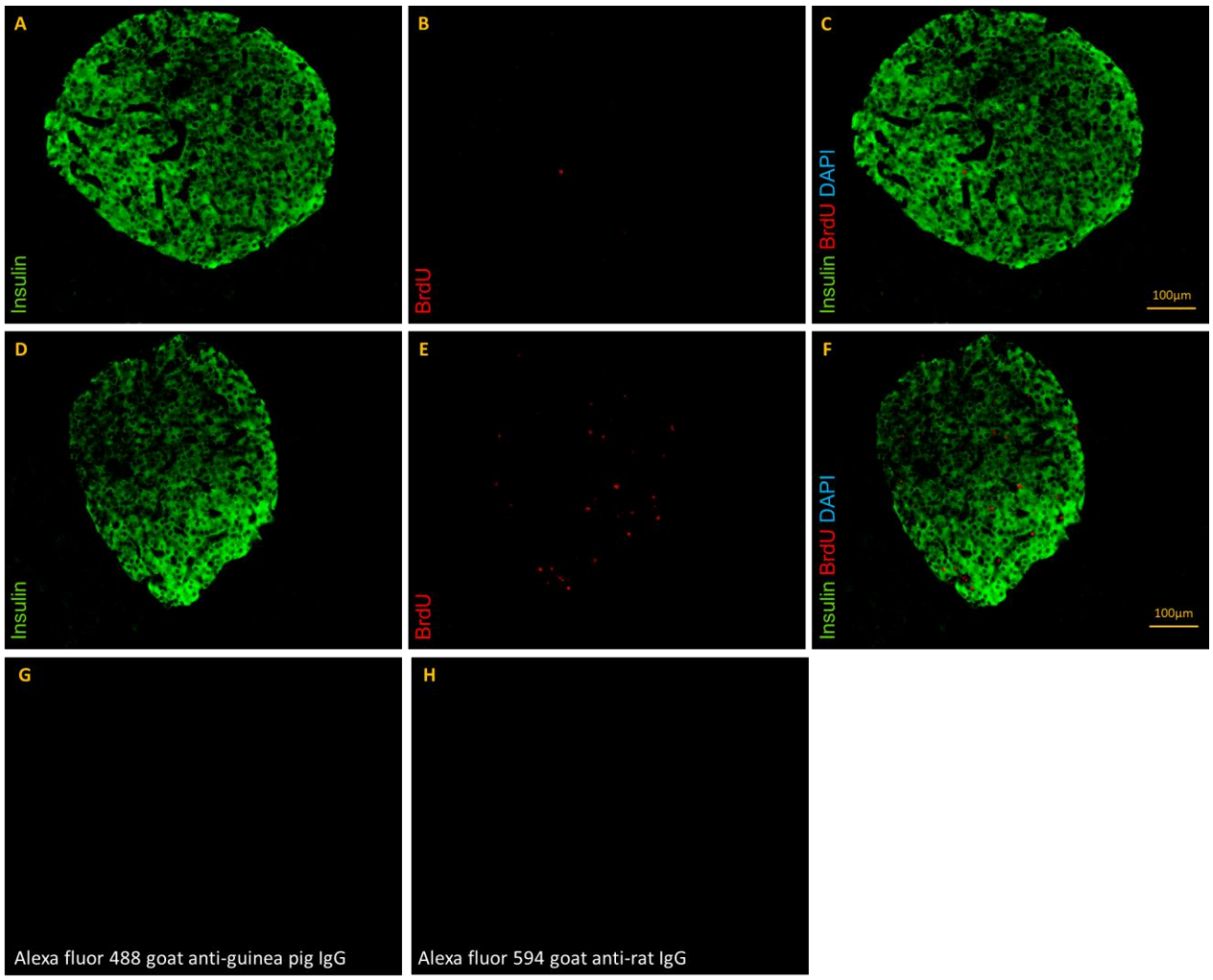

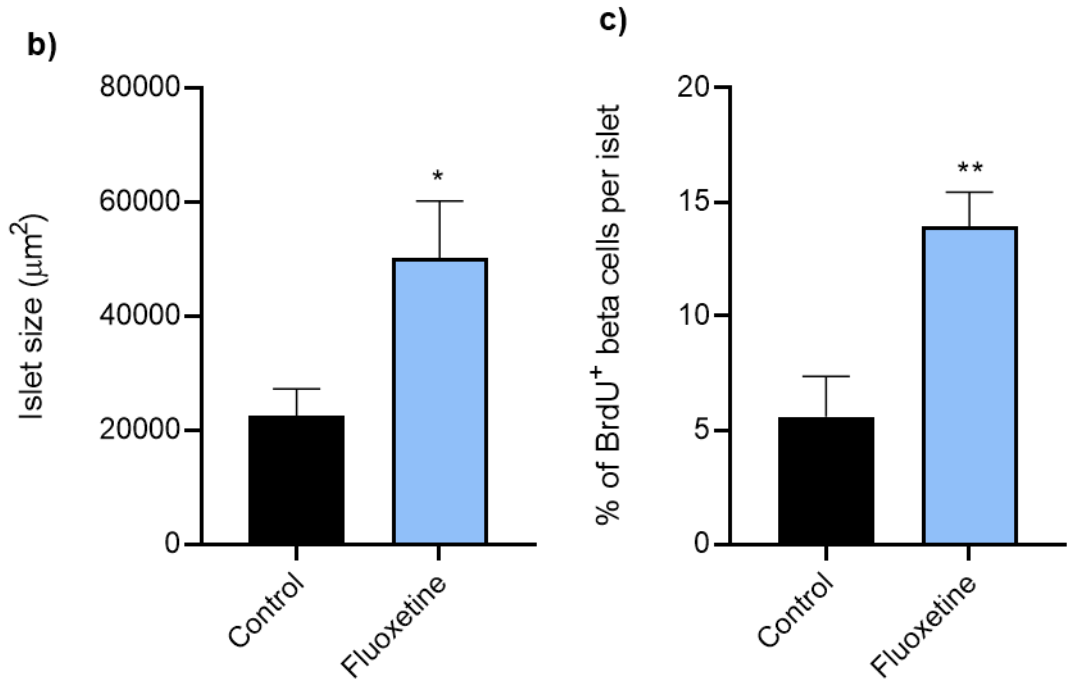

Figure 5.2. Effect of fluoxetine on beta cell proliferation in *ob/ob* mice. BrdU was introduced in drinking water for 7 days prior to the dissection of the pancreases, fixation, and embedding in wax. The pancreatic sections (5µm) were immunostained for BrdU (red) and insulin (green). Representative sections from control mice are shown in panels A-C while those from *ob/ob* mice are shown in panels D-F (a). Scale bar = 100µm. Quantification of islet size (b) and $BrdU^+$ beta cells (c). Data are expressed as mean + SEM; n=19 observations using 6 sections from 4 mice; *p<0.05; **p < 0.01; unpaired t-test.

5.4 Discussion

The *in vitro* data presented in chapter 4 indicated that low and therapeutic concentrations (0.1-1μM) of fluoxetine increased glucose-stimulated insulin secretion from MIN6 cells, mouse islets and human islets, promoted proliferation of MIN6 cells, and reduced cytokine- and palmitate-induced apoptosis of MIN6 cells, mouse islets and human islets. These observations suggest that fluoxetine would be expected to improve glucose tolerance and increase beta cell mass *in vivo*.

As *ob/ob* mice become profoundly obese and hyperglycaemic, they have the capacity to increase beta cell mass to maintain insulin secretion (Bock et al., 2003). Since the majority of people who develop T2D are overtly obese and insulin resistant, *ob/ob* mice are a good model to study potential therapies for T2D (King, 2012).

Short-term treatment with low doses of SSRIs has been linked to improvements in insulin sensitivity and severity of depression (Deuschle, 2013), but long-term use of antidepressants, including SSRIs, in moderate or high daily doses has been associated with an increased risk of developing T2D by 84% (Andersohn et al., 2009). Therefore, it is important to study the chronic effects of antidepressants *in vivo*.

5.4.1 Fluoxetine improves glucose tolerance in *ob/ob* mice *in vivo*

Glucose tolerance tests were used to determine the effect of fluoxetine on the ability of mice to regulate their blood glucose levels. In these experiments glucose was injected intraperitoneally after mice had been injected with a vehicle (DMSO) or fluoxetine four times over 14 days. Consistent with clinical reports that fluoxetine treatment improves glycaemic control in people with depression and anxiety (Deusche, 2013; Tharmaraja et al., 2019), the data presented in this chapter demonstrate that fluoxetine injections improved glucose tolerance in *ob/ob* mice. However, the beneficial effects of fluoxetine were only observed 210 minutes after glucose delivery, suggesting a minor capacity to increase insulin secretion *in vivo*. Nevertheless, the *ob/ob* mice used in this study, which were 31 weeks old at the time of the ipGTTs, were very hyperglycaemic following glucose delivery as plasma glucose concentration exceeded 42mM at minute 60, and the effect of fluoxetine could have been masked by this overt hyperglycaemia. For comparison, the highest blood glucose concentration in lean, young mice undergoing ipGTTs would be 20mM (Kashani et al., 2019). Future studies should be carried out using younger *ob/ob* mice, which are not so overtly glucose intolerant, and which show the typical normalisation of glucose tolerance within 120 minutes. In addition, it would be appropriate to determine whether fluoxetine administration improves glucose tolerance in high fat diet-fed (HFD) mice, to mimic the pathophysiology of diabetes more closely. Thus, HFD-induced phenotypes of T2D in mice share the characteristics of human obesity, including hyperglycaemia, hyperinsulinaemia, insulin resistance, as well as high levels of proinflammatory cytokines (Kleinert et al., 2018; Stott and Marino, 2020). What is more, it has been shown that treatment of rats for 3 weeks with SSRIs, paroxetine and sertraline, diminished SERT function *in vivo* (Benmansour et al., 1999), and that loss of binding sites for SERT was significant after 15 days and had

been reduced by 85% (Frazer and Benmansour, 2002). In addition, serotonin signalling in the rat brain was significantly increased after 15 days of treatment with sertraline and this enhancement of the serotonin signal induced by sertraline was not apparent below two weeks or following acute local administration of the SSRI. This time course for the reduction of binding of SERT is important from the perspective of clinical improvement, and it justifies the timing of the experiment presented in this thesis. However, metabolism of drugs is faster in rodents than in humans, and hence the method of drug administration is important for sustaining high occupancy of SERT, which is key for regulatory effects of SSRIs to take place. Although such occupancy can be achieved when SSRIs are used clinically in patients with depression, it may not be the case in animal models. Because fluoxetine is normally taken orally as tablets, in which concentrations are maintained for long periods, future studies should implement alternative ways of fluoxetine administration, including the use of osmotic minipumps that allow a continuous release of a drug directly into the circulation, and therefore stable serum concentrations, rather than injections that can cause stress and potentially mask the beneficial effects of fluoxetine *in vivo*.

5.4.2. Fluoxetine promotes beta cell proliferation *in vivo*

During the initial phase of hyperglycaemia, beta cells are induced to divide and secrete enough insulin to compensate for insulin resistance. In the current chapter, BrdU and insulin immunostaining of pancreatic sections demonstrated that *ob/ob* mice that had been chronically administered with fluoxetine had an increased number of dividing beta cells when compared to control mice, which led to an overall increase in islet size. This suggests that the pro-proliferative, anti-apoptotic effects of fluoxetine observed *in vitro* also occur *in vivo*, at least in mice, and if this also occurs in humans, it may be at least partly responsible for the

improved glycaemia seen with SSRI use in humans (Tharmaraja et a., 2019; Ye et al., 2011). More experiments are required to understand whether these beneficial effects of fluoxetine on beta cell mass *in vivo* are also observed with sertraline and paroxetine, and how they affect peripheral tissues in diabetic animals.

Chapter 6. Direct effects of second-generation antipsychotics, aripiprazole and clozapine, on beta cell mass and function

6.1. Introduction

Atypical antipsychotics (AAPs) are a class of medication used to manage psychosis in schizophrenia (SCZ) and bipolar disorder or as an add-on therapy of major depressive disorder. AAPs are of relevance to the studies described in this thesis since they have a high binding affinity at 5-HT receptors, including 5-HT1D and 5-HT2A receptors localised to beta cells in the pancreas, and their expression is significantly increased in the islets from type 2 diabetic donors (Bennet et al., 2015; Kim et al., 2010). The 5-HT1D and 5-HT2C receptors are GPCRs that signal via Gi or Gα, respectively, to inhibit or enhance insulin secretion. Therefore, blockade of these receptors may alter downstream signalling pathways, resulting in changes in insulin secretion.

The mechanism of action of most AAPs, including clozapine, is postsynaptic blockade of Gi-coupled dopamine D2 receptors and activation of 5-HT receptors in the brain. Several lines of evidence support the role of D2 receptors in the activity of antipsychotics, and there is strong correlation between D2 receptor binding and clinical potency and efficacy of antipsychotics (Kapur et al., 2000; Seeman, 2010; Thompson et al., 2020). Aripiprazole and brexpiprazole are exceptions as they act as D2 receptor partial agonists, and aripiprazole may display functionally selective properties (Aihara et al., 2004; Burris et al., 2002; Urban et al., 2007). Functionally selective drugs activate specific intracellular pathways to decrease disease symptoms without activating pathways that result in unfavourable side effects (Mailman and Gay, 2007; Tuplin and Holahan, 2017). The unique pharmacological profile of aripiprazole at D2 receptors may account

for the effective management of positive, negative, and cognitive symptoms of schizophrenia, which makes this drug very interesting.

In this thesis, D2 receptors have been shown to be expressed by mouse beta cells and human islets, which is consistent with previous reports (Rubi et al., 2005). Knowing that AAPs act at D2 receptors, the effects of therapeutic concentrations of aripiprazole and clozapine on beta cells were investigated in this chapter. As many schizophrenic patients develop T2D, it is crucial to understand the direct effects of commonly used AAPs on beta cell function and to identify AAPs with no or beneficial effects on beta cells to treat mental disorders in people with metabolic disturbances or T2D.

Consistent with experiments looking at the effects of selective serotonin reuptake inhibitors in chapter 4, viability, proliferation, apoptosis, and insulin secretion from MIN6 cells, mouse islets and human islets were measured following a 48h incubation with two commonly used AAPs: aripiprazole and clozapine. Their plasma concentrations reach maximal levels of 1.12µM and 2.66µM, respectively (Grunder et al., 2008; Keshavarzi et al., 2020; Sparshatt et al., 2010; Stark and Scott, 2012), and therefore aripiprazole and clozapine were used at 1µM and 2µM, respectively, in the experiments described in this chapter. Additionally, concentrations that were 10 times lower and 10 times higher than 1µM and 2µM were also used to study the effects of these AAPs at a wider concentration range.

6.2. Methods

6.2.1. ATP generation in MIN6 beta cells: CellTiter-Glo assay

The CellTiter-Glo assay was used to quantify ATP generation by MIN6 cells. MIN6 cells were seeded into 96-well white plates at a density of 15,000 cells/well, and then incubated in DMEM supplemented with 5.5mM glucose, 10% (v/v) FBS, 1% (v/v) penicillin and streptomycin, and 1% (v/v) L-glutamine, and in the absence or presence of aripiprazole (0.1-10µM) or clozapine (0.2-20 µM) for 48h. The CellTiter-Glo reagent was added to each well 15min prior to the measurement of luminescence as described in Section 2.7.2.

6.2.2. ATP generation in islets: CellTiter-Glo 3D assay

ATP generation by mouse and human islets was measured using a CellTiter-Glo 3D assay. The islets were incubated in RPMI (11.1mM glucose) supplemented with 10% (v/v) FBS, 1% (v/v) penicillin and streptomycin, and 1% (v/v) L-glutamine without or with aripiprazole or clozapine (0.1-20µM) for 48h. Groups of 3 mouse islets or 5 human islets were transferred to white-walled 96-well plates, the CellTiter-Glo 3D reagent was added to the wells containing islets for 15min, and luminescence was measured as described in Section 2.7.2.

6.2.3. Cell viability: Trypan blue exclusion assay

The Trypan blue exclusion assay was performed to assess viability of MIN6 cells and mouse islets. MIN6 cells were seeded into 6-well plates at a density of 300,000 cells/well and incubated in DMEM supplemented with 25mM glucose, 10% (v/v) FBS, 1% (v/v) penicillin and streptomycin, and 1% (v/v) L-glutamine without or with aripiprazole or clozapine (0.1-20µM). Dye uptake by MIN6 cells after a 48h incubation with AAPs was assessed by exposure of the cells for 15min

to Trypan blue (0.2% w/v). Stained (blue; dead) and non-stained (white; viable) cells were visualised by light microscopy (Section 2.7.1).

Mouse islets were incubated in RPMI supplemented with 11.1mM glucose, 10% (v/v) FBS, 1% (v/v) penicillin and streptomycin, and 1% (v/v) L-glutamine and in the absence or presence of aripiprazole or clozapine (0.1-20μM) for 48h in 10cm Petri dishes. Cell membrane permeability and cell viability were assessed by incubation of islets with Trypan blue (0.2% w/v) for 15min, and then the islets were visualised by light microscopy (Section 2.7.1).

6.2.4. Insulin secretion from MIN6 beta cells

MIN6 cells were seeded into 96-well plates at a density of 20,000 cells/well and glucose stimulated insulin secretion (GSIS) was assessed in static insulin secretion experiments.

In acute experiments, MIN6 cells were pre-incubated in DMEM supplemented with 2.5mM glucose, 10% (v/v) FBS, 1% (v/v) penicillin and streptomycin, and 1% (v/v) L-glutamine for 2h at 37°C, and then incubated with DMEM supplemented with 2.5mM or 25mM glucose without or with aripiprazole (0.1-1μM) or clozapine (0.2-2μM) for 30min. The muscarinic receptor agonist carbachol (500μM) was used as a positive control to induce insulin secretion. The supernatants were collected and stored at -20°C until radioimmunoassay for insulin was carried out (Section 2.9.3).

In chronic experiments, MIN6 cells were incubated in DMEM supplemented with 5.5mM glucose in the absence or presence of aripiprazole (0.1-1μM) or clozapine (0.2-2μM) for 48h. Thereafter, the cells were pre-incubated in DMEM (2.5mM glucose) for 2h, and then incubated in DMEM supplemented with either 2.5mM glucose, 25mM glucose or 25mM glucose + 500μM carbachol for 30min without

the presence of AAPs. The supernatants were collected and kept at -20°C until assay for insulin.

6.2.5. Insulin secretion from mouse and human islets

Insulin secretion from mouse and human islets was assessed by static incubation experiments.

In acute experiments, isolated islets were pre-incubated for 1h in Gey & Gey buffer supplemented with 2mM glucose (Section 2.9.1.2), and groups of 3 mouse islets or 5 human islets were incubated with either 2mM or 20mM glucose without or with aripiprazole (0.1-1µM) or clozapine (0.2-2µM) for 1h. Carbachol (500µM) served as a positive control. The supernatants were collected and stored at -20°C for insulin radioimmunoassay (Section 2.9.3).

In chronic experiments, islets were incubated in RPMI (11.1mM glucose) supplemented with 10% (v/v) FBS, 1% (v/v) penicillin and streptomycin, and 1% (v/v) L-glutamine and in the absence or presence of aripiprazole (0.1-1µM) or clozapine (0.2-2µM) for 48h. Following a 1h pre-incubation in buffer containing 2mM glucose, groups of 3-5 islets were incubated in Gey & Gey buffer supplemented with either 2mM or 20mM glucose in the absence of drugs for 1h at 37°C. 500µM carbachol was used as a positive control. The supernatants were kept at -20°C until further assay.

6.2.6. MIN6 cell proliferation: BrdU ELISA

MIN6 cell proliferation was measured using a BrdU ELISA kit. MIN6 cells were seeded into 96-well plates at a density of 20,000 cells/well and cultured in DMEM supplemented with 5.5mM glucose, 1% (v/v) penicillin and streptomycin, and 1% (v/v) L-glutamine, but no FBS, and without or with aripiprazole (0.1-1μM) or clozapine (0.2-2μM) for 48h. 10% (v/v) FBS containing growth factors stimulating cell proliferation was used as a positive control. The cells were exposed to BrdU labelling reagent (100μM) for 2h at 37°C, and proliferation was determined by colorimetric quantification of BrdU incorporation into the DNA of dividing cells as described in Section 2.6.1.

6.2.7. MIN6 cell and islet apoptosis: Caspase-Glo 3/7 assay

Apoptosis of MIN6 cells and islets was assessed by a Caspase-Glo 3/7 apoptosis assay.

MIN6 cells were seeded into 96-well white plates, and they were cultured in DMEM supplemented with 5.5mM glucose, 10% (v/v) FBS, 1% (v/v) penicillin and streptomycin, and 1% (v/v) L-glutamine without or with aripiprazole (0.1-1μM) or clozapine (0.2-2μM) for 48h. The cells were exposed to a pro-inflammatory cytokine cocktail (0.05U/μl IL-1-β, 1U/μl TNF-α and 1U/μl IFN-γ) or 500μM palmitate 24h prior to the quantification of caspase3/7 activities using a Caspase-Glo 3/7 assay following the instructions in Section 2.8.1.

Groups of 3 mouse islets or 5 human islets were cultured in RPMI (11.1mM glucose) supplemented with 10% (v/v) FBS, 1% (v/v) penicillin and streptomycin, and 1% (v/v) L-glutamine in the absence or presence of aripiprazole (0.1-1μM) or clozapine (0.2-2μM) for 48h. The mix of cytokines or palmitate was added for the final 24h of the experiment. Apoptosis was determined by adding the Caspase-

Glo reagent for 1h and measuring caspase3/7 activities as explained in Section 2.8.1.

6.2.8. MIN6 cell apoptosis: Flow cytometry

Apoptosis of single cells was measured by flow cytometry. MIN6 cells were seeded into 6-well plates at a density of 100,000cells/well and incubated with DMEM supplemented with 5.5mM glucose, 10% (v/v) FBS, 1% (v/v) penicillin and streptomycin, and 1% (v/v) L-glutamine without or with aripiprazole (0.1-1µM) or clozapine (0.2-2µM) for 48h. A mix of proinflammatory cytokines was added 24h prior to the assay to induce MIN6 cell death. MIN6 cells were stained with annexin V using an Alexa Fluor 488 annexin V/Dead Cell Apoptosis kit (Section 2.8.2), and apoptosis was assessed using a BD Canto II analyser.

6.3.1. Aripiprazole

6.3.1.1. Effects of aripiprazole on ATP generation by beta cells

ATP is important for insulin release, and it is a key indicator of cell health. ATP production by MIN6 cells, as well as mouse and human islets, was assessed using the CellTiter-Glo assay following a 48h incubation with aripiprazole (0.1-10µM). Figure 6.1a shows that 0.1-1µM of aripiprazole significantly elevated ATP production by MIN6 cells, whereas 10µM aripiprazole significantly reduced luminescence. Inspection of the MIN6 cells indicated that this reduction in luminescence resulted from cells detaching from the well surface at this high aripiprazole concentration. Similar to the data obtained in MIN6 cells, experiments with mouse (Figure 6.1b) and human (Figure 6.1c) islets demonstrated that 0.1-1µM aripiprazole significantly increased ATP generation after 48h exposure, while 10µM aripiprazole significantly decreased ATP generation in mouse islets, which is indicative of lower numbers of metabolically active cells. However, production of ATP by human islets was not affected by high concentrations of aripiprazole, which suggests species-specific differences between mice and humans in response to aripiprazole.

a)

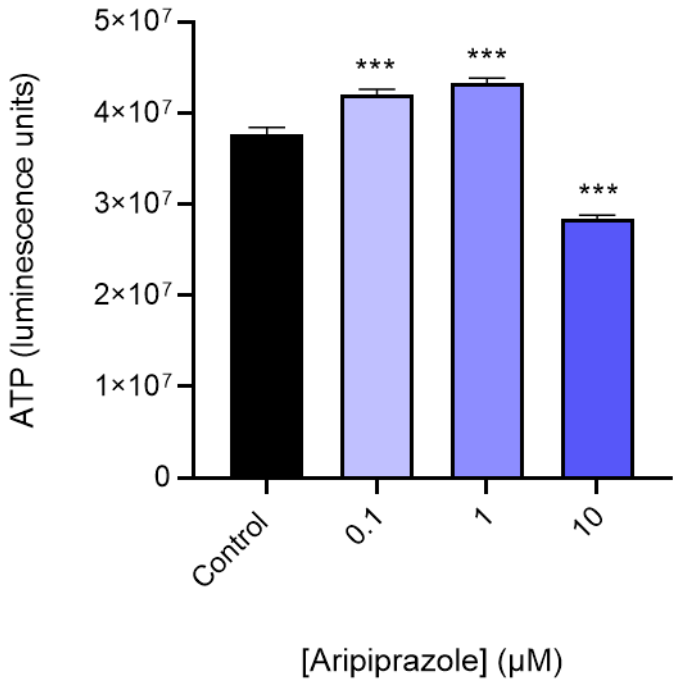
5×10^7
4×10^7
3×10^7
2×10^7
1×10^7
0
ATP (luminescence units)
***
***
***
Control
0.1
1
10
[Aripiprazole] (μM)

b)

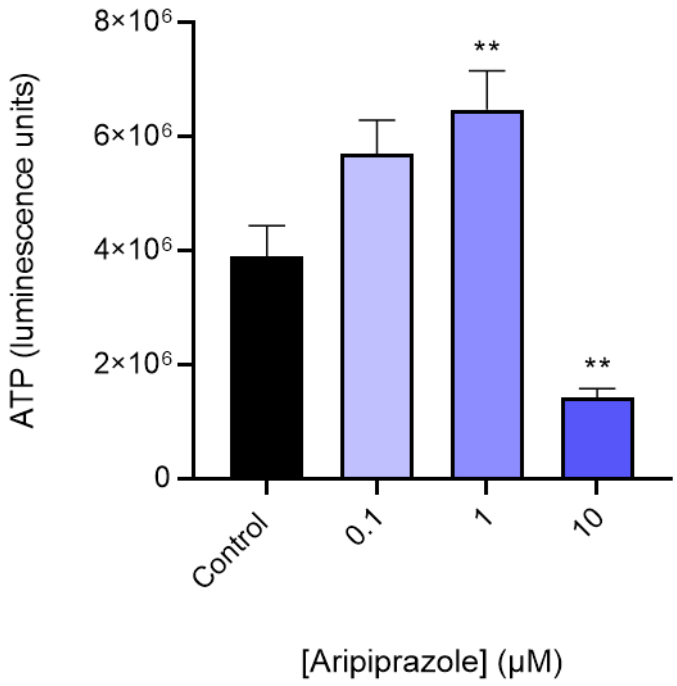
8×10^6
6×10^6
4×10^6
2×10^6
0
ATP (luminescence units)
**
**
Control
0.1
1
10
[Aripiprazole] (μM)

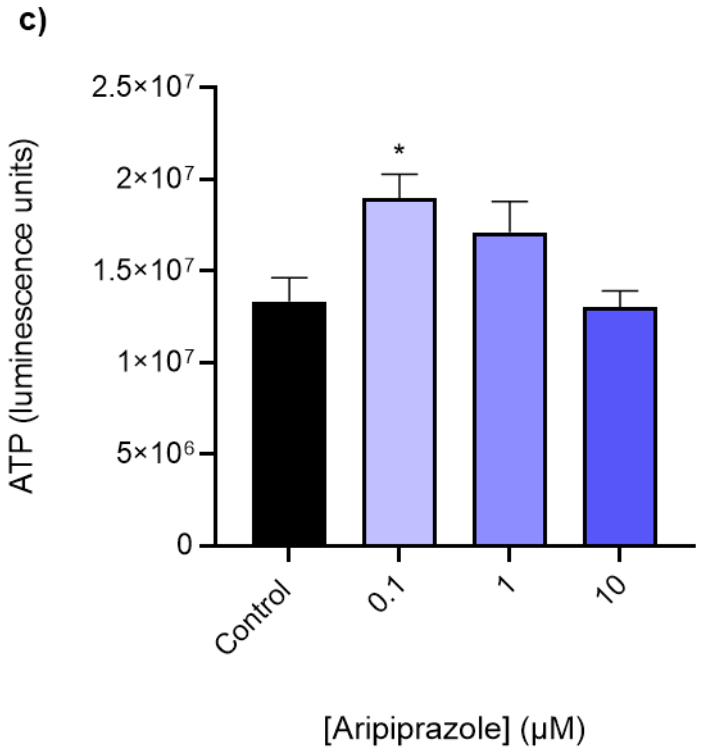

Figure 6.1. Effects of aripiprazole (0.1-10μM) on ATP production by MIN6 cells (a), mouse islets (b) and human islets (c). The cells were incubated without or with aripiprazole for 48h, and ATP generation was measured using the luminescent CellTiter-Glo assays. Data are mean + SEM, n=8 observations, *p<0.05; **p<0.01; ***p<0.001 relative to the control samples, One-way ANOVA, Dunnett's multiple comparisons test.

6.3.1.2. Effects of aripiprazole on beta cell viability

The effects of aripiprazole on MIN6 cell and mouse islet viability were determined by a Trypan blue exclusion test. Following a 48h incubation in the absence or presence of aripiprazole (0.1-10µM), MIN6 cells were stained with Trypan blue dye, and the dye uptake was visualised by light microscopy. The dye was only seen in MIN6 cells or islets that had been treated with 10µM aripiprazole. MIN6 cells that had been treated with 10µM aripiprazole stained blue or detached from the well surface (Figure 6.2a), leading to a decreased percentage of viable cells (Figure 6.2b). Likewise, mouse islets that had been exposed to this high concentration of aripiprazole stained blue in the centre, which is where the majority of beta cells are localised within the islets (Figure 6.2c). These observations indicate that low and therapeutically relevant concentrations of aripiprazole (0.1-1µM) are well tolerated by MIN6 cells and islets, and they do not compromise cell viability, whereas 10µM of this antipsychotic drug is cytotoxic to beta cells, and hence it was not used in the functional experiments described in this chapter.

a)

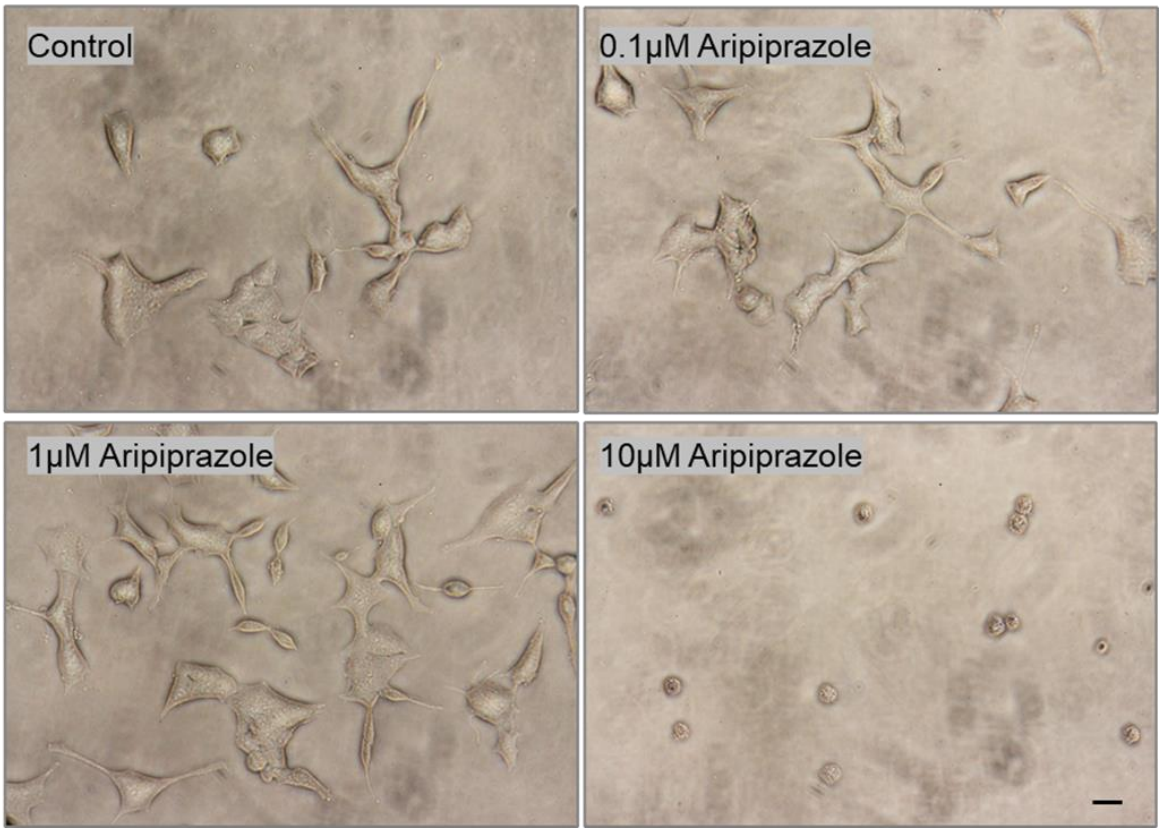
Control
0.1μM Aripiprazole
1μM Aripiprazole
10μM Aripiprazole

b)

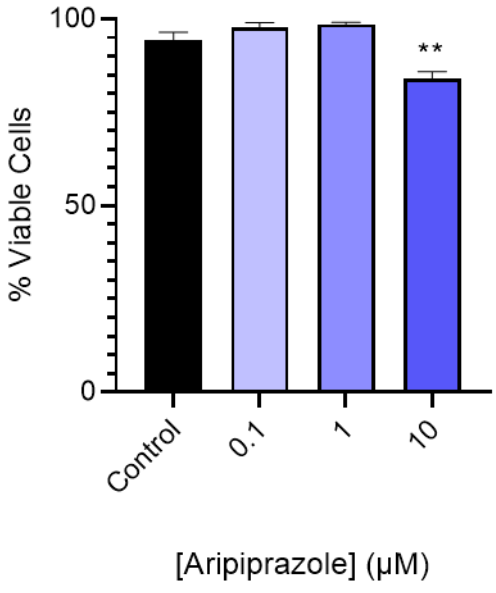
100
50
0
% Viable Cells
**
Control
0.1
1
10
[Aripiprazole] (μM)

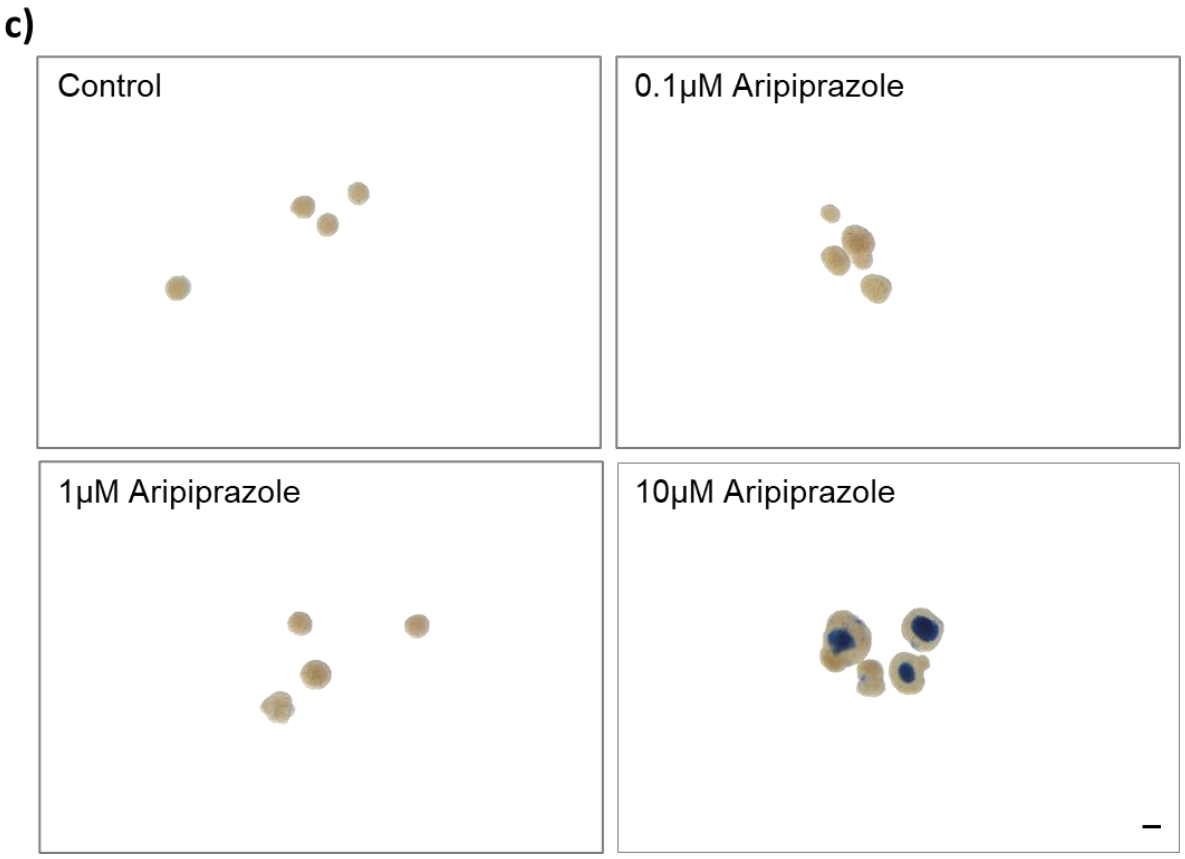

Figure 6.2. Effects of aripiprazole on MIN6 cell and mouse islet viability. Photographs of Trypan blue-stained MIN6 cells (a) and mouse islets (c) after incubation in DMEM (25mM glucose) in the absence (control) or presence of aripiprazole (0.1-10µM) for 48h. Scale bars are 50µm. Percentage viability of MIN6 cells was calculated by counting the numbers of viable and dead cells with a haemocytometer (b). Data are mean + SEM, n =4 technical repeats. **p<0.01 relative to the controls, One-way ANOVA, Dunnett's multiple comparisons test.

6.3.1.3. Effects of aripiprazole on insulin secretion

Given that aripiprazole at 0.1µM and 1µM was well tolerated by MIN6 cells and mouse islets, the effects of these low and therapeutic concentrations of aripiprazole on insulin secretion by MIN6 cells and islets were investigated in acute and chronic static incubation experiments.

In both acute and chronic experiments, exposure of MIN6 cells to 1µM aripiprazole significantly increased insulin release at 25mM glucose (Figure 6.3a, b), whereas 0.1µM of the drug had small, but non-significant effects on glucose-stimulated insulin release. Similar to the data obtained in static incubations using MIN6 cells, both acute and chronic exposure to 1µM aripiprazole significantly potentiated insulin secretion from mouse (Figure 6.3c, d) and human (Figure 6.3e, f) islets at supramaximal glucose levels. In all of the acute and chronic insulin secretion experiments with MIN6 cells, mouse islets and human islets, exposure to either 0.1 or 1µM aripiprazole did not affect basal insulin secretion at 2 or 2.5mM glucose, which means that the secretory mechanisms of the beta cells were not disrupted, suggesting that aripiprazole is unlikely to induce hypoglycaemia when taken therapeutically. In all experiments, beta cells responded to 20 or 25mM glucose and significantly increased insulin release, and this was potentiated by the positive control carbachol.

a)

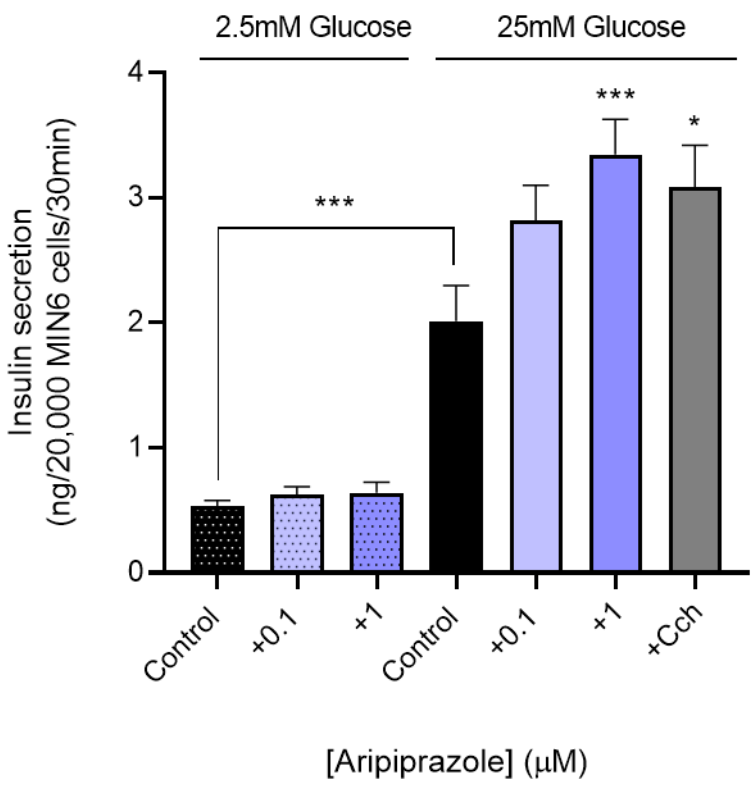
2.5mM Glucose
25mM Glucose
Insulin secretion
(ng/20,000 MIN6 cells/30min)
0
1
2
3
4
***
***
*
Control
+0.1
+1
Control
+0.1
+1
+Cch
[Aripiprazole] (μM)

b)

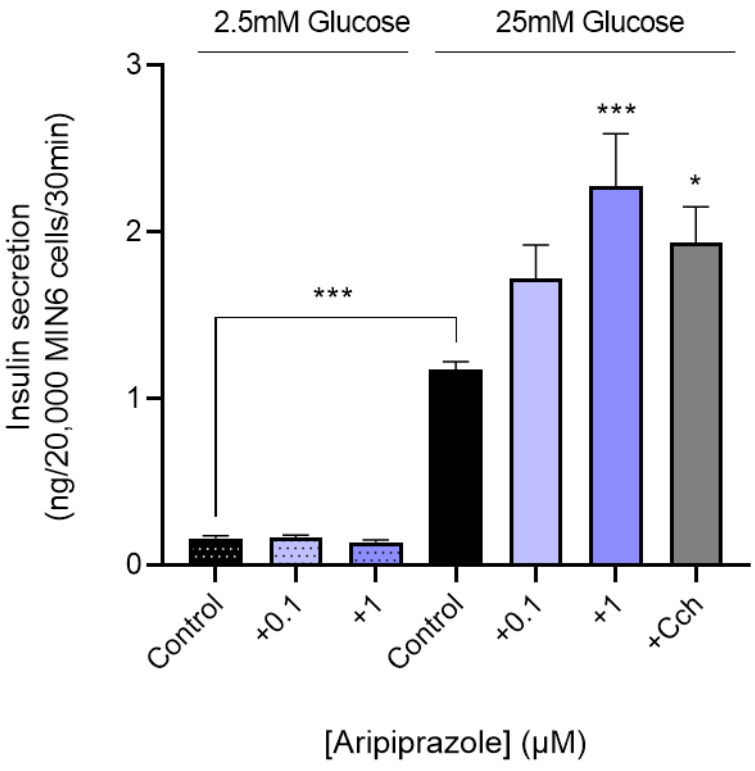
2.5mM Glucose
25mM Glucose
Insulin secretion
(ng/20,000 MIN6 cells/30min)
0
1
2
3
***
***
*
Control
+0.1
+1
Control
+0.1
+1
+Cch
[Aripiprazole] (μM)

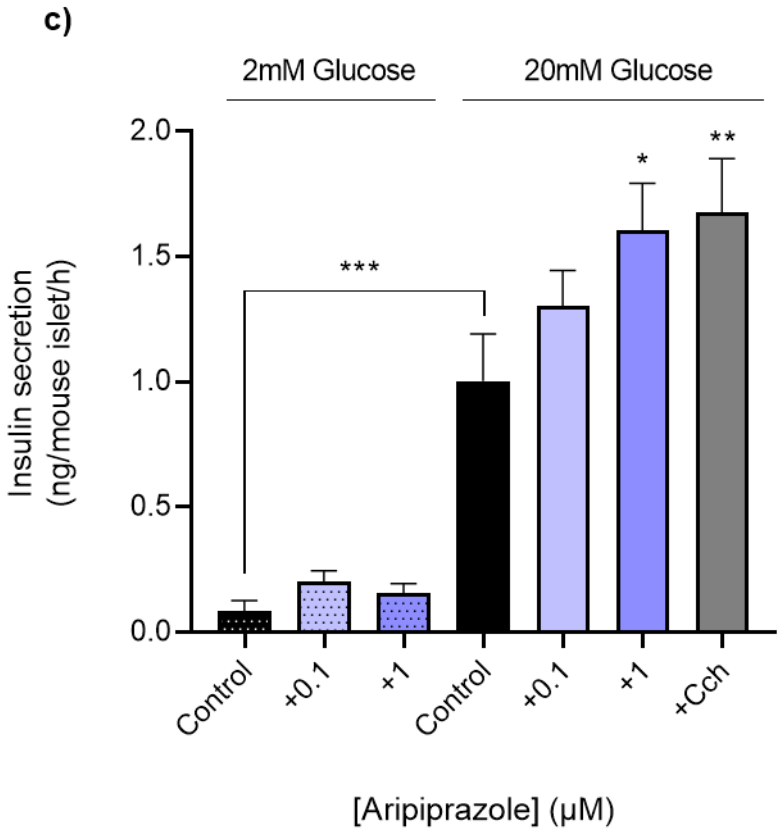
c)
2mM Glucose
20mM Glucose
Insulin secretion (ng/mouse islet/h)
2.0
1.5
1.0
0.5
0.0
***
*
**
Control
+0.1
+1
Control
+0.1
+1
+Cch
[Aripiprazole] (μM)

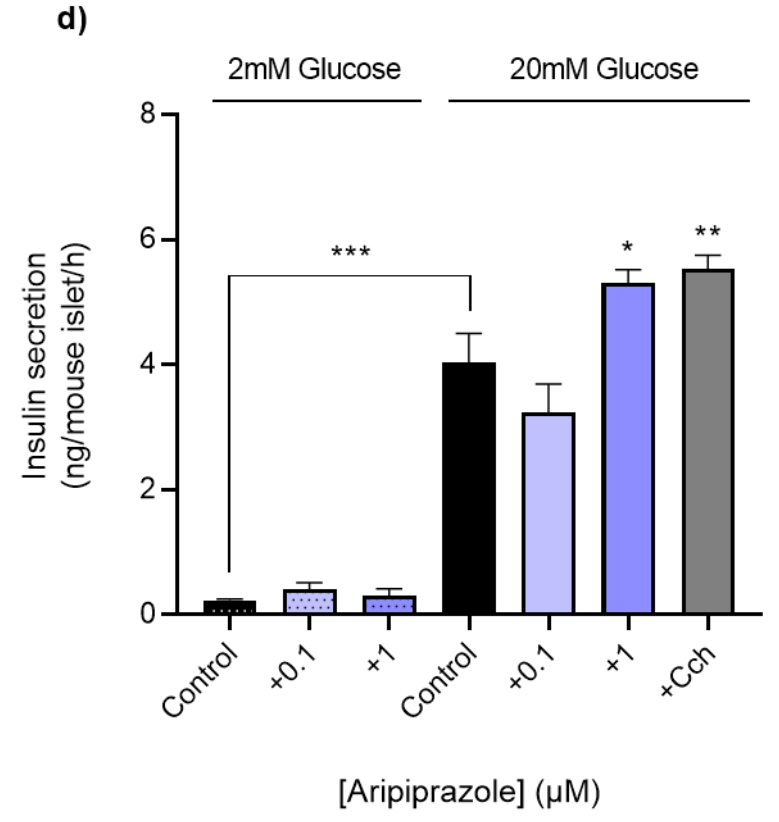
d)
2mM Glucose
20mM Glucose
Insulin secretion (ng/mouse islet/h)
8
6
4
2
0
***
*
**
Control
+0.1
+1
Control
+0.1
+1
+Cch
[Aripiprazole] (μM)

e)

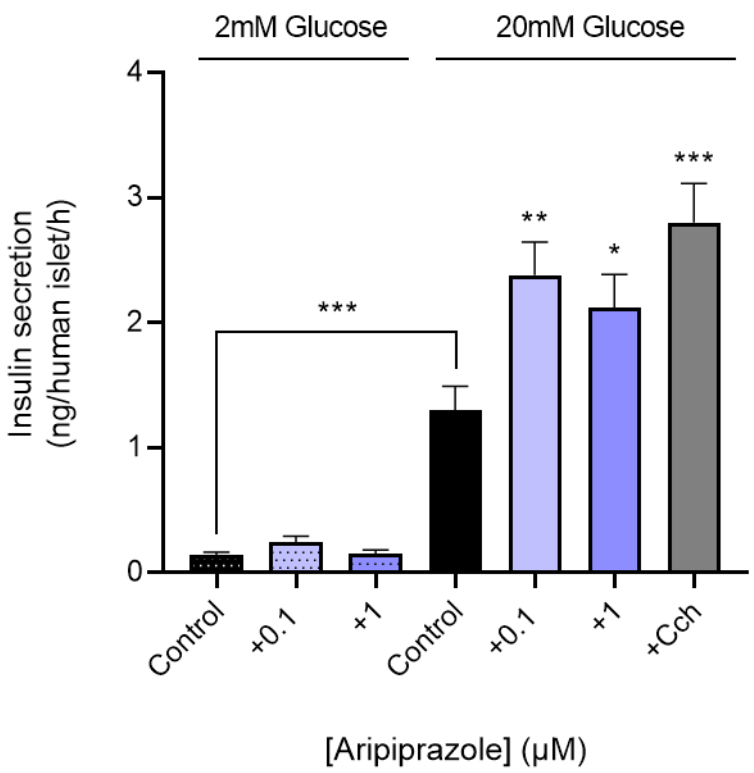
2mM Glucose
20mM Glucose
Insulin secretion (ng/human islet/h)
0
1
2
3
4
***
**
*
***
Control
+0.1
+1
Control
+0.1
+1
+Cch
[Aripiprazole] (μM)

f)

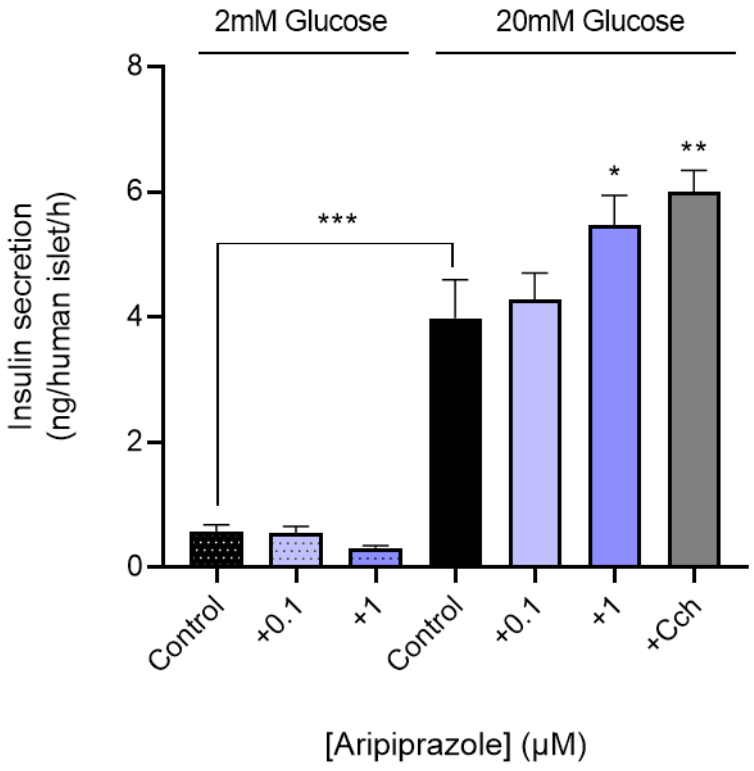
2mM Glucose
20mM Glucose
Insulin secretion (ng/human islet/h)
0
2
4
6
8
***
*
**
Control
+0.1
+1
Control
+0.1
+1
+Cch
[Aripiprazole] (μM)

Figure 6.3. Effects of aripiprazole on insulin secretion from MIN6 cells (a - acute, b - chronic), mouse islets (c - acute, d - chronic) and human islets (e - acute, f - chronic). In static secretion experiments, MIN6 cells or islets were incubated without or with aripiprazole for 30min (MIN6 cells) or 1h (islets) without pre-treatment with aripiprazole (acute experiments) or following a 48h incubation in the absence or presence of aripiprazole (chronic experiments). All data shown are mean + SEM, n=8 observations representative of 2-4 separate experiments, One-way ANOVA, Dunnett's multiple comparisons test. *p<0.05; **p<0.01; ***p<0.001 relative to the control samples at 20 or 25mM glucose.

6.3.1.4. Effects of aripiprazole on beta cell proliferation

Having validated that aripiprazole potentiated glucose-stimulated insulin secretion, the direct effects of this antipsychotic drug on beta cell proliferation were investigated by quantifying the incorporation of the thymidine analogue BrdU into the DNA of dividing MIN6 cells. 48h exposure of MIN6 cells to concentrations of aripiprazole that are well-tolerated by beta cells (0.1-1µM) showed that 1µM aripiprazole significantly increased BrdU incorporation into DNA when compared to control cells that had been cultured in the absence of aripiprazole (Figure 6.4). 10% FBS, which is rich in growth factors that stimulate cell division, was used as a positive control, and it significantly increased MIN6 cell proliferation, as expected.

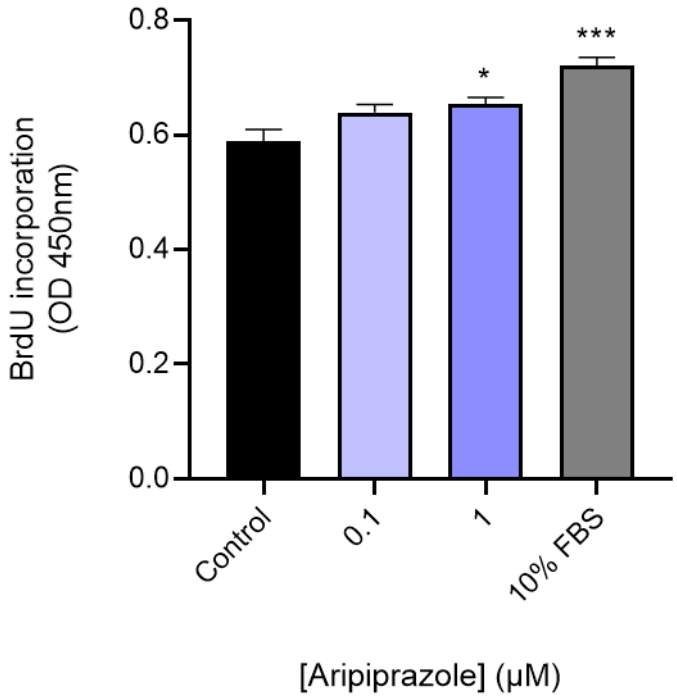

Figure 6.4. Effects of aripiprazole on MIN6 cell proliferation. MIN6 cells were exposed to aripiprazole for 48h, and BrdU incorporation was measured by quantifying absorbance at 450nm. Data are mean + SEM, n=8 observations representative of 3 separate experiments.

*p<0.05; ***p<0.001 relative to the control samples, One-way ANOVA, Dunnett's multiple comparisons test.

6.3.1.5. Effects of aripiprazole on beta cell apoptosis

Beta cell mass expands as a result of increased proliferation and decreased apoptosis. Figure 6.4 shows that aripiprazole increased proliferation of MIN6 cells, and its effects on apoptosis of MIN6 cells, as well as and mouse and human islets, were also investigated by quantifying caspase3/7 activities. Caspases 3 and 7 are important components of the apoptotic pathway. Because basal apoptosis of beta cells is very low, the effects of exposure to aripiprazole on caspase3/7 activities were assessed in the absence and presence of proinflammatory cytokines or a saturated free fatty acid palmitate. Figure 6.5 shows that treatment with 0.1-1μM aripiprazole had no effect on basal or cytokine-induced caspase3/7 activities in MIN6 cells (a). However, 0.1-1μM aripiprazole had a protective effect against cytokine-induced apoptosis of mouse and human islets (b, c). In addition, it also protected MIN6 cells (d), mouse islets (e) and human islets (f) from apoptosis induced by the saturated fatty acid palmitate. By reducing detrimental effects of cytokines and palmitate on beta cell apoptosis, aripiprazole treatment could be beneficial in T2D, which is associated with chronic inflammation and obesity.

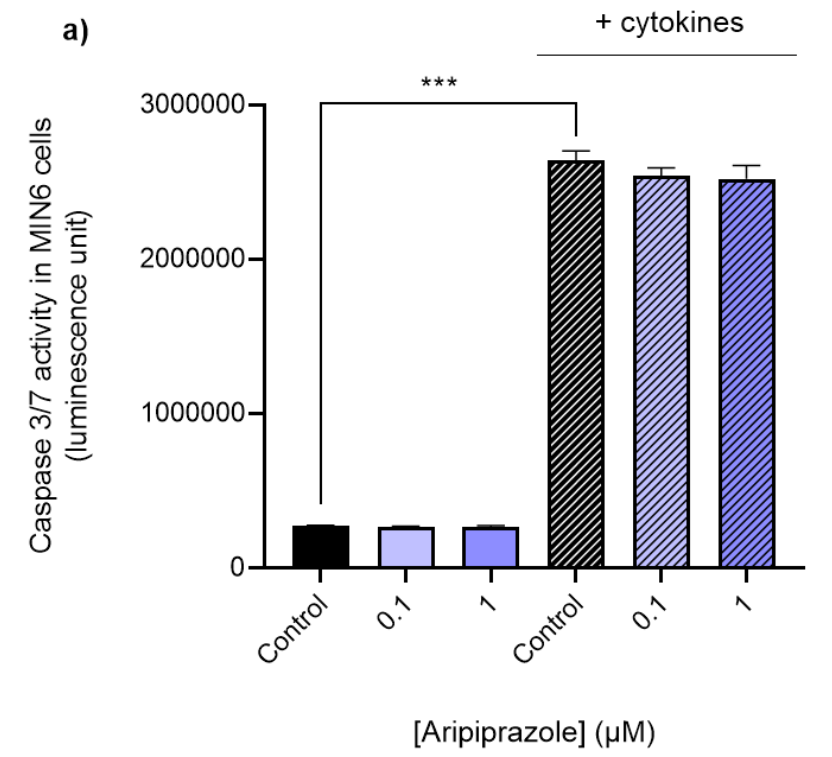
a)
+ cytokines
***
3000000
2000000
1000000
0
Caspase 3/7 activity in MIN6 cells
(luminescence unit)
Control
0.1
1
Control
0.1
1
[Aripiprazole] (μM)

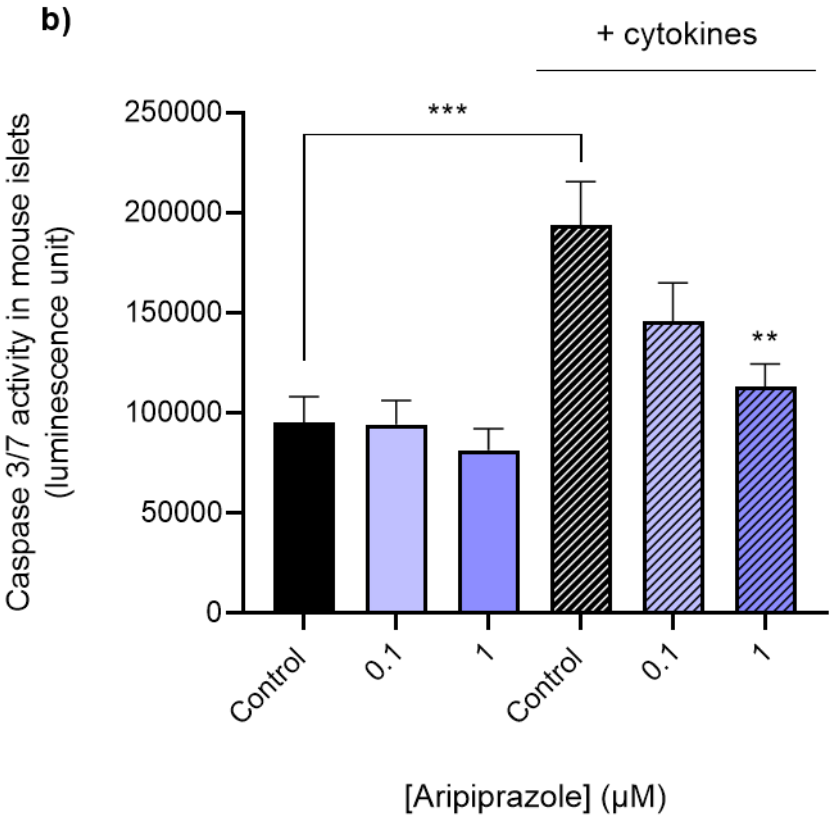
b)
+ cytokines
***
**
250000
200000
150000
100000
50000
0
Caspase 3/7 activity in mouse islets
(luminescence unit)
Control
0.1
1
Control
0.1
1
[Aripiprazole] (μM)

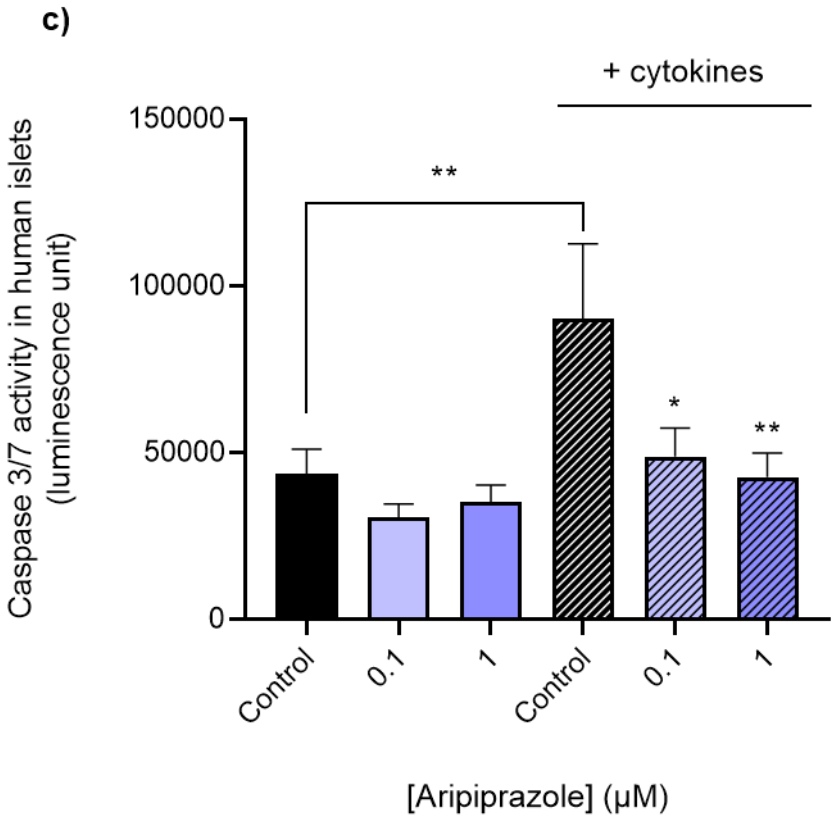
c)
+ cytokines
150000
100000
50000
0
**
*
**
Caspase 3/7 activity in human islets
(luminescence unit)
Control
0.1
1
Control
0.1
1
[Aripiprazole] (μM)

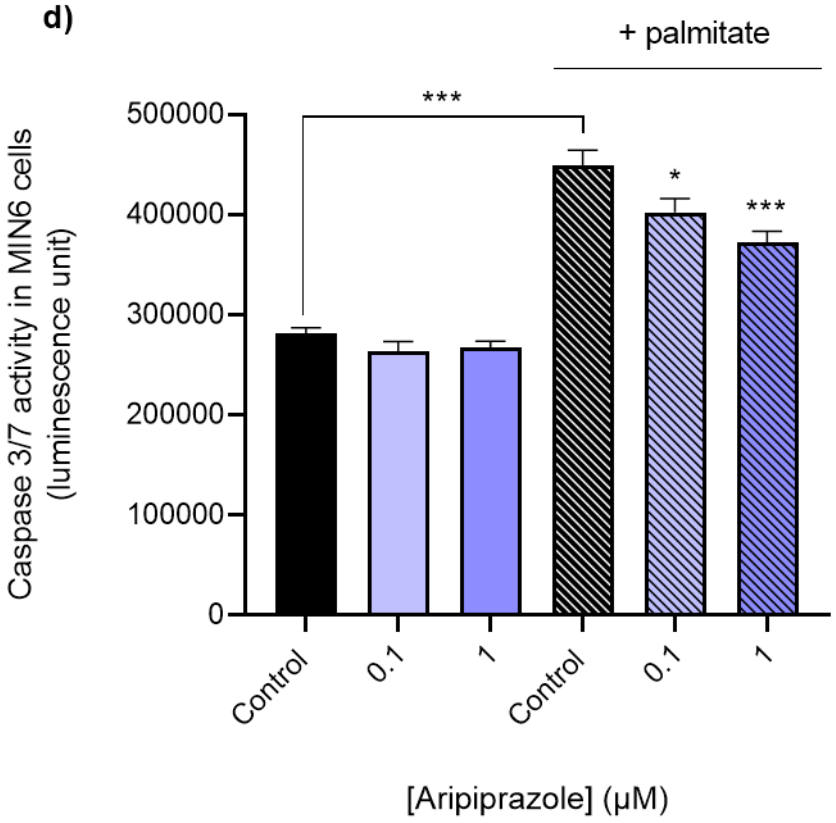
d)
+ palmitate
500000
400000
300000
200000
100000
0
***
*
***
Caspase 3/7 activity in MIN6 cells
(luminescence unit)
Control
0.1
1
Control
0.1
1
[Aripiprazole] (μM)

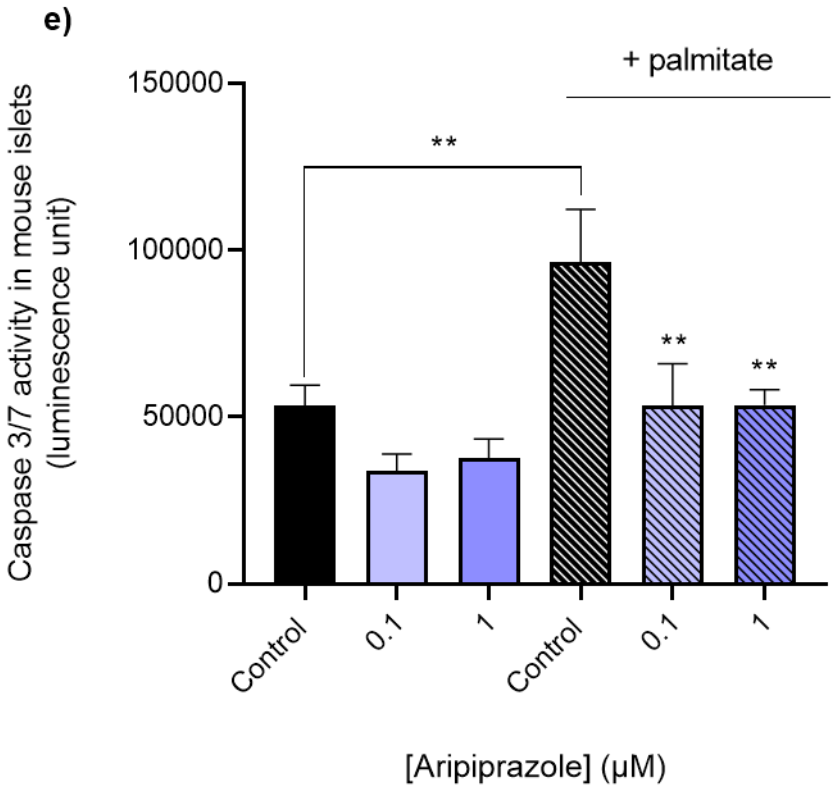
e)
+ palmitate
150000
100000
50000
0
**
**
**
Caspase 3/7 activity in mouse islets
(luminescence unit)
Control
0.1
1
Control
0.1
1
[Aripiprazole] (μM)

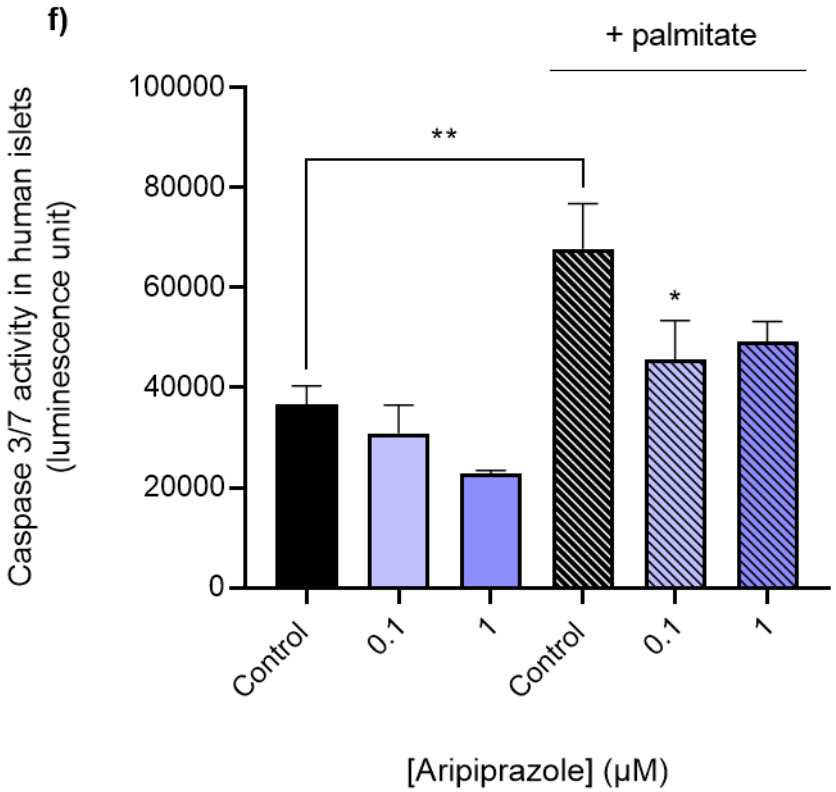
f)
+ palmitate
100000
80000
60000
40000
20000
0
**
*
Caspase 3/7 activity in human islets
(luminescence unit)
Control
0.1
1
Control
0.1
1
[Aripiprazole] (μM)

Figure 6.5. Effects of aripiprazole on apoptosis of MIN6 cells (a, d), mouse islets (b, e) and human islets (c, f) determined by luminescence quantification of caspase3/7 activities. MIN6 cells or islets were treated with aripiprazole for 48h. A proinflammatory cytokine mix or 500µM palmitate were added 24h prior to luminescence measurement. Data are expressed as mean + SEM; n=8 observations representative of 3 and 2 experiments using MIN6 cells and islets, respectively. *p<0.05; **p<0.01; ***p<0.001 versus appropriate control in the absence (black) or presence (striped lines) of cytokines or palmitate; One-way ANOVA, Dunnett's multiple comparisons test.

The lack of protection of aripiprazole against cytokine-induced apoptosis in MIN6 cells (Figure 6.5a) was clearly inconsistent with the significant protective effects observed in mouse and human islets (Fig 6.5b-e). The data shown in Figures 6.1a and 6.4 demonstrate that 48h exposure to 0.1 and 1µM aripiprazole increases MIN6 beta cell ATP generation and proliferation, respectively. Therefore, the protective effects of aripiprazole against cytokine-apoptosis in MIN6 cells could be masked by an increased cell number, and hence increased readings of caspase3/7 activities. Thus, in addition to quantifying apoptosis using the Caspase-Glo assay, apoptosis of MIN6 cells was also assessed by flow cytometry, which allows for quantification of apoptosis in single cells. For these experiments, MIN6 cells were stained with annexin V, and apoptosis was induced by a proinflammatory cytokine cocktail. In contrast to the data obtained in the caspase3/7 luminescence experiments (Figure 6.5a), treatment of MIN6 cells with aripiprazole for 48h led to significantly decreased annexin V binding, indicative of decreased apoptosis (Figure 6.6).

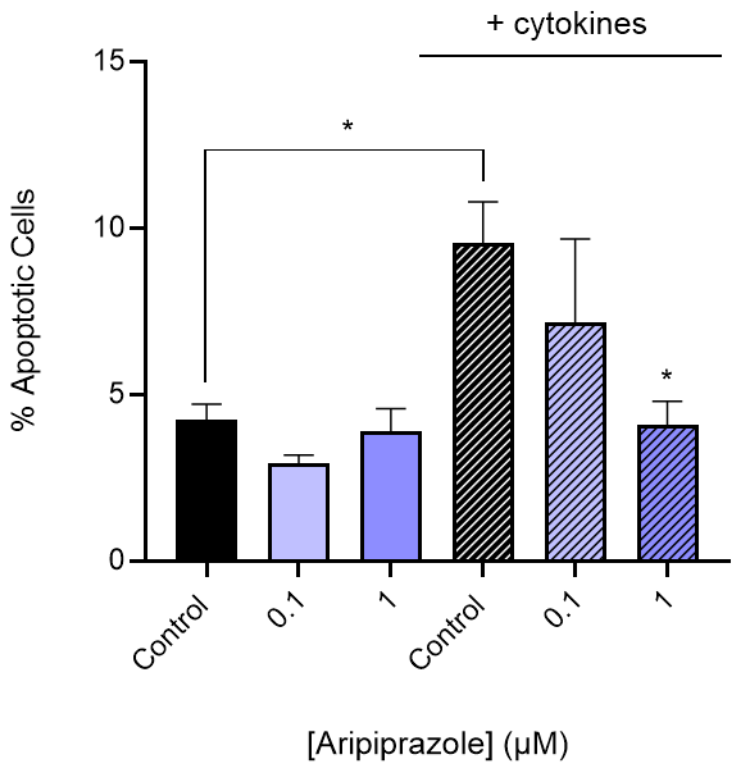

Figure 6.6. Effects of aripiprazole on MIN6 cell apoptosis determined by analysis of annexin V staining. Data are mean + SEM, n=3 separate experiments. *p<0.05 relative to the control samples (black striped), One-way ANOVA, Dunnett's multiple comparisons test.

6.3.2. Clozapine

6.3.2.1. Effects of clozapine on ATP generation by beta cells

Similar to the data obtained with aripiprazole (Figure 6.1), 48h exposure of MIN6 cells to another AAP, clozapine (0.2-2µM), also markedly elevated ATP luminescence (Figure 6.7a), and clozapine at 0.2µM also increased ATP production by mouse islets and human islets (b, c). In contrast to the reductions in ATP luminescence seen with 10µM aripiprazole, 20µM clozapine did not influence the luminescent signal, meaning that it did not lead to decreased ATP levels. In addition, there was no difference between ATP production by islets that had been treated with 2 and 20µM clozapine and the untreated controls.

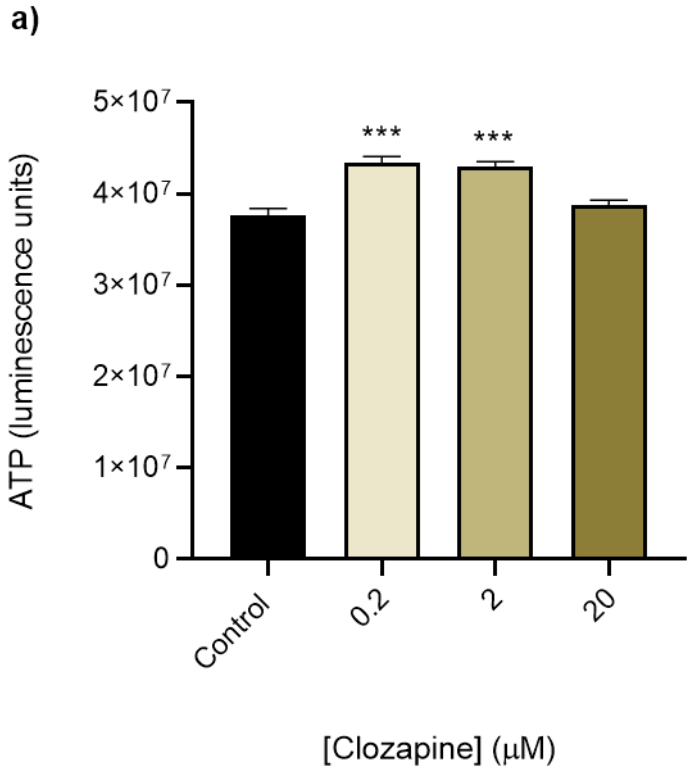

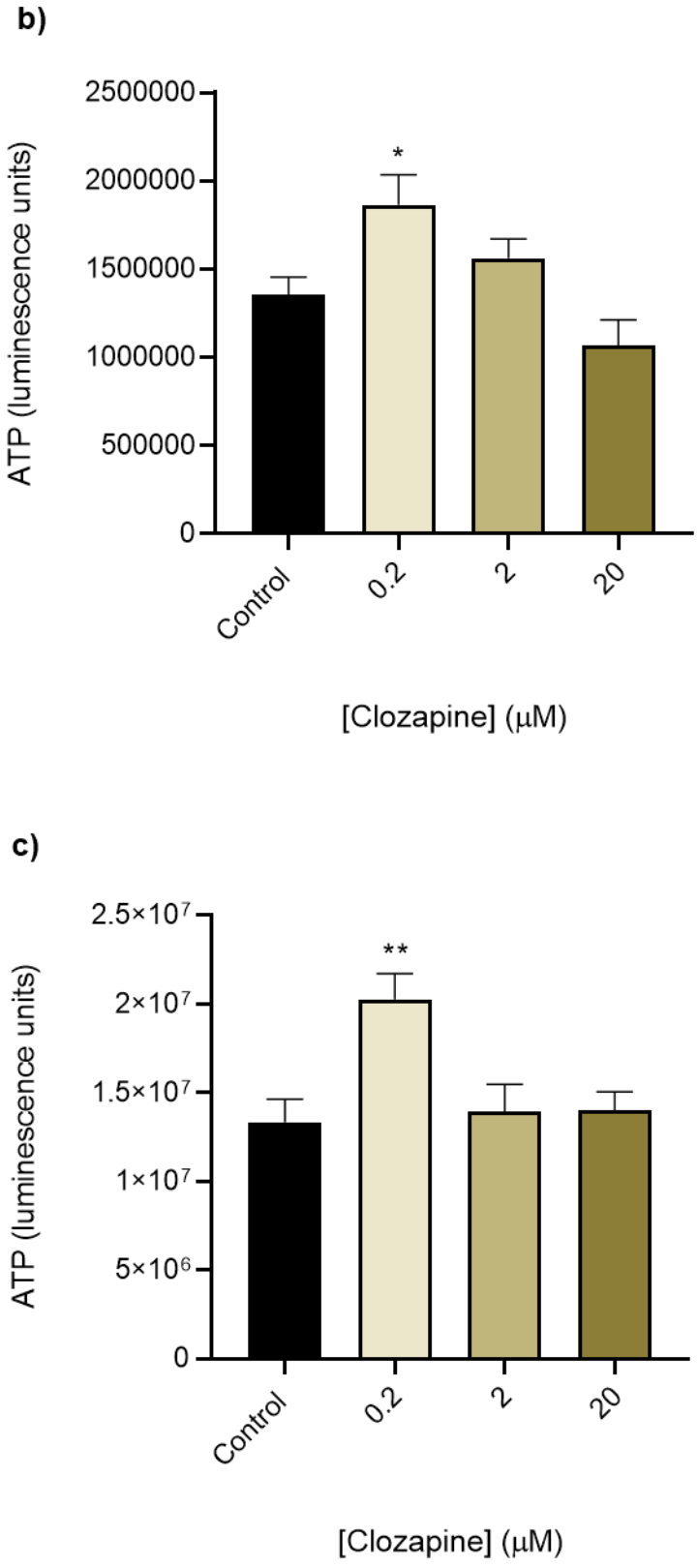

Figure 6.7. Effects of clozapine on ATP generation by MIN6 cells (a), mouse islets (b) and human islets (c). The cells were incubated in the absence or presence of clozapine (0.2-20μM) for 48h,

and ATP generation was quantified using luminescent CellTiter-Glo assays. Data are mean + SEM, n=8 observations representative of 2-3 experiments. *p<0.05; **p<0.01; ***p<0.001 relative to the control samples, One-way ANOVA, Dunnett's multiple comparisons test.

6.3.2.2. Effects of clozapine on beta cell viability

The Trypan blue exclusion assay was used to investigate the effects of clozapine on MIN6 cell and mouse islet viability, and to determine what concentrations are well tolerated by beta cells. Following a 48h incubation in the absence or presence of clozapine (0.2-20µM), MIN6 cells and mouse islets were exposed to 0.2% (w/v) Trypan blue, and its uptake by the cells was visualised by light microscopy (Figure 6.8). Trypan blue uptake was only observed in MIN6 cells or islets that had been exposed to 20µM clozapine, meaning that this concentration was not tolerated by the cells, leading to increased dye update indicative of viability, while lower concentrations did not stain the cells blue or compromise plasma membrane integrity. When compared to microscopy data obtained with 10µM aripiprazole, less Trypan blue staining was observed with 20µM clozapine. Nevertheless, this concentration of clozapine led to a significantly decreased percentage viability of MIN6 cells, and it was not used in further functional experiments.

a)

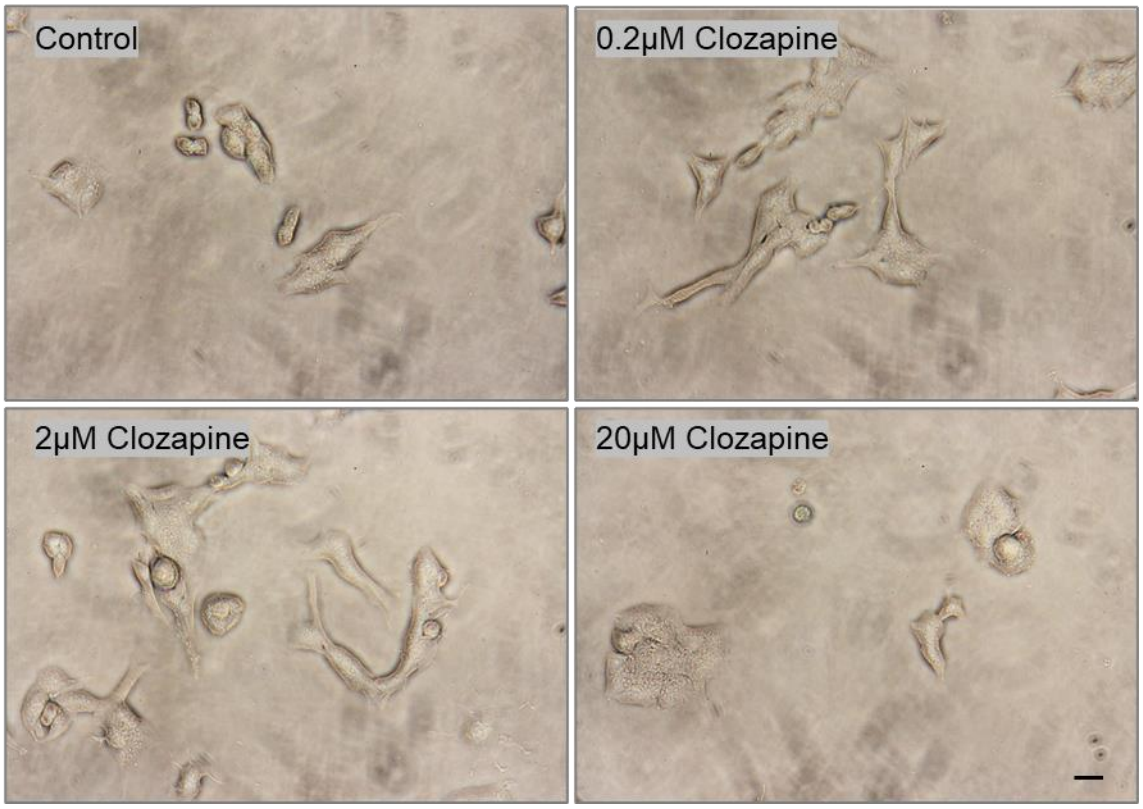
Control
0.2μM Clozapine
2μM Clozapine
20μM Clozapine

b)

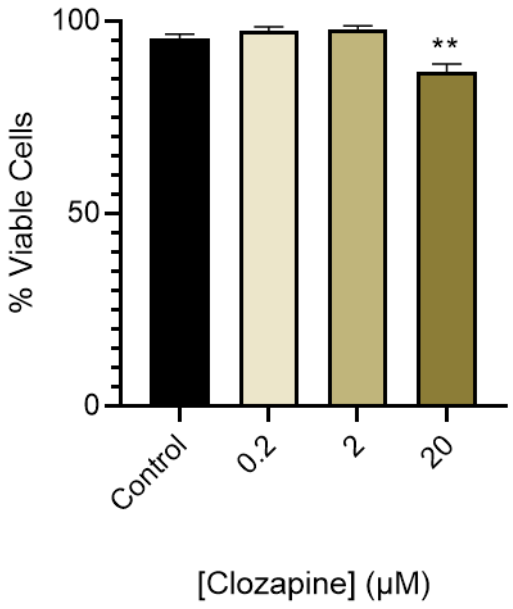
100
50
0
% Viable Cells
**
Control
0.2
2
20
[Clozapine] (μM)

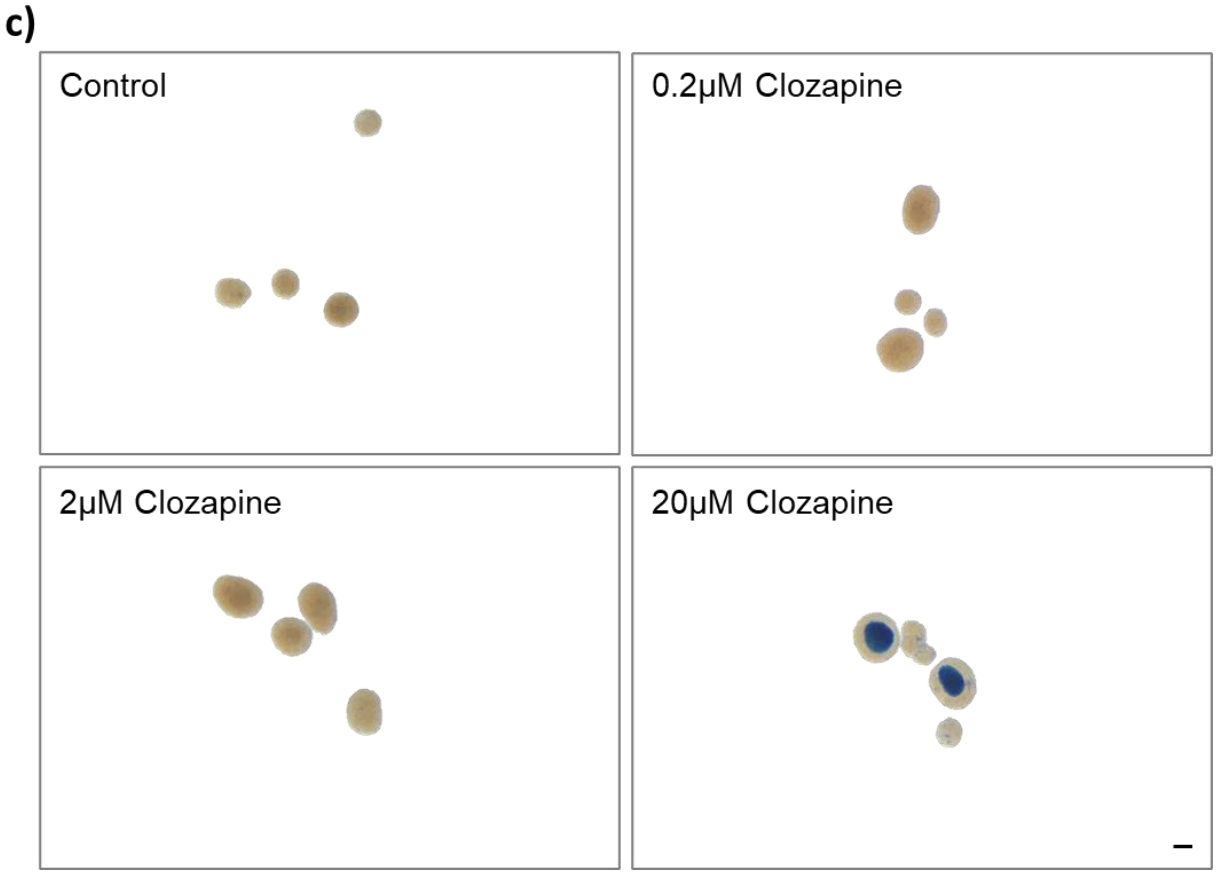

Figure 6.8. Effects of clozapine on MIN6 cell and mouse islet viability. Micrographs of MIN6 cells (a) and mouse islets (c) stained with Trypan blue following 48h incubation without (control) or with clozapine (0.2-20µM). Scale bars show 50µm. % Viability of MIN6 cells was calculated by counting viable and dead cells using a haemocytometer (b). Data are mean + SEM, n =4 technical repeats. **p<0.01 relative to the controls, One-way ANOVA, Dunnett's multiple comparisons test.

6.3.2.3. Effects of clozapine on insulin secretion

Given that clozapine is well tolerated by MIN6 cells and mouse islets at 0.2-2µM, static incubation experiments were carried out to determine the effects of clozapine on insulin secretion by MIN6 cells, mouse islets and human islets. In acute and chronic static incubation experiments, clozapine (0.2-2µM) increased insulin secretion from MIN6 cells and islets at 20-25mM glucose (Figure 6.9), and, as aripiprazole, it did not stimulate basal insulin secretion from beta cells at 2 or 2.5mM glucose, which would be an advantage when prescribing this drug to patients with T2D. In these experiments, clozapine at 2µM had the greatest effects on GSIS from both mouse and human beta cells.

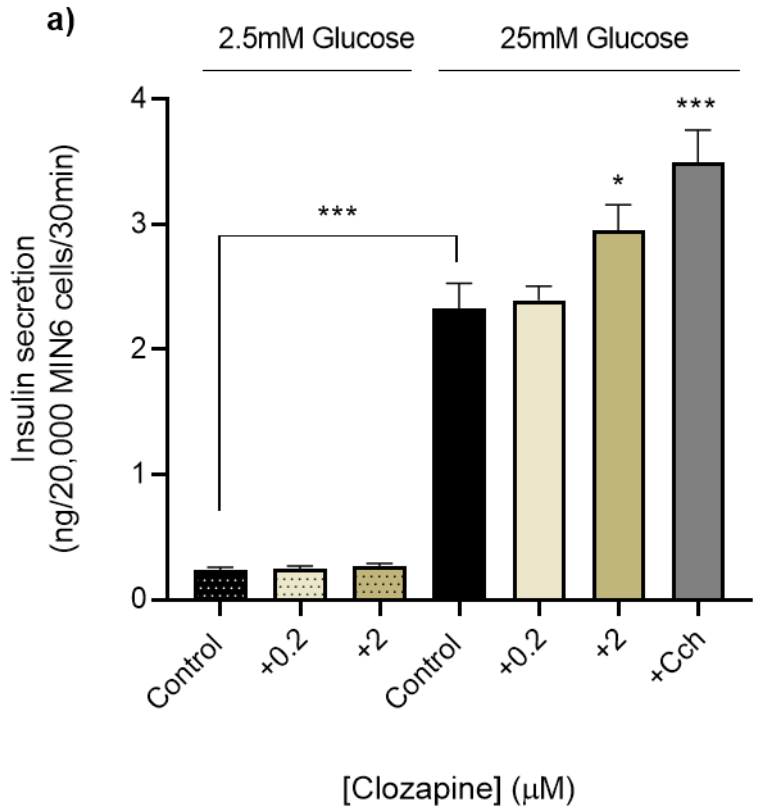

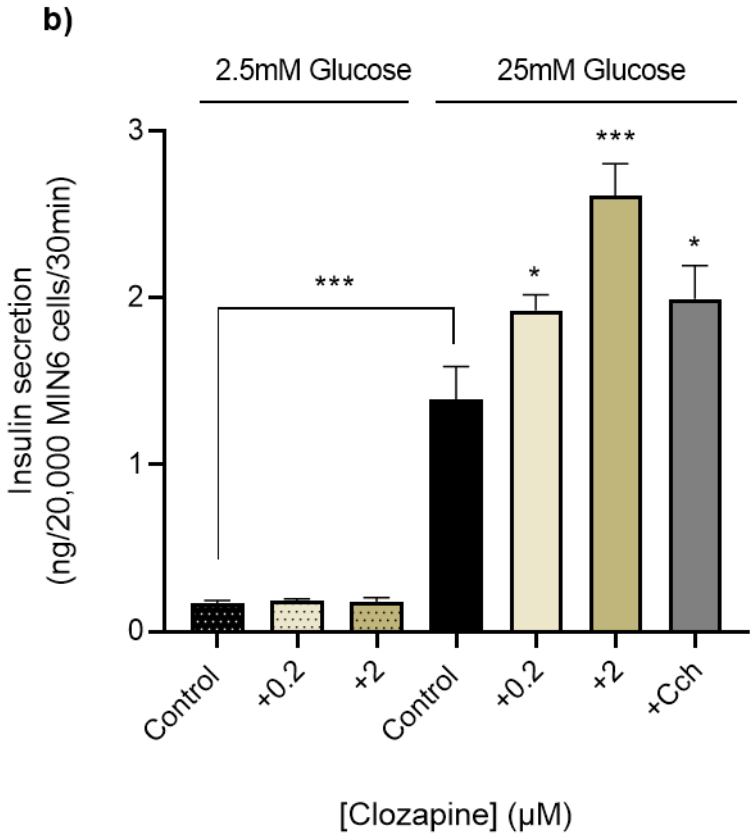
b)
2.5mM Glucose
25mM Glucose
Insulin secretion
(ng/20,000 MIN6 cells/30min)
3
2
1
0
***
*
***
*
Control
+0.2
+2
Control
+0.2
+2
+Cch
[Clozapine] (μM)

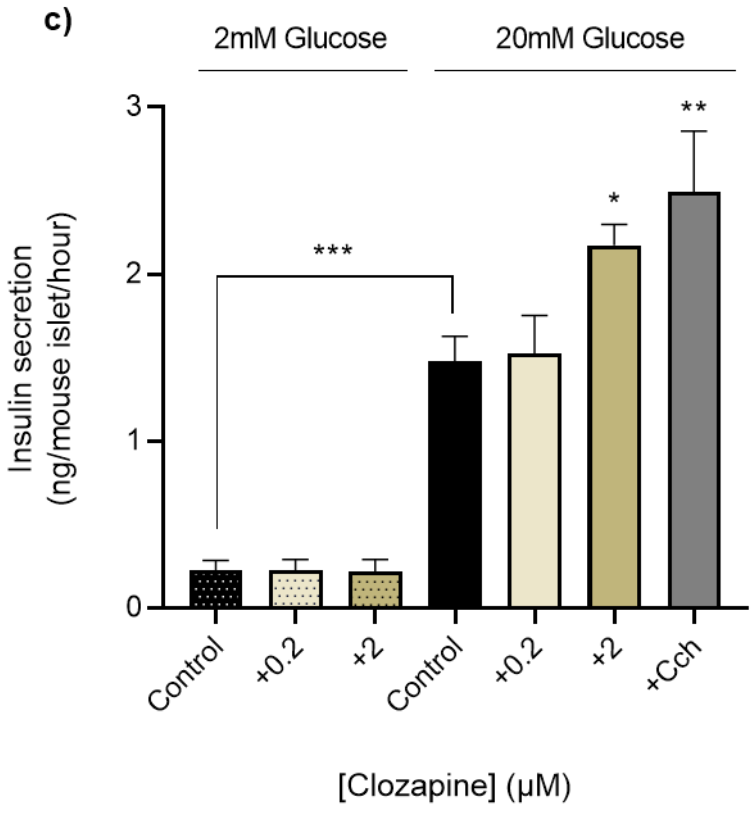
c)
2mM Glucose
20mM Glucose
Insulin secretion
(ng/mouse islet/hour)
3
2
1
0
***
*
**
Control
+0.2
+2
Control
+0.2
+2
+Cch
[Clozapine] (μM)

d)

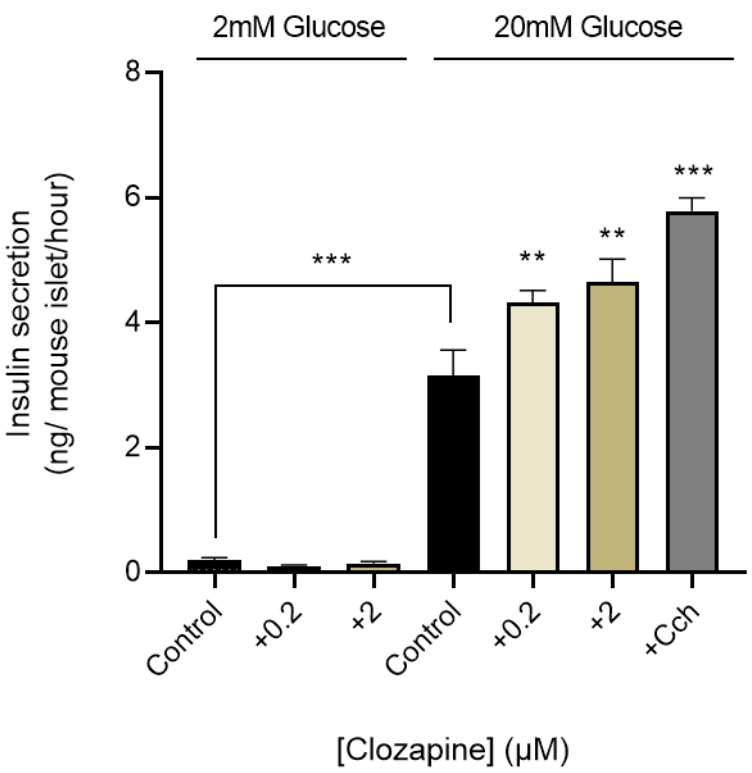
2mM Glucose
20mM Glucose
Insulin secretion
(ng/ mouse islet/hour)
8
6
4
2
0
***
**
**
***
Control
+0.2
+2
Control
+0.2
+2
+Cch
[Clozapine] (μM)

e)

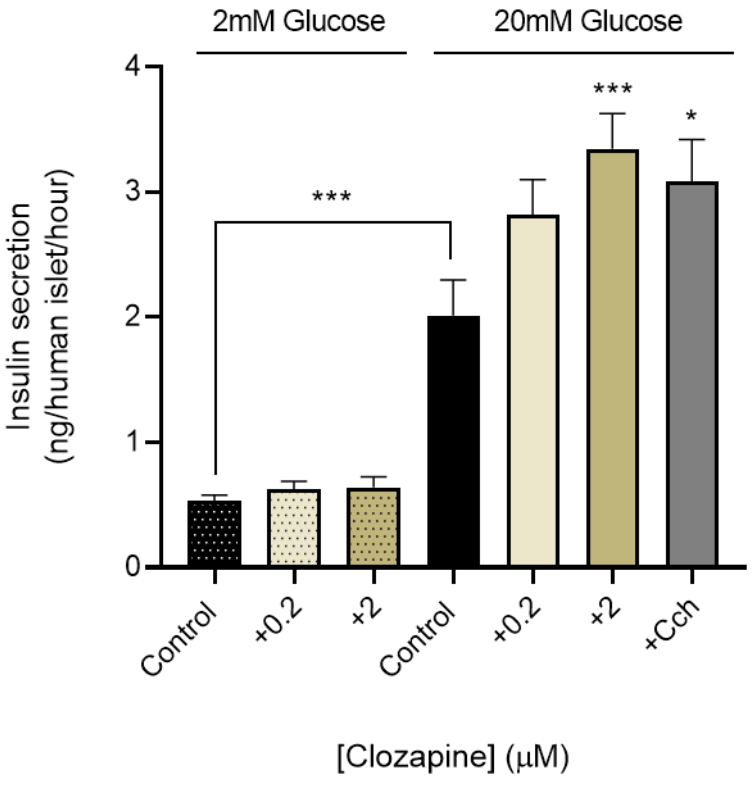
2mM Glucose
20mM Glucose
Insulin secretion
(ng/human islet/hour)
4
3
2
1
0
***
***
*
Control
+0.2
+2
Control
+0.2
+2
+Cch
[Clozapine] (μM)

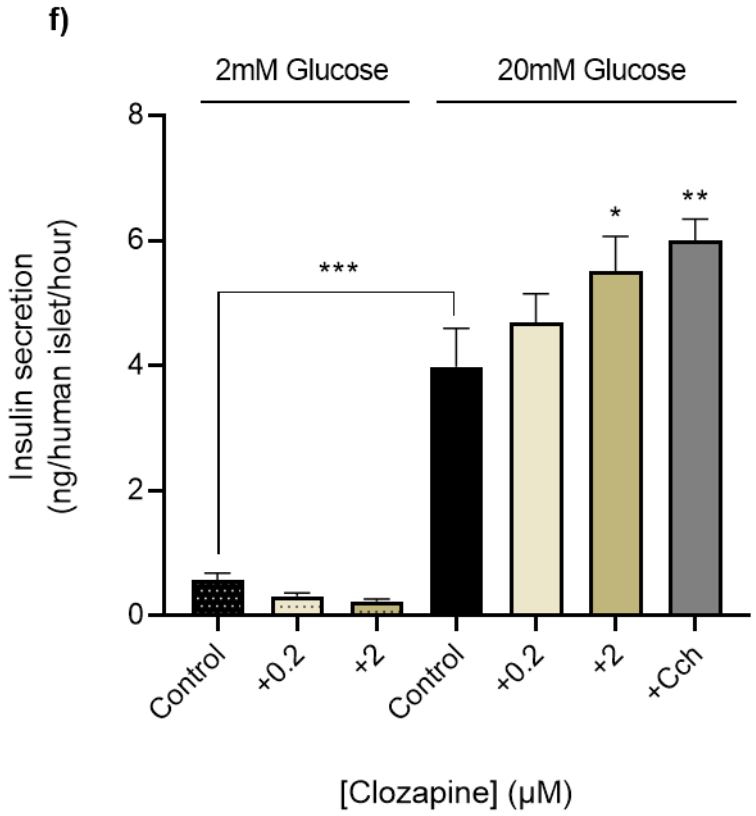

Figure 6.9. Effects of clozapine on insulin secretion from MIN6 cells (a, b), mouse islets (c, d) and human islets (e, f). In static secretion experiments, MIN6 cells or islets were incubated without or with clozapine for 30min (MIN6 cells), 1h (islets) (acute) or 48h (chronic). All data shown are mean + SEM, n=8 observations representative of 2-4 experiments. *p<0.05; **p<0.1; ***p<0.001 relative to the control samples at 20 (islets) or 25mM glucose (MIN6 cells). One-way ANOVA, Dunnett's multiple comparisons test.

6.3.2.4. Effects of clozapine on beta cell proliferation

The ability of clozapine to increase insulin secretion after a 48h incubation period could be due to direct effects to increase insulin secretion and/or secondary to increased numbers of beta cells. To investigate the effects of clozapine on beta cell proliferation, MIN6 cells were labelled with BrdU to quantify DNA replication using a BrdU ELISA kit following a 48h incubation with clozapine. In contrast to the data obtained with aripiprazole (Figure 6.4), low and therapeutic concentrations of clozapine had no effect on BrdU incorporation into the DNA of dividing MIN6 cells (Figure 6.10), meaning that they do not promote proliferation of MIN6 beta cells. 10% FBS, that was used as a positive control, significantly stimulated division of MIN6 cells.

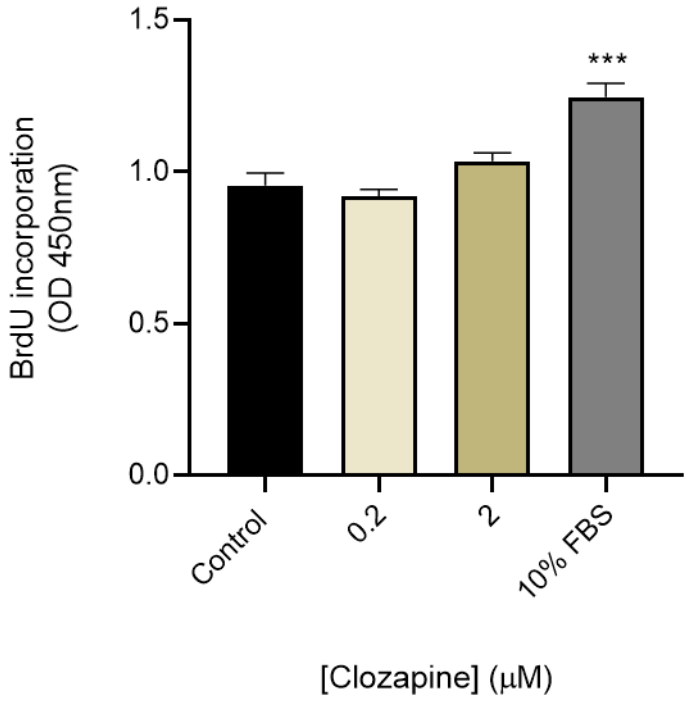

Figure 6.10. Effects of clozapine on MIN6 cell proliferation. MIN6 cells were treated with clozapine at 0.2-2μM for 48h, and BrdU incorporation into the DNA of proliferating cells was quantified using a BrdU ELISA. Data are mean + SEM, n=8 observations representative of 4

experiments. ***p<0.001 relative to the control samples, One-way ANOVA, Dunnett's multiple comparisons test.

6.3.2.5. Effects of clozapine on beta cell apoptosis

Decreased beta cell mass is central to the progression of diabetes (Butler et al., 2003), hence the effects of clozapine on apoptosis were determined by quantifying caspase3/7 activities that are elevated during apoptosis. Following a 48h culture without or with clozapine (0.2-2µM), caspase3/7 activities were measured in MIN6 cells or islets. Apoptosis was induced using a mix of proinflammatory cytokines or palmitate that were added for the final 24h of the experiments. As expected, both cytokines and palmitate significantly elevated caspase3/7 activities when compared to non-treated controls. 48h exposure to clozapine did not affect basal apoptosis of MIN6 cells and islet cells, whereas clozapine had a protective effect against apoptosis of MIN6 cells and islets in the presence of cytokines and palmitate (Figure 6.11). In contrast to the aripiprazole data, clozapine did not promote MIN6 cell proliferation, and the lowest concentration of clozapine was effective in protecting MIN6 cells against cytokine-induced apoptosis. Although clozapine at 2µM was the most effective in decreasing apoptosis in the experiments using mouse and human islets, it did not reduce MIN6 cell apoptosis rates in the presence of cytokines.

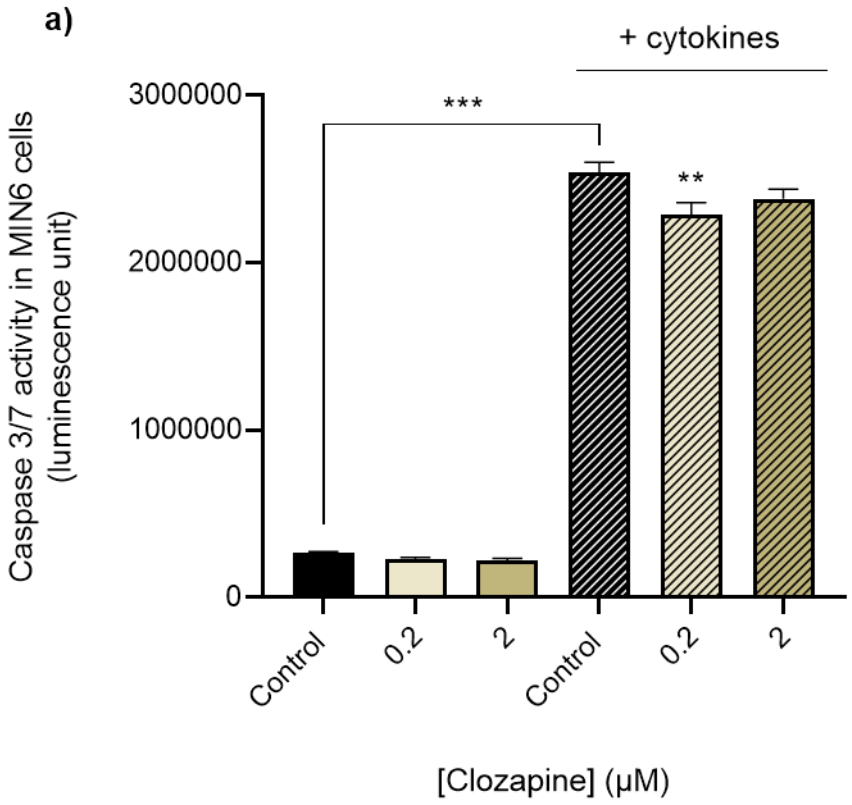
a)
+ cytokines
Caspase 3/7 activity in MIN6 cells
(luminescence unit)
3000000
2000000
1000000
0
***
**
Control
0.2
2
Control
0.2
2
[Clozapine] (µM)

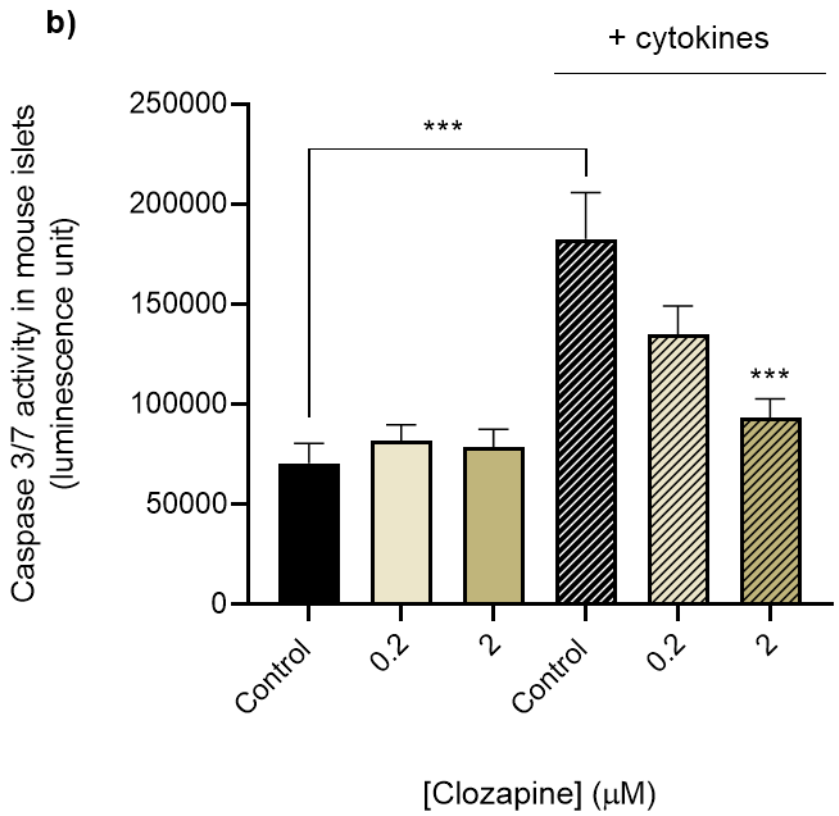
b)
+ cytokines
Caspase 3/7 activity in mouse islets
(luminescence unit)
250000
200000
150000
100000
50000
0
***
***
Control
0.2
2
Control
0.2
2
[Clozapine] (µM)

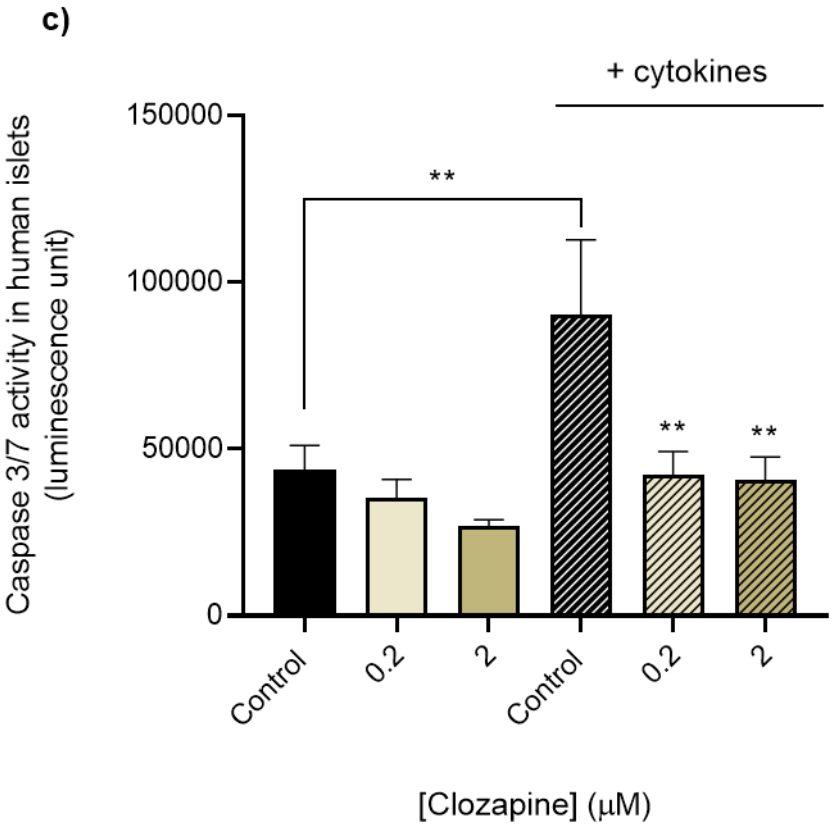
c)
+ cytokines
Caspase 3/7 activity in human islets (luminescence unit)
150000
100000
50000
0
**
**
**
Control
0.2
2
Control
0.2
2
[Clozapine] (µM)

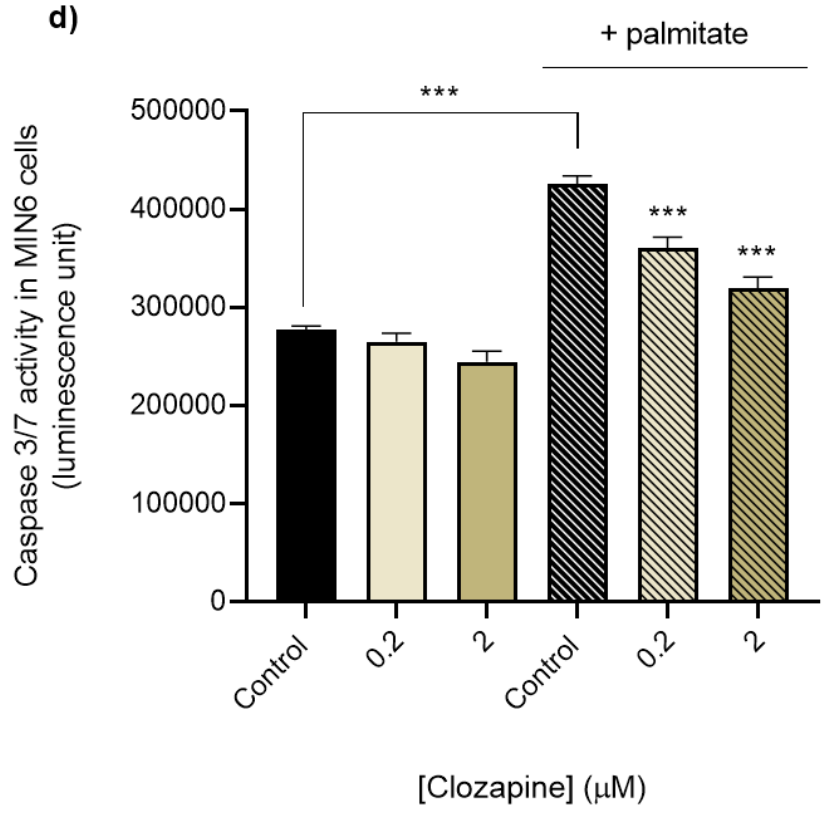
d)
+ palmitate
Caspase 3/7 activity in MIN6 cells (luminescence unit)
500000
400000
300000
200000
100000
0
***
***
***
Control
0.2
2
Control
0.2
2
[Clozapine] (µM)

e)

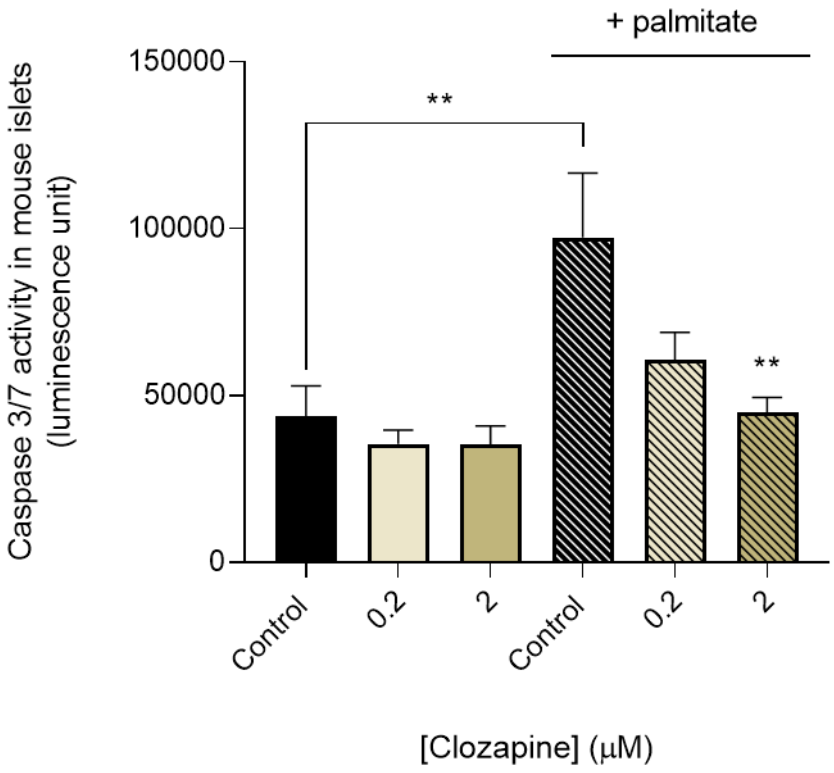
+ palmitate
150000
100000
50000
0
**
**
Caspase 3/7 activity in mouse islets (luminescence unit)
Control
0.2
2
Control
0.2
2
[Clozapine] (μM)

f)

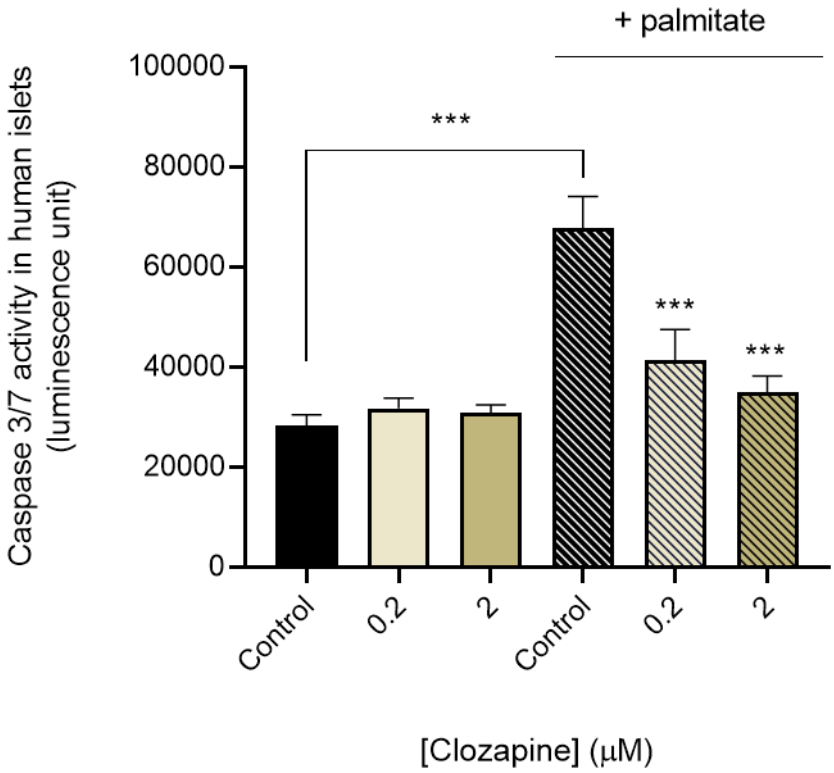
+ palmitate
100000
80000
60000
40000
20000
0
***
***
***
Caspase 3/7 activity in human islets (luminescence unit)
Control
0.2
2
Control
0.2
2
[Clozapine] (μM)

Figure 6.11. Effects of clozapine on cytokine- and palmitate-induced apoptosis of MIN6 cells (a, d), mouse islets (b, e) and human islets (c, f). MIN6 cells or islets were cultured in the absence or presence of clozapine (0.2-2μM) for 48h. Proinflammatory cytokines or palmitate were added 24h prior to quantification of luminescence. Data are expressed as mean + SEM; n=8 observations representative of 2-3 experiments. *p<0.05; **p<0.01; ***p<0.001 versus appropriate control (black striped); One-way ANOVA, Dunnett's multiple comparisons test.

Cytokine-induced apoptosis was also investigated by flow cytometry. This method is more sensitive than the Caspase-Glo assays because it allows for the measurement of apoptosis in single cells. Figure 6.12 shows reduced staining with annexin V of MIN6 cells that had been treated with 0.2 and 2µM clozapine when compared with controls, meaning that clozapine, in the similar way to aripiprazole, had a protective effect against apoptosis in the presence of cytokines.

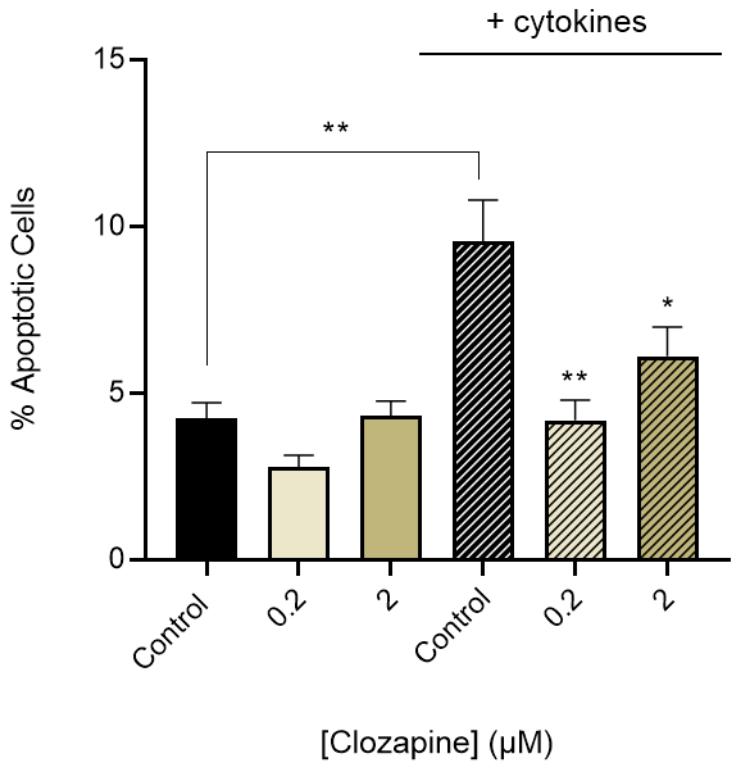

Figure 6.12. Effects of clozapine on apoptosis of MIN6 cells assessed by flow cytometry analysis of annexin V staining. Data are mean + SEM, n=3 separate experiments, *p<0.05; **p<0.01 relative to the control samples (black striped), One-way ANOVA, Dunnett's multiple comparisons test.

6.4. Discussion

The prevalence of diabetes is 3-fold higher in people with severe mental illness than the general population, and it exceeds 10% among schizophrenics treated with antipsychotics (Holt and Peveler, 2009; Holt, 2019). This is of great importance because schizophrenia patients with co-existing diabetes are at an increased risk of excess mortality compared to people with diabetes without SCZ (Chan et al., 2021). Several explanations for this epidemiologic link have been proposed, including environmental factors, shared genetic aetiology, and/or the use of antipsychotic medication (Lin and Shuldiner, 2010; Suvisaari et al., 2016). Therefore, determining the effects of individual AAPs on beta cells is of great importance. Novel data on the direct effects of commonly prescribed AAPs, aripiprazole and clozapine, on mouse and human beta cell function were presented in this chapter. Both aripiprazole and clozapine at low and therapeutic concentrations were well tolerated by beta cells and islets, potentiated glucose stimulated insulin secretion, and decreased apoptosis rates, and it was also demonstrated that aripiprazole increased proliferation of beta cells.

6.4.1. Aripiprazole and clozapine increase ATP generation and viability of MIN6 beta cells and islets

Plasma concentrations of the commonly used AAPs, aripiprazole and clozapine, are 0.24-1.12µM and 0.61-2.66µM, respectively (Grunder et al., 2008; Keshavarzi et al., 2020; Kirschbaum et al., 2008; Sparshatt et al., 2010). However, in several *in vitro* studies, aripiprazole has been used at concentrations as high as 100µM (Badran et al., 2020; Cikankova et al., 2019; Forno et al., 2020), whereas clozapine has been used up to 75µM (Contreras-Shannon et al., 2013; Lundberg et al., 2020), and many of these studies have concluded that these AAPs negatively alter

mitochondrial function and cell viability (Cikankova et al., 2019; Contreras-Shannon et al., 2013). However, when aripiprazole and clozapine were used at low or therapeutic concentrations, they protected neurons from glutamate and ketamine toxicity, respectively (Koprivica et al., 2011; Lundberg et al., 2020). As shown in this chapter, aripiprazole and clozapine at concentrations of 10µM and 20µM, respectively, significantly decreased viability of beta cells. This indicates that high concentrations that exceed the therapeutic range should not be used to assess the effects of these drugs on cell function, which is also true for SSRIs described in chapter 4. In addition to assessment of viability by Trypan blue uptake, ATP generation is a good marker of cell viability, and it was increased by therapeutic concentrations of aripiprazole and clozapine in MIN6 cells and islets. Increased ATP luminescence could be indicative of increased proliferation of beta cells during the 48h incubation period, and hence increased cell numbers. However, since clozapine had no effect on proliferation of MIN6 cells, elevations in ATP levels more likely suggest that the drug was increasing metabolic activity of the cells. ATP is an indicator of mitochondrial function, and therefore, it would be interesting to investigate the direct effects of therapeutically relevant concentrations of AAPs on mitochondria and metabolism of insulin-responsive cells in future studies.

6.4.2. Aripiprazole and clozapine potentiate glucose-stimulated insulin secretion from MIN6 beta cells and islets

By enhancing glucose stimulated insulin secretion, aripiprazole and clozapine could be beneficial in ameliorating diabetic symptoms in SCZ patients. Data presented in this chapter demonstrated that aripiprazole and clozapine at low, therapeutically relevant concentrations significantly potentiated glucose stimulated insulin secretion from mouse and human beta cells, and that they were the most effective in stimulating insulin secretion at concentrations at the higher end of the plasma concentration range. Furthermore, AAPs did not induce insulin secretion at low glucose concentrations, suggesting that they do not favour the occurrence of hypoglycaemia in the fasting state, but only increase insulin secretion at high glucose levels when it is required. In addition to these findings, a recent study has shown that clozapine at 1μM induce insulin secretion from human islets downstream of D2/D3 receptors blockade (Aslanoglou et al., 2021). Other two studies have demonstrated a role for D2 and D3 receptors in insulin secretion from rodent beta cells (Farino et al., 2020; Rubi et al., 2005), and it is shown in this thesis that mouse and human islets express D2 receptors. However, the levels of receptor expression are very low, and further studies are required to determine whether aripiprazole and clozapine exert their favourable effects on insulin secretion from beta cells solely downstream of D2 receptor blockade.

6.4.3. Aripiprazole and clozapine promote beta cell mass expansion

Identifying agents that maintain or expand beta cell mass by increasing proliferation and/or decreasing apoptosis is desired for optimised therapy of hyperglycaemia. Results presented in this chapter demonstrate that both aripiprazole and clozapine had protective effects against apoptosis in the presence of proinflammatory cytokines and palmitate, and that aripiprazole increased proliferative rates of MIN6 cells. In addition to these data, it has been shown that a D2 receptor antagonist, domperidone, promotes mouse and human beta cell mass by enhancing proliferation and decreasing apoptosis (Sakano et al., 2016). This is consistent with the ATP and BrdU data presented in this chapter and suggests that dopamine may inhibit proliferation and promote apoptosis, and that inhibition of dopamine signalling with AAPs could increase beta cell mass. Nevertheless, clozapine had no significant effect on BrdU incorporation into MIN6 cells. What is more, as shown in chapter 3, D2 receptor mRNA expression levels were low in islets and the exact molecular mechanism of action of aripiprazole and clozapine on beta cells is not fully understood. Therefore, more experiments are required to unravel the role of AAPs and the D2 receptor in the endocrine pancreas.

Chapter 7. Culture of mouse and human islet-derived pseudoislets on glass surfaces to study beta cell proliferation and macrophage infiltration

7.1. Introduction

The three-dimensional structure of islets supports maintenance of beta cell viability and function of through cell-cell and cell-matrix interactions (Arous and Wehrle-Haller 2017; Briant et al., 2018). In this respect islets are superior to cell lines derived from pancreatic endocrine tumours, such as INS-1 and MIN6 cell lines, but imaging of islets is challenging due to their thickness and non-adherence to glass coverslips. Generation of adherent reformed primary islets, referred to as pseudoislets, is a recently developed platform that allows high resolution imaging of primary islet cells (Phelps et al., 2017). The pseudoislets can be cultured on glass and adhere to a coating, they can be easily exposed to different treatment media, fixed, stained, and analysed using high-resolution imaging. In addition to their advantage in high resolution microscopy, islet-derived pseudoislets can be used in invasion and migration experiments because they are adherent and more suitable for macrophage infiltration studies. Therefore, this novel technique was used to investigate the effects of SSRIs and AAPs on beta cell proliferation and on macrophage invasion into islets.

7.2. Methods

7.2.1. Preparation of pseudoislets

Mouse and human islets were dispersed into single cells and seeded onto laminin-coated glass coverslips as described in Section 2.3.2. Islet cells required 3 days to adhere to the laminin coating and aggregate to form pseudoislets. The coverslips with pseudoislets were cultured for 2 weeks in neurobasal media

supplemented with B-27 (1x), 1% (v/v) penicillin and streptomycin, 1M Hepes buffer and 5% (v/v) FBS to allow formation of mature pseudoislets.

7.2.2. Immunofluorescence

Pseudoislets were stained using immunofluorescence as described in Section 2.5.3, using antibodies directed against insulin, glucagon, somatostatin, Ki67 and CD80, a macrophage marker (Table 2.13).

7.2.3. Insulin secretion from mouse and human pseudoislets

Insulin secretion from mouse and human pseudoislets was measured by static insulin secretion experiments. Pseudoislets were pre-incubated for 1h in a physiological salt solution (Gey & Gey buffer) supplemented with 2mM glucose, as described in Section 2.9.1.2. Pseudoislets were counted and groups of 6-14 pseudoislets were incubated with buffer supplemented with either 2mM or 20mM glucose in the absence or presence of 1µM aripiprazole or 2µM clozapine for 1h (100µl buffer per pseudoislet). Carbachol (500µM) was used as a positive control. The supernatants were collected and stored at -20°C prior to the insulin radioimmunoassay (Section 2.9.3).

7.2.4. Beta cell proliferation: Ki67 assay

Fully formed pseudoislets were treated with DMEM supplemented with 5.5mM glucose, 1% (v/v) penicillin and streptomycin, and 1% (v/v) L-glutamine and 10% (v/v) FBS and in the absence or presence of clozapine or aripiprazole for 30h. Exendin-4 (20nM), a GLP-1 receptor agonist, was used as a positive control as there is strong evidence that it increases beta cell proliferation (Bowe et al., 2013; Fusco et al., 2017; Wang et al., 2015). Thereafter, pseudoislets were fixed and immunostained for insulin and a proliferation marker, Ki67, as described in Section 2.5.3.

7.2.5. Islet destruction: Macrophage invasion assay

The effects of fluoxetine, aripiprazole and clozapine on cytokine-induced destruction of mouse and human pseudoislets in the presence of monocyte/macrophage-like cells Raw 264.7 (Taciak et al., 2018) were studied using an invasion assay. Pseudoislets were incubated in DMEM supplemented with 5.5mM glucose without or with a drug of interest for 24h. Thereafter, Raw 264.7 cells were activated by exposure to 100mg/ml lipopolysaccharide (LPS) for 1h. Activated RAW 264.7 cells were trypsinised, seeded into inserts at a density of 100,000 cells/insert then placed over coverslips containing pseudoislets. A mix of proinflammatory cytokines was added to the wells containing coverslips with pseudoislets and inserts for the final 24h. Light microscopy was performed to assess the integrity of the pseudoislets after 24h incubation in the presence of cytokines.

7.2.6. Islet infiltration: Migration assays

To investigate whether fluoxetine, aripiprazole and clozapine were able to modify migration of macrophages towards pseudoislets in the lower chamber in the presence of cytokines, migration assays were performed. Briefly, mouse or human pseudoislets were incubated for 24h in 5.5mM DMEM without or with a drug of interest. Thereafter, Raw 264.7 cells were seeded into inserts at a density of 100,000 cells/insert and placed over coverslips containing pseudoislets, and proinflammatory cytokines were added to the wells with inserts for the final 24h. Migration was assessed by two methods: CytoSelect™ Cell Migration and EZCell™ Cell Migration/Chemotaxis assays were performed as described in Sections 2.10.1 and 2.10.2, respectively.

7.3. Results

7.3.1. Formation and characterisation of pseudoislets

The expression of islet hormones in mouse pseudoislets was determined by immunofluorescence. Figure 7.1 shows that two weeks after dissociation and reformation, mature mouse and human pseudoislets contained alpha, beta and delta cells that stained for glucagon, insulin and somatostatin, respectively. Calculation of cell types in pseudoislets after 14-16 days revealed that they resembled the cell composition of primary islets. Thus, mouse islets are composed of 65–80% of beta cells mainly found in their inner core and 10–20% of peripheral alpha cells, which was recapitulated in the mouse pseudoislets (Figure 7.1a and 7.1b). Importantly, the reformed human pseudoislets reflected the cell proportions of primary human islets, which contain a higher percentage of alpha cells, 30-50%, and a lower percentage of beta cells than rodents, 50-60%

(Figure 7.1c and 7.1d). In both species delta cells constitute approximately 5% of the total islet cell number (Figure 7.1b and Figure 7.1d) (Campbell and Newgard, 2021).

a)

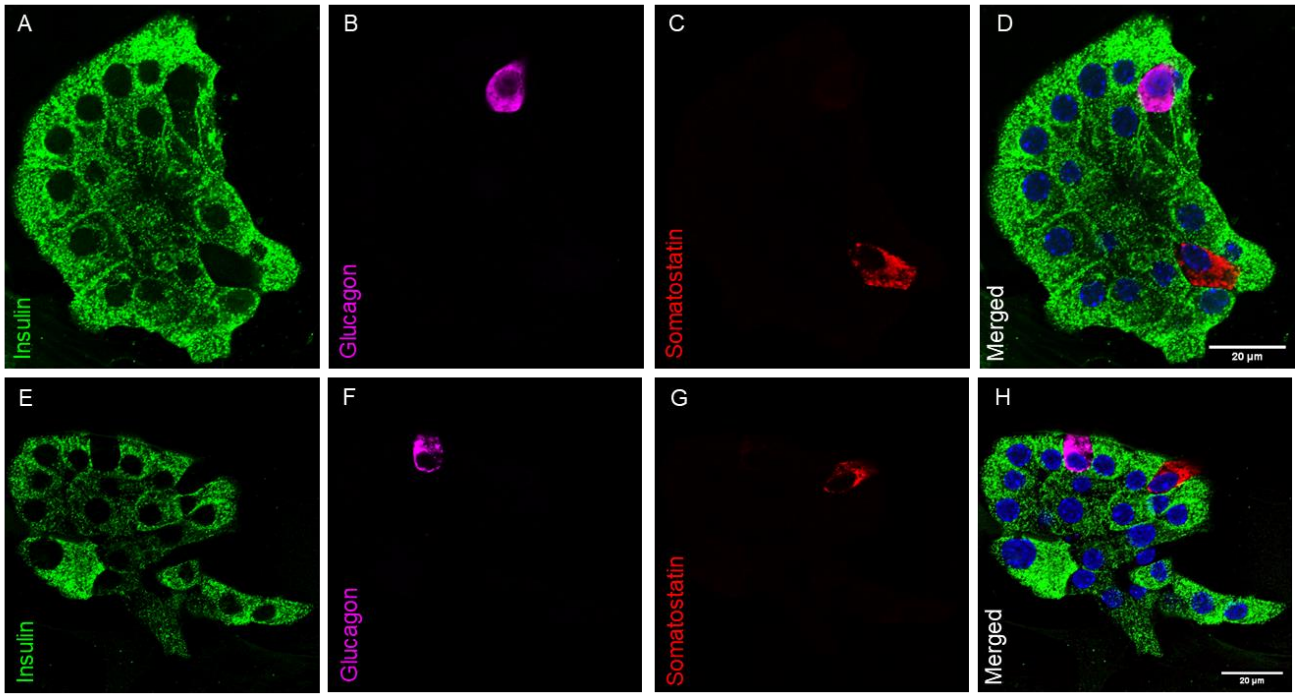

b)

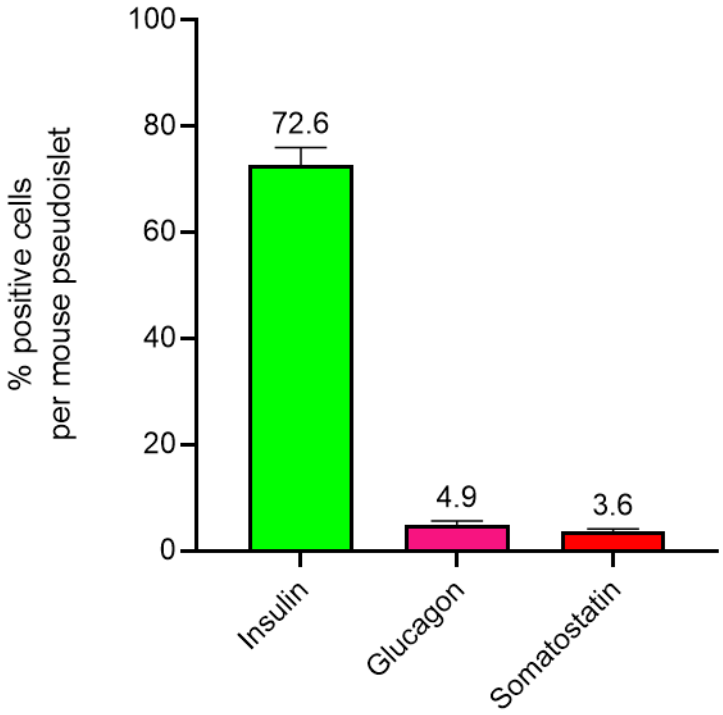
100
80
60
40
20
0
% positive cells
per mouse pseudoislet
72.6
4.9
3.6
Insulin
Glucagon
Somatostatin

c)

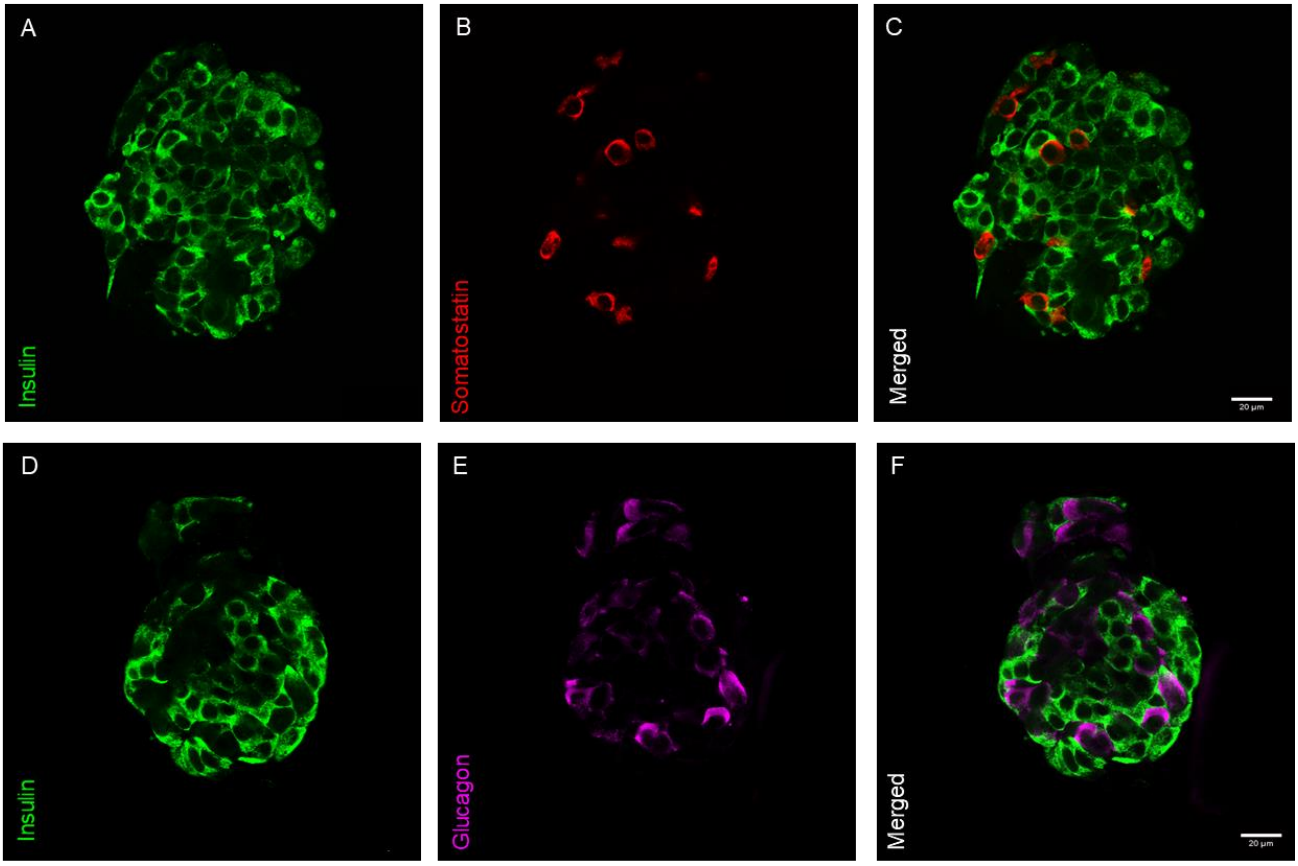
A
Insulin
B
Somatostatin
C
Merged
D
Insulin
E
Glucagon
F
Merged

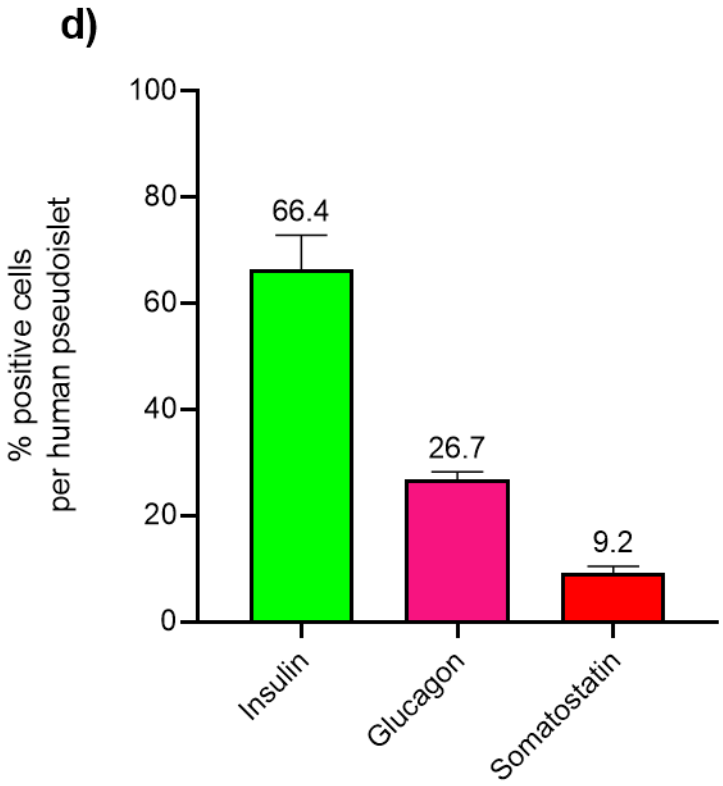

Figure 7.1. Immunofluorescence detection of islet hormones in mature mouse (a) and human (c) pseudoislets formed from single cells after 14 days of seeding. The pseudoislets were immunoprobed with antibodies directed against insulin (green), glucagon (purple) and somatostatin (red). DAPI nuclear staining is shown in blue (a; D, H). Scale bar is 20µm. Percentage calculation of cell types in mature mouse (b) and human (d) pseudoislets was performed with ImageJ software.

7.3.2. Effects of aripiprazole and clozapine on insulin secretion

Insulin secretion was quantified in static incubation experiments using primary islets and pseudoislets generated from primary islets. Acute exposure of mouse and human pseudoislets to 20mM glucose resulted in significantly increased levels of secreted insulin when compared to 2mM glucose, although the magnitude of the secretory response was less from the pseudoislets (Figure 7.2). What is more, Figure 7.3 shows that exposure of mouse pseudoislets to 1µM aripiprazole and 2µM clozapine led to significantly increased insulin secretion at 20mM glucose, similar to the effects of these AAPs in primary islets. This suggests that the pseudoislets were functional and responded in the same way to aripiprazole and clozapine as isolated mouse islets in Figures 6.4 and 6.9. 500µM carbachol was used as a positive control to induce insulin secretion through activation of the M3 muscarinic receptor.

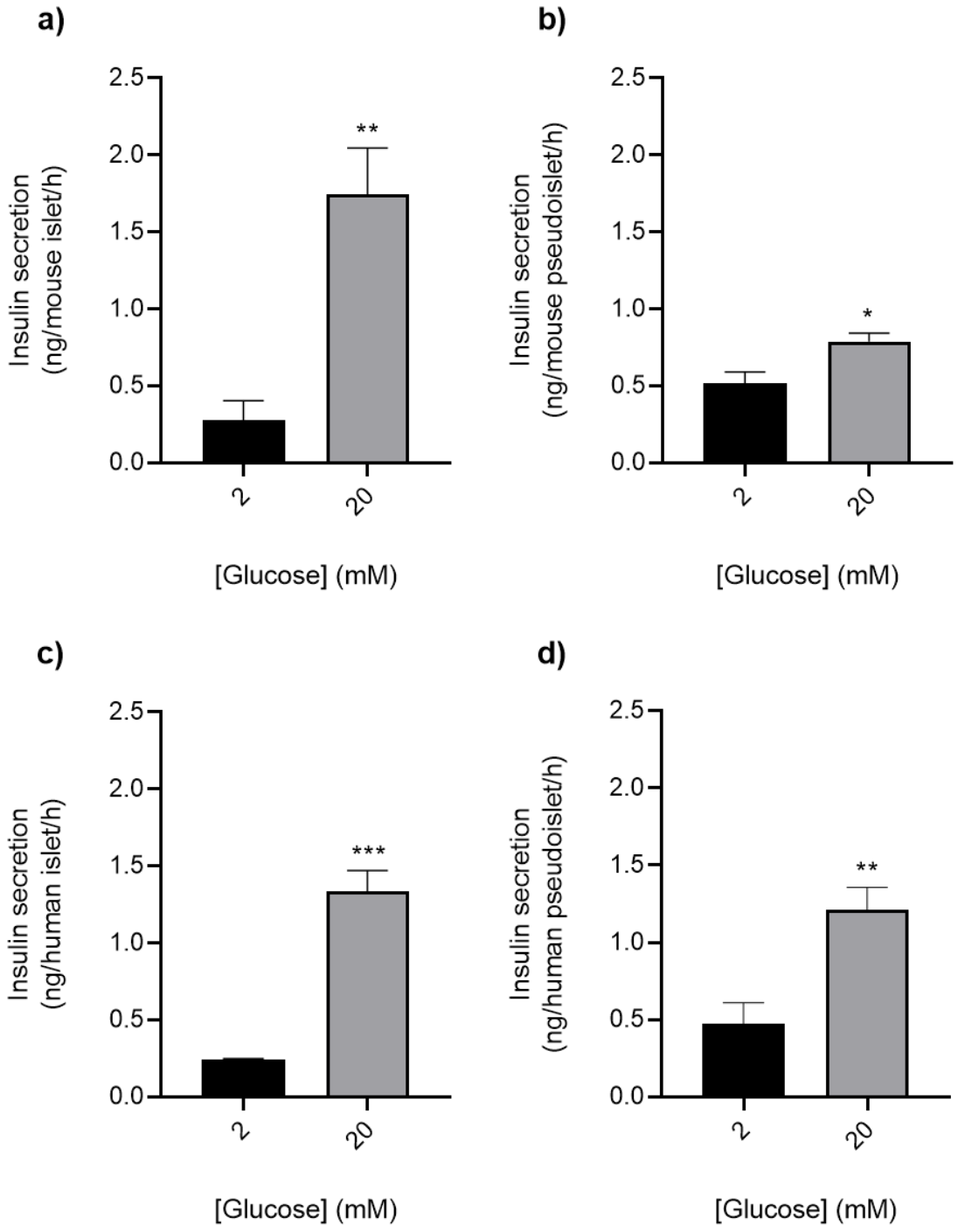

Figure 7.2. Insulin secretory response of primary islets (mouse – a, human – c) and pseudoislets (mouse – b, human – d) to 20mM glucose. In static incubation experiments, islets or pseudoislets were pre-incubated for 2h in the Gey and Gey buffer supplemented with 2mM glucose and then incubated for 1h in the presence of either 2mM or 20mM glucose. All data shown are mean + SEM, n=8 observations. *p<0.05; **p<0.01; ***p<0.001 relative to the control samples at 2mM glucose (black), unpaired Student t-test.

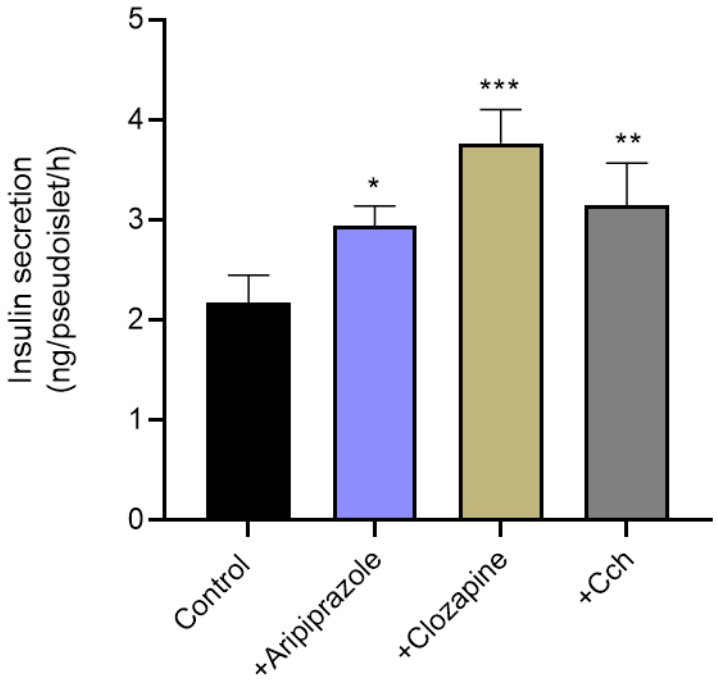

Figure 7.3. Effects of 1µM aripiprazole and 2µM clozapine on glucose-stimulated insulin secretion from mouse pseudoislets. In static secretion experiments, pseudoislets were preincubated in the 2mM glucose Gey and Gey buffer and then incubated at 20mM glucose without or with aripiprazole or clozapine for 1h. 500µM carbachol served as a positive control. All data shown are mean + SEM, n=8 observations. *p<0.05; **p<0.01; ***p<0.001 relative to the control samples at 20mM glucose (Control; black). One-way ANOVA, Dunnett's multiple comparisons test.

7.3.3. Effects of aripiprazole and clozapine on beta cell proliferation

Having demonstrated that aripiprazole and clozapine potentiated glucose-stimulated insulin secretion from mouse and human pseudoislets, the direct effects of these antipsychotic drugs on beta cell proliferation were investigated by immunofluorescence and confocal microscopy imaging. Mouse pseudoislets were exposed to 0.1-1μM aripiprazole and 0.2-2μM clozapine for 30h and fluorescent staining was performed *in situ* using antibodies against a proliferation marker, Ki67, and insulin. Similar to data obtained quantifying BrdU incorporation into MIN6 beta cells, presented in chapter 6, immunostaining revealed that 1μM aripiprazole significantly increased proliferative rates of pseudoislet cells, but 0.1μM aripiprazole was without effect (Figure 7.4). Although 2μM clozapine did not affect BrdU incorporation into the DNA of dividing MIN6 beta cells, it significantly potentiated proliferation of pseudoislet (Figure 7.4). As expected, Exendin-4, also increased pseudoislet proliferation in these experiments, and this effect was similar to the effect of 2μM clozapine.

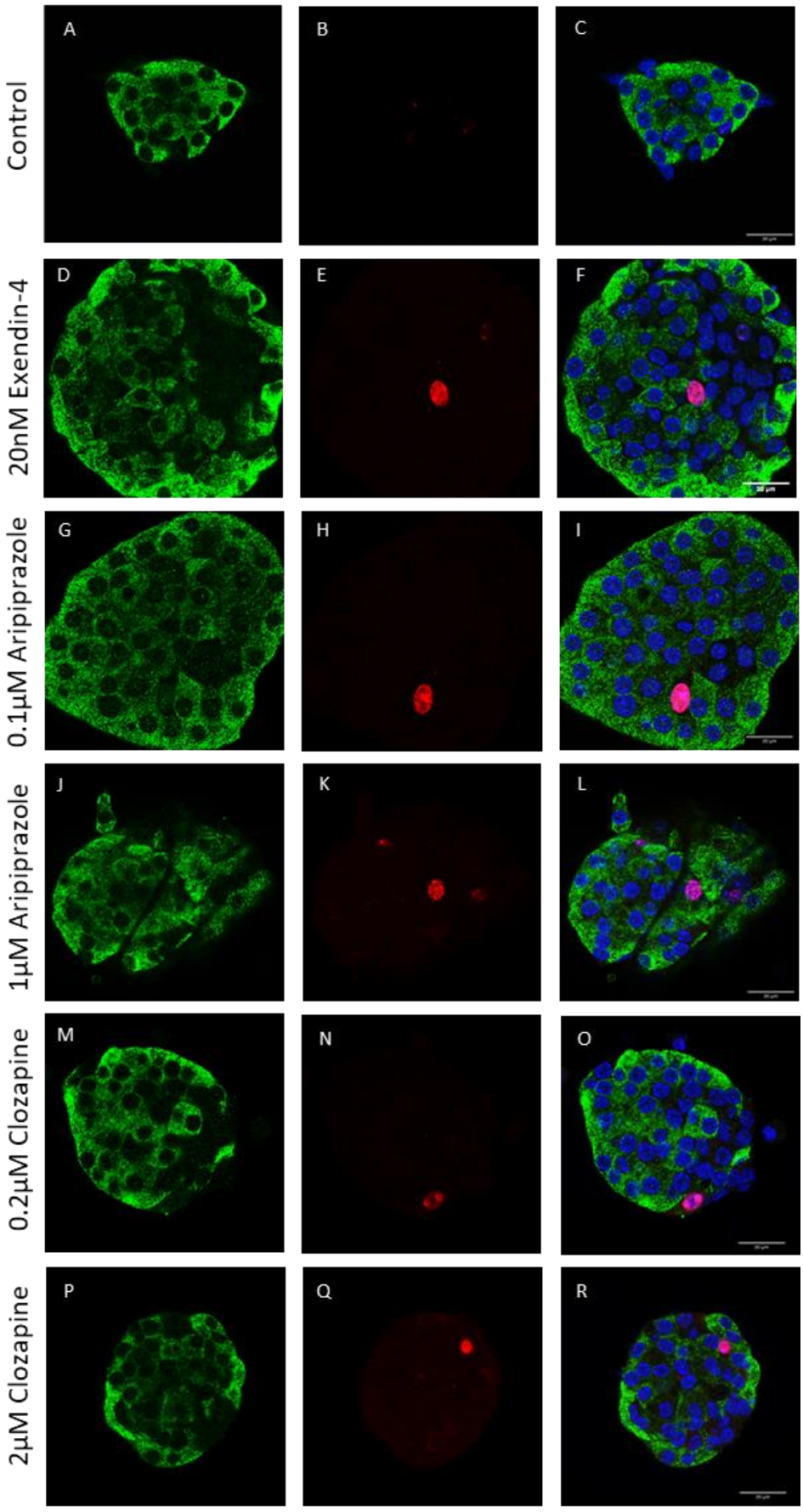
Control
20nM Exendin-4
0.1µM Aripiprazole
1µM Aripiprazole
0.2µM Clozapine
2µM Clozapine
A
B
C
D
E
F
G
H
I
J
K
L
M
N
O
P
Q
R

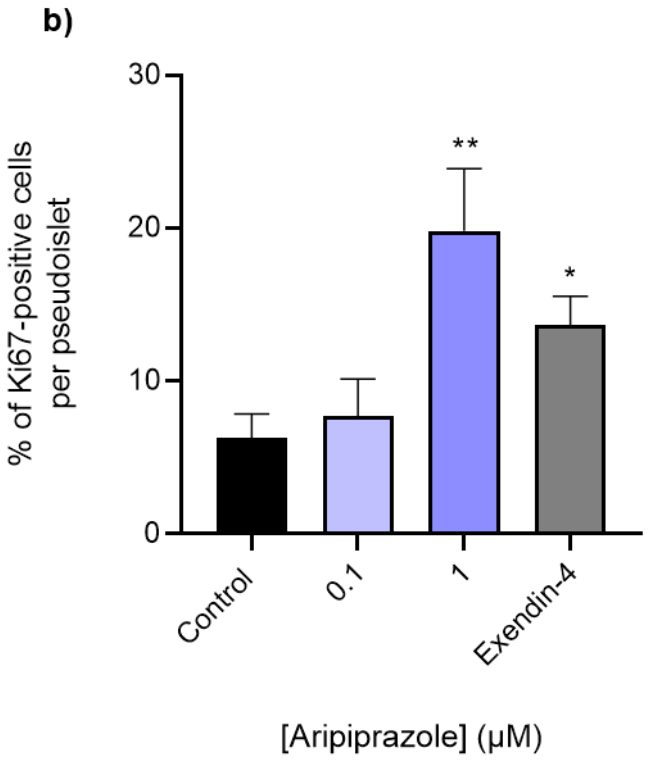
b)
30
20
10
0
% of Ki67-positive cells per pseudoislet
**
*
Control
0.1
1
Exendin-4
[Aripiprazole] (μM)

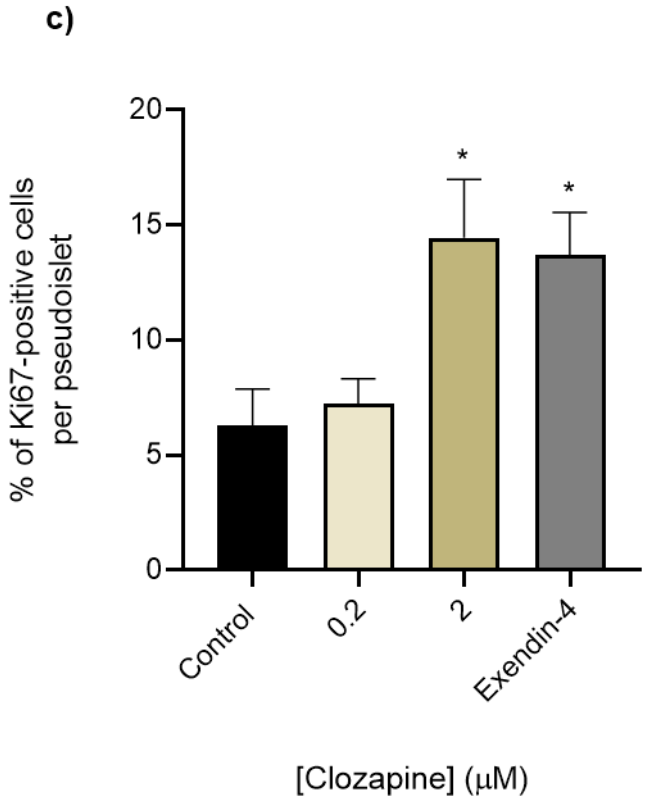
c)
20
15
10
5
0
% of Ki67-positive cells per pseudoislet
*
*
Control
0.2
2
Exendin-4
[Clozapine] (μM)

Figure 7.4. Effects of aripiprazole and clozapine on proliferation of mouse pseudoislets. The pseudoislets were exposed to 0.1-1μM aripiprazole or 0.2-2μM clozapine for 30h and immunoprobed with antibodies directed against insulin (green; A, D, G, J, M, P) and Ki67 (red; B, E, H, K, N, Q). DAPI nuclear staining is shown in blue in merged images (C, F, I, L, O, R) (a). Scale bar is 20μm. Percentage calculation of $Ki67^{+}$ cells within pseudoislets that had been treated with aripiprazole (b) and clozapine (c) was performed using ImageJ software. Numerical data are mean + SEM, n=5 observations from 2 separate experiments. *p<0.05; **p<0.01 relative to the control samples, One-way ANOVA, Dunnett's multiple comparisons test.

7.3.4. Effects of fluoxetine, aripiprazole and clozapine on cytokine-induced destruction of pseudoislets

One of the most prominent features of T1D and T2D is chronic inflammation, with the accompanying presence of cytokines (Randeria et al., 2019; Tsalamandris et al., 2019). Given that SSRIs, including fluoxetine, and AAPs, aripiprazole and clozapine, had protective effects against cytokine-induced apoptosis of mouse and human islets (chapters 4 and 6), the effects of these drugs on cytokine-mediated destruction of pseudoislets were assessed by light microscopy. Mouse and human pseudoislets were exposed to fluoxetine, aripiprazole or clozapine for 48h and the inserts with activated macrophage RAW 264.7 cells and proinflammatory cytokines were added for the final 24h of the experiment. Figure 7.5 shows that mouse (a) and human (b) pseudoislets that had been exposed to cytokines and fluoxetine, aripiprazole or clozapine (panels D-F) sustained a round shape when compared to cytokine-treated controls (panel C). More experiments are required to identify the cells surrounding the pseudoislets, but since islet cells are comingled with other non-islet cell types, including endothelial cells, resident immune cells, neurons, smooth muscle cells and proliferative fibroblasts, (Segerstolpe et al., 2016), it is most likely that they are fibroblast cell populations.

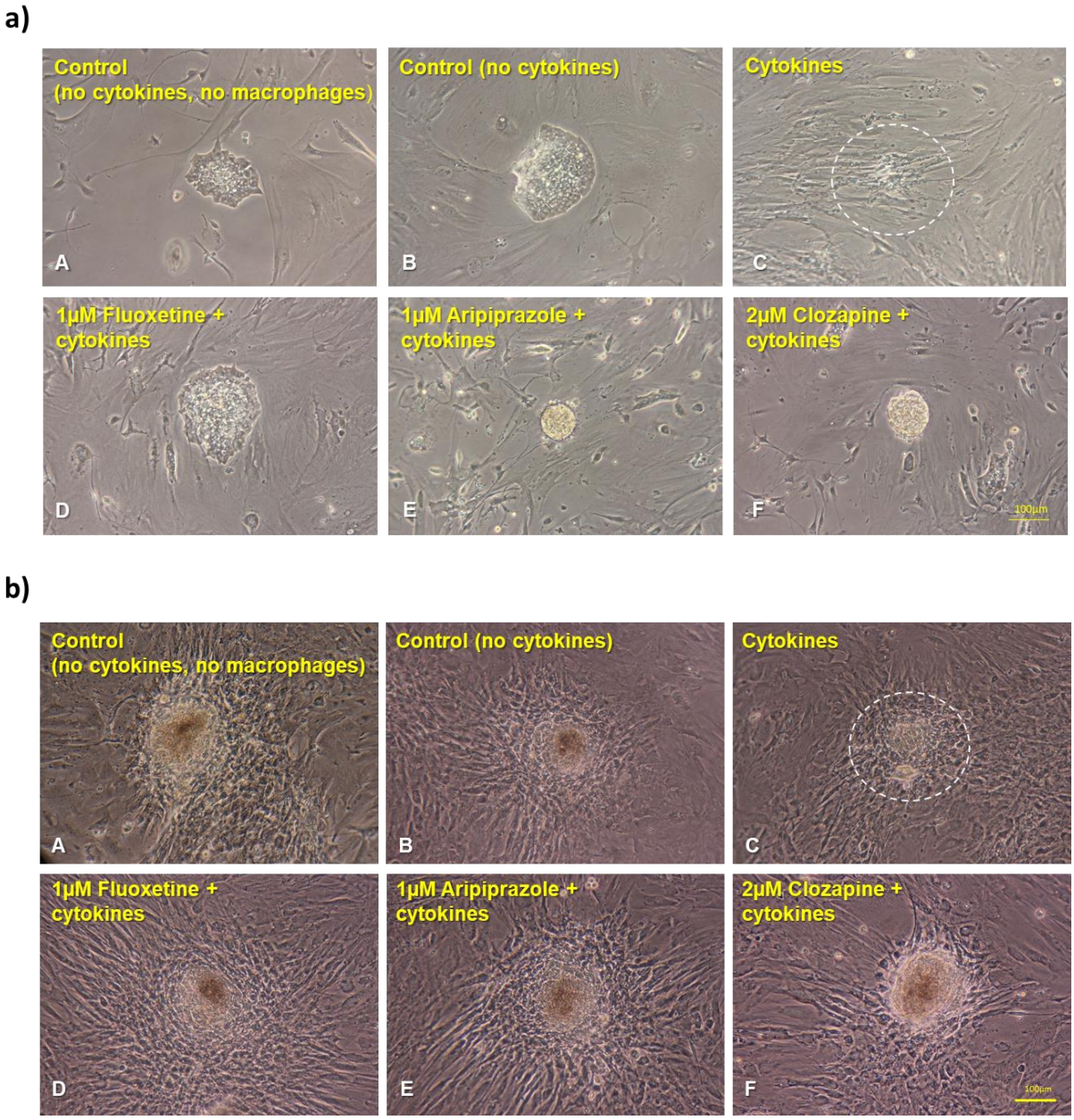

Figure 7.5. Effects of fluoxetine, aripiprazole and clozapine on cytokine-induced destruction of mouse (a) and human pseudoislets (b). The pseudoislets were exposed to 1µM fluoxetine, 1µM aripiprazole or 2µM clozapine for 48h. A mix of proinflammatory cytokines and macrophages were added 24h prior to examination by light microscopy. Destroyed pseudoislets are delimited by a white dotted circle (panels C). Scale bar is 100µm.

7.3.5. Effects of fluoxetine, aripiprazole and clozapine on macrophage infiltration

There is evidence that macrophages accumulate in the islets and that they display a proinflammatory phenotype during progression of T2D (Cucak et al., 2013; Zirpel and Roep, 2021). During development of diabetes islets are characterised by an increased release of inflammatory factors, such as IL-1β, IL-6 and macrophage inflammatory protein 1α, and it has been shown that these factors increase macrophage infiltration (Ehses et al., 2007; Böni-Schnetzler and Meier, 2019). Therefore, islet-derived inflammatory factors may act as a chemoattractant to macrophages and stimulate their migration. Having demonstrated that fluoxetine, aripiprazole and clozapine protected mouse and human pseudoislets against cytokine-induced destruction, the effects of these drugs on the migratory properties of Raw 264.7 macrophage cells were determined using immunofluorescence, as well as cell migration and cell migration/chemotaxis assays (Figure 7.6). CD80 is a costimulatory molecule used to mark activated macrophages, and fluorescent staining demonstrated that macrophages were present within pseudoislets. Panel A confirmed the presence of resident macrophages within untreated pseudoislets, but the CD80 staining was increased in pseudoislets that had been incubated with Raw 264.7 cells and cytokines (Figure 7.6a, b; panel C). The number of Raw 264.7 cells that infiltrated the pseudoislets was significantly higher in the presence of cytokines when compared to untreated controls that had not been exposed to cytokines nor the drugs. The number of islet-associated migratory macrophages in the presence of cytokines was significantly decreased where mouse (b) and human (d) pseudoislets had been incubated with 1µM fluoxetine, 1µM aripiprazole or 2µM clozapine for 48h, which indicates protective effects of these drugs against macrophage infiltration. Similar to data presented in Figure 7.5, the pseudoislets

that had been exposed to fluoxetine and AAPs (Figure 7.6 a, b; Panels D-F) had a preserved round shape in contrast to cytokine-treated controls (Panels C).

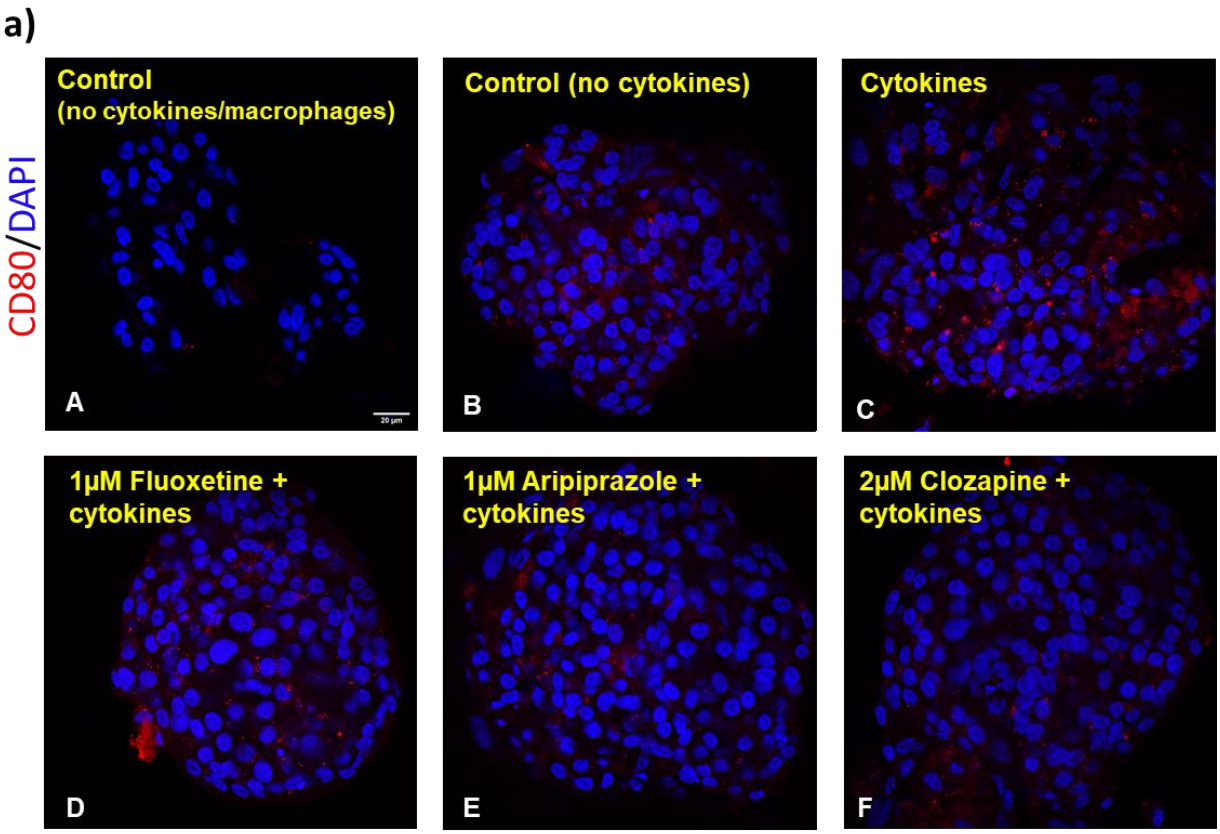

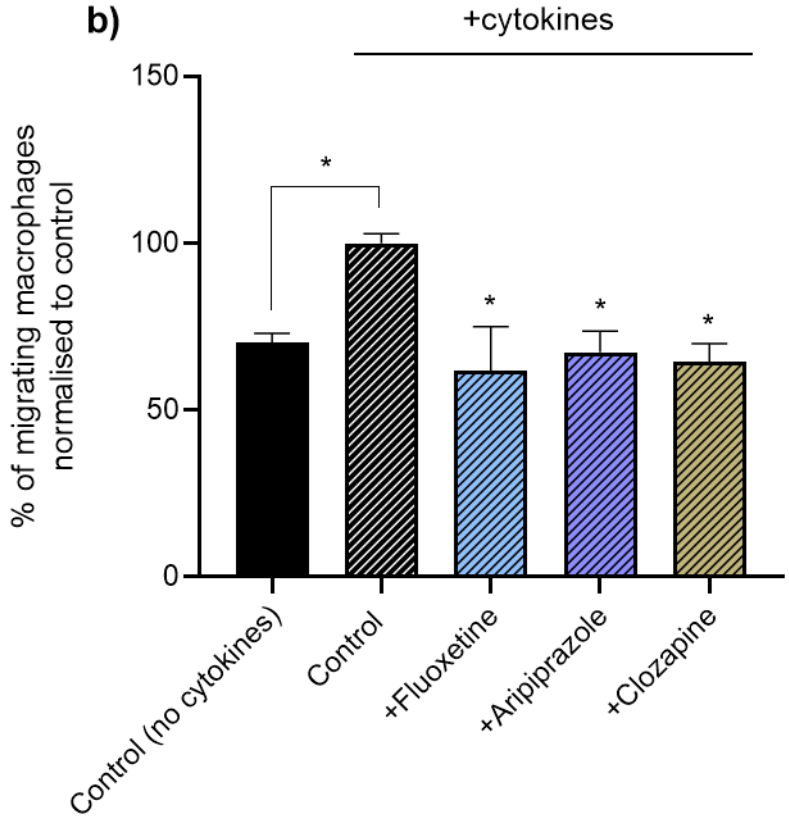
b)
+cytokines
% of migrating macrophages normalised to control
150
100
50
0
*
*
*
*
Control (no cytokines)
Control
+Fluoxetine
+Aripiprazole
+Clozapine

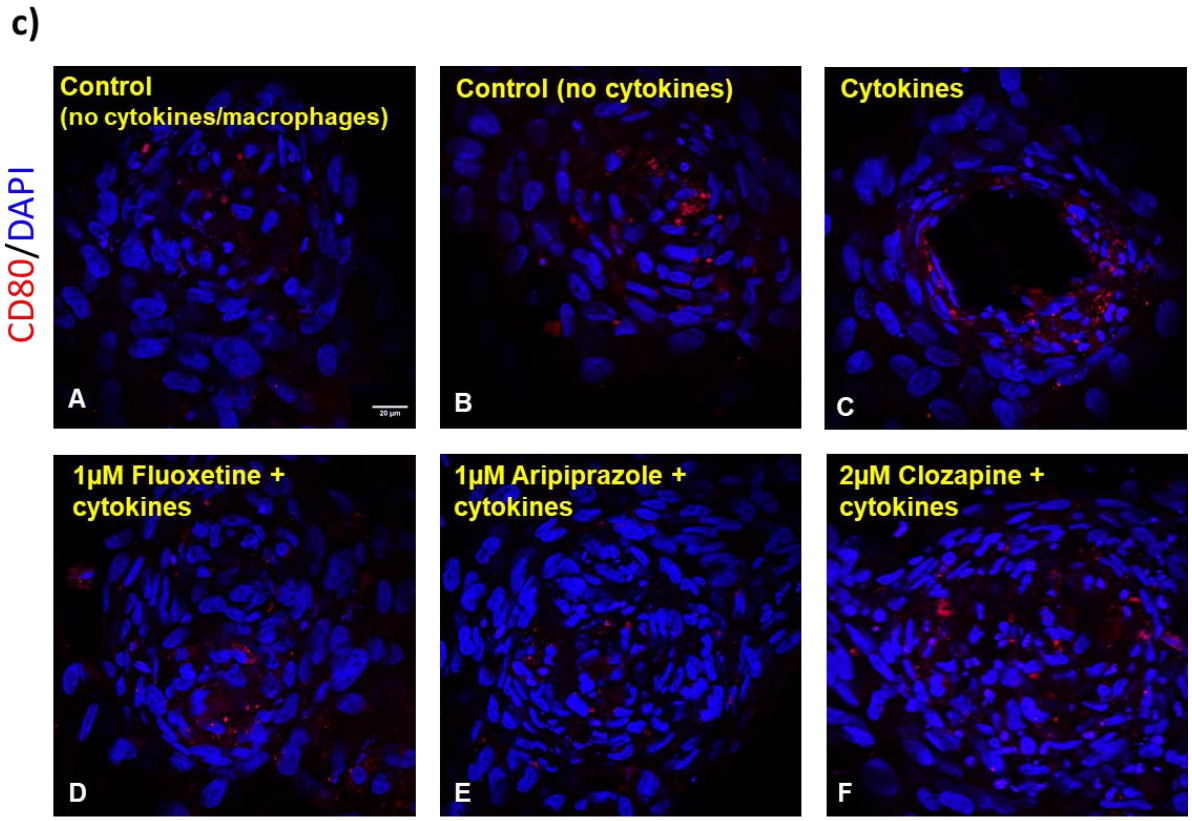
c)
CD80/DAPI
Control
(no cytokines/macrophages)
A
Control (no cytokines)
B
Cytokines
C
1μM Fluoxetine +
cytokines
D
1μM Aripiprazole +
cytokines
E
2μM Clozapine +
cytokines
F

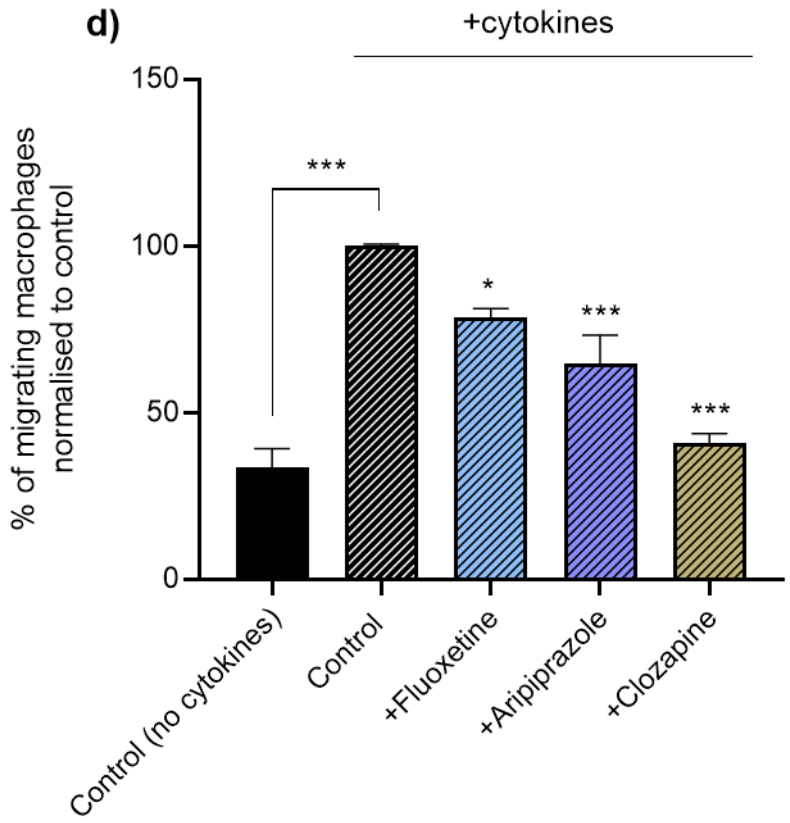

Figure 7.6. Effects of fluoxetine, aripiprazole and clozapine on pseudoislet infiltration by Raw 264.7 macrophage cells. The pseudoislets were incubated with 1µM fluoxetine, 1µM aripiprazole or 2µM clozapine for 48h. Cytokines and macrophages were added 24h prior to fluorescence measurement and imaging. The pseudoislets were immunoprobed with antibodies directed against CD80 (red) and DAPI was stained in blue. Scale bar is 20µm (a, c). Migratory properties of Raw 264.7 cells were assayed by Cell Biolabs' CytoSelect™ cell migration (b) and EZCellTM cell migration/chemotaxis (d) assays followed by quantification of fluorescence (a, c). Data are expressed as mean + SEM; n=3 observations. *p<0.05; **p<0.01; ***p<0.001 versus cytokine control (black; striped lines), One-way ANOVA, Dunnett's multiple comparisons test.

7.4. Discussion

Adherent pseudoislets, generated from dissociated mouse and human islets, were used to allow high resolution imaging since primary islets detach from the coverslip during attempted fixation, whereas free islet cells attach firmly to the coating and form functional pseudoislets. As shown by the immunohistochemical images of insulin, glucagon and somatostatin expression and quantification of glucose-stimulated insulin secretion, the pseudoislets resembled primary islets anatomically and functionally. Therefore, the pseudoislets were used to investigate the effects of fluoxetine, aripiprazole and clozapine on proliferation and macrophage infiltration.

7.4.1. Aripiprazole and clozapine promote proliferation of pseudoislets

The loss of functional beta cell mass is the central pathology for both type 1 and type 2 diabetes (Kahn 2001; Chen et al., 2017), and therefore one of the main goals in diabetes research is to find ways to enhance the mass of beta cells to prevent or delay the onset of diabetes (Kulkarni et al., 2012). Proliferation rates of primary islets are low and difficult to measure, hence the effects of AAPs on beta cell proliferation were measured using primary islet cells cultured on glass. In contrast to a previous report that developed a monolayer culture system (Phelps et al., 2017), our pseudoislets formed 3D structures and resembled primary islets more closely in terms of appearance and architecture. Although adherent pseudoislets enabled visualisation by confocal microscopy and quantification of Ki67 staining, identification of beta cells was not always possible in some central regions, which could be due to sample thickness, and hence poor antibody penetration. Therefore, in proliferation experiments, all $Ki67^+$ cells were counted to assess the effects of aripiprazole and clozapine proliferation of pseudoislet cells. Both AAPs increased the number of $Ki67^+$ cells when compared

to untreated pseudoislets, which is consistent with BrdU ELISAs presented in chapter 3, where aripiprazole increased proliferation rates of MIN6 cells. However, future studies should use alternative antibodies, such as BrdU, another marker for proliferation, or anti-Nkx6.1 antibody that stains the nuclei of beta cells and focus on the effect of those drugs on proliferation of individual islet cell-types.

7.4.2. Fluoxetine, aripiprazole and clozapine prevent cytokine-induced destruction and macrophage infiltration

Macrophages are an integral component of the islets from embryonic development (Morris, 2015), and both resident and recruited islet macrophages are significant regulators of islet inflammation (Ehses et al., 2007). Historically, islet macrophages have been studied as effectors in the autoimmune processes in T1D (Burkart and Kolb, 1996). Light microscopy was used to investigate the effects of fluoxetine, aripiprazole and clozapine on destruction of pseudoislets in the presence of macrophages and proinflammatory cytokines, and data presented in this chapter demonstrated that these drugs had protective effects against cytokine-induced destruction of pseudoislets. Data from invasion and migration assays indicate that macrophage migration and infiltration of pseudoislets were decreased in the presence of fluoxetine, aripiprazole and clozapine, supporting anti-inflammatory effects of these drugs. Fluoxetine has been shown to have anti-inflammatory and immunomodulatory effects in LPS-induced inflammation, and it also decreases levels of the proinflammatory cytokine TNF-α (Kostadinov et al., 2015). Previous studies have documented that aripiprazole limits inflammatory processes by enhancing anti-inflammatory signalling and significantly decreasing levels of proinflammatory cytokines, including IL-1β, TNF-α and IFN-γ, in people with schizophrenia (Sobiś et al., 2014).

In addition, clozapine has been shown to protect dopaminergic neurons from inflammation-induced damage (Hu et al., 2012). Therefore, there is evidence to support these drugs having anti-inflammatory properties and data presented in this chapter indicate that they can also protect against islet inflammation. Nevertheless, future studies should use human macrophage cell lines in addition to mouse macrophage cells, for example widely used TPH-1 cells, and further work is required to unravel the molecular mechanisms by which these drugs protect islets from cytokine-induced destruction and macrophage infiltration. Resident macrophages also play a critical role in beta cell formation during development, and they support beta cell replication in models of pancreas regeneration. Hence, it would be interesting to study islet-associated macrophages in more detail following treatment with fluoxetine, aripiprazole and clozapine.

Chapter 8. Final discussion and Future studies

Diabetes has attained the status of a global pandemic. According to the IDF Diabetes Atlas, over 460 million adults were living with diabetes in 2019, 537 million adults have diabetes in 2021 at the time of writing this thesis, and it is projected that by 2045, diabetes will affect more than 0.7 billion people worldwide (IDF Diabetes Atlas - 10th Edition). Approximately 90% of adults currently diagnosed with diabetes have T2D, which is often accompanied by chronic diseases, including mental health problems. The bidirectional relationship between T2D and mental illness is well documented, though the underlying mechanisms remain unclear (Andersohn et al., 2009). The incidence of psychiatric conditions is about 2-fold greater in patients with T2D than in the general population, and MDD and SCZ have been associated with a higher risk of diabetes, diabetes complications, and increased health care services (Gonzalez et al., 2013; Egede et al., 2002). This association between diabetes and mental health disorders could be exacerbated in the era of COVID-19, as more than half of COVID-19 patients develop psychiatric symptoms (Alessi et al., 2020; Talevi et al., 2020; Zhao et al., 2020). Psychiatric conditions are often treated with cognitive behavioural therapy or medications, including antidepressants and antipsychotics. However, the effects of these drugs on glucose regulation are unclear. The emergence of a pandemic highlights the importance of studying the effects of antidepressants and antipsychotic drugs in patients predisposed to, or with, T2D.

8.1. SSRIs and T2D

Most people with diabetes and psychiatric disorders require long-term antidepressant treatment and there has been an argument about whether the use of SSRIs could lead to glucose dysregulation and increased risk of T2D onset (Deuschle, 2013; Khoza et al., 2011). Although there is evidence in clinical studies that SSRIs improve glycaemia (Tharmaraja et a., 2019; Ye et al., 2011), several *in vitro* studies have reported that fluoxetine decreases insulin secretion, impairs calcium signalling, and promotes ER stress in beta cells (Chang et al., 2017; Elmorsy et al., 2017; De Long et al., 2014). However, in those studies, fluoxetine was used at concentrations exceeding 30µM, which is substantially higher than the plasma concentrations of any SSRI presented in this thesis: fluoxetine and sertraline (0.2-2.6µM) and paroxetine (0.06-0.18µM) (Bolo et al., 2000; Bosch et al., 2008; Lima et al., 2006; Tomita et al., 2014). Additionally, in most of these studies, effects of fluoxetine on beta cell function were determined using cultured beta cell lines. Although these are useful for preliminary functional analyses, they have some disadvantages as models for investigation of insulin secretion when compared to isolated islets. Data presented in this thesis show that 10µM fluoxetine and sertraline, as well as 1µM paroxetine, compromise integrity of MIN6 beta cell and islet cell membranes *in vitro*. What is more, when used at low and therapeutic concentrations, SSRIs exert favourable effects on MIN6 beta cells, and also on mouse and human islets in terms of viability, glucose-stimulated insulin secretion, cell proliferation, and survival.

8.1.1. SSRIs increase ATP generation and viability of beta cells

The assessment of viability allowed determination of the optimal concentration range for investigating the functional effects of fluoxetine, sertraline (0.1-2μM) and paroxetine (0.01-0.1μM) on beta cells. Concentrations that exceeded the plasma concentration range were cytotoxic to MIN6 cells and led to excessive Trypan blue uptake by MIN6 cells and islets. Consistent with this, the risk of T2D increases in depressed patients treated with high dosages of SSRIs (Andersohn et al., 2009), which may be related to direct deleterious effects on beta cells. It has been recently concluded that long-term antidepressant use increases the risk of T2D onset in a time- and dose-dependent manner (Miidera et al., 2020). In the studies described in this thesis, the plasma membrane integrity of MIN6 cells and islet cells was maintained in the presence of low therapeutic concentrations of fluoxetine, sertraline and paroxetine, and therefore concentrations of 0.01-1μM were subsequently used for the assessment of insulin secretion and other functional parameters. The increased ATP generation that is observed in MIN6 cells treated with SSRIs could be a consequence of increased beta cell proliferation. However, beta cells within primary islets have a limited proliferative capacity, so the increased ATP levels detected in the islets that have been exposed to fluoxetine, sertraline and paroxetine may reflect improved cell viability, and therefore increased metabolic activity. SSRIs could also directly alter mitochondrial function to increase ATP production, as the majority of cellular ATP is produced within mitochondria (Haythorne et al., 2019). Importantly for beta cells, ATP is essential for regulated insulin secretion (Koster et al., 2005). It has been reported that fluoxetine penetrates cells by crossing plasma membranes and can be found in the mitochondria (Mukherjee et al., 1998). There is evidence that it affects mitochondria by modulating the activity of respiratory chain components and Krebs cycle enzymes (de Oliveira, 2016). It is possible that SSRIs

generally improve cell viability to increase metabolic activity, but the mechanisms are not fully understood, and it remains unclear how fluoxetine affects mitochondrial function or dynamics.

8.1.2. SSRIs potentiate glucose-stimulated insulin secretion from beta cells

Drugs that enhance insulin secretion are able to lower hyperglycaemia, a major determinant of diabetes, and hence reduce the risk of long-term diabetic complications. As demonstrated in this thesis, fluoxetine, sertraline and paroxetine, at therapeutic concentrations, potentiate glucose-induced insulin secretion (GSIS) following both acute and chronic exposure, but they do not induce basal insulin secretion at 2mM glucose, which indicates that they do not favour the occurrence of hypoglycaemia in the fasting state. It is therefore possible that SSRIs enhance beta cell function to increase insulin secretion in people with diabetes who also suffer from MDD, leading to documented improvements in glycaemia (Gehlawat et al., 2013; Roopan and Larsen, 2016; Tharmaraja et al., 2019; Ye et al., 2011). This suggests that these drugs could be beneficial in the treatment of depression in individuals with diabetes. Nevertheless, the underlying mechanisms of how SSRIs enhance GSIS are not fully understood, but could be attributed to elevated levels of serotonin, which then exerts functional effects on the islets. There is evidence that serotonin is released from beta cells, that it acts to potentiate insulin secretion during pregnancy via 5-HT3A receptor stimulation, and under normal physiological conditions, it acts as an autocrine and paracrine signal in the endocrine pancreas (Almaca et al., 2016; Kim et al., 2010; Ohara-Imaizumi et al., 2013). An activation of 5-HT3A is required for the compensatory increase in insulin secretion during pregnancy by lowering the glucose threshold for insulin release (Ohara-Imaizumi et al., 2013). Data presented in this thesis show that 5-HT3A mRNA is detected in MIN6 cells

and human islets. It is also demonstrated that beta cells express different components of serotonergic machinery, such as SERT, and it has been previously shown that the blockade of SERT by 0.5μM fluvoxamine, another SSRI, induces serotonin secretion from beta cells (Almaca et al., 2016). This suggests that SSRIs could potentially exert their effects directly on beta cells by blocking serotonin reuptake and by increasing endogenous serotonin levels. As in pregnancy, enhanced serotonin signalling may allow islets to cope with increasing insulin demand during T2D by increasing compensatory beta cell mass expansion and insulin secretory responsiveness to glucose, as well as reducing glucagon secretion from alpha cells. On the other hand, it has been suggested that the effect of fluoxetine on GSIS is not mediated by SERT inhibition (Cataldo et al., 2015), and SSRIs could therefore exert favourable effects on insulin secretion and improve glycaemic control through other mechanisms, such as direct effects on K_{ATP} channels. Both fluoxetine and sertraline have been shown to block K^+ channels in platelets and astrocytes, and it is possible that they also inhibit K_{ATP} channels in beta cells, decrease K^+ efflux, and cause cell depolarisation that is crucial for insulin secretion (Frizzo, 2017; Kobayashi et al., 2003; Ohno et al., 2007; Ohno, 2018). Interestingly, fluoxetine increases expression of cytosolic phospholipase A_2 in SERT-deficient cells (Hertz et al., 2015), and activation of phospholipase A_2 leads to a generation of arachidonic acid (AA), which promotes insulin secretion from human islets (Persaud et al., 2007). It is therefore possible that fluoxetine potentiates insulin secretion by increasing AA levels, and this is an area for future research. What is more, fluoxetine promotes phosphorylation of MAPK, cAMP responsive element-binding protein (CREB) and Akt, which have been shown to promote insulin secretion and beta cell proliferation (Blanchet et al., 2015; Le Bacquer et al., 2013; Liu et al., 2012). CREB and Akt are important transcriptional elements for beta cell function, including glucose sensing, insulin

exocytosis, insulin gene transcription, and survival (Dalle et al., 2011; Elghazi and Bernal-Mizrachi, 2009). The molecular mechanisms by which CREB and Akt activate gene transcription in beta cells vary according to the stimulus, and it could be that fluoxetine and other SSRIs affect GSIS through phosphorylation of CREB and Akt.

8.1.3. SSRIs promote beta cell mass expansion

Beta cell mass is defined by a balance between beta cell proliferation and apoptosis (Doyle and Egan, 2007). Data presented in this thesis show that fluoxetine, sertraline and paroxetine increase proliferation of beta cells and protect them against cytokine- and palmitate-induced apoptosis *in vitro,* and fluoxetine increases beta cell proliferation *in vivo*. The exact mechanisms through which SSRIs increase proliferation and decrease apoptosis have not been determined yet, but the beneficial effects of SSRIs on beta cell mass could be attributed to elevated serotonin levels, which is available to exert functional effects. Elevated serotonin could lead to increased beta cell mass, as has been proven in pregnancy, via 5-HT2B receptor stimulation (Kim et al., 2010). Consistent with previous reports that SSRIs improve glycaemic management in people with both diabetes and depression (Gehlawat et al., 2013; Roopan and Larsen, 2016; Tharmaraja et al., 2019), SSRIs could exert their effects on beta cells by blocking SERT, and thus elevating local serotonin concentrations. However, the roles of serotonin and SERT blockade during normal physiological conditions and in conditions of increased metabolic demand, such as obesity and T2D, are yet to be further investigated. In addition to this, human islet beta cells and those from pregnant mice synthesise serotonin (Almaca et al., 2016; Kim et al., 2010; Moon et al., 2020), and, as shown in chapter 3, trace levels of serotonin and TPH were detected in mouse beta cells using IHC. This is important because the

presence of TPH allows serotonin synthesis in beta cells, and this in turn promotes insulin granule exocytosis through serotonylation of small GTPases of the Rab family (Paulmann et al., 2009) and stimulation of beta cell proliferation via 5-HT2B receptors (Bennet et al., 2015; Kim et al., 2015; Ohara-Imaizumi et al., 2013). Interestingly, 5-HT2B mRNA was detected in MIN6 cells and human islets by quantitative PCR as demonstrated in this thesis. Confirmation of the presence of the serotoninergic machinery in MIN6 cells and islets could help to unravel the direct effects of SSRIs on beta cells in people with diabetes. Nevertheless, the levels of TPH and serotonin in mouse beta cells are extremely low, which is consistent with previous reports (Moon et al., 2020; Tharmaraja et al., 2020), and the exact mechanism of action of SSRIs to regulate mouse beta cell proliferation remains to be investigated. On the other hand, there is evidence that SERT is expressed by human beta cells, and that serotonin is synthesised and secreted at detectable levels from islets of healthy humans (Almaca et al., 2016; Bennet et al., 2015). This suggests species-specific differences, as well as possible species-dependent modes of action of SSRIs. In addition to serotonin signalling, there is evidence that insulin acts as an autocrine signalling agent by increasing beta cell proliferation and by inhibiting apoptosis (Muller et al., 2006). It is possible that SSRIs promote beta cell mass expansion and improve glycaemic control by elevating insulin secretion in response to increased glucose levels. As demonstrated in this thesis, fluoxetine, sertraline and paroxetine increase GSIS from mouse and human beta cells. Moreover, sertraline has been shown to potentiate insulin secretion *in vivo* in rats (Gomez et al., 2001). Fluoxetine has been also linked to improvements in the cellular oxidative status (Novio et al., 2011), which suggests a novel mechanism underlying the protective pharmacological effects of fluoxetine against apoptosis. Increases in ROS production are induced by hyperglycaemia in individuals with diabetes, so

inhibitors of oxidative stress could be used to prevent beta cell apoptosis in T2D (Marrif and Al-Sunousi, 2016; Volpe et al., 2018). On the other hand, in the rodent brain, chronic fluoxetine treatment increases CREB phosphorylation downstream of ERK2 (p42 MAPK) phosphorylation (Qi et al., 2008; Taler et al., 2013), and it has been suggested that the ERK-CREB system could be involved in the neuronal mechanism of depression (Qi et al., 2008). Sertraline also upregulates ERK phosphorylation and exerts neuroprotective effects in the brain (Taler et al., 2013). In the endocrine pancreas, ERK and CREB are involved in beta cell mass expansion (Burns et al., 2000; Hussain et al., 2006), and it could be that SSRIs induce beta cell proliferation through similar mechanisms as they use to promote neurogenesis in the brain. Lastly, it is possible that increased beta cell survival and proliferation are due to CaMK4-stimulated CREB activation (Jhala et al., 2003; Liu et al., 2012). It has been reported that this CREB activation regulates the expression of Irs2, and that it results in increased proliferation and decreased apoptosis of beta cells (Liu et al., 2012; Persaud et al., 2011). It could be that SSRIs, by activating signalling through the ERK2/CaMK4/CREB/Irs2 cascade, exert similar effects on beta cell proliferative rate and survival. Moreover, as mentioned earlier, fluoxetine increases expression of cytosolic phospholipase A2, and hence it could increase levels of AA, which has been shown to decrease beta cell apoptosis (Papadimitriou et al., 2007). Although the exact mechanisms of action of SSRIs at the endocrine pancreas are yet to be defined, the ability of SSRIs to promote beta cell proliferation and decrease apoptosis in the presence of factors that accompany inflammation and obesity is crucial in considering these drugs as a possible treatment for T2D.

8.2. AAPs and T2D

The prevalence of diabetes among patients with schizophrenia in the UK is estimated to be 11.3% (Schoepf et al., 2012). The life expectancy of patients with schizophrenia is reduced by up to 25 years (Wildgust et al., 2010), and many of these premature deaths are due to chronic physical disorders associated with SCZ, including T2D. There are concerns that antipsychotics used in the treatment of SCZ increase the risk of developing T2D (Lamberti et al., 2004). Initially antipsychotics are used to manage acute psychosis, but in the longer term they are required to prevent relapse, and therefore they are often used long-term. Nevertheless, the incident of T2D varies between different AAPs, with a high risk observed with clozapine, and low risk observed with aripiprazole (Citrome et al., 2014; Kessing et al., 2010; Pillinger et al., 2020). Other studies consider aripiprazole as "metabolically neutral" (Chipchura et al., 2018). On the other hand, genome-wide association study and polygenic risk score analysis have revealed the presence of a shared genetic background between SCZ and T2D (Hackinger et al., 2018). Patients with comorbid SCZ and T2D have a higher genetic predisposition to both disorders, and metabolic disturbances are observed in people prior to any antipsychotic treatment (Pillinger et al., 2017). In addition, it has been shown that the prevalence of T2D in patients suffering from severe mental illness increases almost 4-fold prior to antipsychotic therapy (Vancampfort et al., 2016).

8.2.1. AAPs increase ATP generation and viability of beta cells

Plasma concentrations of aripiprazole and clozapine are 0.24-1.12µM and 0.61-2.66µM, respectively (Gründer et al., 2008; Keshavarzi et al., 2020; Kirschbaum et al., 2008; Sparshatt et al., 2010), and, as in studies involving SSRIs, these AAPs have been used in *in vitro* beta cell studies at concentrations as high as 75µM (Cikánková et al., 2019; Contreras-Shannon et al., 2013; Lundberg et al., 2020). Many of these studies have concluded that AAPs negatively alter mitochondrial function and cell viability. As shown in this thesis, aripiprazole and clozapine at concentrations of 10-20µM significantly decrease beta cell viability, which indicates that high concentrations exceeding the therapeutic range should not be used to assess the effects of these AAPs on beta cell function. Because ATP is an indicator of mitochondrial function, and its production is increased in the presence of low and therapeutic concentrations of aripiprazole and clozapine, it would be interesting to investigate their direct effects on mitochondria and metabolism of insulin-responsive cells in future studies as nothing is currently known about this.

8.2.2. AAPs increase glucose-stimulated insulin secretion from beta cells

Data presented in this thesis demonstrate that aripiprazole and clozapine at therapeutic concentrations potentiate GSIS from mouse and human beta cells. In addition to these findings, a recent study has shown that clozapine, olanzapine, and haloperidol at 1µM induced both insulin and glucagon secretion from human islets downstream of D2 and D3 receptor blockade (Aslanoglou et al., 2021). This study has suggested a model for dopamine-mediated regulation of insulin and glucagon secretion, where low concentrations of local dopamine stimulate high-affinity D2 receptors to inhibit insulin and glucagon secretion. What is more, at higher concentrations dopamine activates stimulatory low-affinity beta-

adrenergic and alpha-2-adrenergic receptors on alpha and beta cells, respectively, leading to increased glucagon and decreased insulin release. Other studies have also demonstrated a role for D2 and D3 receptors in regulating insulin secretion from mouse beta cells (Farino et al., 2020; Rubi et al., 2005). These studies indicate that D2 and D3 receptors play an important role in glycaemic control through their inhibitory effects on insulin secretion, and they suggest that blockade of peripheral D2 receptors by antipsychotics may contribute to the metabolic disturbances seen clinically. In addition to this, antagonism of D2 receptors on alpha cells has a similar effect on hormone secretion leading to elevated glucagon levels and increased hyperglycaemia. Nevertheless, these studies focused on the effect of D2 receptor blockade at high glucose concentrations and did not include low glucose concentrations. Results presented in this thesis show that AAPs do not induce basal insulin secretion at 2mM glucose, suggesting that they do not favour the occurrence of hypoglycaemia in the fasting state, but only increase insulin secretion at high glucose levels when it is required, following food intake. If insulin secretion is only increased when plasma glucose levels are high, AAPs could be beneficial in ameliorating diabetic symptoms in SCZ patients. In this thesis, it was not possible to determine molecular mechanisms in peripheral tissues and islet cells underlying insulin resistance and glycaemic control after treatment with individual AAPs. They should be investigated in the future because aripiprazole and clozapine may affect peripheral tissues and cause insulin resistance, which could outweigh their beneficial effects on GSIS. What is more, AAPs have high binding affinities at serotonin receptors, including 5-HT1D and 5-HT2A receptors. Both 5-HT1D and 5-HT2A receptors are localised to pancreatic alpha, beta, and delta cells in the pancreas, and their expression is significantly increased in the islets from type 2 diabetic donors (Bennet et al., 2015; Kim et al., 2010).

The 5-HT1D and 5-HT2A receptors are GPCRs that signal via Gi and Gq, respectively, to inhibit or stimulate insulin secretion. Therefore, overexpression of these receptors may either enhance or block specific signalling pathways, resulting in changes in hormone secretion. While clozapine is known as a 5-HT2A receptor antagonist, it also acts as a functionally selective agonist at 5-HT2A by increasing receptor internalisation and Akt phosphorylation (Schmid et al., 2014). What is more, clozapine antagonises the 5-HT1D receptors (Bennet et al., 2015; Meltzer and Massey, 2011), and 5-HT1D receptor activation mediates a decrease of beta cell mass and insulin secretion postpartum (Bennet et al., 2015; Kim et al., 2010). The 5-HT1D receptor antagonist, LY310762, significantly potentiates insulin secretion from human islets (Bennet et al., 2015), and therefore it is possible that the beneficial effects of clozapine and aripiprazole are due to the blockade of 5-HT1D receptors that are linked to increases in beta cell mass and insulin secretion. On the other hand, clozapine acts as functionally selective agonist at 5-HT2A Future studies should therefore not only focus on the effects of individual AAPs on dopamine receptors, but also determine their effects downstream of serotonin receptors.

8.2.3. AAPs increase beta cell mass

Therapeutic agents that increase beta cell mass are desired for optimised T2D therapy. Results presented in this thesis demonstrate that both aripiprazole and clozapine increase proliferative rates of islet cells, and they also decrease rates of beta cell apoptosis in the presence of proinflammatory cytokines and palmitate. There is evidence that a D2 receptor antagonist, domperidone, promotes mouse and human beta cell mass through increases in intracellular cAMP. Moreover, D2 receptor knockdown increases beta cell number, whereas D2 receptor overexpression shows increased apoptosis (Sakano et al., 2016). This

suggests that dopamine inhibits proliferation and promotes apoptosis, and that inhibition of dopamine signalling via D2 receptors by AAPs could increase beta cell mass, which could explain the observations made in this thesis. It is also possible that aripiprazole, and potentially clozapine, exert their beneficial effects on beta cell proliferation and apoptosis in the presence of cytokines or palmitate by a mechanism separate to blocking D2 receptors. For example, cancer studies using aripiprazole have indicated that it can activate adenosine monophosphate-activated protein kinase (AMPK), which is a central regulator of beta cell mass via the mTOR pathway (Lee et al., 2019; Rourke et al., 2018). Furthermore, studies of clozapine in the brain have indicated that it increases levels of the anti-apoptotic protein Bcl-2 and decreases caspase-3 activity (Todorovic et al., 2019), and this is a possible mode of action in beta cells. What is more, increased levels of insulin could act in an autocrine loop and promote beta cell proliferation (Muller et al., 2006). However, more studies are required to unravel the exact molecular mechanism of action of AAPs to promote beta cell mass.

8.3. Limitations of the studies

The experiments described in this thesis have several limitations, some of which were a consequence of Covid-19-related lab closure for several months (March-September 2020), which limited the amount of experimental work that could be done. For a full overview of possible signalling cascades relevant to SSRI and AAP action, qPCR experiments should be performed using mouse islet mRNA in addition to MIN6 cell and human islet mRNA, and fluorescence immunohistochemistry staining should be performed using sections from pregnant mouse islets and human islets. It is important to note that the anti-D2 receptor antibody failed to give pronounced staining in the pancreas and in the

midbrain (positive control), and further antibody optimisation, or use of an alternative antibody, could improve these experiments. In addition, although BrdU is commonly used as a proliferation marker, its use has some limitations. Thus, BrdU is a marker of DNA synthesis, and it does not mark the S-phase of the cell cycle nor cell division, and it can incorporate into DNA during DNA repair processes, as well as abortive re-entry to the cell cycle before apoptosis. In addition, it has been shown that BrdU can be transferred into dividing cells from dying cells (Taupin, 2007). It would therefore be useful to co-stain BrdU with Ki67 that marks active phases of the cell cycle as a component of the mitotic chromosome periphery (Cuylen et al., 2016). As described above, the *in vivo* experiments would have benefitted from the use of younger, obese mice so that were not so overtly glucose intolerant, and inclusion of a positive control, such as Exendin-4 that is known to improve glucose tolerance, should have been used in addition to fluoxetine. Experiments that determined the effects of fluoxetine on insulin-sensitive tissues, such as muscle, liver, and adipose tissue in addition to the endocrine pancreas, would also have provided more detailed information on the effects of fluoxetine delivery *in vivo*. Furthermore, the human macrophage cell line, TPH-1, is more appropriate than mouse Raw 264.7 cells for use in the invasion and migration experiments using human pseudoislets.

8.4. Conclusion

The SSRIs, fluoxetine, sertraline and paroxetine, and AAPs, aripiprazole and clozapine, act directly on beta cells to increase glucose-stimulated insulin secretion and proliferation, and they also have protective effects against apoptosis in the presence of proinflammatory cytokines and palmitate. Data presented in this thesis thus show that SSRIs and AAPs exert favourable effects on beta cells and suggest that although some of these drugs may have deleterious effects on blood glucose levels, this is not because of them impairing beta cell function. Nevertheless, more studies are needed to determine the exact molecular mechanisms of action of these drugs at the endocrine pancreas, as well as unravel their effects in the periphery.

8.4. Future studies

Both antidepressants and antipsychotics have been implicated in increased risk of T2D. As there is no consensus on studies regarding the effects of individual SSRIs and AAPs on beta cells, this thesis aimed to unravel the direct effects of fluoxetine, sertraline, paroxetine, aripiprazole, and clozapine on beta cell function and mass. The experiments described in this thesis established that these drugs potentiate insulin secretion and that they promote beta cell mass expansion *in vitro*. In addition, fluoxetine leads to improved glucose tolerance and increased beta cell proliferation *in vivo*. It is possible that these studies have translational potential to T2D treatment, and that SSRIs that have been selected for this study are responsible for improvements in glycaemia seen in clinical studies (Tharmaraja et a., 2019; Ye et al., 2011). Nevertheless, future studies are required to unravel the effects of individual SSRIs and AAPs on insulin resistance

and glycaemic control *in vivo* using animal models of T2D. Despite their beneficial effects on beta cells, these drugs could also target peripheral tissues and cause insulin resistance. The potential negative effects of SSRIs and AAPs on insulin resistance could outweigh the favourable effects of these drugs in the endocrine pancreas, and hence explain glucose dysregulation reported in many clinical studies. More research is required to understand whether SSRIs and AAPs affect peripheral tissues to promote insulin resistance.

This research would benefit from additional experiments *in vitro*, including perifusions to investigate the effects of aripiprazole and clozapine on dynamic insulin secretion, as well as fluorescence immunohistochemistry to assess the effects of fluoxetine, sertraline, paroxetine, aripiprazole, and clozapine on proliferation using both primary islets and pseudoislets reformed from dissociated primary islets. These pseudoislets offer a novel platform for high resolution imaging of beta cells, and optimisation of this technique would be beneficial for future analysis of beta cell proliferation in islets *in situ*. In addition, data presented in this thesis show that fluoxetine, aripiprazole and clozapine have a protective effect against macrophage infiltration. It would be interesting to repeat those experiments and use primary mouse and human islets in addition to pseudoislets. On the other hand, *in vivo* studies presented in this thesis could be improved by using osmotic minipumps instead of intraperitoneal injections to introduce fluoxetine or other drugs of interest. Because fluoxetine is normally taken orally as tablets, in which concentrations are maintained for long periods, osmotic minipumps may allow a continuous release of the drug directly into the circulation, and therefore produce stable serum concentrations. Moreover, frequent injections can be associated with stress and potentially mask the beneficial effects of fluoxetine *in vivo*.

Although *ob/ob* mice become profoundly obese and develop hyperglycaemia and peripheral insulin resistance (King, 2012), leptin deletion does not represent the underlying aetiology of human obesity. Therefore, different models of T2D should be introduced in future studies, such as the high-fat diet-fed (HFD) mouse, a model that is more representative to T2D in humans, as it is associated not only with hyperglycaemia and insulin resistance, but also beta cell failure. Future studies would also benefit from the use of pregnant mice that have increased levels of expression of serotonergic machinery elements to investigate the effects of SSRIs in pregnancy. Studies using mouse models of depression under conditions of HFD or pregnancy would also benefit this area of research.

The next step after demonstrating how selected SSRIs and AAPs affect beta cells would be investigating their molecular mechanisms of action, starting with analysis of expression of interacting partners by PCR, Western blotting, and immunofluorescence. In addition to this, the SSRIs and AAPs used in this thesis increase beta cell viability and ATP production. As mentioned above, there is evidence that they have an effect on mitochondrial function, and therefore it would be worth studying their action at mitochondria by assessing mitochondria morphology, membrane potential, and mitochondria volume following SSRI or AAP treatment. In addition, the involvement of serotonin could be investigated by comparing perifusion experiments using islets acutely exposed to individual SSRIs without or with commercially available serotonin receptor antagonists SB204741 or tropisetron hydrochloride that block 5-HT2B and 5-HT3A, respectively. It would be interesting to know whether the effects on insulin secretion are lost following deletion of endogenous serotonin by pre-exposure to the tryptophan hydroxylase inhibitor (LX-1031). Calcium microfluorimetry experiments could be performed in parallel to investigate the effects of

fluoxetine, sertraline, paroxetine, aripiprazole, and clozapine on Ca^{2+} signalling in beta cells.

Rodent islets require preloading with serotonin or serotonin precursors *in vitro* in order to allow for detection of serotonin secretion (Barbosa et al., 1998; Rosario et al., 2008; Smith et al., 1995), and it has been suggested that serotonin may play a paracrine role in rodent islets under conditions of increased metabolic demand, such as in pregnancy. There are also substantial differences in expression levels of serotonin and dopamine receptors between mouse and human islets. In addition, human islets have 3 times more serotonin^{+} cells than mouse islets (Amisten et al., 2017). This contrast between mouse and human islets is in line with other species differences in islet architecture and function (Dolensek et al., 2015; Kim et al., 2009; Steiner et al., 2010), and it indicates that serotonin, and potentially dopamine, have functions in human islets not predicted by rodent models. Future studies should therefore aim to fully compare the effects and mechanisms of action of SSRIs and AAPs on both mouse and human beta cells.

Lastly, given the ambivalence in clinical studies that link antidepressant and antipsychotic treatment and changes in glucose regulation (Andersohn et al., 2009; Burcu et al., 2017; Grajales et al., 2019; Newcomer et al., 2002; Tharmaraja et a., 2019; Ye et al., 2011; Zhang et al., 2017), more big scale placebo-controlled trials should be conducted. Research in this area could explain the broad effects of antidepressant therapy on tissues outside the brain, give potential benefits and risk factors, and identify the mechanism of action of SSRIs, and unravel whether these drugs could be found useful in the treatment of metabolic diseases, such as T2D.

Chapter 9. References:

Absher, M., 1973. Hemocytometer Counting. In: Tissue Culture: Methods and Applications, chapter 1. Academic Press, New York.

Agardh, E., Allebeck, P., Hallqvist, J., Moradi, T. and Sidorchuk, A., 2011. Type 2 diabetes incidence and socio-economic position: a systematic review and meta-analysis. *International Journal of Epidemiology*, 40(3), pp.804-818.

Aguilar-Bryan, L. and Bryan, J., 2008. Neonatal Diabetes Mellitus. *Endocrine Reviews*, 29(3), pp.265-291.

Ahren, B., 2009. Islet G protein-coupled receptors as potential targets for treatment of type 2 diabetes. *Nature Reviews Drug Discovery*, 8(5), pp.369-385.

Aihara, K., Shimada, J., Miwa, T., Tottori, K., Burris, K., Yocca, F., Horie, M. and Kikuchi, T., 2004. The novel antipsychotic aripiprazole is a partial agonist at short and long isoforms of D2 receptors linked to the regulation of adenylyl cyclase activity and prolactin release. *Brain Research*, 1003(1-2), pp.9-17.

Alessi, J., Berger de Oliveira, G., Wilke Franco, D., Amaral, B., Scalzilli Becker, A., Padilla Knijnik, C., Luiz Kobe, G., Rosa de Carvalho, T., Heiden Telo, G., Agord Schaan, B. and Heiden Telo, G., 2020. Mental health in the era of COVID-19: prevalence of psychiatric disorders in a cohort of patients with type 1 and type 2 diabetes during the social distancing. Diabetology & metabolic syndrome, 12, pp.76.

Allison, D. B., Mentore, J. L., Heo, M., Chandler, L. P., Cappelleri, J. C., Infante, M. C., Weiden, P. J., 1999. Antipsychotic-induced weight gain: a comprehensive research synthesis. *American Journal of Psychiatry,* 156, pp.1686–1696.

Almaca, J., Molina, J., Menegaz, D., Pronin, A., Tamayo, A., Slepak, V., Berggren, P. and Caicedo, A., 2016. Human Beta Cells Produce and Release Serotonin to Inhibit Glucagon Secretion from Alpha Cells. *Cell Reports*, 17(12), pp.3281-3291.

Alonso-Magdalena, P., Ropero, A., Carrera, M., Cederroth, C., Baquié, M., Gauthier, B., Nef, S., Stefani, E. and Nadal, A., 2008. Pancreatic Insulin Content Regulation by the Estrogen Receptor ERα. PLoS ONE, 3(4), p.e2069.

Altamura, A., Moro, A. and Percudani, M., 1994. Clinical Pharmacokinetics of Fluoxetine. *Clinical Pharmacokinetics*, 26(3), pp.201-214.

Alzoubi, A., Abunaser, R., Khassawneh, A., Alfaqih, M., Khasawneh, A. and Abdo, N., 2018. The Bidirectional Relationship between Diabetes and Depression: A Literature Review. *Korean Journal of Family Medicine*, 39(3), pp.137-146.

Amisten, S., Atanes, P., Hawkes, R., Ruz-Maldonado, I., Liu, B., Parandeh, F., Zhao, M., Huang, G., Salehi, A. and Persaud, S., 2017. A comparative analysis of human and mouse islet G-protein coupled receptor expression. *Scientific Reports*, 7(1).

Amisten, S., Salehi, A., Rorsman, P., Jones, P. and Persaud, S., 2013. An atlas and functional analysis of G-protein coupled receptors in human islets of Langerhans. *Pharmacology & Therapeutics*, 139(3), pp.359-391.

Andersohn, F., Schade, R., Suissa, S. and Garbe, E., 2009. Long-Term Use of Antidepressants for Depressive Disorders and the Risk of Diabetes Mellitus. *American Journal of Psychiatry*, 166(5), pp.591-598.

Ansari, P., Azam, S., Hannan, J., Flatt, P. and Abdel Wahab, Y., 2020. Anti-hyperglycaemic activity of H. rosa-sinensis leaves is partly mediated by inhibition of carbohydrate digestion and absorption, and enhancement of insulin secretion. *Journal of Ethnopharmacology*, 253, p.112647.

Ansari, P., Hannon-Fletcher, M., Flatt, P. and Abdel-Wahab, Y., 2021. Effects of 22 traditional anti-diabetic medicinal plants on DPP-IV enzyme activity and glucose homeostasis in high-fat fed obese diabetic rats. *Bioscience Reports*, 41(1).

Arambewela, M., Somasundaram, N., Ranjan Jayasekara, H., Kumbukage, M., Jayasena, P., Hemanthi Chandrasekara, C., Sudath Fernando, K. and Kusumsiri, D., 2018. Prevalence of

Chronic Complications, Their Risk Factors, and the Cardiovascular Risk Factors among Patients with Type 2 Diabetes Attending the Diabetic Clinic at a Tertiary Care Hospital in Sri Lanka. *Journal of Diabetes Research*, 2018, pp.1-10.

Arous, C. and Wehrle-Haller, B., 2017. Role and impact of the extracellular matrix on integrin-mediated pancreatic β-cell functions. *Biology of the Cell*, 109(6), pp.223-237.

Ascher-Svanum, H., Zagar, A., Jiang, D., Schuster, D., Schmitt, H., Dennehy, E., Kendall, D., Raskin, J. and Heine, R., 2015. Associations Between Glycemic Control, Depressed Mood, Clinical Depression, and Diabetes Distress Before and After Insulin Initiation: An Exploratory, Post Hoc Analysis. *Diabetes Therapy*, 6(3), pp.303-316.

Aslanoglou, D., Bertera, S., Sánchez-Soto, M., Benjamin Free, R., Lee, J., Zong, W., Xue, X., Shrestha, S., Brissova, M., Logan, R., Wollheim, C., Trucco, M., Yechoor, V., Sibley, D., Bottino, R. and Freyberg, Z., 2021. Dopamine regulates pancreatic glucagon and insulin secretion via adrenergic and dopaminergic receptors. *Translational Psychiatry*, 11(1).

Atanes, P. and Persaud, S.J. (2019) GPCR targets in type 2 diabetes. In: GPCRs: Structure, Function, and Drug Discovery, chapter 18, pp. 367–391. Academic Press, London.
Atanes, P., Ruz-Maldonado, I., Oladapo, E., Persaud, S. J., 2020. Assessing Mouse Islet Function. In: Animal Models of Diabetes, chapter 17, pp. 241-268. Humana Press, London.
Atkinson, M., Campbell-Thompson, M., Kusmartseva, I. and Kaestner, K., 2020. Organisation of the human pancreas in health and in diabetes. *Diabetologia*, 63(10), pp.1966-1973.

Au, B., Smith, K., Gariepy, G. and Schmitz, N., 2014. C-reactive protein, depressive symptoms, and risk of diabetes: Results from the English Longitudinal Study of Ageing (ELSA). *Journal of Psychosomatic Research*, 77(3), pp.180-186.

Azuma, J., Hasunuma, T., Kubo, M., Miyatake, M., Koue, T., Higashi, K., Fujiwara, T., Kitahara, S., Katano, T. and Hara, S., 2011. The relationship between clinical pharmacokinetics of aripiprazole and CYP2D6 genetic polymorphism: effects of CYP enzyme inhibition by coadministration of paroxetine or fluvoxamine. *European Journal of Clinical Pharmacology*, 68(1), pp.29-37.

Badescu, S. V., Tataru, C., Kobylinska, L., Georgescu, E. L., Zahiu, D. M., Zagrean, A. M., Zagrean, L., 2016. The association between Diabetes mellitus and Depression. *Journal of Medicine and Life*, 9(2), pp.120–125.

Badran, A., tul-Wahab, A., Zafar, H., Mohammad, N., Imad, R., Ashfaq Khan, M., Baydoun, E. and Choudhary, M., 2020. Antipsychotics drug aripiprazole as a lead against breast cancer cell line (MCF-7) in vitro. *PLOS ONE*, 15(8), p.e0235676.

Barbour, L., Shao, J., Qiao, L., Pulawa, L., Jensen, D., Bartke, A., Garrity, M., Draznin, B. and Friedman, J., 2002. Human placental growth hormone causes severe insulin resistance in transgenic mice. *American Journal of Obstetrics and Gynecology*, 186(3), pp.512-517.

Barnard, K., Peveler, R. and Holt, R., 2013. Antidepressant Medication as a Risk Factor for Type 2 Diabetes and Impaired Glucose Regulation: Systematic review. *Diabetes Care*, 36(10), pp.3337-3345.

Basu, R. and Brar, J., 2006. Dose-dependent rapid-onset akathisia with aripiprazole in patients with schizoaffective disorder. *Neuropsychiatric Disease and Treatment*, 2(2), pp.241-243.

Bauer, C., Kaiser, J., Sikimic, J., Krippeit-Drews, P., Dufer, M. and Drews, G., 2018. ATP mediates a negative autocrine signal on stimulus-secretion coupling in mouse pancreatic β-cells. *Endocrine*, 63(2), pp.270-283.

Beasley, C., Masica, D. and Potvin, J., 1992. Fluoxetine: a review of receptor and functional effects and their clinical implications. *Psychopharmacology*, 107(1), pp.1-10.

Becker, A. and Grecksch, G., 2004. Ketamine-induced changes in rat behaviour: a possible animal model of schizophrenia. Test of predictive validity. *Progress in Neuro-Psychopharmacology and Biological Psychiatry*, 28(8), pp.1267-1277.

Beith, J., Alejandro, E. and Johnson, J., 2008. Insulin Stimulates Primary β-Cell Proliferation via Raf-1 Kinase. *Endocrinology*, 149(5), pp.2251-2260.

Belkina, A. and Denis, G., 2010. Obesity genes and insulin resistance. *Current Opinion in Endocrinology, Diabetes and Obesity*, 17(5), pp.472-477.

Benmansour, S., Cecchi, M., Morilak, D., Gerhardt, G., Javors, M., Gould, G. and Frazer, A., 1999. Effects of Chronic Antidepressant Treatments on Serotonin Transporter Function, Density, and mRNA Level. *The Journal of Neuroscience*, 19(23), pp.10494-10501.

Bennet, H., Balhuizen, A., Medina, A., Dekker Nitert, M., Ottosson Laakso, E., Essén, S., Spégel, P., Storm, P., Krus, U., Wierup, N. and Fex, M., 2015. Altered serotonin (5-HT) 1D and 2A receptor expression may contribute to defective insulin and glucagon secretion in human type 2 diabetes. *Peptides*, 71, pp.113-120.

Berchtold, L., Prause, M., Storling, J. and Mandrup-Poulsen, T., 2016. Cytokines and Pancreatic β-Cell Apoptosis. *Advances in Clinical Chemistry*, pp.99-158.

Berger, M., Gray, J. and Roth, B., 2009. The Expanded Biology of Serotonin. *Annual Review of Medicine*, 60(1), pp.355-366.

Berglund, O., 1987. Lack of glucose-induced priming of insulin release in the perfused mouse pancreas. *Journal of Endocrinology*, 114(2), pp.185-189.

Bernardi, P. and Di Lisa, F., 2015. The mitochondrial permeability transition pore: Molecular nature and role as a target in cardioprotection. *Journal of Molecular and Cellular Cardiology*, 78, pp.100-106.

Bernard-Kargar, C. and Ktorza, A., 2001. Endocrine pancreas plasticity under physiological and pathological conditions. *Diabetes*, 50(Supplement 1), pp.S30-S35.

Bich, L., Mossio, M. and Soto, A., 2020. Glycemia Regulation: From Feedback Loops to Organizational Closure. *Frontiers in Physiology*, 11.

Bischoff, E., Jakobs, K. and Assendelft, W., 2020. Cardiovascular risk management in patients using antipsychotics: it is time to take action. *BMC Medicine*, 18(1).

Bishoyi, A., Roham, P., Rachineni, K., Save, S., Hazari, M., Sharma, S. and Kumar, A., 2021. Human islet amyloid polypeptide (hIAPP) - a curse in type II diabetes mellitus: insights from structure and toxicity studies. *Biological Chemistry*, 402(2), pp.133-153.

Blanchet, E., Van de Velde, S., Matsumura, S., Hao, E., LeLay, J., Kaestner, K. and Montminy, M., 2015. Feedback Inhibition of CREB Signaling Promotes Beta Cell Dysfunction in Insulin Resistance. *Cell Reports*, 10(7), pp.1149-1157.

Bock, T., Pakkenberg, B. and Buschard, K., 2003. Increased Islet Volume but Unchanged Islet Number in *ob/ob* Mice. *Diabetes*, 52(7), pp.1716-1722.

Bock, T., Pakkenberg, B. and Buschard, K., 2003. Increased Islet Volume but Unchanged Islet Number in *ob/ob* Mice. *Diabetes*, 52(7), pp.1716-1722.

Bolo, N. R., Hode, Y., Nedelec, J. F., Laine, E., Wagner, G., Macher, J. P., 2000. Brain pharmacokinetics and tissue distribution *in vivo* of fluvoxamine and fluoxetine by fluorine magnetic resonance spectroscopy. *Neuropsychopharmacology*, 23, pp.28-438.

Bolonna, A. and Kerwin, R., 2005. Partial agonism and schizophrenia. *British Journal of Psychiatry*, 186(1), pp.7-10.

Boni-Schnetzler, M. and Meier, D., 2019. Islet inflammation in type 2 diabetes. *Seminars in Immunopathology*, 41(4), pp.501-513.

Bosch, M. E., Sanchez, A. J., Rojas, F. S., Ojeda, C. B., 2008. Analytical methodologies for the determination of sertraline. *Journal of Pharmaceutical and Biomedical Analysis*, 48, pp.1290-1302.

Bourin, M., Chue, P. and Guillon, Y., 2001. Paroxetine: A Review. *CNS Drug Reviews*, 7(1), pp.25-47.

Bouwens, L. and Rooman, I., 2005. Regulation of Pancreatic Beta-Cell Mass. *Physiological Reviews*, 85(4), pp.1255-1270.

Bowe, J., Chander, A., Liu, B., Persaud, S. and Jones, P., 2013. The permissive effects of glucose on receptor-operated potentiation of insulin secretion from mouse islets: a role for ERK1/2 activation and cytoskeletal remodelling. *Diabetologia*, 56(4), pp.783-791.

Bowe, J., Hill, T., Hunt, K., Smith, L., Simpson, S., Amiel, S. and Jones, P., 2019. A role for placental kisspeptin in β cell adaptation to pregnancy. JCI Insight, 4(20).

Breum, L., Bjerre, U., Bak, J., Jacobsen, S. and Astrup, A., 1995. Long-term effects of fluoxetine on glycemic control in obese patients with non-insulin-dependent diabetes mellitus or glucose intolerance: Influence on muscle glycogen synthase and insulin receptor kinase activity. *Metabolism*, 44(12), pp.1570-1576.

Briant, L., Reinbothe, T., Spiliotis, I., Miranda, C., Rodriguez, B. and Rorsman, P., 2018. δ-cells and β-cells are electrically coupled and regulate α-cell activity via somatostatin. *The Journal of Physiology*, 596(2), pp.197-215.

Briant, L., Salehi, A., Vergari, E., Zhang, Q. and Rorsman, P., 2016. Glucagon secretion from pancreatic α-cells. *Upsala Journal of Medical Sciences*, 121(2), pp.113-119.

Brissova, M., Fowler, M., Nicholson, W., Chu, A., Hirshberg, B., Harlan, D. and Powers, A., 2005. Assessment of Human Pancreatic Islet Architecture and Composition by Laser Scanning Confocal Microscopy. *Journal of Histochemistry & Cytochemistry*, 53(9), pp.1087-1097.

Bromet, E., Andrade, L., Hwang, I., Sampson, N., Alonso, J., de Girolamo, G., de Graaf, R., Demyttenaere, K., Hu, C., Iwata, N., Karam, A., Kaur, J., Kostyuchenko, S., Lépine, J., Levinson, D., Matschinger, H., Mora, M., Browne, M., Posada-Villa, J., Viana, M., Williams, D. and Kessler, R., 2011. Cross-national epidemiology of DSM-IV major depressive episode. *BMC Medicine*, 9(1).

Brun, P., Grijalva, A., Rausch, R., Watson, E., Yuen, J., Das, B., Shudo, K., Kagechika, H., Leibel, R. and Blaner, W., 2014. Retinoic acid receptor signaling is required to maintain glucose-stimulated insulin secretion and β-cell mass. *The FASEB Journal*, 29(2), pp.671-683.

Buchman, N., Strous, R. and Baruch, Y., 2002. Side Effects of Long-Term Treatment with Fluoxetine. *Clinical Neuropharmacology*, 25(1), pp.55-57.

Burcu, M., Zito, J., Safer, D., Magder, L., dosReis, S., Shaya, F. and Rosenthal, G., 2017. Concomitant Use of Atypical Antipsychotics with Other Psychotropic Medication Classes and the Risk of Type 2 Diabetes Mellitus. *Journal of the American Academy of Child & Adolescent Psychiatry*, 56(8), pp.642-651.

Burkart, V. and Kolb, H., 1996. Macrophages in Islet Destruction in Autoimmune Diabetes Mellitus. *Immunobiology*, 195(4-5), pp.601-613.

Burns, C., Squires, P. and Persaud, S., 2000. Signaling through the p38 and p42/44 Mitogen-Activated Families of Protein Kinases in Pancreatic β-Cell Proliferation. *Biochemical and Biophysical Research Communications*, 271(2), p.558.

Burrack, A., Martinov, T. and Fife, B., 2017. T Cell-Mediated Beta Cell Destruction: Autoimmunity and Alloimmunity in the Context of Type 1 Diabetes. *Frontiers in Endocrinology*, 8.

Burris, K., Molski, T., Xu, C., Ryan, E., Tottori, K., Kikuchi, T., Yocca, F. and Molinoff, P., 2002. Aripiprazole, a Novel Antipsychotic, Is a High-Affinity Partial Agonist at Human Dopamine D2 Receptors. *Journal of Pharmacology and Experimental Therapeutics*, 302(1), pp.381-389.

Butler, A., Janson, J., Bonner-Weir, S., Ritzel, R., Rizza, R. and Butler, P., 2003. -Cell Deficit and Increased β-Cell Apoptosis in Humans with Type 2 Diabetes. *Diabetes*, 52(1), pp.102-110.

Cabrera, O., Berman, D., Kenyon, N., Ricordi, C., Berggren, P. and Caicedo, A., 2006. The unique cytoarchitecture of human pancreatic islets has implications for islet cell function. *Proceedings of the National Academy of Sciences*, 103(7), pp.2334-2339.

Cadena-Herrera, D., Esparza-De Lara, J., Ramirez-Ibanez, N., Lopez-Morales, C., Perez, N., Flores-Ortiz, L. and Medina-Rivero, E., 2015. Validation of three viable cell counting methods: Manual, semi-automated, and automated. *Biotechnology Reports*, 7, pp.9-16.

Cakan, N., Kizilbash, S. and Kamat, D., 2012. Changing Spectrum of Diabetes Mellitus in Children. *Clinical Pediatrics*, 51(10), pp.939-944.

Campayo, A., de Jonge, P., Roy, J., Saz, P., de la Cámara, C., Quintanilla, M., Marcos, G., Santabárbara, J. and Lobo, A., 2010. Depressive Disorder and Incident Diabetes Mellitus: The Effect of Characteristics of Depression. *American Journal of Psychiatry*, 167(5), pp.580-588.

Campbell, J. and Newgard, C., 2021. Mechanisms controlling pancreatic islet cell function in insulin secretion. *Nature Reviews Molecular Cell Biology*, 22(2), pp.142-158.

Cataldo Bascunan, L., Lyons, C., Bennet, H., Artner, I. and Fex, M., 2018. Serotonergic regulation of insulin secretion. *Acta Physiologica*, 225(1), p.e13101.

Cataldo, L., Cortes, V., Mizgier, M., Aranda, E., Mezzano, D., Olmos, P., Galgani, J., Suazo, J. and Santos, J., 2015. Fluoxetine Impairs Insulin Secretion without Modifying Extracellular Serotonin Levels in MIN6 β-cells. *Experimental and Clinical Endocrinology & Diabetes*, 123(08), pp.473-478.

Cavelti-Weder, C., Furrer, R., Keller, C., Babians-Brunner, A., Solinger, A., Gast, H., Fontana, A., Donath, M. and Penner, I., 2012. Inhibition of IL-1 Improves Fatigue in Type 2 Diabetes. *Diabetes Care*, 34(10), pp.158-158.

Cell Biolabs, 2016. CytoSelect™ 96-Well Cell Migration Assay (5 µm, Fluorometric Format). San Diego, CA.

Cerf, M., 2013. Beta Cell Dysfunction and Insulin Resistance. *Frontiers in Endocrinology*, 4.

Chan, S., Chan, H., Honer, W., Bastiampillai, T., Suen, Y., Yeung, W., Lam, M., Lee, W., Ng, R., Hui, C., Chang, W., Lee, E. and Chen, E., 2021. Predictors of Treatment-Resistant and Clozapine-Resistant Schizophrenia: A 12-Year Follow-up Study of First-Episode Schizophrenia-Spectrum Disorders. *Schizophrenia Bulletin*, 47(2), pp.485-494.

Chang, H., Chen, S., Shen, M., Kung, M., Chuang, L. and Chen, Y., 2017. Selective serotonin reuptake inhibitor, fluoxetine, impairs E-cadherin-mediated cell adhesion and alters calcium homeostasis in pancreatic beta cells. *Scientific Reports*, 7(1).

Chathoth, V., Ramamurthy, P. and Solomon, S., 2018. Clozapine-induced Insulin-resistant Hyperglycemia in a Diabetic Patient. *Indian Journal of Psychological Medicine*, 40(4), pp.375-377.

Chee, Y., Ng, S. and Yeoh, E., 2020. Diabetic ketoacidosis precipitated by Covid-19 in a patient with newly diagnosed diabetes mellitus. *Diabetes Research and Clinical Practice*, 164, p.108166.

Chen, C., Cohrs, C., Stertmann, J., Bozsak, R. and Speier, S., 2017. Human beta cell mass and function in diabetes: Recent advances in knowledge and technologies to understand disease pathogenesis. *Molecular Metabolism*, 6(9), pp.943-957.

Chen, J., Wu, C., Wang, X., Yu, J. and Sun, Z., 2020. The Impact of COVID-19 on Blood Glucose: A Systematic Review and Meta-Analysis. *Frontiers in Endocrinology*, 11.

Chen, Y., Lin, W., Chen, Y., Mao, W. and Hung, Y., 2010. Antidepressant Effects on Insulin Sensitivity and Proinflammatory Cytokines in the Depressed Males. *Mediators of Inflammation*, 2010, pp.1-7.

Chen, Z., Morris, D., Jiang, L., Liu, Y. and Rui, L., 2014. SH2B1 in β-Cells Regulates Glucose Metabolism by Promoting β-Cell Survival and Islet Expansion. *Diabetes*, 63(2), pp.585-595.

Chesney, E., Goodwin, G. and Fazel, S., 2014. Risks of all-cause and suicide mortality in mental disorders: a meta-review. *World Psychiatry*, 13(2), pp.153-160.

Chikama, K., Yamada, H., Tsukamoto, T., Kajitani, K., Nakabeppu, Y. and Uchimura, N., 2017. Chronic atypical antipsychotics, but not haloperidol, increase neurogenesis in the hippocampus of adult mouse. *Brain Research*, 1676, pp.77-82.

Chiodini, I., Adda, G. and Scillitani, A., 2007. Cortisol Secretion in Patients with Type 2 Diabetes: Relationship With Chronic Complications. *Diabetes Care*, 30(1), pp.83-88.

Chipchura, D., Freyberg, Z., Edwards, C., Leckband, S. and McCarthy, M., 2018. Does the Time of Drug Administration Alter the Metabolic Risk of Aripiprazole?. *Frontiers in Psychiatry*, 9.

Chiwanda, L., Cordiner, M., Thompson, A. and Shajahan, P., 2016. Long-term antidepressant treatment in general practice: changes in body mass index. *BJPsych Bulletin*, 40(6), pp.310-314.

Cho, J., Kim, J., Shin, J., Shin, J. and Yoon, K., 2010. β-cell mass in people with type 2 diabetes. *Journal of Diabetes Investigation*, 2(1), pp.6-17.

Choi, J., Choi, B., Ahn, H., Kim, M., Rhie, D., Yoon, S., Min, D., Jo, Y., Kim, M., Sung, K. and Hahn, S., 2003. Mechanism of block by fluoxetine of 5-hydroxytryptamine3 (5-HT3)-mediated currents in NCB-20 neuroblastoma cells. *Biochemical Pharmacology*, 66(11), pp.2125-2132.

Choi, S., Jang, J. and Park, S., 2005. Estrogen and Exercise May Enhance β-Cell Function and Mass via Insulin Receptor Substrate 2 Induction in Ovariectomized Diabetic Rats. Endocrinology, 146(11), pp.4786-4794.

Chrousos, G., 2009. Stress and disorders of the stress system. *Nature Reviews Endocrinology*, 5(7), pp.374-381.

Cikankova, T., Fisar, Z. and Hroudová, J., 2019. In vitro effects of antidepressants and mood-stabilizing drugs on cell energy metabolism. *Naunyn-Schmiedeberg's Archives of Pharmacology*, 393(5), pp.797-811.

Citrome, L., 2006. A review of aripiprazole in the treatment of patients with schizophrenia or bipolar I disorder. *Neuropsychiatric Disease and Treatment*, 2(4), pp.427-443.

Citrome, L., Kamat, S., Sapin, C., Baker, R., Eramo, A., Ortendahl, J., Gutierrez, B., Hansen, K. and Bentley, T., 2014. Cost-effectiveness of aripiprazole once-monthly compared with paliperidone palmitate once-monthly injectable for the treatment of schizophrenia in the United States. *Journal of Medical Economics*, 17(8), pp.567-576.

Claassen, V., Davies, J., Hertting, G. and Placheta, P., 1977. Fluvoxamine, a specific 5-hydroxytryptamine uptake inhibitor. B*ritish Journal of Pharmacology*, 60(4), pp.505-516.

Clarke, T., Obsteter, J., Hall, L., Hayward, C., Thomson, P., Smith, B., Padmanabhan, S., Hocking, L., Deary, I., Porteous, D. and McIntosh, A., 2016. Investigating shared aetiology between type 2 diabetes and major depressive disorder in a populationbased cohort. *American Journal of Medical Genetics Part B: Neuropsychiatric Genetics*, 174(3), pp.227-234.

Cnop, M., Welsh, N., Jonas, J., Jorns, A., Lenzen, S. and Eizirik, D., 2005. Mechanisms of Pancreatic β-Cell Death in Type 1 and Type 2 Diabetes: Many Differences, Few Similarities. *Diabetes*, 54(Supplement 2), pp.97-107.

Colle, R., de Larminat, D., Rotenberg, S., Hozer, F., Hardy, P., Verstuyft, C., Fève, B. and Corruble, E., 2016. Pioglitazone could induce remission in major depression: a meta-analysis. Neuropsychiatric Disease and Treatment, Volume 13, pp.9-16.

Connolly, V., Gallagher, A. and Kesson, C., 1995. A Study of Fluoxetine in Obese Elderly Patients with Type 2 Diabetes. *Diabetic Medicine*, 12(5), pp.416-418.

Contreras-Shannon, V., Heart, D., Paredes, R., Navaira, E., Catano, G., Maffi, S. and Walss-Bass, C., 2013. Clozapine-Induced Mitochondria Alterations and Inflammation in Brain and Insulin-Responsive Cells. *PLoS ONE*, 8(3), p.e59012.

Covid19.who.int. 2021. *WHO Coronavirus (COVID-19) Dashboard*. [online] Available at: <https://covid19.who.int/> [Accessed 1 December 2021].

Craig, M., Hattersley, A. and Donaghue, K., 2009. Definition, epidemiology and classification of diabetes in children and adolescents. *Pediatric Diabetes*, 10, pp.3-12.

Craske, M. G. and Stein, M. B., 2016. Anxiety. *Lancet*, 388, pp.3048–3059.

Craske, M., Stein, M., Eley, T., 2017. Anxiety disorders. *Nature Reviews Disease Primers*, 3, pp.17024.

Cucak, H., Grunnet, L. and Rosendahl, A., 2013. Accumulation of M1-like macrophages in type 2 diabetic islets is followed by a systemic shift in macrophage polarization. *Journal of Leukocyte Biology*, 95(1), pp.149-160.

Cukierman, T., Gerstein, H. and Williamson, J., 2005. Cognitive decline and dementia in diabetes—systematic overview of prospective observational studies. *Diabetologia*, 48(12), pp.2460-2469.

Cuylen, S., Blaukopf, C., Politi, A., Müller-Reichert, T., Neumann, B., Poser, I., Ellenberg, J., Hyman, A. and Gerlich, D., 2016. Ki-67 acts as a biological surfactant to disperse mitotic chromosomes. Nature, 535(7611), pp.308-312.

Dabelea, D., Mayer-Davis, E., Saydah, S., Imperatore, G., Linder, B., Divers, J., Bell, R., Badaru, A., Talton, J., Crume, T., Liese, A., Merchant, A., Lawrence, J., Reynolds, K., Dolan, L., Liu, L. and Hamman, R., 2014. Prevalence of Type 1 and Type 2 Diabetes Among Children and Adolescents From 2001 to 2009. *JAMA*, 311(17), p.1778.

Dai, B., Wei, D., Zheng, N., Chi, Z., Xin, N., Ma, T., Zheng, L., Sumi, R. and Sun, L., 2018. Coccomyxa Gloeobotrydiformis Polysaccharide Inhibits Lipopolysaccharide-Induced Inflammation in RAW 264.7 Macrophages. *Cellular Physiology and Biochemistry*, 51(6), pp.2523-2535.

Dalle, S., Quoyer, J., Varin, E. and Costes, S., 2011. Roles and Regulation of the Transcription Factor CREB in Pancreatic β -Cells. *Current Molecular Pharmacology*, 4(3), pp.187-195.

Danaei, G., Finucane, M., Lu, Y., Singh, G., Cowan, M., Paciorek, C., Lin, J., Farzadfar, F., Khang, Y., Stevens, G., Rao, M., Ali, M., Riley, L., Robinson, C. and Ezzati, M., 2011. National, regional, and global trends in fasting plasma glucose and diabetes prevalence since 1980: systematic analysis of health examination surveys and epidemiological studies with 370 country-years and 2·7 million participants. *The Lancet*, 378(9785), pp.31-40.

Darmon, M., Al Awabdh, S., Emerit, M. B., & Masson, J., 2015. Insights into Serotonin Receptor Trafficking: Cell Membrane Targeting and Internalization. *Progress in Molecular Biology and Translational Science*, 132, pp.97–126.

Daziano, G., Blondeau, N., Beraud-Dufour, S., Abderrahmani, A., Rovere, C., Heurteaux, C., Mazella, J., Lebrun, P. and Coppola, T., 2021. Sortilin-derived peptides promote pancreatic beta-cell survival through CREB signaling pathway. *Pharmacological Research*, 167, p.105539.

De Bartolomeis, A., Tomasetti, C. and Iasevoli, F., 2015. Update on the Mechanism of Action of Aripiprazole: Translational Insights into Antipsychotic Strategies Beyond Dopamine Receptor Antagonism. *CNS Drugs*, 29(9), pp.773-799.

De Fazio, P., Gaetano, R., Caroleo, M., Cerminara, G., Maida, F., Bruno, A., Muscatello, M., Jaen Moreno, M., Russo, E. and Segura-Garcìa, C., 2015. Rare and very rare adverse effects of clozapine. *Neuropsychiatric Disease and Treatment*, p.1995.

De Long, N., Hardy, D., Ma, N. and Holloway, A., 2017. Increased incidence of non-alcoholic fatty liver disease in male rat offspring exposed to fluoxetine during fetal and neonatal life involves the NLRP3 inflammasome and augmented de novo hepatic lipogenesis. *Journal of Applied Toxicology*, 37(12), pp.1507-1516.

De Oliveira, M., 2016. Fluoxetine and the mitochondria: A review of the toxicological aspects. *Toxicology Letters*, 258, pp.185-191.

De Vries, E., Gietema, J. and de Jong, S., 2006. Tumor Necrosis Factor–Related Apoptosis-Inducing Ligand Pathway and Its Therapeutic Implications. *Clinical Cancer Research*, 12(8), pp.2390-2393.

Dean, P. and Matthews, E., 1968. Electrical Activity in Pancreatic Islet Cells. *Nature*, 219(5152), pp.389-390.

Deshpande, A., Harris-Hayes, M. and Schootman, M., 2008. Epidemiology of Diabetes and Diabetes-Related Complications. *Physical Therapy*, 88(11), pp.1254-1264.

Deuschle, M., 2013. Effects of antidepressants on glucose metabolism and diabetes mellitus type 2 in adults. *Current Opinion in Psychiatry*, 26(1), pp.60-65.

Devaskar, S., Giddings, S., Rajakumar, P., Carnaghi, L., Menon, R. and Zahm, D., 1994. Insulin gene expression and insulin synthesis in mammalian neuronal cells. *Journal of Biological Chemistry*, 269(11), pp.8445-8454.

Devendra, D., Liu, E. and Eisenbarth, G., 2004. Type 1 diabetes: recent developments. *BMJ*, 328(7442), pp.750-754.

Docherty, F. and Sussel, L., 2021. Islet Regeneration: Endogenous and Exogenous Approaches. *International Journal of Molecular Sciences*, 22(7), p.3306.

Dolensek, J., Rupnik, M. and Stozer, A., 2015. Structural similarities and differences between the human and the mouse pancreas. *Islets*, 7(1), p.e1024405.

Donath, M. and Halban, P., 2004. Decreased beta-cell mass in diabetes: significance, mechanisms and therapeutic implications. *Diabetologia*, 47(3), pp.581-589.

Donath, M., Ehses, J., Maedler, K., Schumann, D., Ellingsgaard, H., Eppler, E. and Reinecke, M., 2005. Mechanisms of β-Cell Death in Type 2 Diabetes. *Diabetes*, 54(Supplement 2), pp.108-113.

Doupis, J., Baris, N. and Avramidis, K., 2021. Imeglimin: A New Promising and Effective Weapon in the Treatment of Type 2 Diabetes. *European Endocrinology*, 17(2), p.88.

Doyle, M. and Egan, J., 2007. Mechanisms of action of glucagon-like peptide 1 in the pancreas. *Pharmacology & Therapeutics*, 113(3), pp.546-593.

Duan, W., Peng, Q., Masuda, N., Ford, E., Tryggestad, E., Ladenheim, B., Zhao, M., Cadet, J., Wong, J. and Ross, C., 2008. Sertraline slows disease progression and increases neurogenesis in N171-82Q mouse model of Huntington's disease. *Neurobiology of Disease*, 30(3), pp.312-322.

Duttaroy, A., Zimliki, C., Gautam, D., Cui, Y., Mears, D. and Wess, J., 2004. Muscarinic Stimulation of Pancreatic Insulin and Glucagon Release Is Abolished in M3 Muscarinic Acetylcholine Receptor-Deficient Mice. *Diabetes*, 53(7), pp.1714-1720.

Dyson, P., 2010. The therapeutics of lifestyle management on obesity. *Diabetes, Obesity and Metabolism*, 12(11), pp.941-946.

Ebekozien, O., Agarwal, S., Noor, N., Albanese-O'Neill, A., Wong, J., Seeherunvong, T., Sanchez, J., DeSalvo, D., Lyons, S., Majidi, S., Wood, J., Acharya, R., Aleppo, G., Sumpter, K., Cymbaluk, A., Shah, N., Van Name, M., Cruz-Aviles, L., Alonso, G., Gallagher, M., Sanda, S., Feuer, A., Cossen, K., Rioles, N., Jones, N., Kamboj, M. and Hirsch, I., 2020. Inequities in Diabetic Ketoacidosis Among Patients with Type 1 Diabetes and COVID-19: Data From 52 US Clinical Centers. *The Journal of Clinical Endocrinology & Metabolism*, 106(4), pp.1755-1762.

Egede, L., Zheng, D. and Simpson, K., 2002. Comorbid Depression is Associated with Increased Health Care Use and Expenditures in Individuals with Diabetes. *Diabetes Care*, 25(3), pp.464-470.

Ehses, J., Perren, A., Eppler, E., Ribaux, P., Pospisilik, J., Maor-Cahn, R., Gueripel, X., Ellingsgaard, H., Schneider, M., Biollaz, G., Fontana, A., Reinecke, M., Homo-Delarche, F. and Donath, M., 2007. Increased Number of Islet-Associated Macrophages in Type 2 Diabetes. *Diabetes*, 56(9), pp.2356-2370.

Eisenhofer, G., Goldstein, D., Sullivan, P., Csako, G., Brouwers, F., Lai, E., Adams, K. and Pacak, K., 2005. Biochemical and Clinical Manifestations of Dopamine-Producing Paragangliomas: Utility of Plasma Methoxytyramine. *The Journal of Clinical Endocrinology & Metabolism*, 90(4), pp.2068-2075.

Elghazi, L. and Bernal-Mizrachi, E., 2009. Akt and PTEN: β-cell mass and pancreas plasticity. *Trends in Endocrinology & Metabolism*, 20(5), pp.243-251.

El-Merahbi, R., Löffler, M., Mayer, A. and Sumara, G., 2015. The roles of peripheral serotonin in metabolic homeostasis. *FEBS Letters*, 589(15), pp.1728-1734.

Elmorsy, E., Al-Ghafari, A., Helaly, A., Hisab, A., Oehrle, B. and Smith, P., 2017. Editor's Highlight: Therapeutic Concentrations of Antidepressants Inhibit Pancreatic Beta-Cell Function via Mitochondrial Complex Inhibition. *Toxicological Sciences*, 158(2), pp.286-301.

Eryilmaz, G., Hizli Sayar, G., Ozten, E., Gül, I., Karamustafalioglu, O. and Yorbik, Ö., 2014. Effect of valproate on the plasma concentrations of aripiprazole in bipolar patients. *International Journal of Psychiatry in Clinical Practice*, 18(4), pp.288-292.

Fan, X., Borba, C., Copeland, P., Hayden, D., Freudenreich, O., Goff, D. and Henderson, D., 2012. Metabolic effects of adjunctive aripiprazole in clozapine-treated patients with schizophrenia. *Acta Psychiatrica Scandinavica*, 127(3), pp.217-226.

Fang, J. and Mosier, K., 2014. Literature Values of Terminal Half-Lives of Clozapine are Dependent on the Time of the Last Data Point. *Journal of Pharmacy & Pharmaceutical Sciences*, 17(2), p.187.

Farino, Z. J., Morgenstern, T. J., Maffei, A., Quick, M., De Solis, A. J., Wiriyasermkul, P., Freyberg, R. J., Aslanoglou, D., Sorisio, D., Inbar, B. P., Free, R. B., Donthamsetti, P., Mosharov, E. V., Kellendonk, C., Schwartz, G. J., Sibley, D. R., Schmauss, C., Zeltser, L. M., Moore, H., Harris, P. E., … Freyberg, Z., 2020. New roles for dopamine D_2 and D_3 receptors in pancreatic beta cell insulin secretion. *Molecular psychiatry,* 25(9), pp.2070–2085.

Farooq, S., Choudry, A., Cohen, D., Naeem, F. and Ayub, M., 2019. Barriers to using clozapine in treatment-resistant schizophrenia: systematic review. *BJPsych Bulletin*, 43(1), pp.8-16.

Fava, M., Judge, R., Hoog, S., Nilsson, M. and Koke, S., 2000. Fluoxetine Versus Sertraline and Paroxetine in Major Depressive Disorder. *The Journal of Clinical Psychiatry*, 61(11), pp.863-867.

Feldman, A., Griffin, S., Ahern, A., Long, G., Weinehall, L., Fharm, E., Norberg, M. and Wennberg, P., 2017. Impact of weight maintenance and loss on diabetes risk and burden: a population-based study in 33,184 participants. *BMC Public Health*, 17(1).

Fellner C., 2016. Novel Treatments Target Type-2 Diabetes. *P T.*, 41(10), pp.650-653.

Fleischhacker, W. W. and Uchida, H., 2014. Critical review of antipsychotic polypharmacy in the treatment of schizophrenia. *The international journal of neuropsychopharmacology*, 17(7), pp.1083–1093.

Forno, F., Maatuf, Y., Boukeileh, S., Dipta, P., Mahameed, M., Darawshi, O., Ferreira, V., Rada, P., García-Martinez, I., Gross, E., Priel, A., Valverde, Á. and Tirosh, B., 2020. Aripiprazole Cytotoxicity Coincides with Activation of the Unfolded Protein Response in Human Hepatic Cells. *Journal of Pharmacology and Experimental Therapeutics*, 374(3), pp.452-461.

Frazer, A. and Benmansour, S., 2002. Delayed pharmacological effects of antidepressants. *Molecular Psychiatry*, 7(S1), pp.23-28.

Frizzo, M., 2017. Can a Selective Serotonin Reuptake Inhibitor Act as a Glutamatergic Modulator?. *Current Therapeutic Research*, 87, pp.9-12.

Fu, Z., R. Gilbert, E. and Liu, D., 2013. Regulation of Insulin Synthesis and Secretion and Pancreatic Beta-Cell Dysfunction in Diabetes. *Current Diabetes Reviews*, 9(1), pp.25-53.

Funderburg, L., True, J., Velligan, D., Miller, A., Moore, T. and Maas, J., 1994. Neurological changes with clozapine treatment. *Neuropsychopharmacology*, 11(4), pp.269-269.

Fusco, J., Xiao, X., Prasadan, K., Sheng, Q., Chen, C., Ming, Y. and Gittes, G., 2017. GLP-1/Exendin-4 induces β-cell proliferation via the epidermal growth factor receptor. *Scientific Reports*, 7(1).

Gaisano, H., MacDonald, P. and Vranic, M., 2012. Glucagon secretion and signaling in the development of diabetes. *Frontiers in Physiology*, 3.

Garcia-Colunga, J., Awad, J. and Miledi, R., 1997. Blockage of muscle and neuronal nicotinic acetylcholine receptors by fluoxetine (Prozac). *Proceedings of the National Academy of Sciences*, 94(5), pp.2041-2044.

García-Ocana, A., Vasavada, R., Takane, K., Cebrian, A., Lopez-Talavera, J. and Stewart, A., 2001. Using β-Cell Growth Factors to Enhance Human Pancreatic Islet Transplantation*. *The Journal of Clinical Endocrinology & Metabolism*, 86(3), pp.984-988.

Garcia-Vargas, L., Addison, S., Nistala, R., Kurukulasuriya, D. and Sowers, J., 2012. Gestational Diabetes and the Offspring: Implications in the Development of the Cardiorenal Metabolic Syndrome in Offspring. *Cardiorenal Medicine*, 2(2), pp.134-142.

Gautam, D., Han, S., Hamdan, F., Jeon, J., Li, B., Li, J., Cui, Y., Mears, D., Lu, H., Deng, C., Heard, T. and Wess, J., 2006. A critical role for β cell M3 muscarinic acetylcholine receptors in regulating insulin release and blood glucose homeostasis *in vivo*. *Cell Metabolism*, 3(6), pp.449-461.

Gehlawat, P., Gupta, R., Rajput, R., Gahlan, D. and Gehlawat, V., 2013. Diabetes with comorbid depression: Role of SSRI in better glycemic control. *Asian Journal of Psychiatry*, 6(5), pp.364-368.

Georgia, S. and Bhushan, A., 2010. Pregnancy hormones boost beta cells via serotonin. *Nature Medicine*, 16(7), pp.756-757.

Geravandi, S., Mahmoudi-Aznaveh, A., Azizi, Z., Maedler, K. and Ardestani, A., 2021. SARS-CoV-2 and pancreas: a potential pathological interaction?. *Trends in Endocrinology & Metabolism*, 32(11), pp.842-845.

Gershon, M., 2013. 5-Hydroxytryptamine (serotonin) in the gastrointestinal tract. *Current Opinion in Endocrinology, Diabetes & Obesity*, 20(1), pp.14-21.

Gerstein, H. C., Colhoun, H. M., Dagenais, G. R., Diaz, R., Lakshmanan, M., Pais, P., Probstfield, J., Riesmeyer, J. S., Riddle, M. C., Rayden, L., 2019. Dulaglutide and cardiovascular outcomes in type 2 diabetes (REWIND): a doubleblind, randomised placebo- controlled trial. *Lancet*, 394, pp. 121–130.

Gey, G. and Gey, M., 1936. The Maintenance of Human Normal Cells and Tumor Cells in Continuous Culture: I. Preliminary Report: Cultivation of Mesoblastic Tumors and Normal Tissue and Notes on Methods of Cultivation. *The American Journal of Cancer*, 27(1), pp.45-76.

Ghavami, S., Shojaei, S., Yeganeh, B., Ande, S., Jangamreddy, J., Mehrpour, M., Christoffersson, J., Chaabane, W., Moghadam, A., Kashani, H., Hashemi, M., Owji, A. and Łos, M., 2014. Autophagy and apoptosis dysfunction in neurodegenerative disorders. *Progress in Neurobiology*, 112, pp.24-49.

Gianfrancesco, F., Pesa, J., Wang, R. and Nasrallah, H., 2006. Assessment of antipsychotic-related risk of diabetes mellitus in a Medicaid psychosis population: Sensitivity to study design. *American Journal of Health-System Pharmacy*, 63(5), pp.431-441.

Ginovart, N., Kapur, S., 2012. Role of dopamine D(2) receptors for antipsychotic activity. *Handbook of Experimental Pharmacology*, 212, pp.27–52.

Goldstein, D., Eisenhofer, G. and Kopin, I., 2003. Sources and Significance of Plasma Levels of Catechols and Their Metabolites in Humans. *Journal of Pharmacology and Experimental Therapeutics*, 305(3), pp.800-811.

Gomez, R., Huber, J., Lhullier, F. and Barros, H., 2001. Plasma insulin levels are increased by sertraline in rats under oral glucose overload. *Brazilian Journal of Medical and Biological Research*, 34(12), pp.1569-1572.

Gonzalez, J., Tanenbaum, M. and Commissariat, P., 2016. Psychosocial factors in medication adherence and diabetes self-management: Implications for research and practice. *American Psychologist*, 71(7), pp.539-551.

Goodnick, P. J., Kumar, A., Henry, J. H., Buki, V. M., Goldberg, R. B.,, 1997. Sertraline in coexisting major depression and diabetes mellitus. *Psychopharmacology Bulletin*, 33, pp.261–264.

Gragnoli, C., 2012. Depression and type 2 diabetes: Cortisol pathway implication and investigational needs. *Journal of Cellular Physiology*, 227(6), pp.2318-2322.

Grajales, D., Ferreira, V. and Valverde, Á., 2019. Second-Generation Antipsychotics and Dysregulation of Glucose Metabolism: Beyond Weight Gain. *Cells*, 8(11), p.1336.

Grange, R., Thompson, J. and Lambert, D., 2014. Radioimmunoassay, enzyme and non-enzyme-based immunoassays. *British Journal of Anaesthesia*, 112(2), pp.213-216.

Grant, R. and Dixit, V., 2013. Mechanisms of disease: inflammasome activation and the development of type 2 diabetes. *Frontiers in Immunology*, 4.

Greenstein, B., Wood, D., 2011. The endocrine system at a glance (1st ed.) Wiley-Blackwell, Chichester, UK.

Grohol, J., 2019. *Top 25 Psychiatric Medications for 2018*. [online] Psych Central. Available at: <https://psychcentral.com/blog/top-25-psychiatric-medications-for-2018?li_source=LI&li_medium=popular17> [Accessed 7 December 2021].

Grover, S., Hazari, N., Chakrabarti, S. and Avasthi, A., 2016. Metabolic Disturbances, Side Effect Profile and Effectiveness of Clozapine in Adolescents. *Indian Journal of Psychological Medicine*, 38(3), pp.224-233.

Grunder, G., Fellows, C., Janouschek, H., Veselinovic, T., Boy, C., Brocheler, A., Kirschbaum, K., Hellmann, S., Spreckelmeyer, K., Hiemke, C., Rosch, F., Schaefer, W. and Vernaleken, I., 2008. Brain and Plasma Pharmacokinetics of Aripiprazole in Patients with Schizophrenia: An [18F] Fallypride PET Study. *American Journal of Psychiatry*, 165(8), pp.988-995.

Grunder, G., Hippius, H. and Carlsson, A., 2009. The 'atypicality' of antipsychotics: a concept re-examined and re-defined. *Nature Reviews Drug Discovery*, 8(3), pp.197-202.

Guo, M., Mi, J., Jiang, Q., Xu, J., Tang, Y., Tian, G. and Wang, B., 2014. Metformin may produce antidepressant effects through improvement of cognitive function among depressed patients with diabetes mellitus. *Clinical and Experimental Pharmacology and Physiology*, p.n/a-n/a.

Gupta, A., Madhavan, M.V., Sehgal, K., Nair, N., Mahajan, S., Sehrawat, T. S., Bikdeli, B., Ahluwalia, N., Ausiello, J. C., Wan, E. Y., Freedberg, D. E., Kirtane, A. J., Parikh , S. A., Maurer,

M. S., Nordvig, A. S., Accili, D., Bathon, J. M., Mohan, S., Bauer, K. A., Leon, M. B., Krumholz, H. M., Uriel, N., Mehra, M. R., Elkind, M. S. V., Stone, G. W., Schwartz, A., Ho, D. D.,Bilezikian, J. P., Landry, D. W., 2020. Extrapulmonary manifestations of COVID-19. *Nature Medicine*, 26, pp.1017–1032.Guzman, F., 2021. *Psychopharmacology Institute*. [online] Psychopharmacologyinstitute.com. Available at: <https://psychopharmacologyinstitute.com/publication/aripiprazole-indications-fda-approved-and-off-label-uses-2120> [Accessed 1 December 2021].

Haapakoski, R., Mathieu, J., Ebmeier, K., Alenius, H. and Kivimäki, M., 2015. Cumulative meta-analysis of interleukins 6 and 1β, tumour necrosis factor α and C-reactive protein in patients with major depressive disorder. *Brain, Behavior, and Immunity*, 49, pp.206-215.

Habeb, A., Al-Magamsi, M., Eid, I., Ali, M., Hattersley, A., Hussain, K. and Ellard, S., 2011. Incidence, genetics, and clinical phenotype of permanent neonatal diabetes mellitus in northwest Saudi Arabia. *Pediatric Diabetes*, 13(6), pp.499-505.

Habegger, K., Heppner, K., Geary, N., Bartness, T., DiMarchi, R. and Tschöp, M., 2010. The metabolic actions of glucagon revisited. *Nature Reviews Endocrinology*, 6(12), pp.689-697.

Hackinger, S., Prins, B., Mamakou, V., Zengini, E., Marouli, E., Brčić, L., Serafetinidis, I., Lamnissou, K., Kontaxakis, V., Dedoussis, G., Gonidakis, F., Thanopoulou, A., Tentolouris, N., Tsezou, A. and Zeggini, E., 2018. Evidence for genetic contribution to the increased risk of type 2 diabetes in schizophrenia. *Translational Psychiatry*, 8(1).

Haidary, H. A., Padhy, R. K., 2020. Clozapine. In: StatPearls [Internet]. Treasure Island (FL): StatPearls Publishing. Available at: https://www.ncbi.nlm.nih.gov/books/NBK535399/

Hajek, T., Calkin, C., Blagdon, R., Slaney, C., Uher, R. and Alda, M., 2014. Insulin Resistance, Diabetes Mellitus, and Brain Structure in Bipolar Disorders. Neuropsychopharmacology, 39(12), pp.2910-2918.

Halim, N., Weickert, C., McClintock, B., Weinberger, D. and Lipska, B., 2004. Effects of Chronic Haloperidol and Clozapine Treatment on Neurogenesis in the Adult Rat Hippocampus. *Neuropsychopharmacology*, 29(6), pp.1063-1069.

Hallakou-Bozec, S., Kergoat, M., Fouqueray, P., Bolze, S. and Moller, D., 2021. Imeglimin amplifies glucose-stimulated insulin release from diabetic islets via a distinct mechanism of action. *PLOS ONE*, 16(2), p.e0241651.

Hammen, C., Watkins, E., 2008. Depression (2nd ed.). Psychology Press, East Sussex.

Harding, H. and Ron, D., 2002. Endoplasmic Reticulum Stress and the Development of Diabetes: A Review. *Diabetes*, 51(Supplement 3), pp.S455-S461.

Hartig, S. and Cox, A., 2020. Correction to: Paracrine signaling in islet function and survival. *Journal of Molecular Medicine*, 98(4), pp.469-469.

Hayden, M. and Sowers, J., 2007. Isletopathy in Type 2 Diabetes Mellitus: Implications of Islet RAS, Islet Fibrosis, Islet Amyloid, Remodeling, and Oxidative Stress. *Antioxidants & Redox Signaling*, 9(7), pp.891-910.

Hayes, H., Peterson, B., Haldeman, J., Newgard, C., Hohmeier, H. and Stephens, S., 2017. Delayed apoptosis allows islet β-cells to implement an autophagic mechanism to promote cell survival. *PLOS ONE*, 12(2), p.e0172567.

Haythorne, E., Rohm, M., van de Bunt, M., Brereton, M., Tarasov, A., Blacker, T., Sachse, G., Silva dos Santos, M., Terron Exposito, R., Davis, S., Baba, O., Fischer, R., Duchen, M., Rorsman, P., MacRae, J. and Ashcroft, F., 2019. Diabetes causes marked inhibition of mitochondrial metabolism in pancreatic β-cells. *Nature Communications*, 10(1).

Henquin, J., 2021. Paracrine and autocrine control of insulin secretion in human islets: evidence and pending questions. *American Journal of Physiology-Endocrinology and Metabolism*, 320(1), pp.E78-E86.

Henquin, J., Ishiyama, N., Nenquin, M., Ravier, M. and Jonas, J., 2002. Signals and Pools Underlying Biphasic Insulin Secretion. *Diabetes*, 51(Supplement 1), pp.S60-S67.

Herbert, J., Goodyer, I., Grossman, A., Hastings, M., de Kloet, E., Lightman, S., Lupien, S., Roozendaal, B. and Seckl, J., 2006. Do Corticosteroids Damage the Brain?. *Journal of Neuroendocrinology*, 18(6), pp.393-411.

Hernandez, A. F., Green, J. B., Janmohamed, S., D'Agostino, R. B., Granger, C. B., Jones, N. P., 2018. Albiglutide and cardiovascular outcomes in patients with type 2 diabetes and cardiovascular disease (Harmony Outcomes): a double- blind, randomised placebo- controlled trial. *Lancet*, 392, pp.1519–1529.

Hertz, L., Rothman, D., Li, B. and Peng, L., 2015. Chronic SSRI stimulation of astrocytic 5-HT2B receptors change multiple gene expressions/editings and metabolism of glutamate, glucose and glycogen: a potential paradigm shift. *Frontiers in Behavioral Neuroscience*, 9.

Hicks, J., Bishop, J., Sangkuhl, K., Müller, D., Ji, Y., Leckband, S., Leeder, J., Graham, R., Chiulli, D., LLerena, A., Skaar, T., Scott, S., Stingl, J., Klein, T., Caudle, K. and Gaedigk, A., 2015. Clinical Pharmacogenetics Implementation Consortium (CPIC) Guideline forCYP2D6andCYP2C19Genotypes and Dosing of Selective Serotonin Reuptake Inhibitors. *Clinical Pharmacology & Therapeutics*, 98(2), pp.127-134.

Hill, D., Hogg, J., Petrik, J., Arany, E. and Han, V., 1999. Cellular distribution and ontogeny of insulin-like growth factors (IGFs) and IGF binding protein messenger RNAs and peptides in developing rat pancreas. *Journal of Endocrinology*, 160(2), pp.305-317.

Hirsch, L. and Pringsheim, T., 2016. Aripiprazole for autism spectrum disorders (ASD). *Cochrane Database of Systematic Reviews*, 2016(6), CD009043.

Hollstein, T., Schulte, D., Schulz, J., Gluck, A., Ziegler, A., Bonifacio, E., Wendorff, M., Franke, A., Schreiber, S., Bornstein, S. and Laudes, M., 2020. Autoantibody-negative insulin-dependent diabetes mellitus after SARS-CoV-2 infection: a case report. *Nature Metabolism*, 2(10), pp.1021-1024.

Holt, H., Talaei, M., Greenig, M., Zenner, D., Symons, J., Relton, C., Young, K., Davies, M., Thompson, K., Ashman, J., Rajpoot, S., Kayyale, A., El Rifai, S., Lloyd, P., Jolliffe, D., Finer, S., Ilidriomiti, S., Miners, A., Hopkinson, N., Alam, B., Pfeffer, P., McCoy, D., Davies, G., Lyons, R.,

Griffiths, C., Kee, F., Sheikh, A., Breen, G., Shaheen, S. and Martineau, A., 2021. Risk Factors for Developing COVID-19: A Population-Based Longitudinal Study (COVIDENCE UK). *Thorax,* thoraxjnl-2021-217487. Advance online publication.

Holt, R. and Peveler, R., 2009. Obesity, serious mental illness and antipsychotic drugs. *Diabetes, Obesity and Metabolism*, 11(7), pp.665-679.

Holt, R., 2019. Association Between Antipsychotic Medication Use and Diabetes. *Current Diabetes Reports*, 19(10).

Howes, O., Bhatnagar, A., Gaughran, F., Amiel, S., Murray, R. and Pilowsky, L., 2004. A Prospective Study of Impairment in Glucose Control Caused by Clozapine Without Changes in Insulin Resistance. *American Journal of Psychiatry*, 161(2), pp.361-363.

Hu, X., Zhou, H., Zhang, D., Yang, S., Qian, L., Wu, H., Chen, P., Wilson, B., Gao, H., Lu, R. and Hong, J., 2011. Clozapine Protects Dopaminergic Neurons from Inflammation-Induced Damage by Inhibiting Microglial Overactivation. *Journal of Neuroimmune Pharmacology*, 7(1), pp.187-201.

Huang, C., Snider, F. and Cross, J., 2008. Prolactin Receptor Is Required for Normal Glucose Homeostasis and Modulation of β-Cell Mass during Pregnancy. *Endocrinology*, 150(4), pp.1618-1626.

Huang, Y., Karuranga, S., Malanda, B. and Williams, D., 2018. Call for data contribution to the IDF Diabetes Atlas 9th Edition 2019. *Diabetes Research and Clinical Practice*, 140, pp.351-352.

Hudish, L., Reusch, J. and Sussel, L., 2019. β Cell dysfunction during progression of metabolic syndrome to type 2 diabetes. *Journal of Clinical Investigation*, 129(10), pp.4001-4008.

Hughes, W., Elgundi, Z., Huang, P., Frohman, M. and Biden, T., 2004. Phospholipase D1 Regulates Secretagogue-stimulated Insulin Release in Pancreatic β-Cells. *Journal of Biological Chemistry*, 279(26), pp.27534-27541.

Hulse, R. E., Ralat, L. A., Wei-Jen, T., 2009. Structure, function, and regulation of insulin-degrading enzyme. *Vitamins and hormones,* 80, pp.635–648.

Hussain, M., Porras, D., Rowe, M., West, J., Song, W., Schreiber, W. and Wondisford, F., 2006. Increased Pancreatic β-Cell Proliferation Mediated by CREB Binding Protein Gene Activation. *Molecular and Cellular Biology*, 26(20), pp.7747-7759.

I. S. Sobczak, A., A. Blindauer, C. and J. Stewart, A., 2019. Changes in Plasma Free Fatty Acids Associated with Type-2 Diabetes. *Nutrients*, 11(9), p.2022.

Imagawa, A., Hanafusa, T., Miyagawa, J. and Matsuzawa, Y., 2000. A Novel Subtype of Type 1 Diabetes Mellitus Characterized by a Rapid Onset and an Absence of Diabetes-Related Antibodies. *New England Journal of Medicine*, 342(5), pp.301-307.

Ingimarsson, O., MacCabe, J., Haraldsson, M., Jonsdottir, H. and Sigurdsson, E., 2017. Risk of diabetes and dyslipidemia during clozapine and other antipsychotic drug treatment of schizophrenia in Iceland. *Nordic Journal of Psychiatry*, 71(7), pp.496-502.

International Diabetes Federation, 2019. IDF Diabetes Atlas (10th ed.) Brussels, Belgium.

International Diabetes Federation, 2021. IDF Diabetes Atlas (9th ed.) Brussels, Belgium.

Isaac, R., Boura-Halfon, S., Gurevitch, D., Shainskaya, A., Levkovitz, Y. and Zick, Y., 2013. Selective Serotonin Reuptake Inhibitors (SSRIs) Inhibit Insulin Secretion and Action in Pancreatic β Cells*. *Journal of Biological Chemistry*, 288(8), pp.5682-5693.

Ishihara, H., Asano, T., Tsukuda, K., Katagiri, H., Inukai, K., Anai, M., Kikuchi, M., Yazaki, Y., Miyazaki, J. and Oka, Y., 1994. Overexpression of hexokinase I but not GLUT1 glucose transporter alters concentration dependence of glucose-stimulated insulin secretion in pancreatic beta-cell line MIN6. *Journal of Biological Chemistry*, 269(4), pp.3081-3087.

Ishihara, H., Asano, T., Tsukuda, K., Katagiri, H., Inukai, K., Anai, M., Kikuchi, M., Yazaki, Y., Miyazaki, J. and Oka, Y., 1993. Pancreatic beta cell line MIN6 exhibits characteristics of glucose metabolism and glucose-stimulated insulin secretion similar to those of normal islets. *Diabetologia*, 36(11), pp.1139-1145.

Ivanova, A., Nitka, D. and Schmitz, N., 2009. Epidemiology of antidepressant medication use in the Canadian diabetes population. Social Psychiatry and Psychiatric Epidemiology, 45(9), pp.911-919.

Iversen, S. and Iversen, L., 2007. Dopamine: 50 years in perspective. *Trends in Neurosciences*, 30(5), pp.188-193.

Jafri, L., Khan, A., Siddiqui, A., Mushtaq, S., Iqbal, R., Ghani, F. and Siddiqui, I., 2011. Comparison of high-performance liquid chromatography, radio immunoassay and electrochemiluminescence immunoassay for quantification of serum 25 hydroxy vitamin D. *Clinical Biochemistry*, 44(10-11), pp.864-868.

Jann, M., Grimsley, S., Gray, E. and Chang, W., 1993. Pharmacokinetics and Pharmacodynamics of Clozapine. *Clinical Pharmacokinetics*, 24(2), pp.161-176.

Janson, J., Ashley, R., Harrison, D., McIntyre, S. and Butler, P., 1999. The mechanism of islet amyloid polypeptide toxicity is membrane disruption by intermediate-sized toxic amyloid particles. *Diabetes*, 48(3), pp.491-498.

Jhala, U., Canettieri, G., Screaton, R., Kulkarni, R., Krajewski, S., Reed, J., Walker, J., Lin, X., White, M. and Montminy, M., 2003. cAMP promotes pancreatic β-cell survival via CREB-mediated induction of IRS2. *Genes & Development*, 17(13), pp.1575-1580.

Ji, H., Zhuang, Q. and Shen, L., 2016. Genetic overlap between type 2 diabetes and major depressive disorder identified by bioinformatics analysis. *Oncotarget*, 7(14), pp.17410-17414.

Jiang, W., Peng, Y. and Yang, K., 2018. Cellular signaling pathways regulating β-cell proliferation as a promising therapeutic target in the treatment of diabetes (Review). *Experimental and Therapeutic Medicine*, 16(4), pp.3275–3285.

Jo, S. and Fang, S., 2021. Therapeutic Strategies for Diabetes: Immune Modulation in Pancreatic β Cells. *Frontiers in Endocrinology*, 12.

Johnson, J., Bernal-Mizrachi, E., Alejandro, E., Han, Z., Kalynyak, T., Li, H., Beith, J., Gross, J., Warnock, G., Townsend, R., Permutt, M. and Polonsky, K., 2006. Insulin protects islets from

apoptosis via Pdx1 and specific changes in the human islet proteome. *Proceedings of the National Academy of Sciences*, 103(51), pp.19575-19580.

Jones, P.M., Persaud S.J., 2017. Islet function and insulin secretion. Textbook of diabetes (5th ed.), chapter 6. Blackwell Scientific Press, UK.

Jordan, S., Koprivica, V., Chen, R., Tottori, K., Kikuchi, T. and Altar, C., 2002. The antipsychotic aripiprazole is a potent, partial agonist at the human 5-HT1A receptor. *European Journal of Pharmacology*, 441(3), pp.137-140.

Kahn, R., Sommer, I., Murray, R.,Meyer-Lindenberg, A., Weinberger, D. R., Cannon, T. D., O'Donovan, M., Correll, C. U., Kane, J. M., van Os, J., Insel, T. R., 2015. Schizophrenia. *Nature Reviews Disease Primers,* 1, pp.15067.

Kahn, S., 2001. The Importance of β-Cell Failure in the Development and Progression of Type 2 Diabetes. *Journal of Clinical Endocrinology & Metabolism*, 86(9), pp.4047-4058.

Kahn, S., Andrikopoulos, S. and Verchere, C., 1999. Islet amyloid: a long-recognized but underappreciated pathological feature of type 2 diabetes. *Diabetes*, 48(2), pp.241-253.

Kahn, S., Hull, R. and Utzschneider, K., 2006. Mechanisms linking obesity to insulin resistance and type 2 diabetes. *Nature*, 444(7121), pp.840-846.

Kaido, T., Yebra, M., Cirulli, V., Rhodes, C., Diaferia, G. and Montgomery, A., 2006. Impact of Defined Matrix Interactions on Insulin Production by Cultured Human β-Cells: Effect on Insulin Content, Secretion, and Gene Transcription. *Diabetes*, 55(10), pp.2723-2729.

Kailey, B., van de Bunt, M., Cheley, S., Johnson, P., MacDonald, P., Gloyn, A., Rorsman, P. and Braun, M., 2012. SSTR2 is the functionally dominant somatostatin receptor in human pancreatic β- and α-cells. *American Journal of Physiology-Endocrinology and Metabolism*, 303(9), pp.E1107-E1116.

Kaiser, N., Leibowitz, G. and Nesher, R., 2003. Glucotoxicity and β-Cell Failure in Type 2 Diabetes Mellitus. *Journal of Pediatric Endocrinology and Metabolism*, 16(1).

Kamata, K., Mizukami, H., Inaba, W., Tsuboi, K., Tateishi, Y., Yoshida, T. and Yagihashi, S., 2014. Islet amyloid with macrophage migration correlates with augmented β-cell deficits in type 2 diabetic patients. *Amyloid*, 21(3), pp.191-201.

Kan, C., Pedersen, N., Christensen, K., Bornstein, S., Licinio, J., MacCabe, J., Ismail, K. and Rijsdijk, F., 2016. Genetic overlap between type 2 diabetes and depression in Swedish and Danish twin registries. *Molecular Psychiatry*, 21(7), pp.903-909.

Kapur, S., Zipursky, R., Jones, C., Remington, G. and Houle, S., 2000. Relationship Between Dopamine D2 Occupancy, Clinical Response, and Side Effects: A Double-Blind PET Study of First-Episode Schizophrenia. *American Journal of Psychiatry*, 157(4), pp.514-520.

Kashani, A., Brejnrod, A., Jin, C., Kern, T., Madsen, A., Holm, L., Gerber, G., Holm, J., Hansen, T., Holst, B. and Arumugam, M., 2019. Impaired glucose metabolism and altered gut microbiome despite calorie restriction of *ob/ob* mice. *Animal Microbiome*, 1(1).

KC, K., Shakya, S. and Zhang, H., 2015. Gestational Diabetes Mellitus and Macrosomia: A Literature Review. *Annals of Nutrition and Metabolism*, 66(Suppl. 2), pp.14-20.

Keck, P. and McElroy, S., 2003. Aripiprazole: a partial dopamine D2 receptor agonist antipsychotic. *Expert Opinion on Investigational Drugs*, 12(4), pp.655-662.

Kegeles, L., Abi-Dargham, A., Frankle, W., Gil, R., Cooper, T., Slifstein, M., Hwang, D., Huang, Y., Haber, S. and Laruelle, M., 2010. Increased Synaptic Dopamine Function in Associative Regions of the Striatum in Schizophrenia. *Archives of General Psychiatry*, 67(3), p.231.

Keller, J. and Layer, P., 2005. Human pancreatic exocrine response to nutrients in health and disease. *Gut*, 54(suppl_6), pp.1-28.

Keshavarzi, F., Fox, T., Whiskey, E. and Taylor, D., 2020. Change in plasma concentration of clozapine and norclozapine following a switch of oral formulation. *Therapeutic Advances in Psychopharmacology*, 10, p.204512531989926.

Kessing, L., Thomsen, A., Mogensen, U. and Andersen, P., 2010. Treatment with antipsychotics and the risk of diabetes in clinical practice. *British Journal of Psychiatry*, 197(4), pp.266-271.

Khoza, S., Barner, J., Bohman, T., Rascati, K., Lawson, K. and Wilson, J., 2011. Use of antidepressant agents and the risk of type 2 diabetes. *European Journal of Clinical Pharmacology*, 68(9), pp.1295-1302.

Kikuchi, Y., Iwase, M., Fujii, H., Ohkuma, T., Kaizu, S., Ide, H., Jodai, T., Idewaki, Y., Nakamura, U. and Kitazono, T., 2015. Association of severe hypoglycemia with depressive symptoms in patients with type 2 diabetes: the Fukuoka Diabetes Registry. *BMJ Open Diabetes Research & Care*, 3(1), p.e000063.

Kim, A., Miller, K., Jo, J., Kilimnik, G., Wojcik, P. and Hara, M., 2009. Islet architecture: A comparative study. *Islets*, 1(2), pp.129-136.

Kim, H., Toyofuku, Y., Lynn, F., Chak, E., Uchida, T., Mizukami, H., Fujitani, Y., Kawamori, R., Miyatsuka, T., Kosaka, Y., Yang, K., Honig, G., van der Hart, M., Kishimoto, N., Wang, J., Yagihashi, S., Tecott, L., Watada, H. and German, M., 2010. Serotonin regulates pancreatic beta cell mass during pregnancy. *Nature Medicine*, 16(7), pp.804-808.

Kim, J., Ko, S. and Cho, J., 2008. Loss of beta-cells with fibrotic islet destruction in type 2 diabetes mellitus. *Frontiers in Bioscience*, 13, p.6022.

Kim, K., Oh, C., Ohara-Imaizumi, M., Park, S., Namkung, J., Yadav, V., Tamarina, N., Roe, M., Philipson, L., Karsenty, G., Nagamatsu, S., German, M. and Kim, H., 2014. Functional Role of Serotonin in Insulin Secretion in a Diet-Induced Insulin-Resistant State. *Endocrinology*, 156(2), pp.444-452.

Kim, S., Huang, A., Snowman, A., Teuscher, C. and Snyder, S., 2007. Antipsychotic drug-induced weight gain mediated by histamine H1 receptor-linked activation of hypothalamic AMP-kinase. *Proceedings of the National Academy of Sciences*, 104(9), pp.3456-3459.

King, A., 2012. The use of animal models in diabetes research. British Journal of Pharmacology, 166(3), pp.877-894.

King, P., 2017. *Diabetes and Pregnancy Part 1: Gestational Diabetes | BJFM*. [online] BJFM. Available at: <https://www.bjfm.co.uk/diabetes-and-pregnancy-part-1-gestational-diabetes> [Accessed 3 December 2021].

Kirschbaum, K., Müller, M., Malevani, J., Mobascher, A., Burchardt, C., Piel, M. and Hiemke, C., 2008. Serum levels of aripiprazole and dehydroaripiprazole, clinical response and side effects. *The World Journal of Biological Psychiatry*, 9(3), pp.212-218.

Kleinert, M., Clemmensen, C., Hofmann, S., Moore, M., Renner, S., Woods, S., Huypens, P., Beckers, J., de Angelis, M., Schürmann, A., Bakhti, M., Klingenspor, M., Heiman, M., Cherrington, A., Ristow, M., Lickert, H., Wolf, E., Havel, P., Müller, T. and Tschöp, M., 2018. Animal models of obesity and diabetes mellitus. Nature Reviews Endocrinology, 14(3), pp.140-162.

Kobayashi, T., Washiyama, K. and Ikeda, K., 2003. Inhibition of G protein-activated inwardly rectifying K+ channels by fluoxetine (Prozac). *British Journal of Pharmacology*, 138(6), pp.1119-1128.

Köhler, C., Freitas, T., Maes, M., de Andrade, N., Liu, C., Fernandes, B., Stubbs, B., Solmi, M., Veronese, N., Herrmann, N., Raison, C., Miller, B., Lanctot, K. and Carvalho, A., 2017. Peripheral cytokine and chemokine alterations in depression: a meta-analysis of 82 studies. *Acta Psychiatrica Scandinavica*, 135(5), pp.373-387.

Kong, K. and Tobin, A., 2011. The role of M3-muscarinic receptor signaling in insulin secretion. *Communicative & Integrative Biology*, 4(4), pp.489-491.

Koprivica, V., Regardie, K., Wolff, C., Fernalld, R., Murphy, J., Kambayashi, J., Kikuchi, T. and Jordan, S., 2011. Aripiprazole protects cortical neurons from glutamate toxicity. *European Journal of Pharmacology*, 651(1-3), pp.73-76.

Koro, C. E., Fedder, D. O., L'Italien, G. J., Weiss, S. S., Magder, L. S., Kreyenbuhl, J., Revicki, D. A., Buchanan, R. W., 2002. Assessment of independent effect of olanzapine and risperidone on risk of diabetes among patients with schizophrenia: population based nested case-control study. *BMJ (Clinical research ed.),* 325(7358), pp.243.

Kostadinov, I., Delev, D., Petrova, A., Stanimirova, I., Draganova, K., Kruzliak, P., Kostadinova, I. and Murdjeva, M., 2015. Study on anti-inflammatory and immunomodulatory effects of fluoxetine in rat models of inflammation. *European Journal of Inflammation*, 13(3), pp.173-182.

Koster, J., Permutt, M. and Nichols, C., 2005. Diabetes and Insulin Secretion: The ATP-Sensitive K+ Channel (KATP) Connection. *Diabetes*, 54(11), pp.3065-3072.

Kralik, P. and Ricchi, M., 2017. A Basic Guide to Real Time PCR in Microbial Diagnostics: Definitions, Parameters, and Everything. *Frontiers in Microbiology*, 8.

Kroeze, W., Hufeisen, S., Popadak, B. , Renock, S. M., Steinberg, S., Ernsberger, P., Jayathilake, K., Meltzer, H. Y., Roth, B. L., 2003. H1-Histamine Receptor Affinity Predicts Short-Term Weight Gain for Typical and Atypical Antipsychotic Drugs. *Neuropsychopharmacology*, 28, pp.519–526.

Kuecker, C. and Vivian, E., 2016. Patient considerations in type 2 diabetes – role of combination dapagliflozin–metformin XR. *Diabetes, Metabolic Syndrome and Obesity: Targets and Therapy*, p.25.

Kulkarni, R., Mizrachi, E., Ocana, A. and Stewart, A., 2012. Human β-Cell Proliferation and Intracellular Signaling: Driving in the Dark Without a Road Map. *Diabetes*, 61(9), pp.2205-2213.

Kumar, P., Mishra, D., Mishra, N., Ahuja, S., Raghuvanshi, G. and Niranjan, V., 2019. Acute onset clozapine-induced hyperglycaemia: A case report. *General Psychiatry*, 32(2), p.e100045.

Kupfer, D., Frank, E. and Phillips, M., 2012. Major depressive disorder: new clinical, neurobiological, and treatment perspectives. *The Lancet*, 379(9820), pp.1045-1055.

Kyrou, I. and Tsigos, C., 2009. Stress hormones: physiological stress and regulation of metabolism. *Current Opinion in Pharmacology*, 9(6), pp.787-793.

Laake, J., Stahl, D., Amiel, S., Petrak, F., Sherwood, R., Pickup, J. and Ismail, K., 2014. The Association Between Depressive Symptoms and Systemic Inflammation in People with Type 2

Diabetes: Findings From the South London Diabetes Study. *Diabetes Care*, 37(8), pp.2186-2192.

Ladyman, S., Hackwell, E. and Brown, R., 2020. The role of prolactin in co-ordinating fertility and metabolic adaptations during reproduction. *Neuropharmacology*, 167, p.107911.

Lamberti, J., Crilly, J., Maharaj, K., Olson, D., Wiener, K., Dvorin, S., Costea, G., Bushey, M. and Dietz, M., 2004. Prevalence of Diabetes Mellitus Among Outpatients with Severe Mental Disorders Receiving Atypical Antipsychotic Drugs. *The Journal of Clinical Psychiatry*, 65(5), pp.702-706.

Lange, R., Von Linsingen, C., Mata, F., Moraes, A., Arruda, M. and Vieira Neto, L., 2015. Endocrine abnormalities in ring chromosome 11: a case report and review of the literature. *Endocrinology, Diabetes & Metabolism Case Reports*, 2015.

Le Bacquer, O., Queniat, G., Gmyr, V., Kerr-Conte, J., Lefebvre, B. and Pattou, F., 2013. mTORC1 and mTORC2 regulate insulin secretion through Akt in INS-1 cells. *Journal of Endocrinology*, 216(1), pp.21-29.

Lee, J., Chinnathambi, A., Alharbi, S., Shair, O., Sethi, G. and Ahn, K., 2019. Farnesol abrogates epithelial to mesenchymal transition process through regulating Akt/mTOR pathway. *Pharmacological Research*, 150, p.104504.

Leighton, S., Nerurkar, L., Krishnadas, R., Johnman, C., Graham, G. and Cavanagh, J., 2017. Chemokines in depression in health and in inflammatory illness: a systematic review and meta-analysis. *Molecular Psychiatry*, 23(1), pp.48-58.

Leitner, D., Frühbeck, G., Yumuk, V., Schindler, K., Micic, D., Woodward, E. and Toplak, H., 2017. Obesity and Type 2 Diabetes: Two Diseases with a Need for Combined Treatment Strategies - EASO Can Lead the Way. *Obesity Facts*, 10(5), pp.483-492.

Levey, A., Hersch, S., Rye, D., Sunahara, R., Niznik, H., Kitt, C., Price, D., Maggio, R., Brann, M. and Ciliax, B., 1993. Localization of D1 and D2 dopamine receptors in brain with subtype-specific antibodies. *Proceedings of the National Academy of Sciences*, 90(19), pp.8861-8865.

Liao, C., Chang, C., Wei, W., Chang, S., Liao, C., Lane, H. and Sung, F., 2011. Schizophrenia patients at higher risk of diabetes, hypertension and hyperlipidemia: A population-based study. *Schizophrenia Research*, 126(1-3), pp.110-116.

Lima, C. A. M., Baumann, P., Eap, C. B., 2008. Paroxetine plasma concentrations in adult and elderly depressed patients. *Revista de Psiquiatria do Rio Grande*, 30(1).

Lin, P. and Shuldiner, A., 2010. Rethinking the genetic basis for comorbidity of schizophrenia and type 2 diabetes. *Schizophrenia Research*, 123(2-3), pp.234-243.

Lin, X., Guan, H., Huang, Z., Liu, J., Li, H., Wei, G., Cao, X. and Li, Y., 2014. Downregulation of Bcl-2 Expression by miR-34a Mediates Palmitate-Induced Min6 Cells Apoptosis. *Journal of Diabetes Research*, 2014, pp.1-7.

Lindstrom, P., 2007. The Physiology of Obese-Hyperglycemic Mice [*ob/ob*Mice]. *The Scientific World JOURNAL*, 7, pp.666-685.

Liu, B., Barbosa-Sampaio, H., Jones, P., Persaud, S. and Muller, D., 2012. The CaMK4/CREB/IRS-2 Cascade Stimulates Proliferation and Inhibits Apoptosis of β-Cells. *PLoS ONE*, 7(9), p.e45711.

Liu, B., Barbosa-Sampaio, H., Jones, P., Persaud, S. and Muller, D., 2012. The CaMK4/CREB/IRS-2 Cascade Stimulates Proliferation and Inhibits Apoptosis of β-Cells. *PLoS ONE*, 7(9), p.e45711.

Lombardo, M., De Angelis, F., Bova, L., Bartolini, B., Bertuzzi, F., Nano, R., Capuani, B., Lauro, R., Federici, M., Lauro, D. and Donadel, G., 2011. Human placental lactogen (hPL-A) activates signaling pathways linked to cell survival and improves insulin secretion in human pancreatic islets. *Islets*, 3(5), pp.250-258.

Lopez-Munoz, F. and Alamo, C., 2009. Monoaminergic Neurotransmission: The History of the Discovery of Antidepressants from 1950s Until Today. *Current Pharmaceutical Design*, 15(14), pp.1563-1586.

Lorenzo, A., Razzaboni, B., Weir, G. and Yankner, B., 1994. Pancreatic islet cell toxicity of amylin associated with type-2 diabetes mellitus. *Nature*, 368(6473), pp.756-760.

Lund, A., Bagger, J. I., Wewer Albrechtsen, N. J., Christensen, M., Grøndahl, M., Hartmann, B., Mathiesen, E. R., Hansen, C. P., Storkholm, J. H., van Hall, G., Rehfeld, J. F., Hornburg, D., Meissner, F., Mann, M., Larsen, S., Holst, J. J., Vilsbøll, T., & Knop, F. K., 2016. Evidence of Extrapancreatic Glucagon Secretion in Man. *Diabetes*, 65(3), pp.585–597.

Lundberg, M., Curbo, S., Bohman, H., Agartz, I., Ogren, S., Patrone, C. and Mansouri, S., 2020. Clozapine protects adult neural stem cells from ketamine-induced cell death in correlation with decreased apoptosis and autophagy. *Bioscience Reports*, 40(1).

Lundberg, M., Curbo, S., Bohman, H., Agartz, I., Ögren, S., Patrone, C. and Mansouri, S., 2020. Clozapine protects adult neural stem cells from ketamine-induced cell death in correlation with decreased apoptosis and autophagy. *Bioscience Reports*, 40(1).

Luo, S. and Huang, E., 2016. Dopaminergic Neurons and Brain Reward Pathways. *The American Journal of Pathology*, 186(3), pp.478-488.

Maahs, D., West, N., Lawrence, J. and Mayer-Davis, E., 2010. Epidemiology of Type 1 Diabetes. *Endocrinology and Metabolism Clinics of North America*, 39(3), pp.481-497.

Maedler, K., Oberholzer, J., Bucher, P., Spinas, G. and Donath, M., 2003. Monounsaturated Fatty Acids Prevent the Deleterious Effects of Palmitate and High Glucose on Human Pancreatic β-Cell Turnover and Function. *Diabetes*, 52(3), pp.726-733.

Maheux, P., Ducros, F., Bourque, J., Garon, J. and Chiasson, J., 1997. Fluoxetine improves insulin sensitivity in obese patients with non-insulin-dependent diabetes mellitus independently of weight loss. *International Journal of Obesity*, 21(2), pp.97-102.

Mailman, R. and Gay, E., 2004. Novel Mechanisms of Drug Action: Functional Selectivity at D2 Dopamine Receptors. *Medicinal Chemistry Research*, 13(1-2), pp.115-126.

Mailman, R. and Murthy, V., 2010. Third Generation Antipsychotic Drugs: Partial Agonism or Receptor Functional Selectivity?. *Current Pharmaceutical Design*, 16(5), pp.488-501.

Mamakou, V., Thanopoulou, A., Gonidakis, F., Tentolouris, N. and Kontaxakis, V., 2018. Schizophrenia and type 2 diabetes mellitus. *Psychiatriki*, 29(1), pp.64-73.

Mansur, R., Zugman, A., Ahmed, J., Cha, D., Subramaniapillai, M., Lee, Y., Lovshin, J., Lee, J., Lee, J., Drobinin, V., Newport, J., Brietzke, E., Reininghaus, E., Sim, K., Vinberg, M., Rasgon, N., Hajek, T. and McIntyre, R., 2017. Treatment with a GLP−1R agonist over four weeks promotes weight loss-moderated changes in frontal-striatal brain structures in individuals with mood disorders. European Neuropsychopharmacology, 27(11), pp.1153-1162.

Marchand, L., Pecquet, M. and Luyton, C., 2020. Type 1 diabetes onset triggered by COVID-19. *Acta Diabetologica*, 57(10), pp.1265-1266.

Marin-Penalver, J., Martín-Timon, I., Sevillano-Collantes, C. and Canizo-Gomez, F., 2016. Update on the treatment of type 2 diabetes mellitus. *World Journal of Diabetes*, 7(17), p.354.

Marrif, H. and Al-Sunousi, S., 2016. Pancreatic β Cell Mass Death. *Frontiers in Pharmacology*, 7.

Marso, S. P., Daniels, G. H., Brown-Frandsen, K., Kristensen, P., Mann, J. F. E., Nauck, M. A., Nissen, S. E., Pocock, S., Poulter, N. R., Ravn, L. S., Steinberg, W. M., Stockner, M., 2016. Liraglutide and cardiovascular outcomes in type 2 diabetes. *The New England journal of medicine*, 375, pp. 311–322.

Matsui-Sakata, A., Ohtani, H. and Sawada, Y., 2005. Receptor Occupancy-based Analysis of the Contributions of Various Receptors to Antipsychotics-induced Weight Gain and Diabetes Mellitus. *Drug Metabolism and Pharmacokinetics*, 20(5), pp.368-378.

McCulloch, L., van de Bunt, M., Braun, M., Frayn, K., Clark, A. and Gloyn, A., 2011. GLUT2 (SLC2A2) is not the principal glucose transporter in human pancreatic beta cells: Implications

for understanding genetic association signals at this locus. *Molecular Genetics and Metabolism*, 104(4), pp.648-653.

McEvoy, J., Meyer, J., Goff, D., Nasrallah, H., Davis, S., Sullivan, L., Meltzer, H., Hsiao, J., Scott Stroup, T. and Lieberman, J., 2005. Prevalence of the metabolic syndrome in patients with schizophrenia: Baseline results from the Clinical Antipsychotic Trials of Intervention Effectiveness (CATIE) schizophrenia trial and comparison with national estimates from NHANES III. *Schizophrenia Research*, 80(1), pp.19-32.

McEvoy, J., VanderZwaag, C., McGee, M., Freudenreich, O., Wilson, W. and Cooper, T., 1996. A double-blind, randomized trial comparing clozapine treatment within three distinct serum level ranges in patients with refractory chronic schizophrenia. *Schizophrenia Research*, 18(2-3), p.127.

Melo, K., Bahia, L., Pasinato, B., Porfirio, G., Martimbianco, A., Riera, R., Calliari, L., Minicucci, W., Turatti, L., Pedrosa, H. and Schaan, B., 2019. Short-acting insulin analogues versus regular human insulin on postprandial glucose and hypoglycemia in type 1 diabetes mellitus: a systematic review and meta-analysis. *Diabetology & Metabolic Syndrome*, 11(1).

Meltzer H. Y., 1994. An overview of the mechanism of action of clozapine. *The Journal of clinical psychiatry*, 55, pp.47–52.

Meltzer, H. and Massey, B., 2011. The role of serotonin receptors in the action of atypical antipsychotic drugs. *Current Opinion in Pharmacology*, 11(1), pp.59-67.

Mezza, T., Cinti, F., Cefalo, C., Pontecorvi, A., Kulkarni, R. and Giaccari, A., 2019. β-Cell Fate in Human Insulin Resistance and Type 2 Diabetes: A Perspective on Islet Plasticity. *Diabetes*, 68(6), pp.1121-1129.

Michalopoulos, G., 2017. Hepatostat: Liver regeneration and normal liver tissue maintenance. *Hepatology*, 65(4), pp.1384-1392.

Miidera, H., Enomoto, M., Kitamura, S., Tachimori, H. and Mishima, K., 2020. Association Between the Use of Antidepressants and the Risk of Type 2 Diabetes: A Large, Population-Based Cohort Study in Japan. *Diabetes Care*, 43(4), pp.885-893.

Miras, A. and le Roux, C., 2014. Can medical therapy mimic the clinical efficacy or physiological effects of bariatric surgery?. *International Journal of Obesity*, 38(3), pp.325-333.

Miyachi, A., Kobayashi, M., Mieno, E., Goto, M., Furusawa, K., Inagaki, T. and Kitamura, T., 2017. Accurate analytical method for human plasma glucagon levels using liquid chromatography-high resolution mass spectrometry: comparison with commercially available immunoassays. *Analytical and Bioanalytical Chemistry*, 409(25), pp.5911-5918.

Miyazaki, J., Araki, K., Yamato, E., Ikegami, H., Asano, T., Shibasaki, Y., Oka, Y. and Yamamura, K., 1990. Establishment of a Pancreatic β Cell Line That Retains Glucose-Inducible Insulin Secretion: Special Reference to Expression of Glucose Transporter Isoforms*. *Endocrinology*, 127(1), pp.126-132.

Miyazaki, S., Tashiro, F., Tsuchiya, T., Sasaki, K. and Miyazaki, J., 2021. Establishment of a long-term stable β-cell line and its application to analyze the effect of Gcg expression on insulin secretion. *Scientific Reports*, 11(1).

Montanya, E., Nacher, V., Biarnes, M. and Soler, J., 2000. Linear correlation between beta-cell mass and body weight throughout the lifespan in Lewis rats: role of beta-cell hyperplasia and hypertrophy. *Diabetes*, 49(8), pp.1341-1346.

Moon, J., Kim, Y., Kim, K., Osonoi, S., Wang, S., Saunders, D., Wang, J., Yang, K., Kim, H., Lee, J., Jeong, J., Banerjee, R., Kim, S., Wu, Y., Mizukami, H., Powers, A., German, M. and Kim, H., 2020. Serotonin Regulates Adult β-Cell Mass by Stimulating Perinatal β-Cell Proliferation. *Diabetes*, 69(2), pp.205-214.

Morris, D., 2015. Minireview: Emerging Concepts in Islet Macrophage Biology in Type 2 Diabetes. *Molecular Endocrinology*, 29(7), pp.946-962.

Moulton, C., Pickup, J. and Ismail, K., 2015. The link between depression and diabetes: the search for shared mechanisms. *The Lancet Diabetes & Endocrinology*, 3(6), pp.461-471.

Mukherjee, A., Morales-Scheihing, D., Butler, P. and Soto, C., 2015. Type 2 diabetes as a protein misfolding disease. *Trends in Molecular Medicine*, 21(7), pp.439-449.

Mukherjee, J., Das, M., Yang, Z. and Lew, R., 1998. Evaluation of the binding of the radiolabeled antidepressant drug, 18F-fluoxetine in the rodent brain: an in vitro and *in vivo* study. *Nuclear Medicine and Biology*, 25(7), pp.605-610.

Muller, D., Huang, G., Amiel, S., Jones, P. and Persaud, S., 2006. Identification of Insulin Signaling Elements in Human -Cells: Autocrine Regulation of Insulin Gene Expression. *Diabetes*, 55(10), pp.2835-2842.

Muller, J. A., Groß, R., Conzelmann, C., Kruger, J., Merle, U., Steinhart, J., Weil, T., Koepke, L., Bozzo, C. P., Read, C., Fois, G., Eiseler, T., Gehrmann, J., van Vuuren, J., Wessbecher, I. M., Frick, M., Costa, I. G., Breunig, M., Grüner, B., Peters, L., … Kleger, A., 2021. SARS-CoV-2 infects and replicates in cells of the human endocrine and exocrine pancreas. *Nature metabolism*, 3(2), pp.149–165.

Naicker, K. 2018, Depression and anxiety in type 2 diabetes: associations with diabetes onset, clinical management, and long-term mortality. PhD thesis, University of Ottawa, Ottawa, Canada.

Nansseu, J., Ngo-Um, S. and Balti, E., 2016. Incidence, prevalence and genetic determinants of neonatal diabetes mellitus: a systematic review and meta-analysis protocol. *Systematic Reviews*, 5(1).

Nasrallah, H., 2008. Atypical antipsychotic-induced metabolic side effects: insights from receptor-binding profiles. *Molecular Psychiatry*, 13(1), pp.27-35.

National Institute for Clinical Excellence, 2015. Diabetes in pregnancy; management from preconception to postnatal period NICE guideline NG3

Nauck, M., Vardarli, I., Deacon, C., Holst, J. and Meier, J., 2010. Secretion of glucagon-like peptide-1 (GLP-1) in type 2 diabetes: what is up, what is down?. *Diabetologia*, 54(1), pp.10-18.

Neal, B., Perkovic, V., Mahaffey, K., de Zeeuw, D., Fulcher, G., Erondu, N., Shaw, W., Law, G., Desai, M. and Matthews, D., 2017. Canagliflozin and Cardiovascular and Renal Events in Type 2 Diabetes. *New England Journal of Medicine*, 377(7), pp.644-657.

Newcomer, J., Haupt, D., Fucetola, R., Melson, A., Schweiger, J., Cooper, B. and Selke, G., 2002. Abnormalities in Glucose Regulation During Antipsychotic Treatment of Schizophrenia. *Archives of General Psychiatry*, 59(4), p.337.

Ni, Y. and Miledi, R., 1997. Blockage of 5HT2C serotonin receptors by fluoxetine (Prozac). *Proceedings of the National Academy of Sciences*, 94(5), pp.2036-2040.

Nielsen, J., Skadhede, S. and Correll, C., 2010. Antipsychotics Associated with the Development of Type 2 Diabetes in Antipsychotic-Naïve Schizophrenia Patients. *Neuropsychopharmacology*, 35(9), pp.1997-2004.

Nomiyama, T. and Yanase, T., 2015. Nihon rinsho. *Japanese journal of clinical medicine*, 73(12), pp.2008–2012.

Nonogaki, K., Strack, A., Dallman, M. and Tecott, L., 1998. Leptin-independent hyperphagia and type 2 diabetes in mice with a mutated serotonin 5-HT2C receptor gene. *Nature Medicine*, 4(10), pp.1152-1156.

Nouwen, A., Nefs, G., Caramlau, I., Connock, M., Winkley, K., Lloyd, C., Peyrot, M. and Pouwer, F., 2011. Prevalence of Depression in Individuals with Impaired Glucose Metabolism or Undiagnosed Diabetes: A systematic review and meta-analysis of the European Depression in Diabetes (EDID) Research Consortium. *Diabetes Care*, 34(3), pp.752-762.

Novío, S., Núñez, M., Amigo, G. and Freire-Garabal, M., 2011. Effects of Fluoxetine on the Oxidative Status of Peripheral Blood Leucocytes of Restraint-Stressed Mice. *Basic & Clinical Pharmacology & Toxicology*, 109(5), pp.365-371.

Numata, S., Umehara, H., Ohmori, T. and Hashimoto, R., 2018. Clozapine Pharmacogenetic Studies in Schizophrenia: Efficacy and Agranulocytosis. *Frontiers in Pharmacology*, 9.

Ofek, K., Schoknecht, K., Melamed-Book, N., Heinemann, U., Friedman, A. and Soreq, H., 2012. Fluoxetine induces vasodilatation of cerebral arterioles by co-modulating NO/muscarinic signalling. *Journal of Cellular and Molecular Medicine*, 16(11), pp.2736-2744.

Oh, Y., Bae, G., Baek, D., Park, E. and Jun, H., 2018. Fatty Acid-Induced Lipotoxicity in Pancreatic Beta-Cells During Development of Type 2 Diabetes. *Frontiers in Endocrinology*, 9.

Ohara-Imaizumi, M., Kim, H., Yoshida, M., Fujiwara, T., Aoyagi, K., Toyofuku, Y., Nakamichi, Y., Nishiwaki, C., Okamura, T., Uchida, T., Fujitani, Y., Akagawa, K., Kakei, M., Watada, H., German, M. and Nagamatsu, S., 2013. Serotonin regulates glucose-stimulated insulin secretion from pancreatic cells during pregnancy. *Proceedings of the National Academy of Sciences*, 110(48), pp.19420-19425.

Ohno, Y., 2018. Astrocytic Kir4.1 potassium channels as a novel therapeutic target for epilepsy and mood disorders. *Neural Regeneration Research*, 13(4), p.651.

Ohno, Y., Hibino, H., Lossin, C., Inanobe, A. and Kurachi, Y., 2007. Inhibition of astroglial Kir4.1 channels by selective serotonin reuptake inhibitors. *Brain Research*, 1178, pp.44-51.

Ohta, Y., Kosaka, Y., Kishimoto, N., Wang, J., Smith, S., Honig, G., Kim, H., Gasa, R., Neubauer, N., Liou, A., Tecott, L., Deneris, E. and German, M., 2011. Convergence of the Insulin and Serotonin Programs in the Pancreatic β-Cell. *Diabetes*, 60(12), pp.3208-3216.

Otani, K., Kulkarni, R., Baldwin, A., Krutzfeldt, J., Ueki, K., Stoffel, M., Kahn, C. and Polonsky, K., 2004. Reduced β-cell mass and altered glucose sensing impair insulin-secretory function in βIRKO mice. *American Journal of Physiology-Endocrinology and Metabolism*, 286(1), pp.E41-E49.

Otte, C., Gold, S. M., Penninx, B. W., Pariante, C. M., Etkin, A., Fava, M., Mohr, D. C., Schatzberg, A. F., 2016. Major depressive disorder. *Nature reviews*. Disease primers, 2, pp. 16065.

Padala, P., Qadri, S. and Madaan, V., 2005. Aripiprazole for the Treatment of Tourette's Disorder. *The Primary Care Companion to The Journal of Clinical Psychiatry*, 07(06), pp.296-299.

Paile-Hyvärinen, M., Wahlbeck, K. and Eriksson, J., 2007. Quality of life and metabolic status in mildly depressed patients with type 2 diabetes treated with paroxetine: A double-blind randomised placebo controlled 6-month trial. *BMC Family Practice*, 8(1).

Pan, A., Lucas, M., Sun, Q., van Dam, R., Franco, O., Manson, J., Willett, W., Ascherio, A. and Hu, F., 2010. Bidirectional Association Between Depression and Type 2 Diabetes Mellitus in Women. *Archives of Internal Medicine*, 170(21).

Pandiri AR., 2014. Overview of exocrine pancreatic pathobiology. *Toxicologic Pathology*, 42(1), pp. 207-216.

Papadimitriou, A., King, A. J., Jones, P. M., & Persaud, S. J., 2007. Anti-apoptotic effects of arachidonic acid and prostaglandin E2 in pancreatic beta-cells. *Cellular physiology and biochemistry: international journal of experimental cellular physiology, biochemistry, and pharmacology*, 20(5), pp.607–616.

Papatheodorou, K., Banach, M., Bekiari, E., Rizzo, M. and Edmonds, M., 2018. Complications of Diabetes 2017. *Journal of Diabetes Research*, 2018, pp.1-4.

Parsons, J., Brelje, T. and Sorenson, R., 1992. Adaptation of islets of Langerhans to pregnancy: increased islet cell proliferation and insulin secretion correlates with the onset of placental lactogen secretion. *Endocrinology*, 130(3), pp.1459-1466.

Paulmann, N., Grohmann, M., Voigt, J., Bert, B., Vowinckel, J., Bader, M., Skelin, M., Jevšek, M., Fink, H., Rupnik, M. and Walther, D., 2009. Intracellular Serotonin Modulates Insulin Secretion from Pancreatic β-Cells by Protein Serotonylation. *PLoS Biology*, 7(10), p.e1000229.

Perkovic, V., Jardine, M., Neal, B., Bompoint, S., Heerspink, H., Charytan, D., Edwards, R., Agarwal, R., Bakris, G., Bull, S., Cannon, C., Capuano, G., Chu, P., de Zeeuw, D., Greene, T., Levin, A., Pollock, C., Wheeler, D., Yavin, Y., Zhang, H., Zinman, B., Meininger, G., Brenner, B. and Mahaffey, K., 2019.

Canagliflozin and Renal Outcomes in Type 2 Diabetes and Nephropathy. New England Journal of Medicine, 380(24), pp.2295-2306.

Perreault, L., Skyler, J. and Rosenstock, J., 2021. Novel therapies with precision mechanisms for type 2 diabetes mellitus. *Nature Reviews Endocrinology*, 17(6), pp.364-377.

Persaud, S., Liu, B., Sampaio, H., Jones, P. and Muller, D., 2011. Calcium/calmodulin-dependent kinase IV controls glucose-induced Irs2 expression in mouse beta cells via activation of cAMP response element-binding protein. *Diabetologia*, 54(5), pp.1109-1120.

Persaud, S., Muller, D., Belin, V., Papadimitriou, A., Huang, G., Amiel, S. and Jones, P., 2007. Expression and function of cyclooxygenase and lipoxygenase enzymes in human islets of Langerhans. *Archives of Physiology and Biochemistry*, 113(3), pp.104-109.

Phelps, E., Cianciaruso, C., Santo-Domingo, J., Pasquier, M., Galliverti, G., Piemonti, L., Berishvili, E., Burri, O., Wiederkehr, A., Hubbell, J. and Baekkeskov, S., 2017. Advances in pancreatic islet monolayer culture on glass surfaces enable super-resolution microscopy and insights into beta cell ciliogenesis and proliferation. *Scientific Reports*, 7(1).

Picard, F., Wanatabe, M., Schoonjans, K., Lydon, J., O'Malley, B. and Auwerx, J., 2002. Nonlinear partial differential equations and applications: Progesterone receptor knockout mice have an improved glucose homeostasis secondary to -cell proliferation. Proceedings of the National Academy of Sciences, 99(24), pp.15644-15648.

Pillinger, T., Beck, K., Gobjila, C., Donocik, J., Jauhar, S. and Howes, O., 2017. Impaired Glucose Homeostasis in First-Episode Schizophrenia. *JAMA Psychiatry*, 74(3), p.261.

Pillinger, T., McCutcheon, R., Vano, L., Mizuno, Y., Arumuham, A., Hindley, G., Beck, K., Natesan, S., Efthimiou, O., Cipriani, A. and Howes, O., 2020. Comparative effects of 18 antipsychotics on metabolic function in patients with schizophrenia, predictors of metabolic dysregulation, and association with psychopathology: a systematic review and network meta-analysis. *The Lancet Psychiatry*, 7(1), pp.64-77.

Prestele, S., Aldenhoff, J. and Reiff, J., 2003. Die HPA-Achse als mögliches Bindeglied zwischen Depression, Diabetes mellitus und kognitiven Störungen. *Fortschritte der Neurologie · Psychiatrie*, 71(1), pp.24-36.

Proudman, R., Pupo, A. and Baker, J., 2020. The affinity and selectivity of α-adrenoceptor antagonists, antidepressants, and antipsychotics for the human α1A, α1B, and α1D-adrenoceptors. *Pharmacology Research & Perspectives*, 8(4).

Puelles, V. G., Lütgehetmann, M., Lindenmeyer, M. T., Sperhake, J. P., Wong, M. N., Allweiss, L., Chilla, S., Heinemann, A., Wanner, N., Liu, S., Braun, F., Lu, S., Pfefferle, S., Schröder, A. S., Edler, C., Gross, O., Glatzel, M., Wichmann, D., Wiech, T., Kluge, S., … Huber, T. B., 2020. Multiorgan and Renal Tropism of SARS-CoV-2. *The New England journal of medicine*, 383(6), pp.590–592.

Qi, X., Lin, W., Li, J., Li, H., Wang, W., Wang, D. and Sun, M., 2008. Fluoxetine increases the activity of the ERK-CREB signal system and alleviates the depressive-like behavior in rats exposed to chronic forced swim stress. *Neurobiology of Disease*, 31(2), pp.278-285.

QIAGEN GmbH, 2017. *RNeasy Plant Mini Kit: Purify total RNA from plants and fungi*. [online] Vimeo. Available at: <https://vimeo.com/248279679> [Accessed 5 December 2021].

Qiao, L., Saget, S., Lu, C., Hay, W., Karsenty, G. and Shao, J., 2021. Adiponectin Promotes Maternal β-Cell Expansion Through Placental Lactogen Expression. Diabetes, 70(1), pp.132-142.

Rado, J. and von Ammon Cavanaugh, S., 2016. A Naturalistic Randomized Placebo-Controlled Trial of Extended-Release Metformin to Prevent Weight Gain Associated with Olanzapine in a US Community-Dwelling Population. *Journal of Clinical Psychopharmacology*, 36(2), pp.163-168.

Rahier, J., Guiot, Y., Goebbels, R., Sempoux, C. and Henquin, J., 2008. Pancreatic β-cell mass in European subjects with type 2 diabetes. *Diabetes, Obesity and Metabolism*, 10, pp.32-42.

Raju, B. and Cryer, P., 2005. Maintenance of the postabsorptive plasma glucose concentration: insulin or insulin plus glucagon?. *American Journal of Physiology-Endocrinology and Metabolism*, 289(2), pp.181-186.

Ramachandraiah, C., Subramaniam, N. and Tancer, M., 2009. The story of antipsychotics: Past and present. *Indian Journal of Psychiatry*, 51(4), p.324.

Randeria, S., Thomson, G., Nell, T., Roberts, T. and Pretorius, E., 2019. Inflammatory cytokines in type 2 diabetes mellitus as facilitators of hypercoagulation and abnormal clot formation. *Cardiovascular Diabetology*, 18(1).

Reynolds, R., Logie, J., Roseweir, A., McKnight, A. and Millar, R., 2009. A role for kisspeptins in pregnancy: facts and speculations. REPRODUCTION, 138(1), pp.1-7.

Richardson, S., Willcox, A., Bone, A., Foulis, A. and Morgan, N., 2009. Islet-associated macrophages in type 2 diabetes. *Diabetologia*, 52(8), pp.1686-1688.

Riggio, G., Mariti, C., Sergi, V., Diverio, S. and Gazzano, A., 2020. Serotonin and Tryptophan Serum Concentrations in Shelter Dogs Showing Different Behavioural Responses to a Potentially Stressful Procedure. *Veterinary Sciences*, 8(1), p.1.

Robinson, R., 2009. Serotonin's Role in the Pancreas Revealed at Last. *PLoS Biology*, 7(10), p.e1000227.

Roddy, D., Farrell, C., Doolin, K., Roman, E., Tozzi, L., Frodl, T., O'Keane, V. and O'Hanlon, E., 2019. The Hippocampus in Depression: More Than the Sum of Its Parts? Advanced Hippocampal Substructure Segmentation in Depression. *Biological Psychiatry*, 85(6), pp.487-497.

Roder, P., Wu, B., Liu, Y. and Han, W., 2016. Pancreatic regulation of glucose homeostasis. *Experimental & Molecular Medicine*, 48(3), pp.219-219.

Roopan, S. and Larsen, E., 2016. Use of antidepressants in patients with depression and comorbid diabetes mellitus: a systematic review. *Acta Neuropsychiatrica*, 29(3), pp.127-139.

Rorsman, P. and Braun, M., 2013. Regulation of Insulin Secretion in Human Pancreatic Islets. *Annual Review of Physiology*, 75(1), pp.155-179.

Rosenvinge, A., Krogh-Madsen, R., Baslund, B. and Pedersen, B., 2007. Insulin resistance in patients with rheumatoid arthritis: effect of anti-TNFα therapy. *Scandinavian Journal of Rheumatology*, 36(2), pp.91-96.

Rougerie, P., Miskolci, V. and Cox, D., 2013. Generation of membrane structures during phagocytosis and chemotaxis of macrophages: role and regulation of the actin cytoskeleton. *Immunological Reviews*, 256(1), pp.222-239.

Rourke, J., Hu, Q. and Screaton, R., 2018. AMPK and Friends: Central Regulators of β Cell Biology. *Trends in Endocrinology & Metabolism*, 29(2), pp.111-122.

Roy, T. and Lloyd, C., 2012. Epidemiology of depression and diabetes: A systematic review. Journal of Affective Disorders, 142, pp.S8-S21.

Ruan, H. and Lodish, H., 2004. Regulation of insulin sensitivity by adipose tissue-derived hormones and inflammatory cytokines. *Current Opinion in Lipidology*, 15(3), pp.297-302.

Rubi, B., Ljubicic, S., Pournourmohammadi, S., Carobbio, S., Armanet, M., Bartley, C. and Maechler, P., 2005. Dopamine D2-like Receptors Are Expressed in Pancreatic Beta Cells and Mediate Inhibition of Insulin Secretion. *Journal of Biological Chemistry*, 280(44), pp.36824-36832.

Rychlik, W., Spencer, W. and Rhoads, R., 1990. Optimization of the annealing temperature for DNA amplificationin vitro. *Nucleic Acids Research*, 18(21), pp.6409-6412.

Sachs, B., Ni, J. and Caron, M., 2015. Brain 5-HT deficiency increases stress vulnerability and impairs antidepressant responses following psychosocial stress. *Proceedings of the National Academy of Sciences*, 112(8), pp.2557-2562.

Sakano, D., Choi, S., Kataoka, M., Shiraki, N., Uesugi, M., Kume, K. and Kume, S., 2016. Dopamine D2 Receptor-Mediated Regulation of Pancreatic β Cell Mass. *Stem Cell Reports*, 7(1), pp.95-109.

Sakuraba, H., Mizukami, H., Yagihashi, N., Wada, R., Hanyu, C. and Yagihashi, S., 2002. Reduced beta-cell mass and expression of oxidative stress-related DNA damage in the islet of Japanese Type II diabetic patients. *Diabetologia*, 45(1), pp.85-96.

Saxena, R., Vallyathan, V. and Lewis, D., 2003. Evidence for lipopolysaccharideinduced differentiation of RAW264.7 murine macrophage cell line into dendritic like cells. *Journal of Biosciences*, 28(1), pp.129-134.

Scaglia, L., Cahill, C., Finegood, D. and Bonner-Weir, S., 1997. Apoptosis Participates in the Remodeling of the Endocrine Pancreas in the Neonatal Rat*. *Endocrinology*, 138(4), pp.1736-1741.

Schmid, C., Streicher, J., Meltzer, H. and Bohn, L., 2014. Clozapine Acts as an Agonist at Serotonin 2A Receptors to Counter MK-801-Induced Behaviors through a βArrestin2-Independent Activation of Akt. *Neuropsychopharmacology*, 39(8), pp.1902-1913.

Schoepf, D., Potluri, R., Uppal, H., Natalwala, A., Narendran, P. and Heun, R., 2012. Type-2 diabetes mellitus in schizophrenia: Increased prevalence and major risk factor of excess mortality in a naturalistic 7-year follow-up. *European Psychiatry*, 27(1), pp.33-42.

Schulte, P., 2003. What is an Adequate Trial with Clozapine?. *Clinical Pharmacokinetics*, 42(7), pp.607-618.

Schultz, W., 1998. Predictive Reward Signal of Dopamine Neurons. *Journal of Neurophysiology*, 80(1), pp.1-27.

Schulze, T., Morsi, M., Bruning, D., Schumacher, K. and Rustenbeck, I., 2016. Different responses of mouse islets and MIN6 pseudo-islets to metabolic stimulation: a note of caution. *Endocrine*, 51(3), pp.440-447.

Schwartz, T., 2018. Fine Tuning the Use of Second-Generation Antipsychotics. J*ournal of Mental Health and Clinical Psychology*, 2(5), pp.22-39.

Seedat, S., Scott, K., Angermeyer, M., Berglund, P., Bromet, E., Brugha, T., Demyttenaere, K., de Girolamo, G., Haro, J., Jin, R., Karam, E., Kovess-Masfety, V., Levinson, D., Medina Mora, M., Ono, Y., Ormel, J., Pennell, B., Posada-Villa, J., Sampson, N., Williams, D. and Kessler, R., 2009. Cross-National Associations Between Gender and Mental Disorders in the World Health Organization World Mental Health Surveys. *Archives of General Psychiatry*, 66(7), p.785.

Seeman, P., 2010. Dopamine D2 Receptors as Treatment Targets in Schizophrenia. *Clinical Schizophrenia & Related Psychoses*, 4(1), pp.56-73.

Segerstolpe, A., Palasantza, A., Eliasson, P., Andersson, E., Andréasson, A., Sun, X., Picelli, S., Sabirsh, A., Clausen, M., Bjursell, M., Smith, D., Kasper, M., Ämmälä, C. and Sandberg, R., 2016. Single-Cell Transcriptome Profiling of Human Pancreatic Islets in Health and Type 2 Diabetes. *Cell Metabolism*, 24(4), pp.593-607.

Sell, H., Habich, C. and Eckel, J., 2012. Adaptive immunity in obesity and insulin resistance. *Nature Reviews Endocrinology*, 8(12), pp.709-716.

Sempoux, C., Guiot, Y., Dubois, D., Moulin, P. and Rahier, J., 2001. Human type 2 diabetes: morphological evidence for abnormal beta-cell function. *Diabetes*, 50(Supplement 1), pp.S172-S177.

Shapiro, A., Pokrywczynska, M. and Ricordi, C., 2016. Clinical pancreatic islet transplantation. *Nature Reviews Endocrinology*, 13(5), pp.268-277.

Shapiro, D., Renock, S., Arrington, E., Chiodo, L., Liu, L., Sibley, D., Roth, B. and Mailman, R., 2003. Aripiprazole, A Novel Atypical Antipsychotic Drug with a Unique and Robust Pharmacology. *Neuropsychopharmacology*, 28(8), pp.1400-1411.

Sherwani, S., Khan, H., Ekhzaimy, A., Masood, A. and Sakharkar, M., 2016. Significance of HbA1c Test in Diagnosis and Prognosis of Diabetic Patients. *Biomarker Insights*, 11, p.BMI.S38440.

Shields, B., Hicks, S., Shepherd, M., Colclough, K., Hattersley, A. and Ellard, S., 2010. Maturity-onset diabetes of the young (MODY): how many cases are we missing?. *Diabetologia*, 53(12), pp.2504-2508.

Shrestha, P., Fariba, K., Abdijadid, S., 2021. Paroxetine. In: StatPearls [Internet]. Treasure Island (FL): StatPearls Publishing. Available at: https://www.ncbi.nlm.nih.gov/books/NBK526022/

Sibiak, R., Jankowski, M., Gutaj, P., Mozdziak, P., Kempisty, B. and Wender-Ożegowska, E., 2020. Placental Lactogen as a Marker of Maternal Obesity, Diabetes, and Fetal Growth Abnormalities: Current Knowledge and Clinical Perspectives. *Journal of Clinical Medicine*, 9(4), p.1142.

Silva, D., Kanazawa, L. and Vecchia, D., 2019. Schizophrenia: effects of aripiprazole in metabolic syndrome. *Brazilian Journal of Pharmaceutical Sciences*, 55.

Simpson, N., Maffei, A., Freeby, M., Burroughs, S., Freyberg, Z., Javitch, J., Leibel, R. and Harris, P., 2012. Dopamine-Mediated Autocrine Inhibitory Circuit Regulating Human Insulin Secretion in Vitro. *Molecular Endocrinology*, 26(10), pp.1757-1772.

Singh HK, Saadabadi A., 2021. Sertraline. In: StatPearls [Internet]. Treasure Island (FL): StatPearls Publishing. Available at: https://www.ncbi.nlm.nih.gov/books/NBK547689/

Skelin, M., Rupnik, M. and Cencic, A., 2010. Pancreatic beta cell lines and their applications in diabetes mellitus research. *ALTEX*, pp.105-113.

Smith, M., Hopkins, D., Peveler, R., Holt, R., Woodward, M. and Ismail, K., 2008. First- v. second-generation antipsychotics and risk for diabetes in schizophrenia: Systematic review and meta-analysis. *British Journal of Psychiatry*, 192(6), pp.406-411.

Sobis, J., Rykaczewska-Czerwinska, M., SwiEtochowska, E. and Gorczyca, P., 2015. Therapeutic effect of aripiprazole in chronic schizophrenia is accompanied by anti-inflammatory activity. *Pharmacological Reports*, 67(2), pp.353-359.

Solmi, M., Murru, A., Pacchiarotti, I., Undurraga, J., Veronese, N., Fornaro, M., Stubbs, B., Monaco, F., Vieta, E., Seeman, M., Correll, C. and Carvalho, A., 2017. Safety, tolerability, and

risks associated with first- and second-generation antipsychotics: a state-of-the-art clinical review. *Therapeutics and Clinical Risk Management*, Volume 13, pp.757-777.

Solovjeva, L., Demin, S., Pleskach, N., Kuznetsova, M. and Svetlova, M., 2012. Characterization of telomeric repeats in metaphase chromosomes and interphase nuclei of Syrian Hamster Fibroblasts. *Molecular Cytogenetics*, 5(1).

Song, E., Zhang, C., Israelow, B., Lu-Culligan, A., Prado, A. V., Skriabine, S., Lu, P., Weizman, O. E., Liu, F., Dai, Y., Szigeti-Buck, K., Yasumoto, Y., Wang, G., Castaldi, C., Heltke, J., Ng, E., Wheeler, J., Alfajaro, M. M., Levavasseur, E., Fontes, B., … Iwasaki, A., 2021. Neuroinvasion of SARS-CoV-2 in human and mouse brain. *The Journal of experimental medicine*, 218(3), e20202135.

Song, G., Pacini, G., Ahrén, B. and D'Argenio, D., 2017. Glucagon increases insulin levels by stimulating insulin secretion without effect on insulin clearance in mice. *Peptides*, 88, pp.74-79.

Sparshatt, A., Taylor, D., Patel, M. and Kapur, S., 2010. A Systematic Review of Aripiprazole—Dose, Plasma Concentration, Receptor Occupancy, and Response. *The Journal of Clinical Psychiatry*, 71(11), pp.1447-1456.

Sparshatt, A., Taylor, D., Patel, M. and Kapur, S., 2010. A Systematic Review of Aripiprazole—Dose, Plasma Concentration, Receptor Occupancy, and Response. *The Journal of Clinical Psychiatry*, 71(11), pp.1447-1456.

Sproule, B., Naranjo, C., Bremner, K. and Hassan, P., 1997. Selective Serotonin Reuptake Inhibitors and CNS Drug Interactions. *Clinical Pharmacokinetics*, 33(6), pp.454-471.

Stamateris, R., Sharma, R., Kong, Y., Ebrahimpour, P., Panday, D., Ranganath, P., Zou, B., Levitt, H., Parambil, N., O'Donnell, C., García-Ocana, A. and Alonso, L., 2016. Glucose Induces Mouse β-Cell Proliferation via IRS2, MTOR, and Cyclin D2 but Not the Insulin Receptor. *Diabetes*, 65(4), pp.981-995.

Stark, A. and Scott, J., 2012. A review of the use of clozapine levels to guide treatment and determine cause of death. *Australian & New Zealand Journal of Psychiatry*, 46(9), pp.816-825.

Starrenburg, F. and Bogers, J., 2009. How can antipsychotics cause diabetes mellitus? Insights based on receptor-binding profiles, humoral factors and transporter proteins. *European Psychiatry*, 24(3), pp.164-170.

Steiner, D., Kim, A., Miller, K. and Hara, M., 2010. Pancreatic islet plasticity: Interspecies comparison of islet architecture and composition. *Islets*, 2(3), pp.135-145.

Stiles, L. and Shirihai, O., 2012. Mitochondrial dynamics and morphology in beta-cells. *Best Practice & Research Clinical Endocrinology & Metabolism*, 26(6), pp.725-738.

Stott, N. and Marino, J., 2020. High Fat Rodent Models of Type 2 Diabetes: From Rodent to Human. Nutrients, 12(12), p.3650.

Stranahan, A., Arumugam, T., Cutler, R., Lee, K., Egan, J. and Mattson, M., 2008. Diabetes impairs hippocampal function through glucocorticoid-mediated effects on new and mature neurons. *Nature Neuroscience*, 11(3), pp.309-317.

Straub, S. and Sharp, G., 2002. Glucose-stimulated signaling pathways in biphasic insulin secretion. *Diabetes/Metabolism Research and Reviews*, 18(6), pp.451-463.

Strober, W., 2015. Trypan Blue Exclusion Test of Cell Viability. *Current Protocols in Immunology*, 111(1).

Stumvoll, M., Goldstein, B. J., and Van Haeften, T. W., 2005. Type2 diabetes: principles of pathogenesis and therapy. *Lancet*, 365, pp.1333–1346.

Subramanian, S., Völlm, B. and Huband, N., 2017. Clozapine dose for schizophrenia. *Cochrane Database of Systematic Reviews*, 2017(6).

Sullivan, L. C., Clarke, W. P. and Berg, K. A., 2015. Atypical antipsychotics and inverse agonism at 5-HT2 receptors. *Current Pharmaceutical Design*, 21(26), pp.3732–3738.

Suvisaari, J., Keinänen, J., Eskelinen, S. and Mantere, O., 2016. Diabetes and Schizophrenia. *Current Diabetes Reports*, 16(2).

Taciak, B., Białasek, M., Braniewska, A., Sas, Z., Sawicka, P., Kiraga, L., Rygiel, T. and Krol, M., 2018. Evaluation of phenotypic and functional stability of RAW 264.7 cell line through serial passages. *PLOS ONE*, 13(6), p.e0198943.

Tahrani, A., Bailey, C., Del Prato, S. and Barnett, A., 2011. Management of type 2 diabetes: new and future developments in treatment. *The Lancet*, 378(9786), pp.182-197.

Takahashi, M., Miyatsuka, T., Suzuki, L., Osonoi, S., Himuro, M., Miura, M., Katahira, T., Wakabayashi, Y., Nishida, Y., Fujitani, Y., Takeda, S., Mizukami, H., Itakura, A. and Watada, H., 2020. Biphasic Changes in β-Cell Mass Around Parturition Accompanied by Increased Serotonin Production. *Scientific reports*, *10*(1), pp.4962.

Takaoka, M., Nagata, D., Kihara, S., Shimomura, I., Kimura, Y., Tabata, Y., Saito, Y., Nagai, R. and Sata, M., 2009. Periadventitial Adipose Tissue Plays a Critical Role in Vascular Remodeling. *Circulation Research*, 105(9), pp.906-911.

Taler, M., Miron, O., Gil-Ad, I. and Weizman, A., 2013. Neuroprotective and procognitive effects of sertraline: In vitro and *in vivo* studies. *Neuroscience Letters*, 550, pp.93-97.

Talevi, D., Socci, V., Carai, M., Carnaghi, G., Faleri, S., Trebbi, E., di Bernardo, A., Capelli, F., & Pacitti, F. (2020). Mental health outcomes of the CoViD-19 pandemic. *Rivista di Psichiatria*, 55(3), pp.137–144.

Taupin, P., 2007. BrdU immunohistochemistry for studying adult neurogenesis: Paradigms, pitfalls, limitations, and validation. Brain Research Reviews, 53(1), pp.198-214.

Teff, K., Rickels, M., Grudziak, J., Fuller, C., Nguyen, H. and Rickels, K., 2013. Antipsychotic-Induced Insulin Resistance and Postprandial Hormonal Dysregulation Independent of Weight Gain or Psychiatric Disease. *Diabetes*, 62(9), pp.3232-3240.

Teta, M., Long, S., Wartschow, L., Rankin, M. and Kushner, J., 2005. Very Slow Turnover of β-Cells in Aged Adult Mice. *Diabetes*, 54(9), pp.2557-2567.

Tharmaraja, T., Stahl, D., Hopkins, C., Persaud, S., Jones, P., Ismail, K. and Moulton, C., 2019. The Association Between Selective Serotonin Reuptake Inhibitors and Glycemia: A Systematic Review and Meta-Analysis of Randomized Controlled Trials. *Psychosomatic Medicine*, 81(7), pp.570-583.

Then, C., Liu, K., Liao, M., Chung, K., Wang, J. and Shen, S., 2017. Antidepressants, sertraline and paroxetine, increase calcium influx and induce mitochondrial damage-mediated apoptosis of astrocytes. *Oncotarget*, 8(70), pp.115490-115502.

Thompson, I., de Vries, E. and Sommer, I., 2020. Dopamine D2 up-regulation in psychosis patients after antipsychotic drug treatment. *Current Opinion in Psychiatry*, 33(3), pp.200-205.

Thorve, V., Kshirsagar, A., Vyawahare, N., Joshi, V., Ingale, K. and Mohite, R., 2011. Diabetes-induced erectile dysfunction: epidemiology, pathophysiology and management. *Journal of Diabetes and its Complications*, 25(2), pp.129-136.

Tilg, H. and Moschen, A., 2008. Inflammatory Mechanisms in the Regulation of Insulin Resistance. *Molecular Medicine*, 14(3-4), pp.222-231.

Ting, E., Yang, A. and Tsai, S., 2020. Role of Interleukin-6 in Depressive Disorder. *International Journal of Molecular Sciences*, 21(6), p.2194.

Todorovic, N., Micic, B., Schwirtlich, M., Stevanovic, M. and Filipovic, D., 2019. Subregion-specific Protective Effects of Fluoxetine and Clozapine on Parvalbumin Expression in Medial Prefrontal Cortex of Chronically Isolated Rats. *Neuroscience*, 396, pp.24-35.

Tomita, T., Yasui-Furukori, N., Nakagami, T., Tsuchimine, S., Ishioka, M., Kaneda, A., Nakamura, K. and Kaneko, S., 2014. Therapeutic Reference Range for Plasma Concentrations of Paroxetine in Patients with Major Depressive Disorders. *Therapeutic Drug Monitoring*, 36(4), pp.480-485.

Tovey, E., Rampes, H. and Livingstone, C., 2005. Clozapine-induced type-2 diabetes mellitus: possible mechanisms and implications for clinical practice. *Journal of Psychopharmacology*, 19(2), pp.207-210.

Tsalamandris, S., Antonopoulos, A., Oikonomou, E., Papamikroulis, G., Vogiatzi, G., Papaioannou, S., Deftereos, S. and Tousoulis, D., 2019. The Role of Inflammation in Diabetes: Current Concepts and Future Perspectives. *European Cardiology Review*, 14(1), pp.50-59.

Tsujimoto, Y., 2001. Role of Bcl-2 family proteins in apoptosis: apoptosomes or mitochondria?. *Genes to Cells*, 3(11), pp.697-707.

Tuplin, E. and Holahan, M., 2017. Aripiprazole, A Drug that Displays Partial Agonism and Functional Selectivity. *Current Neuropharmacology*, 15(8).

Tuttolomondo, A., Maida, C. and Pinto, A., 2015. Diabetic Foot Syndrome as a Possible Cardiovascular Marker in Diabetic Patients. *Journal of Diabetes Research*, 2015, pp.1-12.

Tyrberg, B., Eizirik, D., Hellerstrom, C., Pipeleers, D. and Andersson, A., 1996. Human pancreatic beta-cell deoxyribonucleic acid-synthesis in islet grafts decreases with increasing organ donor age but increases in response to glucose stimulation in vitro. *Endocrinology*, 137(12), pp.5694-5699.

Uchendu, C. and Blake, H., 2016. Effectiveness of cognitive-behavioural therapy on glycaemic control and psychological outcomes in adults with diabetes mellitus: a systematic review and meta-analysis of randomized controlled trials. *Diabetic Medicine*, 34(3), pp.328-339.

Umpierrez, G., Hellman, R., Korytkowski, M., Kosiborod, M., Maynard, G., Montori, V., Seley, J. and Van den Berghe, G., 2012. Management of Hyperglycemia in Hospitalized Patients in Non-Critical Care Setting: An Endocrine Society Clinical Practice Guideline. *The Journal of Clinical Endocrinology & Metabolism*, 97(1), pp.16-38.

Unger, R. and Cherrington, A., 2012. Glucagonocentric restructuring of diabetes: a pathophysiologic and therapeutic makeover. *Journal of Clinical Investigation*, 122(1), pp.4-12.

Unsworth, R., Wallace, S., Oliver, N., Yeung, S., Kshirsagar, A., Naidu, H., Kwong, R., Kumar, P. and Logan, K., 2020. New-Onset Type 1 Diabetes in Children During COVID-19: Multicenter Regional Findings in the U.K. *Diabetes Care*, 43(11), pp.e170-e171.

Urakami T., 2019. Maturity-onset diabetes of the young (MODY): current perspectives on diagnosis and treatment. *Diabetes, metabolic syndrome and obesity: targets and therapy*, 12, pp.1047–1056.

Urban, J., Vargas, G., von Zastrow, M. and Mailman, R., 2006. Aripiprazole has Functionally Selective Actions at Dopamine D2 Receptor-Mediated Signaling Pathways. *Neuropsychopharmacology*, 32(1), pp.67-77.

Ustione, A., Piston, D. and Harris, P., 2013. Minireview: Dopaminergic Regulation of Insulin Secretion from the Pancreatic Islet. *Molecular Endocrinology*, 27(8), pp.1198-1207.

van Harten, B., de Leeuw, F., Weinstein, H., Scheltens, P. and Biessels, G., 2006. Brain Imaging in Patients with Diabetes: A systematic review. *Diabetes Care*, 29(11), pp.2539-2548.

Vancampfort, D., Sienaert, P., Wyckaert, S., De Hert, M., Stubbs, B. and Probst, M., 2016. Sitting time, physical fitness impairments and metabolic abnormalities in people with bipolar disorder: An exploratory study. *Psychiatry Research*, 242, pp.7-12.

Vancampfort, D., Stubbs, B., Mitchell, A., De Hert, M., Wampers, M., Ward, P., Rosenbaum, S. and Correll, C., 2015. Risk of metabolic syndrome and its components in people with schizophrenia and related psychotic disorders, bipolar disorder and major depressive disorder: a systematic review and meta-analysis. *World Psychiatry*, 14(3), pp.339-347.

Vanes, L., Mouchlianitis, E., Patel, K., Barry, E., Wong, K., Thomas, M., Szentgyorgyi, T., Joyce, D. and Shergill, S., 2019. Neural correlates of positive and negative symptoms through the illness course: an fMRI study in early psychosis and chronic schizophrenia. *Scientific Reports*, 9(1).

Vardi, M., Jacobson, E., Nini, A. and Bitterman, H., 2008. Intermediate acting versus long-acting insulin for type 1 diabetes mellitus. *The Cochrane database of systematic reviews,* 2008(3), CD006297.

Varma, S., Bishara, D., Besag, F. and Taylor, D., 2011. Clozapine-related EEG changes and seizures: dose and plasma-level relationships. *Therapeutic Advances in Psychopharmacology*, 1(2), pp.47-66.

Vetere, A., Choudhary, A., Burns, S. and Wagner, B., 2014. Targeting the pancreatic β-cell to treat diabetes. *Nature Reviews Drug Discovery*, 13(4), pp.278-289.

Volpe, C., Villar-Delfino, P., dos Anjos, P. and Nogueira-Machado, J., 2018. Cellular death, reactive oxygen species (ROS) and diabetic complications. *Cell Death & Disease*, 9(2).

Wang, C., Chen, X., Ding, X., He, Y., Gu, C. and Zhou, L., 2015. Exendin-4 Promotes Beta Cell Proliferation via PI3k/Akt Signalling Pathway. *Cellular Physiology and Biochemistry*, 35(6), pp.2223-2232.

Wang, F., Hull, R., Vidal, J., Cnop, M. and Kahn, S., 2001. Islet Amyloid Develops Diffusely Throughout the Pancreas Before Becoming Severe and Replacing Endocrine Cells. *Diabetes*, 50(11), pp.2514-2520.

Wang, L., Ree, S., Huang, Y., Hsiao, C. and Chen, C., 2013. Adjunctive effects of aripiprazole on metabolic profiles: Comparison of patients treated with olanzapine to patients treated with other atypical antipsychotic drugs. *Progress in Neuro-Psychopharmacology and Biological Psychiatry*, 40, pp.260-266.

Wang, P., Fiaschi-Taesch, N., Vasavada, R., Scott, D., García-Ocaña, A. and Stewart, A., 2015. Diabetes mellitus—advances and challenges in human β-cell proliferation. *Nature Reviews Endocrinology*, 11(4), pp.201-212.

Wang, X., Bao, W., Liu, J., OuYang, Y., Wang, D., Rong, S., Xiao, X., Shan, Z., Zhang, Y., Yao, P. and Liu, L., 2013. Inflammatory Markers and Risk of Type 2 Diabetes: A systematic review and meta-analysis. *Diabetes Care*, 36(1), pp.166-175.

Wanner, C., Inzucchi, S., Lachin, J., Fitchett, D., von Eynatten, M., Mattheus, M., Johansen, O., Woerle, H., Broedl, U. and Zinman, B., 2016. Empagliflozin and Progression of Kidney Disease in Type 2 Diabetes. New England Journal of Medicine, 375(4), pp.323-334.

Weinberg, N., Ouziel-Yahalom, L., Knoller, S., Efrat, S. and Dor, Y., 2007. Lineage Tracing Evidence for In Vitro Dedifferentiation but Rare Proliferation of Mouse Pancreatic β-Cells. *Diabetes*, 56(5), pp.1299-1304.

Wenthur, C., Bennett, M. and Lindsley, C., 2015. Classics in Chemical Neuroscience: Fluoxetine (Prozac). *ACS Chemical Neuroscience*, 5(1), pp.14-23.

Westermark, P. and Wilander, E., 1978. The influence of amyloid deposits on the islet volume in maturity onset diabetes mellitus. *Diabetologia*, 15(5), pp.417-421.

Whicher, C., O'Neill, S. and Holt, R., 2020. Diabetes in the UK: 2019. *Diabetic Medicine*, 37(2), pp.242-247.

Wichmann, D., 2020. Autopsy Findings and Venous Thromboembolism in Patients With COVID-19. *Annals of Internal Medicine*, 173(12), p.1030.

Wilcox G., 2005. Insulin and insulin resistance. *The Clinical biochemist. Reviews*, 26(2), pp.19–39.

Wildgust, H., Hodgson, R. and Beary, M., 2010. The paradox of premature mortality in schizophrenia: new research questions. *Journal of Psychopharmacology*, 24(4_suppl), pp.9-15.

Wilson, M., Scheel, D. and German, M., 2003. Gene expression cascades in pancreatic development. *Mechanisms of Development*, 120(1), pp.65-80.

Winans, E., 2003. Aripiprazole. *American Journal of Health-System Pharmacy*, 60(23), pp.2437-2445.

Wiviott, S. D., Raz, I., Bonaca, M. P., Mosenzon, O., Kato, E. T., Cahn, A., Silverman, M. G., Zelniker, T. A., Kuder, J. F., Murphy, S. A., Bhatt, D. L., Leiter, L. A., 2019. Dapagliflozin and cardiovascular outcomes in type 2 diabetes. *The New England journal of medicine*, 380, pp.347–35.

Wlodkowic, D., Skommer, J., Darzynkiewicz, Z., 2009. Flow cytometry-based apoptosis detection. *Methods in Molecular Biology*, 559, pp.19–32.

Wong, D., Perry, K. and Bymaster, F., 2005. The Discovery of Fluoxetine Hydrochloride (Prozac). *Nature Reviews Drug Discovery*, 4(9), pp.764-774.

Wood, M. and Reavill, C., 2007. Aripiprazole acts as a selective dopamine D2receptor partial agonist. *Expert Opinion on Investigational Drugs*, 16(6), pp.771-775.

World Health Organization, 2019. World Health Organization model list of essential medicines: 21st list 2019. Geneva.

Wu, Y., Blichowski, M., Daskalakis, Z., Wu, Z., Liu, C., Cortez, M. and Snead, O., 2011. Evidence that clozapine directly interacts on the GABAB receptor. *NeuroReport*, 22(13), pp.637-641.

Wu, Y., Ding, Y., Tanaka, Y. and Zhang, W., 2014. Risk Factors Contributing to Type 2 Diabetes and Recent Advances in the Treatment and Prevention. *International Journal of Medical Sciences*, 11(11), pp.1185-1200.

Wyler, S., Lord, C., Lee, S., Elmquist, J. and Liu, C., 2017. Serotonergic Control of Metabolic Homeostasis. *Frontiers in Cellular Neuroscience*, 11.

Xin, Y., Davies, A., Briggs, A., McCombie, L., Messow, C., Grieve, E., Leslie, W., Taylor, R. and Lean, M., 2020. Type 2 diabetes remission: 2 year within-trial and lifetime-horizon cost-effectiveness of the Diabetes Remission Clinical Trial (DiRECT)/Counterweight-Plus weight management programme. *Diabetologia*, 63(10), pp.2112-2122.

Xiong, Q., Yu, C., Zhang, Y., Ling, L., Wang, L. and Gao, J., 2017. Key proteins involved in insulin vesicle exocytosis and secretion. *Biomedical Reports*, 6(2), pp.134-139.

Yada, Y., Kitagawa, K., Sakamoto, S., Ozawa, A., Nakada, A., Kashiwagi, H., Okahisa, Y., Takao, S., Takaki, M., Kishi, Y. and Yamada, N., 2020. The relationship between plasma clozapine concentration and clinical outcome: a cross-sectional study. *Acta Psychiatrica Scandinavica*, 143(3), pp.227-237.

Yamazaki, H., Philbrick, W., Zawalich, K. and Zawalich, W., 2006. Acute and chronic effects of glucose and carbachol on insulin secretion and phospholipase C activation: studies with diazoxide and atropine. *American Journal of Physiology-Endocrinology and Metabolism*, 290(1), pp.E26-E33.

Yang, F., Ma, Q., Liu, J., Ma, B., Guo, M., Liu, F., Li, J., Wang, Z. and Liu, M., 2020. Prevalence and major risk factors of type 2 diabetes mellitus among adult psychiatric inpatients from 2005 to 2018 in Beijing, China: a longitudinal observational study. *BMJ Open Diabetes Research & Care*, 8(1), p.e000996.

Yang, H., Lin, J., Li, H., Liu, Z., Chen, X. and Chen, Q., 2021. Prolactin Is Associated with Insulin Resistance and Beta-Cell Dysfunction in Infertile Women With Polycystic Ovary Syndrome. *Frontiers in Endocrinology*, 12.

Yang, Y. and Chan, L., 2016. Monogenic Diabetes: What It Teaches Us on the Common Forms of Type 1 and Type 2 Diabetes. *Endocrine Reviews*, 37(3), pp.190-222.

Ye, Z., Chen, L., Yang, Z., Li, Q., Huang, Y., He, M., Zhang, S., Zhang, Z., Wang, X., Zhao, W., Hu, J., Liu, C., Qu, S. and Hu, R., 2011. Metabolic Effects of Fluoxetine in Adults with Type 2 Diabetes Mellitus: A Meta-Analysis of Randomized Placebo-Controlled Trials. *PLoS ONE*, 6(7), p.e21551.

Ying, W., Fu, W., Lee, Y. and Olefsky, J., 2020. The role of macrophages in obesity-associated islet inflammation and β-cell abnormalities. *Nature Reviews Endocrinology*, 16(2), pp.81-90.

Yood, M., deLorenze, G., Quesenberry, C., Oliveria, S., Tsai, A., Willey, V., McQuade, R., Newcomer, J. and L'Italien, G., 2009. The incidence of diabetes in atypical antipsychotic users differs according to agent-results from a multisite epidemiologic study. *Pharmacoepidemiology and Drug Safety*, 18(9), pp.791-799.

Young, L., Darios, E. and Watts, S., 2015. An immunohistochemical analysis of SERT in the blood–brain barrier of the male rat brain. *Histochemistry and Cell Biology*, 144(4), pp.321-329.

Yusufi, B., Mukherjee, S., Flanagan, R., Paton, C., Dunn, G., Page, E. and Barnes, T., 2007. Prevalence and nature of side effects during clozapine maintenance treatment and the relationship with clozapine dose and plasma concentration. *International Clinical Psychopharmacology*, 22(4), pp.238-243.

Zhang, N., Yun, R., Liu, L. and Yang, L., 2020. Association of glycosylated hemoglobin and outcomes in patients with COVID-19 and pre-existing type 2 diabetes. *Medicine*, 99(47), p.e23392.

Zhang, S. and Kuhn, J., 2013. Cell isolation and culture. *WormBook*, pp.1-39.

Zhang, Y., Liu, Y., Su, Y., You, Y., Ma, Y., Yang, G., Song, Y., Liu, X., Wang, M., Zhang, L. and Kou, C., 2017. The metabolic side effects of 12 antipsychotic drugs used for the treatment of schizophrenia on glucose: a network meta-analysis. *BMC Psychiatry*, 17(1).

Zhang, Y., Zheng, R., Meng, X., Wang, L., Liu, L. and Gao, Y., 2015. Pancreatic Endocrine Effects of Dopamine Receptors in Human Islet Cells. *Pancreas*, 44(6), pp.925-929.

Zhao, Q., Hu, C., Feng, R., Yang, Y., 2020. Investigation of the mental health of patients with novel coronavirus pneumonia. *Chinese Journal of Contemporary Neurology and Neurosurgery*, 53.

Zheng, Y., Ley, S. and Hu, F., 2017. Global aetiology and epidemiology of type 2 diabetes mellitus and its complications. *Nature Reviews Endocrinology*, 14(2), pp.88-98.

Zhou, Z., Ribas, V., Rajbhandari, P., Drew, B., Moore, T., Fluitt, A., Reddish, B., Whitney, K., Georgia, S., Vergnes, L., Reue, K., Liesa, M., Shirihai, O., van der Bliek, A., Chi, N., Mahata, S., Tiano, J., Hewitt, S., Tontonoz, P., Korach, K., Mauvais-Jarvis, F. and Hevener, A., 2018. Estrogen receptor α protects pancreatic β-cells from apoptosis by preserving mitochondrial function and suppressing endoplasmic reticulum stress. Journal of Biological Chemistry, 293(13), pp.4735-4751.

Zhuang, Q., Shen, L. and Ji, H., 2017. Quantitative assessment of the bidirectional relationships between diabetes and depression. *Oncotarget*, 8(14), pp.23389-23400.

Zinman, B., Wanner, C., Lachin, J. M., Fitchett, D., Bluhmki, E., Hantel, S., Mattheus, M., Devins, T., Johansen, O. E., Woerle, H. J., Broedl, U. C., Inzucchi, S. E.,2015. Empagliflozin, cardiovascular outcomes, and mortality in type 2 diabetes. *The New England journal of medicine*, 373, pp.2117–2128.

Zinman, B., Wanner, C., Lachin, J., Fitchett, D., Bluhmki, E., Hantel, S., Mattheus, M., Devins, T., Johansen, O., Woerle, H., Broedl, U. and Inzucchi, S., 2015. Empagliflozin, Cardiovascular Outcomes, and Mortality in Type 2 Diabetes. New England Journal of Medicine, 373(22), pp.2117-2128.

Zirpel, H., Roep, B. O., 2021. Islet-Resident Dendritic Cells and Macrophages in Type 1 Diabetes: In Search of Bigfoot's Print. *Frontiers in endocrinology*, 12, pp.666795.

Zraika, S., Aston-Mourney, K., Laybutt, D., Kebede, M., Dunlop, M., Proietto, J. and Andrikopoulos, S., 2006. The influence of genetic background on the induction of oxidative stress and impaired insulin secretion in mouse islets. *Diabetologia*, 49(6), pp.1254-1263.

Conference publications:

Olaniru OE, Toczyska K, Giera S, Piao X, Jones PM, Persaud SJ. Characterising the role of the adhesion receptor GPR56 in islet development. Abstracts of 53rd EASD Annual Meeting, Diabetologia. 2017

Liu B, Zariwala M, Toczyska K, Ruz-Maldonado I, Persaud SJ, Moulton C, Jones PM, Ismail K, Huang G. The selective serotonin reuptake inhibitor fluoxetine improves glucose homeostasis in mice and humans: effects on insulin secretion and functional beta cell mass. Abstracts of 54th EASD Annual Meeting, Diabetologia. 2018

Toczyska K, Ruz-Maldonado I, Liu B, Persaud PJ. Direct effects of the selective serotonin reuptake inhibitors, fluoxetine and sertraline, to improve beta cell mass and function *in vitro* and *in vivo*" Abstracts of 55th EASD Annual Meeting, Diabetologia. 2019

Toczyska K, Ruz-Maldonado I, Liu B, Persaud PJ. The selective serotonin reuptake inhibitors, fluoxetine and sertraline, improve beta cell mass and function. Abstracts of the Diabetes UK Professional Conference 2019. Diabetic Med. 2019

Toczyska K, Hubber EL, Liu B, Persaud PJ. Effect of the selective serotonin reuptake inhibitor paroxetine on mouse beta cell function. Abstracts of 56th EASD Annual Meeting, Diabetologia. 2020

Toczyska K, Hubber EL, Liu B, Persaud PJ. Evaluation of the effects of the selective serotonin reuptake inhibitor paroxetine on Mouse beta-cell function. Abstracts of the Diabetes UK Professional Conference 2020. Diabetic Med. 2020

Toczyska K, Day G, Guccio N, Liu B and Persaud SJ. The atypical antipsychotic drugs aripiprazole and clozapine have direct effects on beta-cells to stimulate proliferation and decrease apoptosis. Abstracts of the Diabetes UK Professional Conference 2021. Diabetic Med. 2021

Toczyska K, Day G, Guccio N, Rosa H, Liu B and Persaud SJ. Therapeutically relevant concentrations of atypical antipsychotic drugs, aripiprazole and clozapine, promote beta-cell mass expansion. Abstracts of 57th EASD Annual Meeting, Diabetologia. 2021